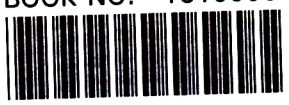

Intelligent autopilots for ships

Thesis submitted to the University of Wales for the degree of

Doctor of Philosophy

By

Antonio Zirilli,
Mechatronics Research Centre
University of Wales College, Newport
October 2000

Declarations

DECLARATION

This work has not previously been accepted in any substance for any degree and is not being currently submitted in candidature for any degree

Signed.....(Candidate)

Date.....

STATEMENT 1

This thesis is the result of my own investigations except where otherwise stated.
Other sources are acknowledged by footnotes giving explicit references. A bibliography is appended.

Signed.....(Candidate)

Date.....

STATEMENT 2

I hereby give consent for my thesis, if accepted to be available for photocopying and for inter-library loan, and for the title and summary to be made available to outside organisations.

Signed.....(Candidate)

Date

To my mother, Fabio and Ciccio...

The greatest inspirations,
The most sublime ideas of living that have come down to humanity,
Come from a higher realm,
A happier realm,
A place of pure dreams,
A heaven of blessed notions.
Ideas and infinite possibilities dwell there in absolute tranquillity.

Before these ideas come to us they were pure,
They were silent and their living possibilities were splendid.
But when they come to our earthly realm they acquire weight and words.
They become less.

We began before words and we will end beyond them.
What is the real meaning,
The real idea of love ?

Yes, the highest things are beyond words.
If only words were a kind of fluid that turns into the visible physical equivalent of their true value,
Then ...

Acknowledgements

After three years of studying in a foreign country the list of people to thank is enormous. I would like to thank my three supervisors, Prof. Antonio Tiano who always believed in me and Prof. Geoff Roberts who give me the opportunity to study at the Mechatronics Research Centre and most importantly he supported and encouraged me throughout all the period of my study. Last but certainly not least Dr. Robert Sutton, who with his red pen corrected the overall thesis making it readable and more understandable even to me. From all of them I learnt both technical and non-technical aspects of this work. I am truly indebted to all of them.

Of course there are also all the friends of the Mechatronics Research Centre but in particular I would like to thank Mrs Jane John for her genuine disposability in helping me with all sorts of matter. In the final stage of my writing-up she even helped me with my english spelling.

I would like to thank all the staff of the library, in particular Mrs Jenifer Coleman and Mrs Bronwen Stone who always with passion and dedication helped me to find all the papers and books I requested. Without them all the precious information I gathered from those papers and books would have been impossible.

Some people are very lucky because they have big and happy families. I am certainly one of these. All this will not have any sense without the awareness that I had and I will constantly have the support and the encouragement of my family. There are no words to express the real meaning of love I will just say, my father Gianfranco and his wife Beatrice, my sister Matilde and her husband Angelo, my two little sisters Renata and Claudia, my love Sonia and our faithful friends Birba and Cuba. Thanks to all of you.

Summary

The design of automatic systems for steering a ship presents difficult challenges because of their dynamic properties which vary considerably within the range of sailing conditions. Automatic steering of ships has its origin at the beginning of the century and was prompted by the introduction of the gyrocompass. Until the earlier 70s almost all autopilots for a ship were based on the proportional-derivative-integral (PID) controller. The main disadvantage with PID controllers is that the optimal parameters setting can be achieved only for a particular sailing condition. This shortcoming was and is still dealt with in the framework of adaptive theory where the controller parameters are adjusted in the attempt to seek the optimum of a pre-set performance function. Despite such a potential advantage, at present adaptive control theory is limited to linear plants and requires a certain amount of *a-priori* information for a successful application.

This thesis is concerned with the applicability of intelligent control techniques to the problem of designing course-keeping and course-changing autopilots for ships. For this reason the framework of intelligent control theory is introduced and a pragmatic definition of intelligent controllers is stated. The learning and adaptive features of neural networks and fuzzy logic systems are exploited and used to solve advantageously the control design problem. Adaptive networks are used as a unifying structure where different kinds of neural networks and fuzzy logic paradigms can be described. In this framework, comparisons between neural networks and fuzzy logic systems are made and results from one field can be easily extended to the other.

Although the use of such systems for the design of autopilots is in its early stage, the majority of the contributions which have appeared in literature have focused on the use of feedforward networks trained with the back-propagation algorithm. The main contributions of this thesis are the critical analysis of the feedforward network controller trained with the back-propagation algorithm, the proposition of an alternative controller architecture based on the use of radial basis function networks and to give conditions under which the stability analysis of the intelligent controllers so designed can be evaluated.

Table of Contents

Chapter 1 Introduction and overview *1-1*

1.1 Introduction **1-1**

1.2 Autopilots for ships: brief overview **1-3**

1.2.1 Earlier approaches 1-3

1.2.2 Classical approaches 1-5

1.2.3 Intelligent approaches 1-7

1.3 Steering criteria for course-changing and course-keeping **1-9**

1.4 Adaptive approach: objectives and motivations **1-12**

1.5 Structure of the thesis **1-18**

1.6 Reference List **1-19**

Chapter 2 Neural networks and Fuzzy logic systems *2-1*

2.1 Introduction **2-1**

2.2 Artificial Neural Networks **2-2**

2.2.1 Perceptrons 2-4

2.2.2 Multilayer Perceptron Networks 2-6

2.2.3 Cerebellar Model Articulated Controller 2-8

2.2.4 Radial Basis Function Networks 2-9

2.3 Fuzzy systems for control **2-12**

2.3.1 Mamdani fuzzy models 2-25

2.3.2 Sugeno fuzzy models 2-26

2.4 Summary **2-28**

2.5 Reference List **2-28**

Chapter 3 Adaptive networks *3-1*

3.1 Introduction **3-1**

3.1.1 Adaptive Network Based Fuzzy Inference System 3-1

3.2 Adaptive networks for control **3-4**

3.3 Universal approximation capability **3-8**

3.4 Adaptation and learning in intelligent control **3-10**

3.4.1 Least square and least mean square algorithm 3-11

3.4.2 Back-propagation 3-13

3.4.3 Hybrid learning 3-19

3.5 Summary **3-20**

3.6 Reference List **3-20**

Chapter 4 Ship's dynamics *4-1*

4.1 Introduction **4-1**

4.2 Equation of motion in six degrees of freedom **4-2**

4.3 Hydrodynamic derivatives **4-6**

4.4 Stability index and Lateral stability **4-8**

4.5 Models used for control **4-13**
4.5.1 Nomoto's model 4-14
4.5.2 Bech's model 4-15
4.5.3 Norrbin's model 4-17

4.6 Summary **4-19**

4.7 Reference List **4-20**

Chapter 5 Non-linear model of a containership *5-1*

5.1 Introduction **5-1**

5.2 Non-linear model of a containership **5-3**
5.2.1 Deterministic forces and moments 5-5
5.2.2 Disturbances modelling 5-8
5.2.3 The overall system 5-11

5.3 Manoeuvring characteristics **5-12**

5.4 Summary **5-16**

5.5 Reference List **5-17**

Chapter 6 Autopilots designed with fuzzy set theory *6-1*

6.1 Introduction **6-1**

6.2 Fuzzy course-keeping controller **6-3**

6.3 Fuzzy course-changing controller **6-9**

6.4 Conclusions **6-19**

6.5 Reference List **6-20**

Chapter 7 Intelligent Autopilots *7-1*

7.1 Introduction **7-1**

7.2 Model-reference neural autopilots **7-2**

7.3 Course-keeping autopilots **7-9**

7.4 Stable adaptive autopilots based on NN and fuzzy logic **7-17**
7.4.1 Statement of the problem 7-18
7.4.2 Controller design 7-21
7.4.3 Simulation results 7-25

7.5 Conclusions **7-33**

7.6 Reference List **7-36**

Chapter 8 Conclusions and further recommendations *8-1*

8.1 Review **8-1**

8.2 Discussion and conclusion **8-5**

Appendix A *A-1*

A.1 Geometrical data and hydrodynamics coefficients **A-1**

A.2 Linear model **A-4**

A.3 Reference List **A-10**

Appendix B Disturbances Modelling ***B-1***

B.1 Introduction **B-1**

B.2 Waves effects **B-2**

B.2.1 Simply Gravity Waves Theory (Regular waves) B-3

B.2.2 Harmonic waves theory (Irregular waves) B-6

B.2.3 Waves forces and moments B-8

B.2.4 Response operators B-10

B.3 Wind effects **B-12**

B.4 Ocean Current **B-16**

B.5 Shallow water effects **B-17**

B.6 Summary **B-19**

B.7 Reference List **B-19**

Appendix C ***C-1***

C.1 Stability proof **C-1**

C.2 Reference List **C-6**

Appendix D Published papers ***D-1***

D.1 List of journal paper **D-1**

D.2 List of conference papers **D-1**

List of Figures

Chapter 1 **Page**

Figure 1.1: Course changing manoeuvre 1-11

Chapter 2

Figure 2.1: Biological neuron structure 2-2
Figure 2.2: Basic structure of neuron 2-3
Figure 2.3: Three layer neural network 2-6
Figure 2.4: Block diagram of CMAC 2-9
Figure 2.5: Radial Basis Network 2-11
Figure 2.6: General Fuzzy Logic System structure 2-13
Figure 2.7: Two rules, two inputs Mamdani fuzzy model 2-24
Figure 2.8: Two rules, two inputs fuzzy Sugeno model 2-26

Chapter 3

Figure 3.1: ANFIS architecture for the first order Sugeno model 3-3
Figure 3.2: Controller mapping 3-4
Figure 3.3: Direct adaptive controller 3-5
Figure 3.4: State estimation mapping 3-5
Figure 3.5: Indirect adaptive controller 3-6
Figure 3.6: Three layer adaptive network 3-14
Figure 3.8: Back-propagation for one layer non-linear network 3-18
Figure 3.8: Two inputs two outputs adaptive back-propagation network 3-18

Chapter 4

Figure 4.1: Ship's systems frame 4-2
Figure 4.2: Different kinds of stability 4-9
Figure 4.3: Fully symmetric buoy 4-11
Figure 4.4: Lateral ship's section 4-13
Figure 4.7: Reversal spiral test for stable and unstable ships 4-17

Chapter 5

Figure 5.1: Three possible relationships between X and v 5-2
Figure 5.2: Solid Pierson-Moskowitz spectrum. With circle reconstructed from response operators 5-10
Figure 5.3: Steering machine dynamics 5-11
Figure 5.4: Block diagram of the complete simulated system 5-12
Figure 5.5: 30° course-changing manoeuvre 5-13
Figure 5.6: 15°/15° zig-zag manoeuvre 5-14
Figure 5.7: 15°/15° zig-zag manoeuvre 5-14
Figure 5.8: Bech's reverse spiral manoeuvre 5-15

Chapter 6

Figure 6.1: Fuzzy PD_like controller 6-2
Figure 6.2: Rudder sequence during course-keeping 6-3
Figure 6.3: Membership functions for the absolute value of the course error 6-6
Figure 6.4: Membership functions for the pulse width 6-6
Figure 6.5: Membership functions for the yaw rate 6-6
Figure 6.6: Surge velocity and yaw angle for a course-keeping in beam sea 6-7
Figure 6.7: Rudder angle and yaw rate for a course-keeping in beam sea 6-7
Figure 6.8: Surge velocity and yaw angle for a course-keeping in beam sea 6-8
Figure 6.9: Rudder angle and yaw rate for a course-keeping in beam sea 6-8
Figure 6.10: Input membership functions fired for e(t)=0.2 and ce(t)=-0.8 6-10

Figure 6.11: Model reference adaptive fuzzy autopilot 6-12
Figure 6.12: 30° course-changing manoeuvre 6-16
Figure 6.13: State variables and correction signals for the 30° course-changing manoeuvre 6-16
Figure 6.7: Sequence of course-changing manoeuvres 6-11
Figure 6.8: State variables and correction signals for the sequence of course-changing manoeuvres 6-11
Figure 6.14: Sequence of course-changing manoeuvres 6-18
Figure 6.15: State variables and correction signals for the sequence of course-changing manoeuvres 6-18
Figure 6.16: Heading and rudder angle for a step change in the surge velocity 6-19
Figure 6.17: State variables and correction signals for a step change in the surge velocity 6-19

Chapter 7

Figure 7.1: Direct adaptive neural controller 7-3
Figure 7.2: The indirect neural controller 7-4
Figure 7.3: Series-parallel identification schema 7-5
Figure 7.4: 20°/20° zig-zag manoeuvre. Solid line ship's non-linear model. Dotted line neural network model 7-5
Figure 7.5: NN_g mapping 7-6
Figure 7.6: $NN_{g^{-1}}$ mapping 7-6
Figure 7.7: A 10° course-changing manoeuvre. (x-axis time in seconds, y-axis degree) 7-8
Figure 7.8: A 30° course-changing manoeuvre. (x-axis time in seconds, y-axis degree) 7-9
Figure 7.9: Feed-back linearised system 7-11
Figure 7.10: Architecture for feedback linearisation 7-13
Figure 7.11: Course-keeping with linear quadratic controller (x-axis time in seconds) 7-14
Figure 7.12: Course-keeping with the non- linear controller (x-axis time in seconds) 7-14
Figure 7.13: Linear quadratic controller for initial surge velocity of 5 m/sec 7-15
Figure 7.14: Non-linear controller for initial surge velocity of 5 m/sec 7-15
Figure 7.15: Linear controller for initial roll rate of 0.2 deg/sec 7-16
Figure 7.16: Non-linear controller for the initial roll rate of 0.2 deg/sec 7-16
Figure 7.17: Structure of the identifier using radial basis network 7-24
Figure 7.18: Controller structure based on radial basis function network 7-24
Figure 7.19: Water's depth and hydrodynamics parameters 7-26
Figure 7.20: Heading and rudder angle for course-changing 7-27
Figure 7.21: Controller parameters, tracking and estimation error for the course-changing manoeuvre 7-27
Figure 7.22: Heading and rudder angle for the course changing manoeuvre 7-28
Figure 7.23: Heading and rudder angle for a dead-zone in the adaptive law 7-29
Figure 7.24: Controller parameters, tracking and estimation error for a dead-zone in the adaptive law 7-29
Figure 7.25: Heading and rudder angle for a step change in the surge velocity 7-31
Figure 7.26: Controller parameters, tracking and estimation error for a for a step change in the surge velocity 7-31
Figure 7.27: Heading and rudder angle for a surge velocity of 7 m/sec 7-32

Figure 7.28: Controller parameters, tracking and estimation error for a surge velocity of 7 m/sec 7-32
Figure 7.29: Heading and rudder angle for a course change manoeuvre without disturbances 7-33
Figure 7.30: Controller parameters, tracking and estimation error for the course change without disturbances 7-33

Appendix A

Figure A.1: Bode plot, turning rate/rudder angle A-6
Figure A.2: Bode plot, roll angle/rudder angle A-6
Figure A.3: $5^{\circ}/5^{\circ}$ zig-zag manoeuvre. Dotted linear model, solid non-linear model A-7
Figure A.4: $15^{\circ}/15^{\circ}$ zig-zag manoeuvre. Dotted linear model, solid non-linear model A-7
Figure A.5: 10° course-changing manoeuvre A-8
Figure A.6: 30° course-changing manoeuvre A-9
Figure A.7: 30° step response of the linear (dotted line_) and non-linear (solid line) model A-10

Chapter B

Figure B.1: Pierson-Moskowitz spectral density for different values of T and $h_{1/3}$ B-8
Figure B.2: Spectral density of the ship's induced motion B-10
Figure B.3: The ship in shallow water B-20

List of Tables

Chapter 4 Page

Table I: Motion terminology 4-3

Chapter 6

Table I: 49 rules base knowledge for the fuzzy controller 6-11

Table II: 121 rules base knowledge for the fuzzy controller 6-17

Appendix A

Table I: Containership main data A-1

Table II: Hydrodynamic coefficients for the containership A-2

Table III: Hydrodynamics parameters re-tuned to match the full scale experiments A-3

Table IV: Wind coefficients A-3

Glossary and Terms

The use of the same notation has tried to be avoided, however where the some notation is used in different presentations its correct meaning will be evident from the context it is used in.
If not otherwise specified in the particular context the following symbol assume the corresponding meaning:

δ	Rudder angle
ψ	Yaw angle
φ	Roll angle
$\dot{\psi} = r$	Yaw rate
p	Roll rate
u	Surge velocity
v	Sway velocity
τ	Time constant
NN	Neural Network approximator
θ	Parameters vector
∇	Gradient
e	Error
k	Time step
ζ	Wave amplitude
V_w	Wave velocity
ω	Frequency in radiant/second
ω_e	Encounter frequency
λ_w	Wave length
β	Wave encounter angle
T_w	Wave period
$h_{1/3}$	Significant wave height
S_ζ	Wave spectral density
S_{zz}	Spectral density of the ship induced motion
$R_{z\zeta}$	Response operators
V_{wind}	Wind velocity
S_w	Wind spectral density
χ_w	Wind encounter angle

Chapter 1 Introduction and overview

1.1 Introduction

This thesis investigates the applicability of *intelligent control systems* for the design of autopilots for ships. The main difficulty in defining what it is meant by *intelligent control* stems from the fact that there is not general agreement upon definitions for human intelligence and intelligent behaviour. One of the earliest definitions of "machine intelligence", is that by the British mathematician A. Turing. Turing was convinced that if a computer could do all mathematical operations, it could also do anything a person can do, which is still a highly controversial opinion. To argue from this position a criterion of intelligence was needed. Turing expressed this criterion as a test. The test is undertaken in the following manner: A person communicates with a computer through a terminal. When the person is unable to decide whether he/she is talking to a computer or another person, the computer can safely be said to possess all the important characteristics of intelligence. Turing was convinced that the building of such a machine was possible.

The Turing test clearly emphasises the external behaviours requested from a computer (or machine) to be safely defined as an intelligent machine. These external behaviours do not have to be distinguished from that of a human being and most importantly this has to happen from a human point of view (that is the observer). The problem of differentiating between an external manifestation of such behaviours and the internal mechanism that produces it, is also mentioned by (Zadeh, 1963) as the main reason why a clear definition of adaptation is still lacking.

The viewpoint adopted throughout the thesis is that *intelligent control* is the discipline that involves both artificial intelligence and control theory. The design of intelligent control systems should be based on the attempt to understand and duplicate some or part of the phenomena that ultimately produces a kind of behaviour that can be termed "intelligent", i.e. generalisation, flexibility adaptation etc. All these characteristics, to a differing extent are appreciated in what are recognised as intelligent species. For instance, when a virus is difficult to neutralise, it is usually labelled as an intelligent virus. This is also in accordance with the Turing experiment, where the intelligent classification of a machine is observer dependent.

In (Astrom and McAvoy, 1992), a very demanding definition of intelligent control is stated as follows: "An intelligent control system has the ability to comprehend, reason and learn about process, disturbances and operating conditions". Clearly with such a demanding definition, it appears that current control systems have a long way to go before they can qualify for this attribute. However, in the above paper a framework for intelligent control is discussed. For this purpose, a multidimensional space constituted by rules, objects and algorithms is introduced. Each artificial intelligent technique therefore, is seen as a subspace where the appropriate combination of the different attributes is defined. It is argued then, that in designing intelligent control systems the goal should be to locate the appropriate region where the intersection of fundamental attribute is achieved in an optimal way. In other words, the designer has to decide, based on her/his experience of the problem, about the combination of different design techniques that will lead to the attainment of the control objects. From this point of view, the design of intelligent control can be reduced to the combination of different techniques for the purpose of achieving more sophisticate and reliable control systems. This is probably why traditionally, intelligent control has embraced classical control

theory, neural networks, fuzzy logic and a wide variety of search techniques (i.e. backpropagation, genetic algorithms simulated annealing etc.). Based on this point of view, the theoretical foundation of intelligent control system can be found at the intersection of disciplines like cybernetic artificial intelligence and informatics (Zi-Xing, 1997). Adaptive neurofuzzy control is such an example, where ideas germinated in the field of neural networks are used for the design of optimal fuzzy logic based controllers.

1.2 Autopilots for ships: brief overview

1.2.1 Earlier approaches

The introduction of automatic autopilots for steering a ship can be traced back to the 1922 with the pioneering work of (Sperry, 1922) and (Minorsky, 1922). According to (Bennet, 1979), the major contribution of Sperry, compared to the simple proportional autopilots proposed by other inventors of the time, was the inclusion of a derivative term in the control law. In fact, as emphasised in (Bennet, 1979), Sperry observed that an experienced helmsman would also, "meet" the helm, that is, back off the helm and put it over the other way to prevent the angular momentum of the ship carrying it past the desired heading. Therefore he proposed the use of an "anticipator" to build into his autopilot the "intuition" of an experienced helmsman. The name "Metal-Mike" given to the new automatic system by an officer of the ship which had been used for the trials, emphasis both the purpose (replace the helmsman) and the origin of the proposed system. Apparently, Sperry went further and argued that the amount of "anticipation" should be proportional to the overshoot which would occur in the absence of the "anticipator". Since this overshoot will vary for different sailing conditions he proposed

a mechanism to adjust the amount of anticipation. However, it is not certain whether or not the full "adaptive" mechanism was included in the commercial production of Metal-Mike.

Minorsky's contribution was of more theoretical basis. He was interested in solving the problem of controlling the motion of a ship analytically rather then practically (Minorsky, 1922). With respect the linearised equation of motion (Bennet, 1979):

$$\frac{Ad^2\alpha}{dt^2} + \frac{Bd\alpha}{dt} + K\rho = D \tag{1.1}$$

where A is the moment of inertia of the ship, B is the viscous damping coefficient, K is a constant, α is the heading error, ρ is the rudder angle and D is the disturbances force, he argued that the control problem is completely solved when the rudder angle ρ and its derivative are obtained as a function of α. He proposed several methods of regulation, one of this is expressed by equation (1.2):

$$\frac{d\rho}{dt} = m_1\alpha + n_1\frac{d\alpha}{dt} + p_1\frac{d^2\alpha}{dt^2} \tag{1.2}$$

which nowadays is the celebrated proportional-integral-derivative (PID) controller. Minorsky went further and by substituting (1.2) into (1.1) he managed, by applying the Hurwitz theorem, to find the condition under which the motion of the controlled ship is stable. According to (Bennet, 1979) this was the first theoretical analysis of a control system.

1.2.2 Classical approaches

Subsequent enhancements of the autopilot proposed by Minorsky were the inclusion of a limiter in order to prevent rudder saturation. A dead band and a filter were also included in order to smooth the control effort preventing calls from not compensative disturbances (i.e. high frequency yaw motion due to waves). Manual adjustment of the PID parameters was introduced in order to account for the different sailing conditions (i.e. different load, speed and weather conditions). To this aim a suitable terminology close to the mariner was developed, so that typical autopilots posses the Rudder Action button to regulate the proportional action, the Counter Rudder button to regulate the derivative control action and the Automatic Permanent Helm to regulate the integral action. In addition to the above buttons, for preventing rudder angle saturation and excessive rudder movement the two buttons Rudder Limit and Weather were introduced, regulating respectively the maximum rudder angle allowable and the dead-band width.

Mainly due to its relatively simplicity, these kinds of autopilots dominated the scenario until the early 1970s. Although the use of an appropriate nomenclature made the manual setting of the autopilot parameters much more suitable for non control experts, such as crew members, the impetus to move towards a more sophisticated autopilot, can be explained by the need to maintain optimal performance in all different sailing conditions. In fact, the optimal achievement of the two main steering modes of an autopilot, namely course-keeping and course-changing, can be properly defined only with respect a particular sailing conditions. For instance, with respect the course-keeping mode of operation, the autopilot has to select the best trade-off between precision (which will minimise the elongation of the sailed distance) and control effort

(rudder movement, which will produce additional drag force and consequent loss of speed and increase of fuel expenditure). However, this trade-off is not always the same and more importantly is difficult to be deduced heuristically by crew members. In different sailing conditions a different priority (or weight) can be assigned to the precision and control effort. For instance, when the ship is sailing in restricted water precision is of main concern, while in open sea fuel consumption is of major interest.

The most popular approach for dealing with the above mentioned autopilot demands, was the Linear Quadratic (LQ) Controller, in which the controller parameters are selected in order to satisfy certain optimal criteria expressed as a quadratic cost function. Different cost functions taking into account yaw and rudder deviation, fuel consumption, etc., were proposed (Norrbin, 1972), (Broome *et al*, 1980). Although the LQ technique fits very nicely in the formulation of the ship's course-keeping control problem and appeared to be robust for parameter changes, other researchers were investigating the applicability of adaptive control techniques such as model reference (Honderd and Winkelman, 1972), (Amerongen and Udink Ten Cate, 1975) or self-tuning adaptive controller (Kallstrom *et al*, 1979), (Brink *et al*, 1978), which are much appropriate for the formulation of the ship's course-changing problem. In parallel to the adaptive approach, where the controller parameters are constantly adjusted in order to seek the optimum of a cost function, robust methods were applied in the attempt to find the set of control parameters able to guarantee acceptable performances in a wide range of operation conditions, (Grimble and Katebi, 1999), (Katebi *et al*, 1987).

1.2.3 Intelligent approaches

Prompted by advances in computing technology, more sophisticated control algorithms became applicable. Neural networks and fuzzy logic paradigms, represents the most popular of these approaches, where the principle aim in the controller design is to emulate some intelligent behaviours such as learning and adaptation.

The most popular neural network structure used to solve the ship autopilot design problem is the multilayer perceptron network with the back-propagation algorithm. Different controller structures such as supervised control, direct inverse control, indirect and direct controls were employed for training the controller parameters (Hearn *et al*, 1997). An alternative possibility is to train the same neural network for different operating conditions in such a way that while in a particular situation the neural controller can extrapolate the proper control actions (Burns and Richter, 1995). In (Balasuriya and Hoole, 1995) it is shown how a feedforward neural network can be trained, in a supervised fashion using the back-propagation algorithm. The contribution of the paper is that the training data are collected from manoeuvres performed by an helmsmen. It is concluded therefore, that the proposed feedforward neural network is able to reproduce the behaviours of a skilled helmsman. The feedforward neural network can also be used to solve the multivariable problem. In (Tiano *et al*, 1994) it is shown how a rudder roll damping controller can be trained using back-propagation.

One of the first autopilot designed with fuzzy set theory was presented in (Amerongen *et al*, 1977). The proposed autopilot was using two different inputs with five linguistic variables and a fixed rule base. It was shown that compared to a PID controller the proposed fuzzy autopilot showed a significantly enhanced performance in a noisy

environment with fewer rudder calls. However, the tuning of the fuzzy controller parameters was based on an extended trials and error procedure. A different application of fuzzy set theory was pursued in (Sutton, 1987) were fuzzy logic is proposed and used to design a cognitive model of a helmsman. Following this work it was argued that the fuzzy system so achieved could have been used to replace the helmsman. However, it seemed that in order to guarantee acceptable performances in different operating conditions, the proposed controller needed further adjustment. This led to different adaptation and learning structures. One of these is the self-organising controller proposed in (Sutton and Jess, 1991). Usually, the problem of parameter optimisation for a fuzzy controller has been addressed in the framework of neural networks where back-propagation algorithm has been used (Sutton *et al*, 1997) or in the general framework of optimisation theory (Sutton and Marsden, 1997). However, all of the above optimisation approaches are based on the similarity between neural networks and fuzzy systems when the latter are described in the framework of adaptive networks.

All of the papers cited in section 1.2.3, shown the possibility to pose and solve the autopilot design problem in the framework of intelligent control theory. However, none of them addresses the problem of stability of the overall system and more importantly all of them rely on a heavy computational effort to guarantee the proper learning of the controller. At the present the last points represent the two main drawbacks of intelligent autopilots. It is argued that, until these two issues are properly addressed and solved, the design of intelligent autopilots for ships cannot be fully developed.

1.3 Steering criteria for course-changing and course-keeping

As mentioned in the previous section, the definition of optimal performance criteria, for the design of autopilots is not always a trivial task. There may be conflicting objectives for a particular sailing condition. In this respect, for the design of ship's autopilots, traditionally it has been distinguished between two main modes of operating, *course-changing* and *course-keeping*.

Course-keeping: In the course-keeping mode of operating, the control system has to maintain a fixed direction of sailing, compensating for the different external environmental disturbances (i.e. wind, waves and current). The controller has to select the best trade-off between precision (which will minimise the elongation of the sailed distance) and control effort (rudder movement, which will produce additional drag force and consequent loss of speed). It seems natural therefore, to formulate this control design problem in the framework of Linear Quadratic optimal theory, where the cost function to be optimised can be expressed as follows:

$$J = \frac{1}{T}\int_0^T \left(\varepsilon^2 + \lambda\delta^2\right)dt \tag{1.3}$$

where $\varepsilon = (\psi_d - \psi)$ denote the heading error, δ is the rudder angle and λ is a weighting factor. (Koyama, 1970), first proposed equation (1.3) for the solution of the course-keeping control problem. In equation (1.3), the term ε^2 translates the elongation of the distance due to course errors into a loss of speed, while δ^2 account for the increased resistance introduced by the rudder motion. The proper choice of the weighting factor is made with the aid of full scale experiments or model based tests,

however Koyama and further (Norrbin, 1972) proposed values for λ based on two different analytical approaches. Koyama considered that the loss of speed is mainly due to the increased distance to be sailed and to the rudder motion. Based on this hypothesis he suggested values of λ approximately between 8 and 10. Norrbin totally neglected the contribution on the loss of speed from course errors and elongation of the sailed distance. He considered the loss of speed mainly due to the increased resistance of the rudder movement and to the centrifugal force. As shown in (Blanke M. 1981), the relative increase in drag and in path elongation due to steering should be expressed as:

$$\frac{\Delta R}{R} = -\frac{1}{T}\int_0^T \left(\begin{bmatrix} v & r & \varepsilon \end{bmatrix} \begin{bmatrix} 0 & \mu & 0 \\ \mu & 0 & 0 \\ 0 & 0 & \gamma \end{bmatrix} \begin{bmatrix} v \\ r \\ \varepsilon \end{bmatrix} - \lambda\delta^2 \right) dt \tag{1.4}$$

where μ, γ and λ are positive numbers. (On page 250 of Blanke thesis the sign of the terms $\lambda\delta^2$ is incorrect. The correct form is as above.)

The above criterion expresses the work necessary to bring the ship from an initial state vector $\begin{bmatrix} v & r & \varepsilon \end{bmatrix}^T$ to the zero state vector. This is the integral over time of the added resistance plus the contribution from the elongation of the path sailed due to the heading error. It is worth noting that the existence of an optimal state feedback control law is not affected by the weighting matrix being negative defined.

Although the cost function expressed by equation (1.4) has a strong physical motivation, its minimisation involves three weighting factor μ, γ and λ to be assessed. As pointed out in (Kallstrom and Norrbin, 1980) the proper choice of the weighting factors can be properly done with the aid of sea or model based trials. For this reason

the Koyama criterion given in equation (1.3), which by far is easier to be assessed, has received more attention for the autopilot design.

Course-changing: During a course-changing manoeuvre the heading angle of the ship, is changed in such a way that the ship can sail in the new direction specified by a new (desired) heading angle. Although the purpose is still to change the sailing direction, according to the actual circumstances this manoeuvre can be performed in different way i.e. by minimising the overshoot of the manoeuvre or by maximising the settling time. In any case, as discussed in (Amerongen and Naute Lemke, 1980), this kind of manoeuvre can be described by the step response of a second order linear system with transfer function:

$$\frac{\psi(s)}{\delta(s)} = \frac{\omega_m^2}{s^2 + 2\xi\omega_m s + \omega_m^2} \tag{1.6}$$

From this response, shown in figure 1.1, it is possible to distinguish three different phases of the manoeuvre as: 1) the start of the manoeuvre, where for safety reasons, the intention of the manoeuvre must be clearly indicated to others ships, 2) a stationary turning, characterised by a constant slope (turning rate), and 3) the end of the manoeuvre, where again for safety reasons it is important to be able to control the overshoot in order to avoid dangerous paths. The realisation of each of the three phases, will depend upon the particular situations, for instance in the stationary phase, the roll angle induced by the rudder rate can be kept under certain values. Alternatively, if in restricted water, the turning radius should be minimised, but in any cases the optimal parameters of the desired manoeuvre (equation (1.6)) should be chosen keeping in mind the dynamics of the particular ship.

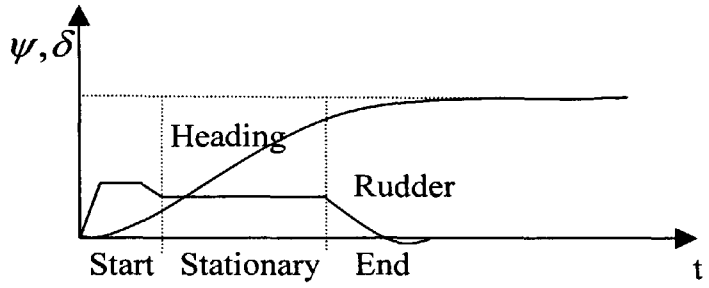

Figure 1.1: Course changing manoeuvre

Having represented the desired manoeuvre as the response of a second-order transfer function, the design of the autopilot for course-changing manoeuvre, can be formulated in the framework of the model reference control approach. Model reference adaptive technique can be used to automatically tune the resultant controller parameters to account for the different sailing conditions (Amerongen, 1982).

1.4 Adaptive approach: objectives and motivations

During the last twenty years the fields of artificial neural networks and fuzzy logic systems have witnessed a growing interest in control applications (Hunt *et al*, 1992) (Sugeno, 1985). The primary characteristic that rendered these systems attractive, is the fact that under certain conditions, the parameters of the network can be adjusted from input/output data. This has led to the use of such systems, under different conditions of uncertainties, as adaptive or learning systems. As pointed out in (Farrell and Baker, 1996), the main difference between an adaptive system and a learning one relies on the spatial emphasis of the later in the approximation of the functional mapping representing the controller. In fact, adopting the viewpoint of approximation theory, the controller design reduces to finding an appropriate functional mapping from the measured and desired system's output, to a control action that will produce a satisfactory

behaviour of the closed-loop system. A control system that, during functional approximation, treats every distinct operating situation as a novel one is limited to adaptive operation, whereas a system that correlates past experiences with past situations, and that can recall and exploit those past experiences, is capable of learning (Baker and Farrell, 1992).

Although a comprehensive definition of an adaptive system is still lacking, the emphasis in the above distinction is in the two different behaviours required by an intelligent controller. For instance, the compensation of external disturbances, achieved by local optimisation, does not account for unmodelled dynamics, which require a global optimisation approach. A well-known drawback of adaptive systems is their relatively slow transient response, due partially to the fact that they do not exploit past experience. For example, in the presence of time invariant non-linearities not accounted for in the controller structure, the adaptation process will not converge. Recent work in this respect by (Narendra and Balakrishnan, 1997), consider the use of multiple models with switching criteria in order to guarantee a good initialisation of the adaptive system for every different operating conditions. The choice of models, either fixed or adaptive, with different orders accounts for parameter uncertainties as well for structural uncertainties. In this respect, the use of multiple models introduces the spatial emphasis of learning algorithm mentioned in (Farrell and Baker, 1996).

Traditionally, the design of adaptive control systems, as introduced in (Astrom and Wittenmark, 1995), deals primarily with the problem of controlling a plant in the presence of structural or parametric uncertainty. The approach to follow in designing such systems is not unique and mostly will depend upon the kind and the degree of uncertainty presents in the problem definition.

One of the earlier definitions of adaptive systems, introduced by (Bellman and Kalaba, 1959), outline the adaptive process as the last of three stages in the evolution of control process. According to Bellman and Kalaba, the first stage of the control process, appears when the plant to be controlled is fully characterised and the controller has complete information about its signals. In this situation the control process is labelled to be a *deterministic control process*. When unknown factors, such as noise or parameters uncertainty are present in the process and they appear mathematically characterised by random variables with known spectral density, the control process is labelled as a *stochastic control process.* Finally, when even less information about the uncertainty is available and the controller has to learn how to improve its performances by input/output measurements the control process is labelled as an *adaptive control process.*

The adaptive control process definition given above is entirely qualitative and though it states when an adaptive controller has to be used, it does not give any information about the extent of uncertainty that the system is able to manipulate. Even in less rigorous definitions, especially those borrowed from biological fields where *adaptation* i.e. is defined as "an advantageous conformation of an organism to changes in its environment", the appreciation of truly adaptive behaviour of a plant is not well understood. An example of adaptive definition which clearly germinates from that used in biology is given by Eveleigh 1967 (as described in (Narendra and Annaswamy, 1989) page 9). "An adaptive system is a system which is provided with a means of continuously monitoring its own performance in relation to a given figure of merit or optimal condition and a means of modifying its own parameters by a closed-loop action so as to approach this optimum".

With respect to the last definition, it is difficult even to distinguish between a conventional feedback controller and an adaptive one, since the former may also be considered as a controller that monitors its behaviour for improving the overall system's performances. According to (Zadeh, 1963), the difficulty in finding a comprehensive definition of adaptivity, relies on the lack of clearly differentiating the *external manifestation* of adaptive behaviours and the *internal mechanism* by which the adaptivity is achieved. By concentrating on the former Zadeh gave the following definition of adaptation.

> "Denoting with S a system, with P its performances and with W the set of acceptable performance. Specifying with $\{S_\mu\}$ the family of function which the system is subjected to and with P_μ the correspondent performances, the system S is said to be adaptive with respect to $\{S_\mu\}$ and W, if it performs acceptably well with every source in the family $\{S_\mu\}$, that is $P_\mu \in W$. In other words, S is adaptive with respect to $\{S_\mu\}$ and W if it maps $\{S_\mu\}$ into W. "

Although this definition clearly states what is demanded from an adaptive system, literally map $\{S_\mu\}$ into W, it is clear that by a proper choice of the family $\{S_\mu\}$ and the set W, any system can be adaptive. In fact, it is well known that if a feedback linear time invariant system is stable in x_0, then it is also asymptotically stable in some neighbourhood of x_0. This may answer the question whether a feedback system is also adaptive or not. Moreover, the definition given by Zadeh, is similar to the definition used for *robust* systems.

According to (Narendra and Annaswamy, 1989) and (Landau, 1999) the difficulty in clearly distinguishing between adaptive behaviours and robustness is due to the present limitation encountered in the non-linear analysis. This fact is particularly true if it is bare in mind that, no matter how complex an adaptive systems is, it can be seen merely

as a feedback system where the two steps of identification and control are repeated according to the circumstances. The difficulty in analysing such systems lie on the fundamental fact that a subset of the system's parameters are adjusted according to an adaptation law, making them (these parameters) part of the state variable for the successive step of control. Finally, the complexity of the adaptation law increase when the family $\{S_\mu\}$ (introduced in the above definition of Zadeh) is enlarged and the set W is reduced.

Because of the above mentioned difficulties, at the present day, the analysis and synthesis of adaptive systems is generally restricted for linear plants with unknown parameters. While the overall control system is non-linear, its behaviour asymptotically approaches that of a linear time invariant system.

Landau in (Landau, 1999), speculates about the relationship and similarity that adaptive and robust system gained during the last decade. The advance in closed loop identification methods recently used to enhance the performance of robust controllers is one of the examples where the two approaches are merged for better performance achievement (Landau and Karini, 1997a) (Landau and Karini, 1997b). The successful use of supervisory control (or model-switching) as a way to ensure good adaptation transients, in the presence of large parameters change, is another example where the two control design techniques share common results (Morse *et al*, 1992) (Narendra *et al*, 1995). Although these recent examples shown that a unified treatment of the robust and adaptive approaches will clearly produce some advantages in the achievement of better control systems, the two approaches in the classical control literature are treated separately. It is believed, that, when a more comprehensive theory for the analysis and

synthesis of non-linear time variant systems is established, the gap between robust and adaptive approach will be bridged.

The motivations for using an adaptive control approach for the design of ship motion control systems, is primarily related to the considerable changes in the dynamical response that a ship manifests with respect to different sailing conditions (i.e. speed, load trim and weather conditions). Motivated by the need to guarantee acceptable performances in divers operating conditions, different adaptive autopilots have been proposed. In (Amerongen and Udink Ten Cate, 1975) is emphasised how, in a certain range of depth of water, ships with a poor course stability characteristic can even become course unstable. An adaptive autopilot, based on model reference technique, that can cope with such situations ensuring course stability for all ranges of water depth is therefore proposed. In (Kallstrom *et al*, 1979) two adaptive autopilot based on velocity scheduling and self tuning regulator for course-keeping and high gain turning regulator are proposed. These autopilots are proved to work excellently under different load, speed and weather conditions. In (Tiano *et al*, 1980) an extended self-tuning controller that minimises a preset cost function, whose form depends on the operational situations and the environmental conditions is proposed and tested for different ships. All the simulation results indicated that the proposed autopilot is a feasible and efficient solution for the automatic steering of ships in different sailing conditions. In (Fortuna and Muscato, 1996), an adaptive Linear Quadratic controller is proposed for the compensation of the waves induced roll motion for a high-speed passenger monohull ship. The results obtained both by see trials and computer simulation revealed the superior performance that can be achieved by the adaptive approach compared to traditional lead-lag compensator. Finally (Astrom, 1980) presents an analytical analysis describing why it is beneficial to use adaptive controllers for the design of ship's

autopilots. Although the analytical treatment is based on the linear theory, it still gives the flavour and motivation of why adaptive techniques should be used. It is shown that indeed it is possible to design a constant gain controller which guarantees stability for the different sailing conditions, but at the cost of poor performance. An adaptive approach, where the gain is automatically tuned to optimise a performance function, is therefore desirable.

1.5 Structure of the thesis

The structure of the remainder of the thesis follows broadly that of this chapter. Prompted by advances in computing technology and motivated by the need to produce more efficient ship control systems, the design of course-changing and course-keeping autopilots in the framework of intelligent control theory (as defined in section 1.1) is investigated. The aim and contribution of the thesis, is to exploit the adaptation and learning properties of intelligent paradigms based on neural networks and fuzzy logic systems for an efficient solution of the ship autopilots control design problem. The latter properties are studied in the framework of adaptive control theory, where well-known results can be adopted and applied to the particular case. The advantages of fuzzy algorithms, in easily representing and exploiting heuristic knowledge will be also discussed. However, all the proposed control algorithms have their foundation in the control theory framework where the analytical analysis of the proposed control algorithms will be attempted. In particular it is shown how this can be achieved within the framework of linear adaptive theory, when some constraint on the structure of the autopilots is fulfilled.

The outline of the thesis is as follows:

Chapter two presents a review of neural networks and fuzzy logic based systems. As stated in the introduction these systems represent the major tools on which intelligent controllers are based. Chapter three describes the framework of adaptive networks, where neural networks and fuzzy logic systems are described in a unified fashion. This will allow comparisons and similarities between the control algorithms based on neural networks and fuzzy logic systems that are presented in Chapters six and seven. In particular in the former Chapter it is emphasised the major difference between neural network and fuzzy logic system and how fuzzy set theory can be used advantageously for the design of autopilots for ships. Chapters four and five, describes respectively, the ship's dynamics, and the mathematical model of a containership used during the simulation of the proposed control algorithms. Finally, Chapters eight summarises the conclusions and highlights some recommendation for future work.

In appendix A the main data of the containership are given while appendix B describes the environmental disturbances and their analytical description. Appendix C gives the analytical proof of the stability of the intelligent autopilot presented in Chapter 7. Finally appendix D gives the papers which are related to the work of this thesis.

The work carried out in the course of this thesis has produced the following contributions.

- A working definition of intelligent systems is given.
- Neural Networks and Fuzzy Inference Systems are described under a unifying theory.
- A comparison between Radial Basis Function and Multilayer Perceptron Networks is given.
- Software for the implementation of the non-linear model of a containership was designed.

- A description in the frequency domain of the rudder sequence used for the course-keeping control problem is presented.
- The use of the indirect method of adaptation for the autopilot implemented with Mltilayer Perceptron Networks within the comparison with the direct method of adaptation.
- The proposition of a different controller structure for which the on-line implementation of the control algorithm can be guarantee.
- Sufficient conditions under which a detailed analysis of the closed-loop systems performance can be made and stability of the overall system can be proved.
- Conditions under which the proposed control structure can be implemented either with Fuzzy Inference systems as well as with Neural networks.

The following list of papers relate directly with the work presented in this thesis and they have been or are accepted for publication.

Journal paper

A. Zirilli, G.N. Roberts, A. Tiano and R. Sutton, "Adaptive Steering of a containership based on Neural Networks". Accepted for publication in International Journal of Adaptive Control and Signal Processing, January 2001

Conference papers

ZIRILLI, A., ROBERTS, G., TIANO, A. and SUTTON, R. 1999. A model-reference neural autopilot for ships. IMarE Conference: Computers and Ships, London. pp 25-35

ZIRILLI, A., ROBERTS, G.N., TIANO, A. and SUTTON, R. 1999. A Neuro-Fuzzy Model Reference Autopilot for Ships. Twelfth ship control systems symposium. The Hague, Netherlands.

ZIRILLI, A., ROBERTS, G.N., TIANO, A. and SUTTON, R. 2000. An adaptive autopilot for ships based on neural networks controller. International Conference & Exhibition on Gearing, Transmissions and Mechanical Systems. 3-6 July 2000, Nottingham, UK. Pp.493-502

ZIRILLI, A., ROBERTS, G.N., TIANO, A. and SUTTON, R. 2000. An adaptive Fuzzy autopilot for a containership. 5th IFAC Conference on Manoeuvring and Control of Marine Craft. 24-27 August 2000 Aalborg University, Denmark. pp 317-322

ZIRILLI, A., ROBERTS, G.N., TIANO, A. and SUTTON, R. 2000. Feedback-linearisation controller based on neural networks for the course-keeping problem of a containership. UKACC International Conference, Control 2000, 4-7 September University of Cambridge, UK.

1.6 Reference List

Amerongen, J. van 1982. *Adaptive Steering of Ships: A model-reference approach to improved manoeuvring and economical course keeping.* Husdrukkerij, Delft University of Technology. Ph.D. Thesis.

Amerongen, J. van,Naute Lenke, H. R., and Veen der van, J. C. T. 1977. *An autopilot for ships designed with fussy sets.* Proc. IFAC Conference on Digital Computer Applications to Process Control. pp. 479-487, The Hauge.

Amerongen, J. van, and Udink Ten Cate, A. J. 1975. Model reference adaptive autopilots for ships. *Automatica,* **11**, pp. 441-449.

Amerongen, van J., and Naute Lemke, van H. R. 1980. *Criteria for optimum steering of ships.* Proc. Ship Steering Automatic Control. pp. 3-22, Genova.

Astrom, K. J. 1980. Why Use Adaptive Techniques for Steering Large Tankers. *International Journal of Control,* **32** (4), pp. 689-708.

Astrom, K. J, and McAvoy, T. J. 1992. Intelligent control: an overview and evaluation. *In:* David A. White and Donald A. Sofge ed. *Handbook of Intelligent Control.*

Neural, Fuzzy and Adaptive approaches. Van Nostrand Reinhold. New York, pp. 3-34.

Astrom, K. J., and Wittenmark, B. 1995. *Adaptive Control* . 2nd ed. Addison-Wesley. 0-201-55866-1.

Baker, W. L., and Farrell, J. A. 1992. An introduction to connectionist learning control systems. *In:* David A. White and Donald A. Sofge ed. *Handbook of Intelligent Control: Neural, fuzzy and adaptive approaches.* New York: pp. 35-64.

Balasuriya, B. A. A. P., and Hoole, P. R. P. 1995. *Feedforword neural network controller for ship steering.* Proc. of the 3th IFAC Workshop on Control Applications in Marine Systems. CAMS '95. pp. 400-404, Trodheim, Norway.

Bellman, R., and Kalaba, R. 1959. On adaptive control processes. *IRE Transactions on Automatic Control,* **4**, pp. 1-9.

Bennet, S. 1979. *A history of control engineering 1800-1930.* The Institution of Electrical Engineers. 0-906048-07-9.

Blanke, M. 1981. *Ship Propulsion Losses related to Automated Steering and Prime Mover Control.* Ph.D. Thesis, The Technical University of Denmark, Lyngby.

Brink, A. W.,Baas, G. E.,Tiano, A., and Volta, E. 1978. *Adaptive automatic course-keeping control of a supertanker and a container ship: a simulation study.* Proc. 5th Ship Control Systems Symposium Vol. 4. Annapolis.

Broome, D. R.,Keane, A. J., and Marshall, L. 1980. *The effect of variations in ship operations on an adaptive autopilot.* Proc. Ship Steering and Automatic Control. pp. 77-95, Genova.

Burns, R., and Richter, R. 1995. *The application of neural networks for the control of small and large vessels.* Proc. of the 3th IFAC Workshop on Control Application in MArine Systems. CAMS '95. pp. 393-399, Trondheim, Norway.

Farrell, J., and Baker, Walter 1996. Learning Control Systems: Motivation and Implementation. *In:* Madan M. Gupta and Naresh K. Sinha ed. *Intelligent Control Systems, Theory and Applications. (Chapter 17).* New York: IEEE Press.

Fortuna, L., and Muscato, G. 1996. A Roll Stabilization System for a Monohull Ship: Modelling, Identification and Adaptive Control. *IEEE Transactions on Control Systems Technology,* **4** (1), pp. 18-28.

Grimble, M. J, and Katebi, M. R. 1999. *Robust Ship Autopilot Control System Desing.* 12th Ship Control Systems Symposium Vol. II. The Hague, The Netherlands.

Hearn, G. E.,Zhang, Y., and Sen, P. 1997. *Alternative designs of neural network based autopilots: A comparative study.* 4th IFAC Conference on Manoeuvring and Control of Marine Craft. MCMC '97. pp. 54-59, Brijuni, Croatia.

Honderd, G., and Winkelman, J. E. 1972. *An Adaptive Autopilot for Ships.* Proc. 3rd Ship Control Systems Symposium Vol.2. Bath.

Hunt, K. J.,Sbarbaro, D.,Zbikowsky, R., and Gawthrop, P. J. 1992. Neural Networks for Control Systems - A survey. *Automatica,* **28** (6), pp. 1083-1112.

Kallstrom, C. G.,Astrom, K. J.,Thorell, N. E.,Eriksson, J., and Sten, L. 1979. Adaptive autopilots for tankers. *Automatica,* **15**, pp. 254-284.

Kallstrom, C. G., and Norrbin, N. H. 1980. *Performance criteria for ship autopilots: An analysis of shipboard experiments.* Proc. Ship Steering Automatic Control. pp. 23-41, Genoa.

Katebi, M. R.,Wong, D. D. K., and Grimble, M. J. 1987. *LQG autopilot and rudder roll stabilisation control system design.* Proc. 8th Ship Control Systems Symposium Vol.3. pp. 69-84, The Hauge, The Netherlands .

Koyama, T. 1970. On the optimum automatic steering system of ships at sea. *Selected papers from: Journal Society of Naval Architect of Japan,* **4**, pp. 142-156.

Landau, I. D. 1999. From robust control to adaptive control. *Control Engineering Practice,* **7**, pp. 1113-1124.

Landau, I., and Karini, A. 1997a. An output error recursive algorithm for unbiased identification in closed loop. *Automatica,* **33** (5), pp. 933-938.

Landau, I., and Karini, A. 1997b. Recursive algorithms for identification in closed loop-a unified approach and evaluation. *Automatica,* **33** (8), pp. 1499-1523.

Minorsky, N. 1922. Directional Stability of Automatically Steered Bodies. *Journal of*

American Society of Naval Engineers, **34**, pp. 280 309.

Morse, A. S.,Mayne, D. Q., and Goodwin, G. C. 1992. Applications of Hysteresis Switching in Parameter Adaptive Control. *IEEE Transactions on Automatic Control,* **37** (9), pp. 1343-1354.

Narendra, K. S., and Annaswamy, A. M. 1989. *Stable Adaptive Systems.*

Narendra, K. S.,Balakrishnam, J., and Ciliz, M. K. 1995. Adaptation and learning using multiple models, switching and tuning. *IEEE Control System Magazine,* pp. 37-51.

Narendra, K., and Balakrishnan, S. 1997. Adaptive control using multiple models. *IEEE Transaction on Automatic Control,* (AC-42), pp. 171-187.

Norrbin, N. H. 1972. *On the added resistance due to steering on a straight course.* Proc. 13th International Towing Tank . pp. 282-408 Vol.1, Berlin.

Sugeno, M. 1985. *Industrial applications of Fuzzy Control.* Elsevier Science Pub.: New York.

Sutton, R. 1987. *Fuzzy set models of the helmsman steering a ship in course-keeping and course-changing modes.* University of Wales Institute of Science and Technology, Cardiff. Ph.D. Thesis.

Sutton, R., and Jess, I. M. 1991. A design study of a self-organizing fuzzy autopilot for ship control. *Proc. INstitution Mechanical Engeneerings,* **205**, pp. 35-47.

Sutton, R., and Marsden, G. D. 1997. A fuzzy autopilot optimized using a genetic algorithm. *Journal of Navigation,* **Vol 50** (No 1), pp. pp 120-131.

Sutton, R., Taylor S.D.H. and Roberts, G. N. 1997. Tuning Fuzzy ship autopilot using artificial neural networks. *Transactions of The Institute of Mesurement and Control,* **19** (2), pp. 94-106.

Tiano, A.,Mort, N.,Derradji, D. A.,Cuneo, M.,Ranzi, A., and Zhou, W. W. 1994. *Rudder Roll Stabilisation by Neural Network-Based Control Systems.* Proc. 3rd Int. Conferenc on MAnoeuvring and Control of Marine Craft. MCMC '94. pp. 33-44,

Tiano, A.,Volta, E.,Brink, A. W., and Verbruggen, T. W. 1980. *Adaptive control of large ships in non-stationary conditions -a simulation study-.* Proc. Ship Steering and Automatic Control. pp. 189-209, Genoa.

Zadeh, L. A. 1963. On the definition of adaptivity. *In Proceeding of the IEEE,* **51**, pp. 569-570.

Zi-Xing, Cai 1997. *Intelligent Control: Principles, Techniques and Applications.* Singapore: World Scientific Publishing Co. Pte. Ltd. 981-02-2564-4.

Chapter 2 Neural networks and Fuzzy logic systems

2.1 Introduction

This chapter introduces neural networks (NN) and fuzzy logic (FL) based systems. After a brief introduction the description of these systems is focused on those particular structures that are used for control purposes. In fact as stated in the previous chapter regardless of the definition of intelligent systems, NN and FL can be seen as the traditional tools used for the design of intelligent controllers.

In section 2.2, after a brief introduction on artificial neural networks, the perceptron network, the multilayer perceptron network, radial basis function network and the cerebellar model articulated controller are described in some details. These particular neural network configurations are in fact present in a wide range of control applications. At the end of the section, a brief comparison between multilayer perceptron networks and radial basis function networks is addressed.

In section 2.3, fuzzy systems used for control applications are presented. Each block component of a fuzzy logic system is described in its purpose and mathematical formulation. Two particular fuzzy systems used in control applications, namely the Mamdani and the Sugeno fuzzy model, are presented at the end of this section.

Section 2.4 finally summarises the chapter.

2.2 Artificial Neural Networks

An artificial neural network (ANN or simply NN), is a massively parallel connected network, the structure of which is mainly inspired by the human biological neural system. Historically, much of the inspirations for the field of NNs came from the desire to produce artificial systems capable of sophisticated, perhaps "intelligent", computations similar to those that the human brain routinely performs. The basic element of artificial neural networks is the neuron, which represents a very simple model of the neuron of the human brain. Figure 2.1 shows a schematic representation of biological neurons. In this figure the four main parts of the neuron, (dendrites, cell body, synapses and axon) are specified.

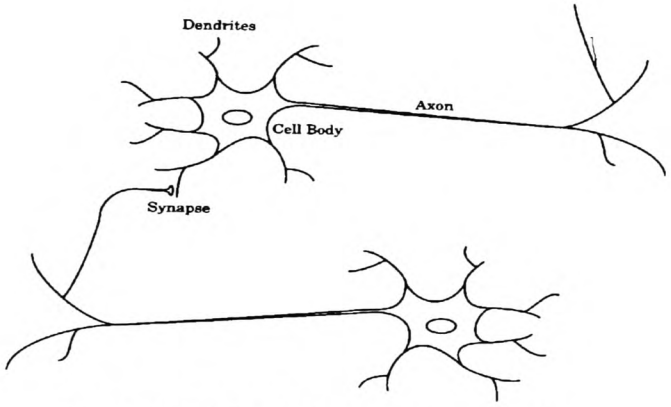

Fig. 2.1: Biological neuron structure

The dendrites are tree-like receptive networks of nerve fibres that carry electrical signals into the cell body. The cell body, effectively sums and thresholds these incoming signals. The axon is a single long fibre that carries the signal from the cell body out to other neurons. The point of contact between the axon of one cell and a dendrite of another cell is called synapse. It is the arrangement of neurons and the strengths of the individual synapses, determined by a not well-know complex chemical process that establishes the function of the neural network.

A block diagram representing the simplified biological neuron is shown in figure 2.2.

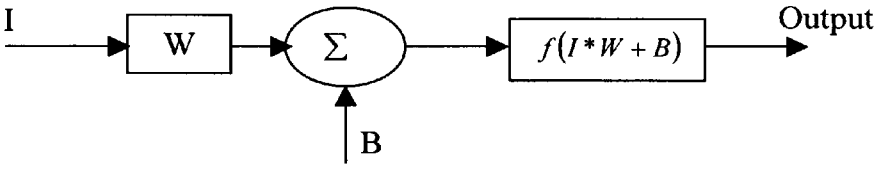

Fig.2.2: Basic structure of a neuron.

The input signal multiplied by a weight is added to a bias, this operation in the above description of the biological neuron, is performed in the cell body. The output of the artificial neuron then is calculated through a function (linear or non-linear) also known as the activation function, that accounts for the synapse connections in the biological neuron. By itself the artificial neuron of figure 2.2, is not able to perform particular tasks. It is the connection of different neurons and the choice of different activation function that classify different artificial neural networks i.e. perceptrons neural networks, radial basis function neural networks, to name just two.

Once the structure of a neural network is chosen, its behaviour is determined by the values of its weights and biases. The way to determine the proper values for those parameters is termed learning. There are three different type of learning, namely supervised learning (or with a teacher), unsupervised learning and reinforcement learning. In supervised learning, the learning rule is provided by a set of inputs and corresponding desired targets. The difference between the desired target (or network output) and the actual network output is used to drive the change in the network's parameters. Reinforcement learning is similar to the supervised learning, except that the learning rule is provided with a measure of the network performance. This measure is used to drive the network's parameter changes. Finally in the unsupervised learning rule,

the network's parameters are changed in response only to its input signals. The research effort, since the first introduction of ANNs, was to develop different structures of neuron connection (neural networks) with associated learning rules capable of performing different tasks, such as classification and pattern recognition. The most widely used ANNs for control purpose are the multilayer perceptron network (MPN), the radial basis function neural network (RBFN) and the cerebellar model articulated controller network (CMAC). All these neural networks share the ability to be universal approximator. The ability to approximate any continuos function in a compact set, in conjunction with the ability to learn this approximation from data (using appropriate learning rule), rendered these systems attractive as adaptive or learning systems under different conditions of uncertainties. In the next section, the structure and the analytical formulation of MPNs, RBFNs and CMAC is presented. The later in fact are used as building blocks for the design of the ship's autopilots presented in this thesis.

2.2.1 Perceptrons

The perceptron neural network is one of the first artificial neural networks proposed by (Rosenblatt, 1958). Like the basic neuron, the perceptron produces a weighted sum of the input signals that is compared with a threshold to determine its output. When the weighted sum of the input is greater then or equal to the threshold the output is 1, while it is 0 if the sum is less then the threshold. This can be achieved by an hard limit function as the activation function. The major contribution of Rosenblatt was the definition of a learning rule for training the perceptron parameters to solve pattern recognition problems. The perceptron learning rule proposed by Rosenblatt is expressed by equation (2.1):

$$\theta(k+1) = \theta(k) + e(k)x(k) \tag{2.1}$$

where the parameter vector include the input weights and biases ($\theta = [w, b]$) and the input vector p is extended to the vector $x = [p, 1]$ (since the threshold can be considered as an input to the networks always equal to 1). The error e, in equation (2.1) is defined as:

$$e = d - a \tag{2.2}$$

where d is the desired output value and a is the output of the network. The learning rule expressed by equation (2.1) falls in to the so-called supervised learning rule, since the desired output has to be available to compute the output error. Although the perceptron network can solve many pattern classifications, its limitation stems in the fact that the input space can only be linearly separate. This problem was emphasised in the book Perceptron (Minsky and Papert, 1969), where it was shown that the perceptron network cannot implement the logical OR function. This intrinsic limitation of the perceptron led to a diminishing in the interest about neural networks. It was felt that this limitation could have been solved with the use of a connection of different perceptron neurons. However, it was not clear how to train such a network. It was after the formulation of the backpropagation learning rule (Rumelhart *et al*, 1988), that this problem was overcame and the introduction of the multilayer perceptron networks produced new interest in the field of neural networks.

2.2.2 Multilayer Perceptron Networks

The structure of three layered MPN with n inputs and m outputs is shown in figure 2.3. It was proved by many authors that such a neural network structure with non-linear activation function in the hidden layer is able to approximate any non-linear functions defined in a compact set (Cybenko, 1989), (Hornick *et al*, 1989). The same result holds if the network is formed by more then one non-linear hidden layer. Since one hidden non-linear layer is sufficient to approximate any non-linear function, whether it is necessary to use multiple hidden layers is still not completely clear.

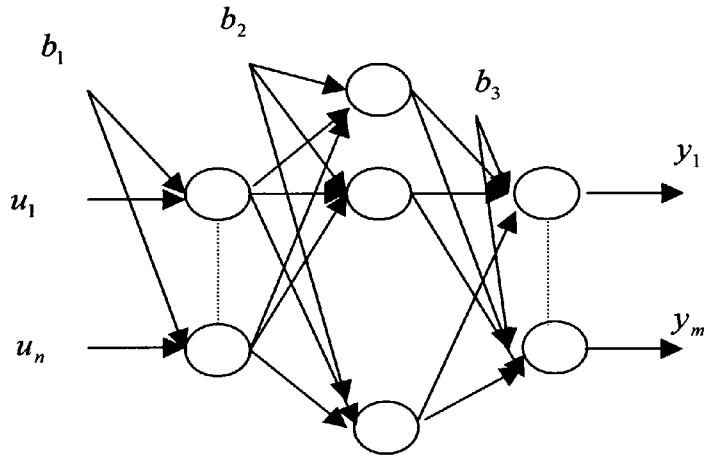

Fig. 2.3: Three layer neural network

The relationship between the input u and the output vectors y is represented by equation (2.3).

$$\mathrm{y}(\theta,\mathrm{u}) = f\left(\sum_n \theta_n f\left(\sum_j \theta_j f\left(\cdots f\left(\sum_i \theta_i u_i\right)\right)\right)\right) \tag{2.3}$$

In the particular case of one hidden layer, equation (2.3) reduces to:

$$y(\theta,u) = f_3(\theta_3 f_2(\theta_2 f_1(\theta_1 u))) \tag{2.4}$$

where θ_i with $i = 1,2,3$ is the vector parameter of each layer (i.e. $\theta_i = [w_i, b_i]$, where w are the weights and b are the biases) u is the input vector and f are the activation functions of each layer of neurons. In order to allow the output of the network to be any real number within a certain bound (i.e. to take account for actuator saturation), the activation function of the output layer is usually chosen to be a linear saturated function or simply a linear function. In order to guarantee the approximation properties of the network, the hidden layer activation function is chosen to be any non-linear function with known derivative. (The requirement on the derivative of the activation function is due to the backpropagation algorithm). Two of the commonly used non-linear functions in the hidden layer are: the logaritmic sigmoidal function, $y = \frac{1}{1+e^{-x}}$ with values in [0,1] and the tangent sigmoidal function, $y = \frac{2}{1+e^{-2x}} - 1$ with values in [-1,1].

Since the earlier days of research into artificial neural networks, it was expected that such a network of neurons massively interconnected could perform many tasks that a simple neuron cannot. Moreover, due to the parallelism in the network structure, computation can be performed simultaneously for different nodes leading to a speed up in the overall computational time. Due to the connections between neurons, failure in an internal node does not result in major changes in performance. As a consequence, artificial neural networks have the potential for being useful components in the design of complex systems. However, the major problem encountered with such networks is due to the inability to find appropriate learning rules to train the parameter values for a specific task. This problem was solved by different authors during the 1980s. The most referenced and promulgated one is due to Rumelhart and his colleagues of the Parallel Distributed Processing laboratory and termed backpropagation learning algorithm (Rumelhart *et al*, 1988).

2.2.3 Cerebellar Model Articulated Controller

The cerebellar model articulated Controller (CMAC) was first proposed by (Albus, 1971) after studying the functions of the cerebellum. A structural description of the CMAC is presented in figure 2.4, where the three main steps of the information process are highlighted. The input vector space, represented by the set U, is mapped through a non-linear function into what is called the conceptual memory. This mapping assigns to each point of the input space a set of C points in the conceptual memory. The mapping occurs in such a way that near points in the input space are mapped into sets of the conceptual memory that overlaps. Closer the input vectors bigger will be the overlap of the corresponding sets in the conceptual memory. On the contrary, if the two points in the input space are far from each other, no overlapping in the corresponding sets of the conceptual memory will occur. The sets of points so far activated in the conceptual memory will be combined (possibly in a linear weighted fashion) in the final stage to produce the output of the CMAC. The definition of the sets in the conceptual memory and of the non-linear mapping will determine the non-linear behaviours of the network and are usually based on heuristic knowledge.

In (Miller *et al*, 1990), it is claimed that this network, due to its fixed non-linearity, can be trained easier then MPNs. The training consists of just adjusting the weights of the output layer by well-known least mean square algorithms. A number of successful applications of this network are also reported. However, the problem to design the conceptual memory and the non-linear mapping, especially for high dimensional input space, is still the major drawback encountered for the CMAC.

The CMAC can be seen as a network that performs a look-up table in the input space. To each inputs, representing certain information, the network associates possible decisions in the conceptual memory. These decisions are then weighted to produce the final output. When the problem to be solved dictates a high level of quantization of the input space, the dimension of the conceptual memory can became numerically intractable.

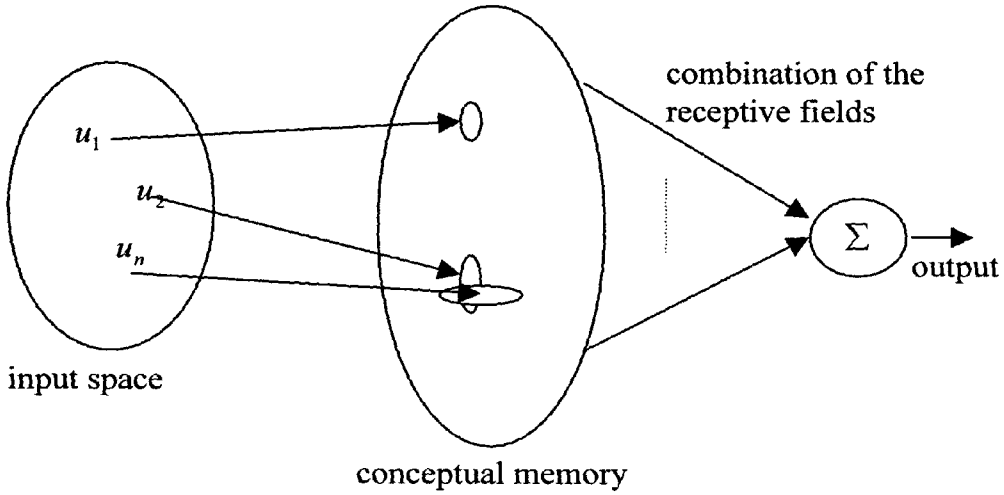

Fig.2.4: Block diagram of CMAC

2.2.4 Radial Basis Function Networks

A radial basis function neural network with n inputs $u = [x_1, ..., x_n]$ and m outputs y is shown in figure 2.5. It can be considered as a two layers network, in which the first layer performs a non-linear transformation of the input space, through the basis functions, into a new vector space. The output of the hidden layer is then combined in a linear fashion to produce the output of the network y. The equation describing the input/output relation of the RBFN is as follows:

$$y(\theta,u)=\sum_{j=1}^{n}\theta_j\Phi_j(u) \tag{2.5}$$

where the non-linear functions, Φ_j performs the input vector transformation and are of the form:

$$\Phi_j(u)=\varphi(\|u-c_j\|)\text{with } c_j \in \Re^n \tag{2.6}$$

$\varphi(\cdot)$, has its maximum value at the origin and drops off rapidly as its argument increase. A possible choice for the functions Φ_j is then the Gaussian function, which has the form of equation (2.7):

$$\Phi_j(u)=e^{-\frac{(u-c_j)^2}{2\sigma_j^2}} \tag{2.7}$$

When the Gaussian functions are specified in terms of its parameters c_j (centre) and σ_j^2 (deviation), the only adjustable parameter of the network are the weights of the output layer θ_j.

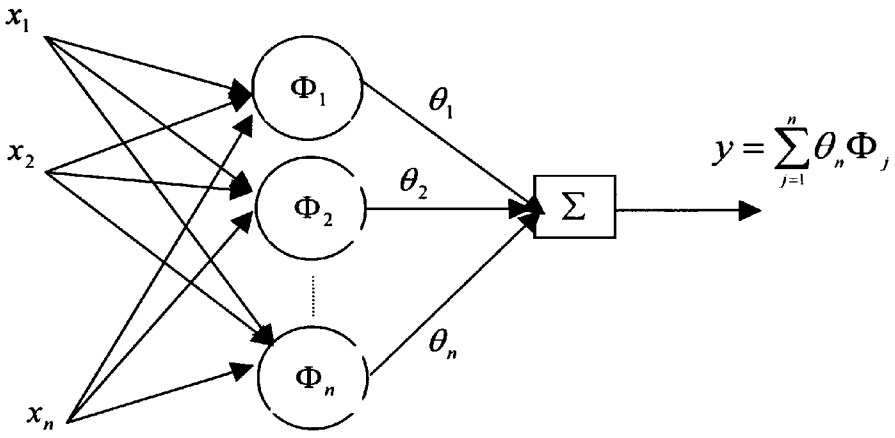

Fig. 2.5: Radial Basis Network

The similarity to the CMAC is then clear. In both the non-linearity of the network is confined to the input layer. When the parameters of this layer are fixed, a straightforward least mean square algorithm can be used to adjust the output parameters that are linear in the network output (equation (2.5)). For high input space dimensionality both the RBFN and CMAC can became numerically intractable.

A brief comparison of MPNs and RBFNs can be made by considering some advantages and disadvantages of both. From equation (2.3) it is clear that the parameters of a MPN are related in a non-linear fashion with respect to the output. Hence, derivative based algorithms are mandatory for the adjustment of the parameters. This, in turn, implies that the parameters can converge to local minima unless other derivative-free methods are used which in general, due to their low speed of convergence, are not well suited for on-line implementation. Moreover, the adjustment of a single parameter of the network affects the output globally. For this reason, all the weights have to be adjusted simultaneously for each training data set, reducing the effect of previous learning and slowing down the convergence rates of the algorithm. On the contrary, in the RBFN,

once the parameters defining the basis functions are fixed, the adjustable parameters are related in a linear fashion to the output. This allows the use of the least mean square algorithm which is considerably faster then the derivative based algorithms. Moreover, when the input vector is close to the centre of the ith basis function, the response of this is large while it is virtually zero when the input vector is very far from the centre. It is possible to consider this local behaviour of the network in order to speed up the learning and to retain previous learned patterns. However, the overall behaviour of the network is highly affected by the choice of the basis function parameters.

Some heuristic methods exist in order to ensure good approximation properties of the network and a good rule is to ensure a sufficient overlapping of the basis function in the input domain. Other non-heuristic methods based on cluster analysis can be used only if a significant amount of data can be collected. As a consequence of this, for a high dimensional input space, the number of the basis functions that are needed to ensure good approximation properties may became numerically intractable.

2.3 Fuzzy systems for control

Traditional control designs are usually based on physical models of the system to be controlled. A set of differential equations (linear or non-linear) characterising the mathematical model of the system, have to be solved in order to determine the relationship between the input values and the corresponding output values of the control system. If mathematical models are difficult to be defined, i.e. due to the complexity of the system or to the kind of available information (rather vague and uncertain), cognitive modelling represents a more viable alternative.

Using a cognitive based modelling approach, the aim is to design control system based on a model of the expert, who is able to specify the general properties of the system, rather than on a model of the system to be controlled. In this respect, fuzzy logic has proved to be a powerful tool. The control strategy is specified by a set of rules deduced by *a-priori* knowledge of the system, that constitutes the rule knowledge base of the controller. Based on this stored knowledge, the actual situation is evaluated in order to infer the appropriate control action. The deduced control action, performed by the so-called inference machine, is based on fuzzy logic where uncertainties are easily handled. In fact, fuzzy logic as introduced in the paper of (Zadeh, 1965), is based on an extension of the classical idea of set inclusion. While in crisp set theory, an element of a universe of discourse either belongs or not belongs to a set, in fuzzy logic each element of the universe of discourse belongs to a set with a different degree of belonging defined by a membership function.

Figure 2.6 shows the basic structure of a fuzzy logic system used for control purpose with its four principal blocks. These four principal blocks are named 1) fuzzy rule knowledge base, 2) fuzzy inference engine, 3) fuzzifier and 4) defuzzifier and constitute the four building blocks of a fuzzy inference system.

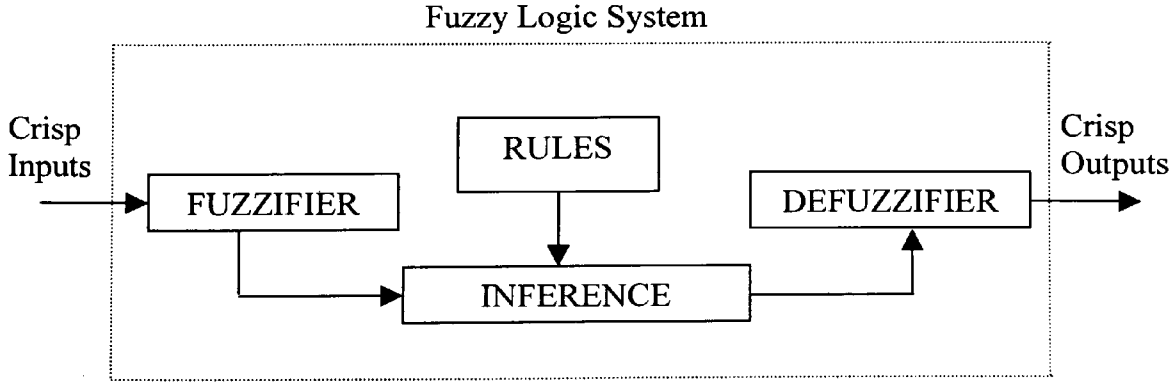

Fig.2.6: General Fuzzy Logic System structure

The *fuzzy rule knowledge base* represents the block were heuristic knowledge in the form of **IF-THEN** rules can be stored. The rules for a multi-input-single-output (MISO) system are expressed in the form of equation (2.8), (it can be proved that any multi-input-multi-output (MIMO) system, with *m* outputs, can be represented by *m* MISO):

$$R^{(i)}: IF \quad x_1 \quad is \quad A_1^i \quad and \quad \cdots \quad and \quad x_n \quad is \quad A_n^i \quad THEN \quad y \quad is \quad B^i \tag{2.8}$$

where i is the number of rules, $\bar{x} = (x_1, x_2, ..., x_n)^T \in U$ is the input vector, $y \in \Re$ is the output, A_n^i and B^i are fuzzy sets defined in U and $\Re$ respectively.

Each rule of equation (2.8) defines an implication from $\mathrm{A}_1^{\mathrm{i}} \times \mathrm{A}_2^{\mathrm{i}} \times \cdots \times \mathrm{A}_{\mathrm{n}}^{\mathrm{i}}$ into B^i that is a fuzzy set defined in the Cartesian product space $U \times \Re$. There are different fuzzy implication rules proposed in the literature. The two following rules are an extension from the crisp implication rules to the equivalent fuzzy logic counterpart:

$$\mu_{A_1^i \times \cdots \times A_n^i \to B^i}(\bar{x}, y) = 1 - \min\left[\mu_{A_1^i \times \cdots \times A_n^i}(\bar{x}), 1 - \mu_{B^i}(y)\right] \tag{2.9}$$

$$\mu_{A_1^i \times \cdots \times A_n^i \to B^i}(\bar{x}, y) = \max\left[1 - \mu_{A_1^i \times \cdots \times A_n^i}(\bar{x}), \mu_{B^i}(y)\right] \tag{2.10}$$

The above equations are obtained from the following tautologies respectively:

$$A \to B \leftrightarrow \sim [A \cap (\sim B)] \tag{2.11}$$

$$A \to B \leftrightarrow [\sim A \cup (B)] \tag{2.12}$$

where the symbol $\sim$ represents the not operator (or negation), $\cup$ and $\cap$ are the union and interception respectively and $\leftrightarrow$ represents equivalence. Equation (2.11) and (2.12)

states the isomorphic equivalence between set theory and propositional logic. It is possible to prove that the use of the above implication rules lead to a fuzzy system that is not causal (Mendel, 1995). This is the reason why in engineering applications the two used implication rules are the *min* and *product* implication rules, expressed in equations (2.13) and (2.14), introduced by (Mamdani, 1974) and (Larsen, 1980) respectively:

- Min-operation rule of fuzzy implication:

$$\mu_{A_1^i \times \cdots \times A_n^i \to B^i}(\bar{x}, y) = \min\left[\mu_{A_1^i \times \cdots \times A_n^i}(\bar{x}), \mu_{B^i}(y)\right] \tag{2.13}$$

- Product-operation rule for fuzzy implication:

$$\mu_{A_1^i \times \cdots \times A_n^i \to B^i}(\bar{x}, y) = \left[\mu_{A_1^i \times \cdots \times A_n^i}(\bar{x}) \cdot \mu_{B^i}(y)\right] \tag{2.14}$$

In the equations (2.13) and (2.14), $\mu_{A_1^i \times \cdots \times A_n^i}(\bar{x})$ represents the degree of certainty of the antecedent part of the ith rule and is expressed as:

$$\mu_{A_1^i \times \cdots \times A_n^i}(\bar{x}) = \mu_{A_1^i}(x_1) * \mu_{A_2^i}(x_2) * \cdots * \mu_{A_n^i}(x_n) \tag{2.15}$$

The symbol $*$ denotes the t-norm which correspond to the conjunction term "and" in the antecedent part of (2.8). Three commonly used operations for the t-norm are:

1) Fuzzy intersection or *minimum* operator defined as:

$$\mu_\alpha(x_1) * \mu_\beta(x_2) = \mu_{\alpha \cap \beta}(\bar{x}) = \min\left\{\mu_\alpha(x_1), \mu_\beta(x_2)\right\} \tag{2.16}$$

2) Algebraic product operator defined as:

$$\mu_{\alpha}(x_1) * \mu_{\beta}(x_2) = \mu_{\alpha \cap \beta}(\bar{x}) = \mu_{\alpha}(x_1) \cdot \mu_{\beta}(x_2) \tag{2.17}$$

3) Bounded product:

$$\mu_{\alpha}(x_1) * \mu_{\beta}(x_2) = \mu_{\alpha \cap \beta}(\bar{x}) = \max[0, \mu_{\alpha} + \mu_{\beta} - 1] \tag{2.18}$$

As be seen from the equations (2.16), (2.17) and (2.18), the degree of certainty assigned to the antecedent part $\mu_{\alpha \times \beta}(\bar{x})$, is always less or equal to the lowest degree of certainty of each membership functions that constitute the premise. This is in accordance with the meaning of the logical "and" operator.

The construction of the *rule knowledge base* has a great impact on the behaviour of a fuzzy system. Two main aspects of the rule base to be considered carefully are the *consistency* and the *completeness*. Consistency of the rule base refers to the condition in which there are no rules with the same antecedent and different consequent part leading therefore to contradiction. While completeness refers to the property where for any input value within the domain of the input variable there is at least one rule with a degree of certainty different then zero. A sufficient condition for the completeness of the rule base is that:

$$\exists i, such \quad that \; \mu_{A_1^i \times \cdots \times A_n^i}(\bar{x}) \neq 0, \quad \forall \bar{x} \in U \tag{2.19}$$

The *fuzzy inference* block, performs the logical functions evaluation on the rules specified in the knowledge base equation (2.8). The generalisation of the classical inference rules (i.e. modus ponens, modus tollens and hypothetical syllogism), to the

fuzzy counterpart, is based on the so-called *compositional rule of inference* (Zadeh, 1973). In contrast with the classical Boolean logic, where the logical functions may be either true or false, in fuzzy logic each rule is true with different degree of certainty. In others words, if A is a fuzzy set describing the current inputs, each rule R^i in (2.8) determine a fuzzy set $A \circ R^i$ in $\Re$ based on the following compositional rule of inference:

$$\mu_{A\circ R^i}(y) = \sup_{x\in U}\left[\mu_A(\bar{x}) * \mu_{A_1^i\times\cdots\times A_n^i\to B^i}(x,y)\right] \tag{2.20}$$

where $\mu_A(\bar{x})$ is the membership function describing the fuzzification of the input $\bar{x}$, $*$ is the t-norm and $\mu_{A_1^i\times\cdots\times A_n^i\to B^i}(\bar{x},y)$ is computed by one of the above fuzzy implication rules (equations (2.13) or (2.14))). The final fuzzy set describing the entire set of i rules is obtained from the fuzzy sets $\mu_{A\circ R^i}(y)$ for i=1,...,n (number of rules) using the fuzzy disjunction operation defined as:

$$\mu_{A\circ R^1,\ldots,R^m}(y) = \mu_{A\circ R^1}(y)\otimes\mu_{A\circ R^2}(y)\otimes\ldots\otimes\mu_{A\circ R^m}(y) \tag{2.21}$$

where $\mu_{A\circ R^1,\ldots,R^n}(y)$ is the aggregated fuzzy set of the consequent (that represent the deducted inferred reasoning) and the symbol $\otimes$ denotes the t-conorm. The three most commonly used t-conorm operations are:

1) Fuzzy union or *maximum operator*:

$$\mu_\alpha \otimes \mu_\beta = \max\left[\mu_\alpha, \mu_\beta\right] \tag{2.22}$$

2) Algebraic sum:

$$\mu_\alpha \otimes \mu_\beta = \left[\mu_\alpha + \mu_\beta - \mu_\alpha \mu_\beta\right] \tag{2.23}$$

3) Bounded sum:

$$\mu_\alpha \otimes \mu_\beta = \min\left[1, \mu_\alpha + \mu_\beta\right] \tag{2.24}$$

Equation (2.21) is the mathematical statement of the approximate reasoning capability of the fuzzy logic systems.

The *fuzzifier* performs the fuzzification operation that consists in mapping the crisp input $\bar{x}$ into a membership function defined in the interval $[0,1]$. As stated above the fuzzy inference engine performs deductive reasoning applying logical function evaluation on fuzzy sets instead of crisp values. The fuzzifier therefore is used to transform the crisp input $\bar{x}$ in a fuzzy set while the *defuzzifier* performs the opposite operation, it transforms the output of the fuzzy inference engine (which is a fuzzy set) into a crisp value.

For the fuzzification process at least two methods exist:

1) singleton fuzzification: which define the fuzzy set for the crisp value $\bar{x}_1$ as:

$$\begin{aligned} \mu_A(\bar{x}) &= 1 \quad for\ \bar{x} = \bar{x}_1 \\ \mu_A(\bar{x}) &= 0 \quad for\ \bar{x} \neq \bar{x}_1 \end{aligned} \tag{2.25}$$

Note that with this fuzzification method, equation (2.20) simplify in:

$$\mu_{A\circ R^i}(y) = \sup_{x\in U}\left[\mu_A(\bar{x}) * \mu_{A_1^i\times\cdots\times A_n^i\to B^i}(x,y)\right] = \sup_{x\in U}\left[1 * \mu_{A_1^i\times\cdots\times A_n^i\to B^i}(x,y)\right] = \left[\mu_{A_1^i\times\cdots\times A_n^i\to B^i}(x,y)\right] \tag{2.26}$$

whether minimum or product operation is used for the t-norm, (equation (2.16) or (2.17)).

2) general fuzzification: which define the fuzzy set for the crisp value $\bar{x}_1$ as:

$$\mu_A(\bar{x}) = 1 \quad for \quad \bar{x} = \bar{x}_1$$

$\mu_A(\bar{x})$ decreases from 1 as $\bar{x}$ moves away from $\bar{x}_1$. (2.27)

For control purposes, due to its computational efficiency, a singleton fuzzifier is normally used, however in the presence of noisy input the general fuzzification methods may be useful. In fact the general fuzzification method can be interpreted as a pre-filtering of the noisy input signal. As an example, consider a SISO fuzzy system. Using the product for both, t-norm (equation (2.17)) as well for the implication rule (equation (2.14)), equation (2.20) that represents the inferred fuzzy set will have the follows form:

$$\mu_{A\circ R^i}(y) = \sup_{x\in U}\left[\mu_A(\bar{x}) * \mu_{A^i\to B^i}(x,y)\right] = \sup_{x\in U}\left[\mu_A(\bar{x})\cdot\mu_{A^i}(x)\cdot\mu_{B^i}(y)\right] \tag{2.28}$$

Since the superior is calculated over all $x \in U$, equation (2.28) can be rewritten as:

$$\mu_{A\circ R^i}(y) = \mu_{B^i}(y)\sup_{x\in U}\left[\mu_A(\bar{x})\cdot\mu_{A^i}(x)\right] \tag{2.29}$$

Suppose now, that the membership function associated to the crisp input $\bar{x}$ (during the fuzzification process), is a Gaussian function defined as $\mu_A(\bar{x}) = e^{-\frac{(x-\bar{x})^2}{2\sigma_{\bar{x}}}}$, with centre $\bar{x}$

and standard deviation $\sigma_{\bar{x}}$. If the membership function associated with the antecedent part of the ith rule is chosen as well as a Gaussian function of the form $\mu_{A^i}(x) = e^{-\frac{(x-m_i)^2}{2\sigma_i}}$, defining the membership function product such as:

$$\mu_{PR^i}(x) = \mu_A(\bar{x})\mu_{A^i}(x) \tag{2.30}$$

It can be proved that the point:

$$x_{\max} = \frac{m_i\sigma_{\bar{x}}^2 - \bar{x}\sigma_i^2}{\sigma_i^2 + \sigma_{\bar{x}}^2} \tag{2.31}$$

will maximise the function $\mu_{PR^i}(x)$ expressed in equation (2.30). Equation (2.29) then reduces to:

$$\mu_{A\circ R^i}(y) = \mu_{B^i}(y)\mu_{PR^i}(x_{\max}) \tag{2.32}$$

Equation (2.31) can be interpreted as a pre-filtering of the noisy data $\bar{x}$ achieved by the fuzzification process (Mouzouris and Mendel, 1997a) (Mouzouris and Mendel, 1997b).

For the defuzzification process different strategies exist, based either on the implied fuzzy sets (equation 2.20) or on the overall implied fuzzy set (equation 2.21). With respect the implied fuzzy sets the two most common defuzzification methods are:

1) Centre of gravity, defined as:

$$y(\bar{x}) = \frac{\sum_{i=1}^{m} b_i \int \mu_{A \circ R^i}(y) dy}{\sum_{i=1}^{m} \int \mu_{A \circ R^i}(y) dy} \tag{2.33}$$

where b_i is the centre of area of the membership function of the consequent part associated to the *ith* rule. Note that the fuzzy system must be defined so that:

$$\sum_{i=1}^{m} \int \mu_{A \circ R^i}(y) dy \neq 0$$

This value will be not zero if there is a rule that is on for every possible combination of the fuzzy system inputs (the rule base is complete) and the consequent fuzzy sets have a nonzero area.

2) Centre-average defined as:

$$y(\bar{x}) = \frac{\sum_{i=1}^{m} b_i \left(\mu_{A \circ R^i}(y)\right)}{\sum_{i=1}^{m} \mu_{A \circ R^i}(y)} \tag{2.34}$$

where b_i is the point in $\Re$ at which the output membership function achieves its maximum value. Also with this defuzzification formula it is necessary that:

$$\sum_{i=1}^{m} \mu_{A \circ R^i}(y) \neq 0$$

With respect the overall implied fuzzy set (equation 2.21) three possible defuzzification formula are:

1) Max criterion defined as:

$$y(\bar{x}) = \arg\sup_y \left\{ \mu_{A \circ R^1, \ldots, R^m}(y) \right\} \tag{2.35}$$

This criterion returns the value of y that result in the supremum of the overall implied fuzzy set. Sometimes the supremum can occur in more then one point in $\Re$. In this case a different strategy can be specified in order to choose the proper point. One of these criteria is the mean of maximum.

2) Mean of maximum defuzzification criterion is defined as the mean value of all elements whose membership is maximum:

$$y(\bar{x}) = \frac{\int y \hat{\mu}_{A \circ R^i \times \cdots \times R^m}(y) dy}{\int \hat{\mu}_{A \circ R^i \times \cdots \times R^m}(y) dy} \tag{2.36}$$

where $\hat{\mu}_{A \circ R^i \times \cdots \times R^m}(y)$ is a new membership function defined as:

$$\hat{\mu}_{A \circ R^1 \times \cdots \times R^m}(y) = \begin{Bmatrix} 1 & if \mu_{A \circ R^1 \times \cdots \times R^m}(y) is \max \\ 0 & otherwise \end{Bmatrix}$$

Here also $\int \hat{\mu}_{A \circ R^i \times \cdots \times R^m}(y) dy \neq 0$, moreover this integral has to be computed each time instant since it depends on $\hat{\mu}$ which changes with time. This can require excessive computational resource for continuous universe of discourse.

3) Centre of Area defuzzification method selects the crisp value of the output as the centre of area of the overall implied fuzzy set. For a continuos output universe of discourse the formula can be expressed as:

$$y(\bar{x}) = \frac{\int y \mu_{A \circ R^1 \times \cdots \times R^m}(y) dy}{\int \mu_{A \circ R^1 \times \cdots \times R^m}(y) dy} \tag{2.37}$$

Also, here it is necessary that the integral $\int \mu_{A \circ R^1 \times \cdots \times R^m}(y) dy \neq 0$, moreover similar to the previous method it can be computational expensive.

As a result of the above discussion, the fuzzy system given in figure 2.6 represents a very rich class of static systems mapping $U \subset \Re^n$ into $\Re$, because within each block there are many different choices. Different combinations of these choices may result in different subclasses of fuzzy logic systems with interesting properties. For instance, the fuzzy logic systems with *center-average defuzzifier*, *product inference* and *singleton fuzzifier* have the following form:

$$y(\bar{x}) = \frac{\sum_{i=1}^{m} b_i \left(\prod_{j=1}^{n} \mu_{A_j}(x_j) \right)}{\sum_{i=1}^{m} \left(\prod_{j=1}^{n} \mu_{A_j}(x_j) \right)} \tag{2.38}$$

The above statement follows straightforward from the application of the equations (2.14), (2.27) and (2.34).

An interesting parameterisation of equation (2.38) can be achieved considering the parameters of the input membership functions fixed, therefore defining:

$$\xi^m(\bar{x}) = \frac{\prod_{j=1}^{n} \mu_{A_j}(x_j)}{\sum_{i=1}^{m} \left(\prod_{j=1}^{n} \mu_{A_j}(x_j) \right)} \quad ; \text{ and } \quad \theta^T = [b_i, \ldots, b_m] \tag{2.39}$$

as regressor and parameters vectors respectively, the fuzzy systems of equation (2.38) can be linearly re-parameterised with respect b_i as:

$$y(\bar{x}) = \theta^T \xi(\bar{x}) \tag{2.40}$$

The main reasons for considering the fuzzy system expressed in equation (2.38) as a building block for the design of adaptive fuzzy systems are: 1) It has been proved that equation (2.38) is a universal approximator function, 2) the fuzzy logic systems expressed by equation (2.38) is constructed from a set of IF-THEN rules, therefore linguistic information from human experts can be easily incorporated into the system, 3) the parameterisation of equation (2.40) allow for the application of well-known result in linear adaptive control theory 4) by comparing equation (2.5) with (2.40) it is clear the relationship between RBFN and FIS of the form expressed by equation (2.38). The last point allows the generalisation of results from the field of neural network to that of fuzzy logic systems and vice versa.

To summarise, the design of a fuzzy logic system involves the specification of the following operations:

AND operator: for calculating the firing strength of a rule with *and* antecedents. (usually *t-norm*).

OR operator: for calculating the firing strength of a rule with *or* antecedents. (usually *t-conorm*).

Implication operator: for calculating the inferred consequent of each rule (usually *t-norm*).

Aggregate operator: to aggregate the inferred consequences of each rule in an overall membership function (usually *t-conorm*).

Fuzzification operator: to associate a membership function to the measured crisp value.

Defuzzification operator: to associate a crisp value to the inferred fuzzy set.

Two of the most well known fuzzy logic systems used for control purpose are the *Mamdani* and *Sugeno* fuzzy inference systems. These are briefly described in the following section.

2.3.1 Mamdani fuzzy models

Mamdani first used the idea of fuzzy sets to design a control system for a steam engine, based on linguistic interpretation of rules specified by a human expert operator (Mamdani and Assilian, 1975). Mamdani used the min operator to perform the *and* and implication and the *max* operator to perform aggregation. Figure 2.7 shows the steps involved in a two inputs one output Mamdani fuzzy inference system with singleton fuzzification.

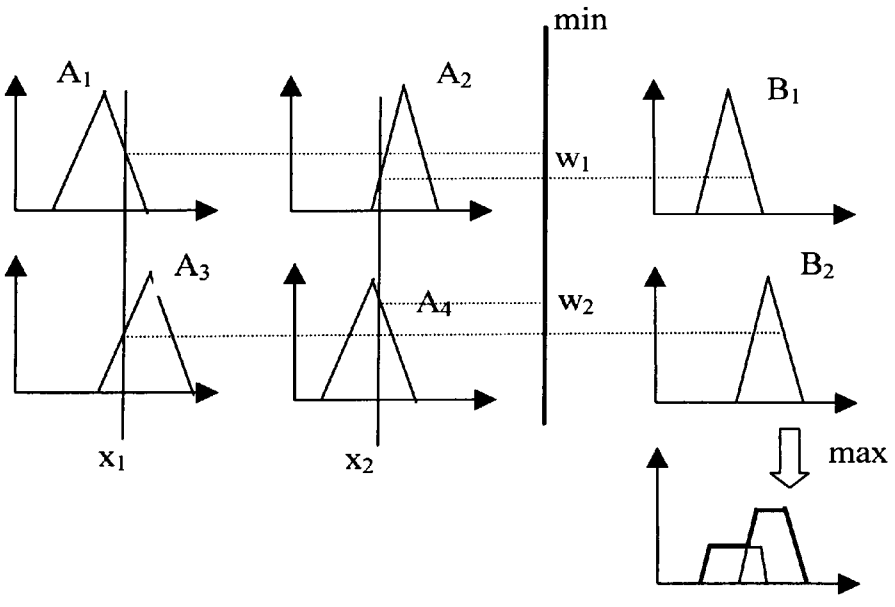

Fig.2.7: Two rules, two inputs Mamdani fuzzy model

In the Mamdani fuzzy model of figure 2.7, the two singleton membership functions associated to the inputs x_1 and x_2 are mapped into the membership functions describing the antecedent part of each rule. These firing strengths are combined with the *min* operator to give the degree of belief of each antecedent rule (w_1 and w_2). These are used to shape the output membership function of each rule to give the membership function of the consequence. Each consequent membership functions are then aggregated using the *max* operator to represent the inferred fuzzy set (represented in bold in the bottom-right of the figure).

In general, for a *Mamdani fuzzy model,* is intended any fuzzy systems with *min* or *product* operator to define the *t-norm*, with aggregation as defined in equation (2.22) and *defuzzification* as defined by equations (2.35), (2.36) or (2.37). The computational complexity of this fuzzy inference system will finally depend upon the particular choice of the different operators.

2.3.2 Sugeno fuzzy models

The peculiarity of the *Sugeno fuzzy model* (also known as the Takagi Sugeno Kang model), is that while the antecedent part is still defined in terms of linguistic fuzzy sets, the consequent part is defined by a crisp function. Equation (2.41) is an example of the Sugeno's type rules:

$$R^{(i)}: IF \quad x_1 \quad is \quad A_1^i \quad and \quad \cdots \quad and \quad x_n \quad is \quad A_n^i \quad THEN \quad y = f(x_1,..,x_n) \tag{2.41}$$

In general, $f(x_1,...,x_n)$ can be any function, however usually it is a polynomial function of the input variables. When the polynomial is of the first-order the resultant fuzzy system is termed first-order Sugeno fuzzy model. When the function $f(.)$ is a constant the resultant fuzzy system is termed zero-order Sugeno model. In general the advantage of the Sugeno fuzzy model is its numerical computability compared to the Mamdani model. In the Sugeno model, in fact the defuzzification process is reduced to the weighted combination of the functions defining the consequent part of each rule. It is important to note, that while in the Mamdani model the output is always a fuzzy set that can be further defuzzified, in the Sugeno model the output is always a crisp value. In other words, the Sugeno model is a mapping from fuzzy sets defined in the antecedent part to crisp values defined by the consequent functions. Figure 2.8 is a graphical representation of a Sugeno fuzzy model with two inputs and one output .

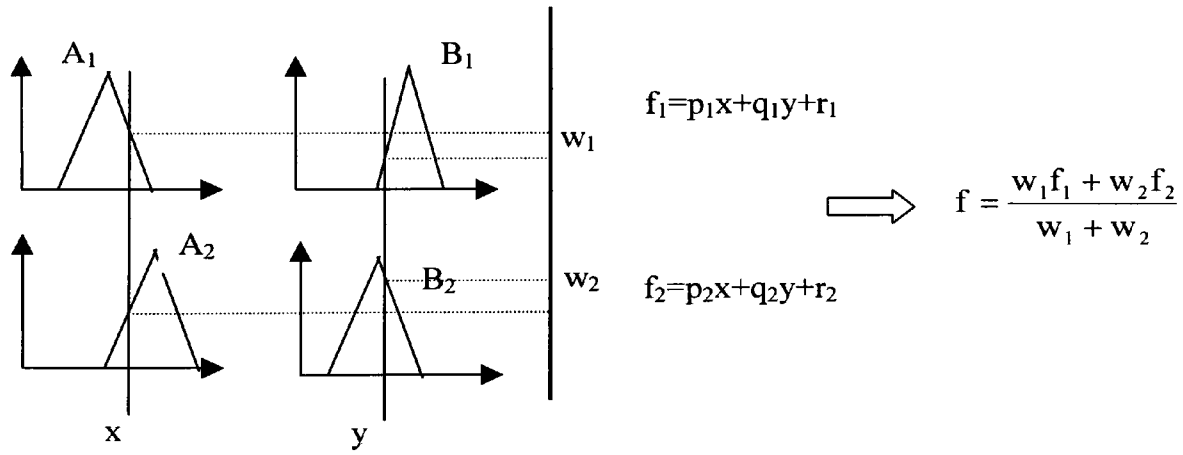

Fig.2.8: Two rules, two inputs fuzzy Sugeno model

From a brief comparison with figure 2.7 it is clear that the main difference between the two fuzzy models are in the consequent part. In the Sugeno type fuzzy model the consequent part of each rule is represented by a function. Therefore, the defuzzification in more straightforward.

2.4 Summary

In this chapter a review of neural networks and fuzzy logic systems has been presented. Both, the analytical formulation and as well the structure of the systems have been discussed. When focusing on the analytical representation, similarities between the two systems are highlighted. An example for a particular configuration of fuzzy logic system and radial basis function neural network was given.

Neural networks and fuzzy logic systems germinated from the aim to emulate and reproduce peculiar characteristics of what are recognised as intelligent species. The neuron that is the basic element of any neural networks is in fact nothing more then a simplified model of the biological neuron. On the contrary, fuzzy logic based systems have had the aim to extend the rigid two value Boolean logic, on which all the digital systems are based, to a way of inferring which is much closer to the human being. Fuzzy logic can be seen as a way to translate imprecise and vague statements in a precise mathematical formulation. In this sense, neural networks and fuzzy logic systems can be seen as two complementary systems. On one hand, neural networks tries to emulate the hardware on which intelligent behaviours are based (the brain), and on the other hand fuzzy logic tries to manipulates and quantify imprecision and fuzziness that characterises the real world.

2.5 Reference List

Albus, J. S. 1971. A theory of cerebellar functions. *Mathematical Biosciences,* **10**, pp. 25-61.

Cybenko, G. 1989. Approximation by superposition of sigmoidal functions. *Mathematics of Cotrol, Signals and Systems,* **2**, pp. 183-192.

Hornick, K.,Stinchcombe, M., and White, H. 1989. Multilayer Feedforward Networks are Universal Approximators. *Neural Network,* **2**, pp. 359-366.

Larsen, P. M. 1980. Industrial applications of fuzzy logic control. *International Journal Man Machine Studies,* **12** (1), pp. 3-10.

Mamdani, E. H. 1974. Applications of fuzzy algorithms for simple dynamic plant. *Proceedings of IEE,* **121**, pp. 1585-1588.

Mamdani, E. H., and Assilian, S. 1975. An experiment in linguistic synthesis with a fuzzy logic controller. *International journal of Man-Machine Studies,* **7** (1), pp. 1-13.

Mendel, J. M. 1995. Fuzzy Logic Systems for Engineering: A Tutorial. *Proceedings of the IEEE,* **83** (3), pp. 345-377.

Miller, W. T. III,Glanz, F. H., and Kraft, L. G. III 1990. CMAC: An Associative Neural Network Alternative to Backpropagation. *Proceedings of the IEEE,* **78** (10), pp. 1561-1567.

Minsky, M., and Papert, S. 1969. *Perceptrons.* MIT Press, Cambridge, MA.

Mouzouris, G. C., and Mendel, J. M. 1997a. Dynamic non-Singleton fuzzy logic systems for nonlinear modeling. *IEEE Transactions on Fuzzy Systems,* **5** (2), pp.

199-208.

Mouzouris, G. C., and Mendel, J. M. 1997b. Non-Singleton Fuzzy Logic Systems: Theory and Application. *IEEE Transection on Fuzzy Systems,* **5** (1), pp. 56-71.

Rosenblatt, F. 1958. The perceptron: A probabilistic model for information storage and organisation in the brain. *Psychological Review,* **65**, pp. 386-408.

Rumelhart, D.,Mcclelland, J. L., and the PDP Research Group 1988. *Parallel Distributed Processing.* 8th ed. USA: The Massachusetts Institute of Technology.

Zadeh, L. A. 1965. Fuzzy sets. *Information and Control,* **8**, pp. 338-353.

Zadeh, L. A. 1973. Outline of a new approach to the analysis of complex systems and decision process. *IEEE Transactions Syst. Man and Cybernetics,* **SMC-3** (1), pp. 28-44.

Chapter 3 Adaptive networks

3.1 Introduction

Adaptive networks, as introduced in (Jang *et al*, 1997), are used as a unifying framework that subsumes different kinds of neural network paradigms with supervised learning capabilities. Within this framework, different kinds of neural networks and fuzzy inference systems (NN and FIS) can be represented by an interconnection of basis nodes with adjustable parameters (adaptive networks). By focusing on the functional evaluation performed by each node, the two systems (NN and FIS) can be combined in a synergistic fashion. Well-established learning paradigms introduced in the context of neural networks can be easily extended to fuzzy systems and new architectures combining advantages of both fields can be proposed. In this extent the most well-known neural-fuzzy architecture proposed by Jang in the earlier 1990s is the ANFIS (Adaptive Network Based Fuzzy Inference System), (Jang, 1993). This architecture is discussed next as an example of a combination of neural network and fuzzy logic paradigms.

3.1.1 Adaptive Network Based Fuzzy Inference System

Figure 2.8 (section 2.3.2 of Chapter 2) shows, the graphical representation of the inference mechanism of a two rules first order Sugeno fuzzy model, with two inputs and one output. Singleton fuzzification, weighted averages defuzzification and product *and* is used. With respect to figure 2.8, the knowledge base is specified by the following two rules:

1. If x is A_1 *and* y is B_1 Then $f_1=p_1x+q_1y+r_1$
2. If x is A_2 *and* y is B_2 Then $f_2=p_2x+q_2y+r_2$

The steps performed by the inference mechanism can be summarised as follows:

1. The firing strengths of the input singletons are calculated for each membership functions of the antecedent part.
2. The firing strengths of each rule's antecedent are combined by the *and* operator in order to quantify the degree of belief of the antecedent part (w_1 and w_2).
3. The consequence of each rule is weighted according to the associated degree of belief to quantify the inferred consequent (w_1f_1 and w_2f_2).
4. The consequences of each rule are combined to quantify the inferred result (f).

An adaptive network can be designed in order to perform each of the above four steps. Figure 3.1 shows such a feedforward network. Each node of layer one performs the function evaluation of the membership function associated to the antecedent part of each rule. The output of this layer is therefore the firing strength of the antecedent membership function. This operation corresponds to step 1 in the inference mechanism described above. In layer two the antecedent part of each rule is combined according to the selected *t-norm* (product or minimum operation). The output of this layer is therefore the degree of belief associated to the antecedent part of each rule. This operation corresponds to step 2. In layer three, the consequent part of each rule is weighted according to the degree of belief associated to the antecedent part. This corresponds to step 3. Finally, in the fourth layer and output layer, the weighted average defuzzification is applied to the consequence of each rule. This corresponds to step 4 in the inference mechanism described above.

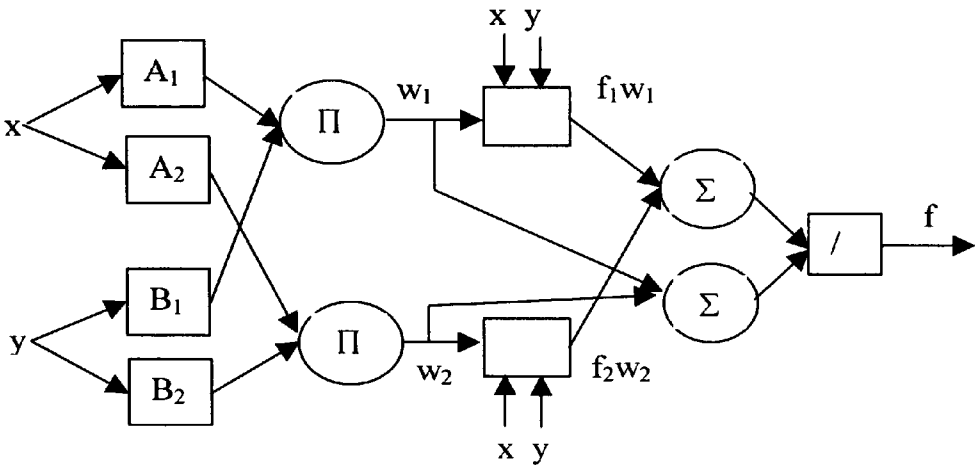

Fig.3.1: ANFIS architecture for the first order Sugeno model.

The convention adopted in the representation of figure 3.1 is that square nodes represents nodes with adjustable parameters (adaptive nodes), while circular node have fixed parameters. Any optimisation or learning methods (i.e. back-propagation) can be applied to the network of figure 3.1 in order to identify the optimal parameters of the membership function and/or the parameters of the consequent part. In principle each node in the network of figure 3.1 can be adaptive, in the sense that the optimisation can be carried out with respect the *t-norm* as well, which is represented in layer two. A least square learning algorithm, a back-propagation algorithm and its modification can be applied to this adaptive network which in fact is functionally equivalent to the Sugeno fuzzy inference system of figure 2.8. Other fuzzy inference systems, different from the one used in the above example, can be represented by an equivalent adaptive network (Kung *et al*, 1999) (Jang and Sun, 1993). In particular in the latter paper it is emphasised how RBFN and a particular class of FIS can be implemented by the same adaptive network. This is a consequence of the functional equivalence of the two systems which emphasised in the paper (Jang and Sun, 1993) and has already been mentioned in section 2.3 of Chapter 2.

3.2 Adaptive networks for control

The idea of adaptive networks, introduced in section 3.1, is to design a network (defined as the interconnection between bases nodes) such that it is functionaly equivalent to the system used to implement the controller. The learning properties of the adaptive networks can then be used in order to automatically synthesis (or optimise) the controller parameters.

The principal benefits of intelligent control stems on the ability of NN and FS, to automatically synthesise mappings that can be used advantageously within a control system architectures. Examples of such architectures that employ approximation mappings are shown in figures 3.2, 3.3, 3.4 and 3.5.

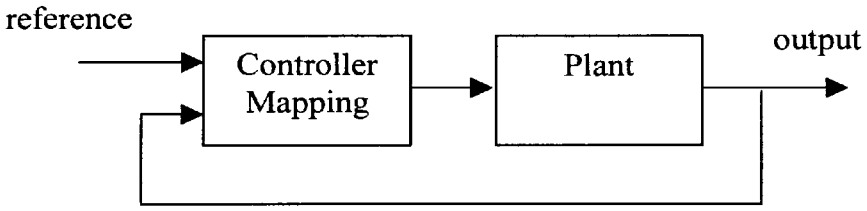

Fig.3.2: Controller mapping

They include:

1) a controller mapping that relates measured and desired plant outputs to an appropriate set of control actions (figure 3.2). Different neural networks and fuzzy systems have been trained in a supervised fashion in order to replace proportional plus integral plus derivative (PID), linear quadratic gaussian (LQG) and other traditional controllers.
2) A control parameters mapping that generates parameters for a controller from measured system's performance (i.e. direct adaptive control shown in figure 3.3).

3) A model state mapping that produces state estimation (i.e. identifier or estimator shown in figure 3.4).

4) A model parameters mapping that relates the plant operating conditions to an accurate set of model parameters (i.e. indirect adaptive control shown in figure 3.5).

All these control architectures have their foundations in traditional control theory. In accordance with the definition of intelligent control given in section 1.1, neural networks and fuzzy logic systems are used to solve the analytical part of the control design problem which now consist of approximating a suitable control mapping.

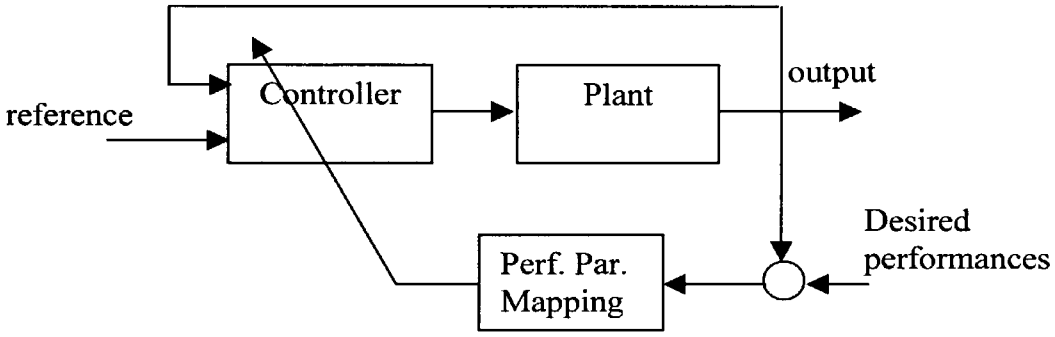

Fig.3.3: Direct adaptive control

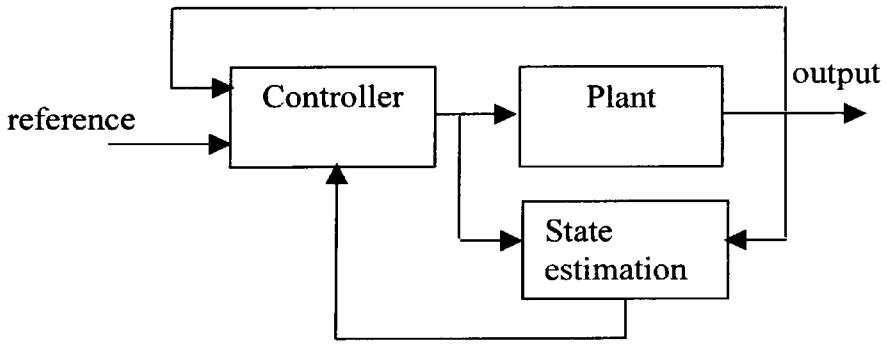

Fig.3.4: State estimation mapping

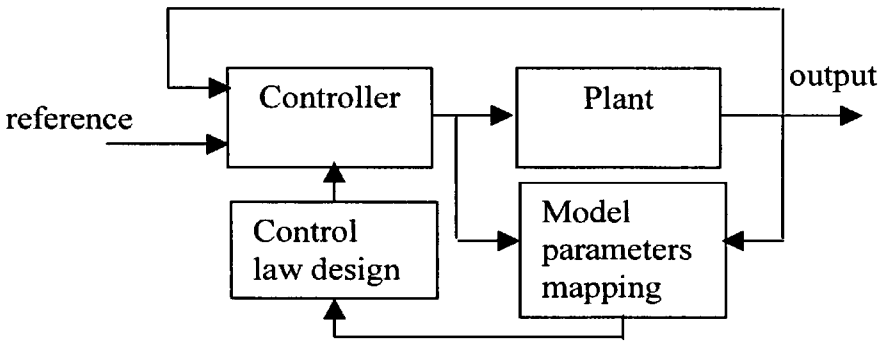

Fig.3.5: Indirect adaptive controller

In general, the problem to approximate a multivariate function $f(\bar{x})$ by an approximating function or functional mapping $NN(\theta,\bar{x})$, is dealt with in the framework of approximation theory and the related fields of system identification and system estimation. Its raises three main questions (Poggio and Girosi, 1990):

1) What kind of approximator has to be used? In other words, what classes of functions $f(\bar{x})$ the selected functional approximator $NN(\theta,\bar{x})$ can approximate?

2) What kind of algorithm has to be used for finding the optimal parameters θ^* for a given choice of $NN(\theta,\bar{x})$?

3) Is the selected approximator with the selected algorithm realisable in practice?

The proper answers to the above questions are application dependent. However, the above questions motivate the choice of the particular controller structure and adaptation/learning algorithm. They also represent a systematic procedure to find the most suitable combination of different identification and control design techniques. In

the context of neural networks and fuzzy systems, the first question refers primarily to the problem of choosing a particular network, (i.e. MPN, RBFN, CMAC, Mamdani, Sugeno etc.), while the second question is related to the particular parameterisation that can be achieved. For instance, as mentioned in 2.2.4, for a RBFN with fixed parameters in the input non-linear layer, least mean square algorithm can be used. Finally, the last question dictates the hardware specification and whether or not the adaptation can be performed on line.

To measure the quality of the approximation, the idea of distance between the function to be approximated $f(\bar{x})$ and the approximator $NN(\theta,\bar{x})$ is used. A function ρ is defined in order to quantify such distance. A common choice for the function ρ is the Euclidean norm. Once the function ρ has been defined and the approximator $NN(\theta,\bar{x})$ has been chosen, the approximation problem reduces to find the parameter θ^* for which:

$$\rho[NN(\theta^*,\bar{x}), f(\bar{x})] \leq \rho[NN(\theta,\bar{x}), f(\bar{x})] \tag{3.1}$$

for any θ belonging to the set of admissible values.

A solution to this problem, if it exists, is said to be the best approximation. It is clear that the existence of the best approximation depends ultimately on the class of the functions to which $NN(\theta,\bar{x})$ belongs.

Since other more conventional approximator methods, such as orthogonal functions, splines and polynomial, enjoy the characteristic to be universal approximators the question why neural networks or fuzzy systems should be used is legitimated.

Ultimately, the choice of which approximator to be used is dictated by practical considerations, however, it is possible to highlight some advantages that both MPN, RBFN and Fuzzy logic systems have over conventional approximation methods. One of these advantages is that all signal levels always lies in amenable bounds. On the contrary, for example when a polynomial of high-order is used to approximate a function and the magnitude of the input variable exceeds unity, the output can be very large, causing numerical problems for the determination of the parameters. The basis functions for orthogonal series are usually given in terms of look-up tables. For some application a good resolution may dictate a large number of samples requiring a large memory for storing the look-up table. All these practical disadvantages are not present in neural network and fuzzy logic based systems. Moreover, due to their parallel strongly interconnected structure, neural networks and fuzzy systems posses hardware robustness. For instance, the failure of one single component of the network will not produce major changes in the overall system's performances. These advantages in conjunction with the objective to mimic the most sophisticated controller ever designed, the brain, represents the major reasons for the research efforts made during the last twenty years in the field of intelligent control.

3.3 Universal approximation capability

The universal approximation capability of the selected approximator, is a fundamental requirement in order to guarantee the existence of a solution (i.e. the existence of the best approximator). This property, characteristic of some specific networks, will ensure that the network can approximate, with any degree of accuracy, any continous function defined in a compact set. The analytical proof of this characteristic is based on the fulfilment of the Stone-Weierstrass theorem. Originally used to prove the approximation

capability of polynomial functions, the Stone-Weierstrass theorem can be stated in different forms. The one more useful for applications, is as follows (Jin Liang *et al*, 1996):

Stone-Weierstrass theorem:

Let S be a compact set with N dimensions and let $\Omega \supset C(S)$ be a set of continuous real-valued functions on S satisfying the following conditions:

a) Identity function: The constant function $f(x) = 1$ is in Ω.

b) Separability: For any two points $x_1 \neq x_2$ in S, there exist an $f \in \Omega$ such that $f(x_1) \neq f(x_2)$.

c) Algebraic closure: For any f and $g \in \Omega$ and α and $\beta \in \Re$, the functions fg and $\alpha f + \beta g \in \Omega$.

Then Ω is dense in $C(S)$, which implies that, for any $\varepsilon > 0$ and any function $g \in C(S)$, there is a function $f \in \Omega$ such that:

$$|g(x) - f(x)| < \varepsilon \text{ for all } x \in S \tag{3.2}$$

The accomplishment of conditions *a)* and *b)* is simple to be verified, while condition *c)* will depend on the particular non-linear function used to implement the activation function. Examples of neural networks that can satisfy the Stone-Weierstrass theorem are reported in (Cybenko, 1989), where networks with sigmoidal activation functions in the hidden non-linear layer are used. (Hornick *et al*, 1989) shows that with squashing activation functions in the hidden layer the same approximation capability, of the sigmoidal networks, can be achieved.

The above results obtained for neural networks have been applied by (Wang, 1992), to prove that a fuzzy system with product inference, centroid defuzzification and Gaussian membership function satisfies the Stone-Weierstrass theorem. The result obtained by Wang however is a natural consequence of the functional equivalence between RBFNs and FISs of the type defined above (Jang and Sun, 1993). A different proof of the approximation capabilities of a fuzzy system has been given by Kosko based on the idea of fuzzy patches (Kosko, 1992).

Although all the above papers have a great practical importance and have contributed to a better understanding of network functions approximation, none of them provide a way on how many nodes (networks parameters) are needed to achieve a desired approximation error. These have to be determined by trials and error in a specific context. However, too small a network may not be able to sufficiently approximate accurately the observed input-output data, while too large a network may not be able to sufficiently generalise (i.e. interpolate) accurately.

3.4 Adaptation and learning in intelligent control

The way the adjustable parameters θ of the adaptive network are changed specify the learning or adaptation algorithm. The problem to find the best approximator, as defined above, can be formulated as an optimisation problem to find the minimum of a specified cost function. Least mean square and back-propagation algorithms are the two most used optimisation algorithms, originally formulated in the content of neural networks. More recently hybrid combinations of those approach are being used. These are briefly discussed in the following sections.

3.4.1 Least square and least mean square algorithm

Least mean square (LMS) algorithm, also known as delta rule or Widrow-Hoff learning algorithm, is an approximated steepest descent optimisation algorithm, used for the minimisation of the mean square error for linear networks (networks for which the input/output relationship is of the form: $y(\theta,u)=u\theta$). LMS algorithm falls in the supervised learning rule type. It is assumed therefore that a set of desired targets and outputs are available. The optimisation criteria to be minimised is the mean square error defined as the sum of the squares of the differences between the actually observed and the computed values and expressed in equation (3.3),

$$J(\theta)=\frac{1}{2}\sum_{i=1}^{k}\left[(d_i-y_i(\theta,u))^2\right] \tag{3.3}$$

where k is the number of data pairs d_i and y are the desired and measured output respectively. Since the measured variable is linear in the parameters θ, and the criterion (3.3) is quadratic the minimisation problem admit an analytical solution of the form: (Astrom and Wittenmark, 1995):

$$\hat{\theta}_{opt}=\left(A^TA\right)^{-1}A^Ty \tag{3.4}$$

In equation (3.4) $A\in\Re^{k\times n}$ is the matrix of input signals, n is the number of inputs and $\hat{\theta}_{opt}$ is the vector of optimal parameters in the mean square sense. In order to be able to account for new data pairs a recursive version of the mean square algorithm expressed in equation (3.4) is also available (Astrom and Wittenmark, 1995).

The problems of the least square estimator algorithm are related to the computational effort in calculating the matrix $(A^T A)^{-1}$ especially when A is not quadratic (that is when the number of measured data exceed the number of inputs $k > n$). The LMS algorithm proposed by (Widrow and Lehr, 1990) overcame this problem using a steepest descent algorithm to minimise an estimate of equation (3.3), defined by equation (3.5):

$$J(\theta) = (d_k - y_k(\theta, u))^2 = e^2(k) \tag{3.5}$$

where the sum of the squared error has been replaced by the squared error at iteration k. The gradient of equation (3.5), is then calculated at each iteration as follows:

$$\nabla J(\theta) = \nabla e^2(k) = -2(d_k - y_k(\theta, u))\frac{\partial}{\partial \theta} y_k(\theta, u) \tag{3.6}$$

In the simple case of a linear network, where the output is expressed as $y_k(\theta, u) = \theta u_k$, equation (3.6) reduces to:

$$\nabla J(\theta) = \nabla e^2(k) = -2(d_k - y_k(\theta, u))u_k = -2e(k)u_k \tag{3.7}$$

The iterative optimisation of equation (3.3) based on the approximated function (equation (3.5)) and the gradient method is expressed by equation (3.8):

$$\hat{\theta}_{k+1} - \hat{\theta}_k = -\eta \nabla J(\theta) = \eta e(k) u_k \tag{3.8}$$

where η is an adaptation gain. The beauty of equation (3.8) is its simple implementation due primarily to the available signals u_k and $e(k)$. It is possible to prove that under a proper choice of the adaptation gain and some condition on the input signals the steady state solution of equation (3.8) converges to the solution of the least square estimator (equation (3.4)). However, the main drawback of this adaptation algorithm is that it relies on the assumption that the network is linear in its parameters (equation (3.7)). If this assumption is relaxed, as in the case of MPN and general FS, the calculation of the partial derivative of the cost function (equation (3.6)), is not a trivial task. The lack in learning algorithms that could be applied to non-linear networks and the inherent limitation of the linear networks, were the main reasons for a loss of popularity of artificial neural networks techniques in the middle of the 70s. This problem was solved with the introduction of the back-propagation learning algorithm.

3.4.2 Back-propagation

The LMS algorithm or the perceptron learning rules (briefly discussed in Chapter 2 section 2.2.1) were designed to train single-layer perceptron-like networks. These networks, as pointed out in (Minsky and Papert, 1969), are able to solve only linearly separable classification problems. The awareness that this limitation could have been overcome with the use of multilayer networks was frustrated by the inability to develop efficient learning algorithms.

The major difficulty in designing a steepest descent adaptation algorithm for these class of non-linear networks, is represented by the calculation of the gradient of the approximated cost function expressed by equation (3.6), due to the non-linear relationship between the output of the network and its parameters. This problem was

efficiently solved and advertised within the neural network community by the work of (Rumelhart *et al*, 1988) and co-worker. The calculation of the partial derivative of the error signal with respect to the parameters of each single neurons of the network is solved by the use of the chain rule of calculus.

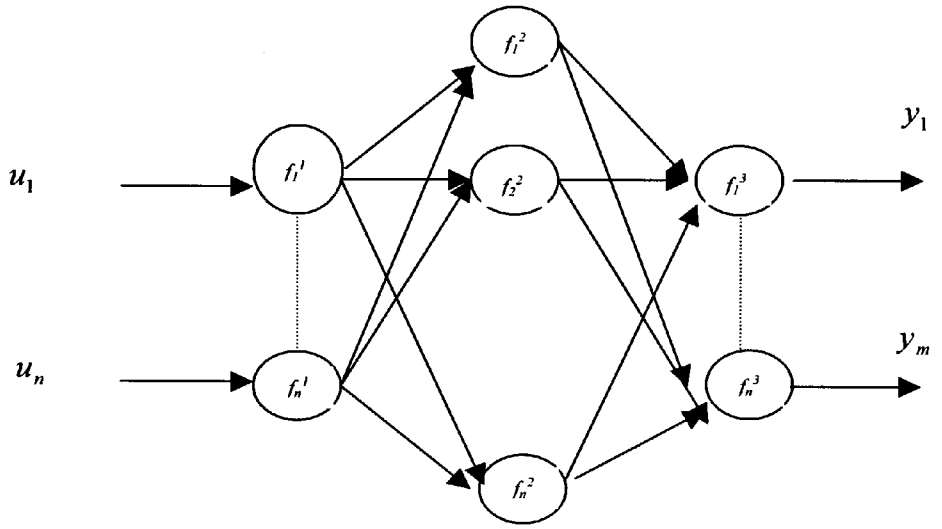

Fig.3.6: Three layer adaptive network

Suppose that a given adaptive network has L layers and N(l) nodes in layer l (see figure 3.6 with l=3). The output and function of node i of layer l can be represented as s_i^l and f_i^l respectively. Since the output of a node depends on the incoming signals and the parameter set of the node, the general expression for the output s_i^l is as follows:

$$s_i^l = f_i^l\left(s_1^{l-1},\ldots,s_n^{l-1},\theta_i^l\right) \tag{3.9}$$

In equation (3.9) θ_i^l is the parameter vector of the node and s_i^{l-1} with $i = 1,\ldots,n$ are the outputs of the n nodes of the previous layer. The error signal ε_i^l defined as:

$$\varepsilon_i^l = \frac{\partial J(\theta)}{\partial s_i^l} \tag{3.10}$$

can be interpreted as the sensitivity of the cost function (equation (3.6)) with respect the output of node i of later l. Applying the chain rule to equation (3.10), the error signal can be rewritten:

$$\varepsilon_i^l = \frac{\partial J(\theta)}{\partial s_i^l} = \sum_{m=1}^{N(l+1)} \frac{\partial J(\theta)}{\partial s_m^{l+1}} \cdot \frac{\partial s_m^{l+1}}{\partial s_i^l} = \sum_{m=1}^{N(l+1)} \varepsilon_m^{l+1} \frac{\partial f_m^{l+1}}{\partial s_i^l} \tag{3.11}$$

where N(l+1) is the number of nodes in layer l+1. Equation (3.11) states how the error signal is back-propagate from layer l+1 to layer l. At the output layer L $\varepsilon_i^L = t_{i,k} - y_{1,k}$ where $t_{i,k}$ and $y_{i,k}$, are the desired and the actual value respectively of the ith output at time k. To calculate the partial derivative of the cost function with respect the node's parameters θ_i, it is possible to apply again the chain rule of calculus as follow:

$$\nabla J(\theta) = \frac{\partial J}{\partial \theta_i} = \frac{\partial J}{\partial s_i^l} \frac{\partial s_i^l}{\partial \theta_i} = \varepsilon_i^l \frac{\partial s_i^l}{\partial \theta_i} \tag{3.12}$$

Provided the existence of the partial derivative $\frac{\partial s_i^l}{\partial \theta_i}$, the iterative optimisation of equation (3.3), based on the approximated function of equation (3.5) and the gradient method is then expressed by the following equation:

$$\hat{\theta}_{i,k+1} - \hat{\theta}_{i,k} = -\eta \frac{\partial J(\theta)}{\partial \theta_{i,k}} = -\eta \varepsilon_i^l \frac{\partial s_i^l}{\partial \theta_i} \tag{3.13}$$

Equation (3.13) is the back-propagation learning algorithm. It is implemented in two steps, a forward step where, in order to compute the output error of the network, the input u_k is propagated through the network and a back word step where the error, calculated at the output layer, is back-propagated through the network in order to calculate the partial derivative of the cost function with respect to each node parameter (equation (3.12)).

A graphical interpretation of the backpropagation learning rule can be explained by studying the single layer non-linear network represented in figure 3.7, where the non-linear function is represented by an hyperbolic tangent $y_k = \tanh(s_k) = \frac{1-e^{-2s_k}}{1+e^{-2s_k}}$ and $s_k = \theta_k u_k$.

The instantaneous error to be minimised is defined as:

$$\varepsilon_k = t_k - \tanh(s_k) \tag{3.14}$$

Equation (3.6) becomes:

$$\nabla J(\theta) = \nabla \varepsilon_k^{\,2} = \frac{\partial \varepsilon_k^{\,2}}{\partial \theta_k} = 2\varepsilon_k \frac{\partial \varepsilon_k}{\partial \theta_k} \tag{3.15}$$

From equation (3.14), the partial derivative of equation (3.15) becomes:

$$\frac{\partial \varepsilon_k}{\partial \theta_k} = -\tanh'(s_k)\frac{\partial s_k}{\partial \theta_k} = -\tanh'(s_k)u_k \tag{3.16}$$

where $\tanh'$ is the differential function of $\tanh$. Substituting equation (3.16) into (3.15) yields:

$$\nabla J(\theta) = 2\varepsilon_k \frac{\partial \varepsilon_k}{\partial \theta_k} = -2\varepsilon_k \tanh'(s_k) u_k \tag{3.17}$$

Equation (3.17) represents the equivalent of equation (3.7) when the output of the network is the tanh non-linear function. Applying the steepest descent method, the iterative optimisation of equation (3.3), based on the approximated function (equation (3.5)) becomes:

$$\hat{\theta}_{k+1} - \hat{\theta}_k = -\eta \nabla J(\theta) = \eta \varepsilon(k) \tanh'(s_k) u_k \tag{3.18}$$

which is the equivalent of equation (3.8) when the output of the activation function is a non-linear function. It should be noted that in order to implement equation (3.18) the derivative of the activation function has to be known. This constrains the applicability of the above adaptation rule (equation (3.13)) and all back-propagation based rules to networks with non-linear differentiable functions. The extension of the back-propagation algorithm, shown in figure 3.7, to an adaptive network with two inputs and two outputs is shown in figure 3.8. The network represented inside the dotted line, also known as the sensitivity network, is used for the calculation of the partial derivatives and represents the backward step in the computation of the adaptation algorithm.

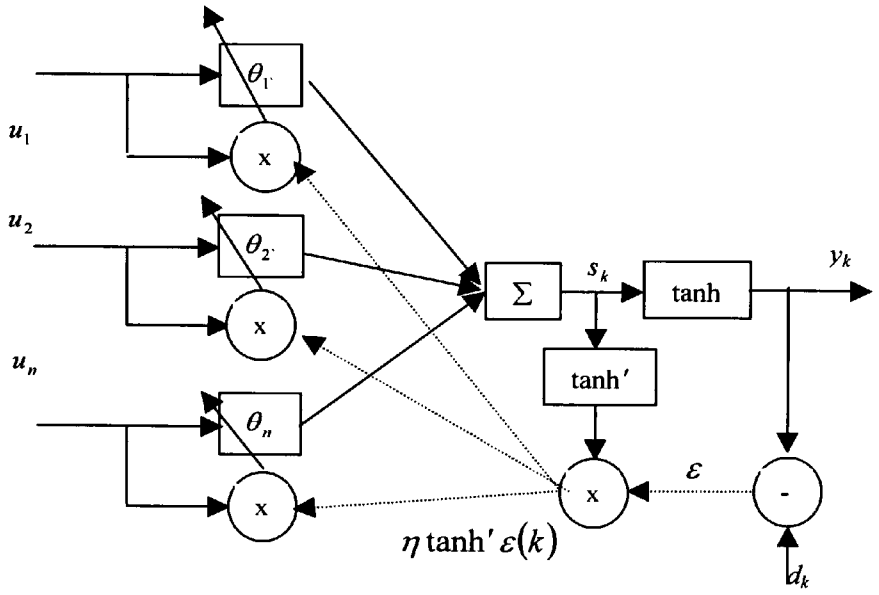

Fig.3.7: Back-propagation for one layer non-linear network

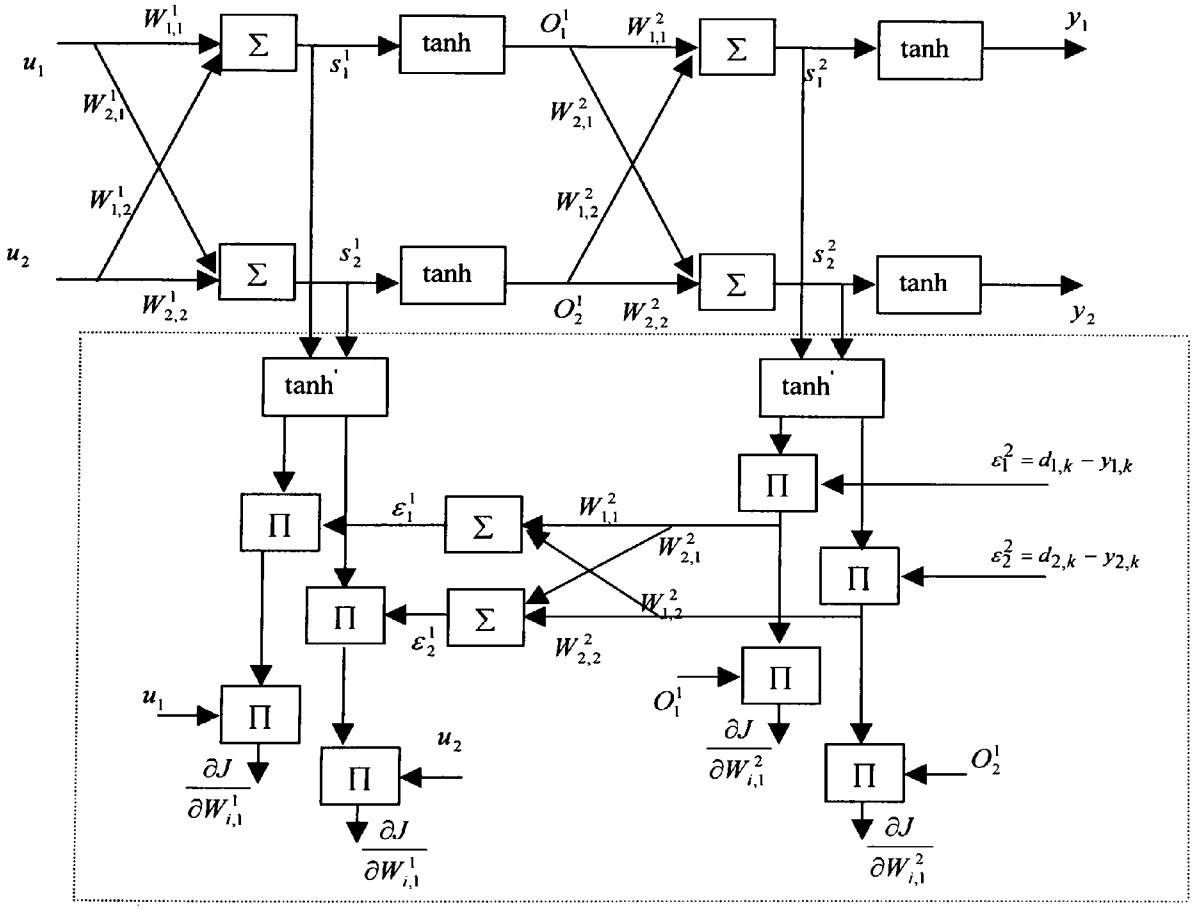

Fig.3.8: Two inputs two outputs adaptive back-propagation network

3.4.3 Hybrid learning

A combination of the back-propagation or general steepest descent methods and least square algorithm, can be used in order to speed up the learning process. By noting that all the parameters in the output layer of the adaptive network appears linear, it is possible to use the least mean square algorithm, which is faster then back-propagation, to update such parameters. Once the optimal output parameters, in the least square sense, are found back-propagation can be used to adapt the other parameters in the network. In general, as expressed in equation (3.19), the output of an adaptive node is a function of its inputs and a set of modifiable parameters.

$$y = f(x, \theta) \tag{3.19}$$

If a suitable transformation T can be applied to the function *f* such that the new output, which is the composition of T and y (written as $T \circ y$) results to be linear in some of the network parameters θ, these parameters can be adapted by least square method. It is important to note, that with this method the optimality in the choice of the linear parameters is guaranteed with respect to the transformed space parameters. However, in practical application this seams not to be of major concern. Different combination of the two learning algorithms leads to a variety of adaptive systems. For instance, it is possible to consider a first optimisation of the linear parameter only using least mean square algorithm to bootstrap the learning process based on back-propagation algorithm or it is possible to use back-propagation for the non-linear parameters while least-square for the linear ones.

3.5 Summary

In this chapter adaptive networks has been introduced. In this framework, the similarities between neural networks and fuzzy logic based systems can be exploited. In section one an example on how RBFN are functionally equivalent to a particular structure of FIS is shown. In section 2.2 it is shown how these networks can be used for solving control problem. Also the pragmatic definition of intelligent control given in the first chapter is enhanced by the presentation of few control architectures where adaptive networks can be employed. In section 2.3, the universal approximation capabilities of these networks is stated and briefly discussed. Motivated by this characteristic, the control design process reduces to finding an approximation mapping from the performance measurements to command signals. The last section describes in some detail the most widely used learning algorithms for adjusting the nodes parameters of the adaptive network.

3.6 Reference List

Astrom, K. J., and Wittenmark, B. 1995. *Adaptive Control* . 2nd ed. Addison-Wesley. 0-201-55866-1.

Cybenko, G. 1989. Approximation by superposition of sigmoidal functions. *Mathematics of Cotrol, Signals and Systems,* **2**, pp. 183-192.

Hornick, K.,Stinchcombe, M., and White, H. 1989. Multilayer Feedforward Networks are Universal Approximators. *Neural Network,* **2**, pp. 359-366.

Jang, J. S. R., and Sun, C. T. 1993. Functional Equivalence Between Radial Basis

Function Networks and Fuzzy Inference Systems. *IEEE Transactions on Neural Networks,* **4** (1), pp. 156-159.

Jin Liang,Gupta, M. M., and Nikiforuk, P. N. 1996. Approximation Capabilities of Feedforward and Recurrent Neural Networks. *In:* Madan M. Gupta and Naresh K. Sinha ed. *INtelligent Control Systems: Theory and Applications.* IEEE Press New York, pp. 234-264.

Kosko, B. 1992. *Fuzzy systems as universal approximators.* IEEE International conference on fuzzy systems. pp. 1153-1162,

Kung, S. Y.,Taur, J., and Lin, S. H. 1999. Synergistic Modeling and Applications of Hierarchical Fuzzy Neural Networks. *Proceedings of the IEEE, special issue on Computational Intelligence,* **87** (9), pp. 1550-1574.

Minsky, M., and Papert, S. 1969. *Perceptrons.* MIT Press, Cambridge, MA.

Wang, Li-Xin 1992. *Fuzzy Systems are Universal Approximators.* Proc. IEEE International Conference on Fuzzy Systems. pp. 1163-1169, San Diego.

Widrow, B., and Lehr, M. A. 1990. 30 Years of Adaptive Neural Newtorks: Perceptron, Madaline, and Backpropagation. *Proceedings of The IEEE,* **78** (9), pp. 1415-1442.

Chapter 4 Ship dynamics

4.1 Introduction

For the design of control systems the importance of a mathematical model, describing the system to be controlled, is well recognised. In the case of a ship, modelling is quite a complex task. Generally the model should describe, acceptably well, the relevant dynamics of the ship. The more complex a model is, the more difficult the controller design will become. For this reason, it is common practice to distinguish between models used for control design purposes from those used for simulation purposes. In the former, only the relevant dynamics are represented, often in a way that are compatible with the selected control design technique, while in the later it is important that the discrepancies between the real plant response and the model response is reduced. When the model used for simulation purposes is closer to the real dynamics of the ship, the simulation results will be closer to the real system performance.

This chapter introduces the Newton's equations describing the kinetics of a rigid body. Assuming the ship as a rigid body moving in six degrees of freedom, the equation describing the ship dynamics are formulated in section 4.2. In section 4.3, the hydrodynamic derivative theory is used for the formulation of the hydrodynamic forces and moments acting on the hull while criteria for the definition of different motion stability are formulated in section 4.4 (stability index and lateral stability respectively). Section 4.5 deals with the effects produced by control surfaces such as a rudder and fins, and finally in section 4.6 the most common ship mathematical models used for control design purposes are discussed.

4.2 Equation of motion in six degrees of freedom

Considering the ship as a rigid body moving in six degrees of freedom, for the description of the different motions, Newton's law can be utilised. For this purpose it is convenient to define two system frames. The inertial system frame fixed with the earth and a second system frame fixed with the rigid body. Figure 4.1 shown the two system frames while table I summarises the terminology adopted by naval architects for the description of the different motions.

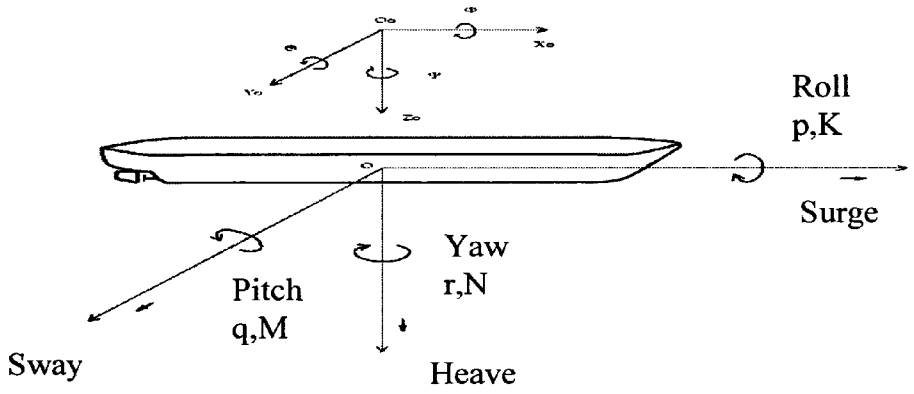

Figure 4.1: Ship's system frame

With respect the system frame shown in figure 4.1 with the origin corresponding to the centre of gravity the Newtonian equation are written as in equation (4.1) and (4.2):

$$\vec{F} = \frac{d\vec{Q}}{dt} \tag{4.1}$$

$$\vec{M} = \frac{d\vec{K}}{dt} \tag{4.2}$$

where $\vec{F}$ and $\vec{M}$ are the total force and moment acting on the hull with components:

$$\vec{F} = \hat{i}X + \hat{j}Y + \hat{k}Z$$
$$\vec{M} = \hat{i}K + \hat{j}M + \hat{k}N \tag{4.3}$$

while $\vec{Q}$ and $\vec{K}$ are the momentum and the angular momentum respectively defined as:

$$\vec{Q} = \hat{i}mu + \hat{j}mv + \hat{k}mw$$
$$\vec{K} = \hat{i}I_x p + \hat{j}I_y q + \hat{k}I_z r \tag{4.4}$$

In equation (4.4) m is the ship's mass while I_x, I_y and I_z are the moments of inertia of the body about the x, y and z axis. $\hat{i}, \hat{j}$ and $\hat{k}$ are the versors (unity vector) of the system's frame fixed with the body.

Table I (Motions terminology)

Surge	Translation along x-axis
Sway	Translation along y-axis
Heave	Translation along z-axis
Roll	Rotation along x-axis
Pitch	Rotation along y-axis
Yaw	Rotation along z-axis

The vector representation of the linear and angular velocities is respectively:

$$\vec{U} = \hat{i}u + \hat{j}v + \hat{k}w \tag{4.5}$$

$$\vec{\omega} = \hat{i}p + \hat{j}q + \hat{k}r \tag{4.6}$$

Using the following Poisson's formulae (equation 4.7):

$$\begin{aligned}\frac{d\hat{i}}{dt} &= \hat{j}r - \hat{k}q \\ \frac{d\hat{j}}{dt} &= \hat{k}p - \hat{i}r \\ \frac{d\hat{k}}{dt} &= \hat{i}q - \hat{j}p\end{aligned} \tag{4.7}$$

it is possible to prove that equation (4.1) and (4.2) become (Abkowitz, 1964):

$$\begin{aligned}X &= m(\dot{u} + qw - rv) \\ Y &= m(\dot{v} + ru - pw) \\ Z &= m(\dot{w} + pv - qu)\end{aligned} \tag{4.8}$$

$$\begin{aligned}K &= I_x\dot{p} + (I_z - I_y)qr \\ M &= I_y\dot{q} + (I_x - I_z)rp \\ N &= I_z\dot{r} + (I_y - I_x)pq\end{aligned} \tag{4.9}$$

Usually, it is convenient to choose the origin of the system's frame not corresponding with the centre of gravity. Denoting with $\vec{R}_g = \hat{i}x_g + \hat{j}y_g + \hat{k}z_g$ the vector distance from the centre of gravity to the new origin, equation (4.8) and (4.9) become:

$$\begin{aligned}&m[\dot{u} + qw - rv - x_g(q^2 + r^2) + y_g(pq - \dot{r}) + z_g(pr + \dot{q})] = X \\ &m[\dot{v} + ru - pw - y_g(r^2 + p^2) + z_g(qr - \dot{p}) + x_g(qp + \dot{r})] = Y \\ &m[\dot{w} + pv - qu - z_g(p^2 + q^2) + x_g(rp - \dot{q}) + y_g(rq + \dot{p})] = Z \\ &I_x\dot{p} + (I_z - I_y)qr + m[y_g(\dot{w} + pv - qu) - z_g(\dot{v} + ru - pw)] = K \\ &I_y\dot{q} + (I_x - I_z)rp + m[z_g(\dot{u} + qw - rv) - x_g(\dot{w} + pv - qu)] = M \\ &I_z\dot{r} + (I_y - I_x)pq + m[x_g(\dot{v} + ru - pw) - y_g(\dot{u} + qw - rv)] = N\end{aligned} \tag{4.10}$$

One of the difficulties in modelling dynamics of a ship is the way in which the hydrodynamic forces and moments acting on the hull, represented on the right hand side of equation (4.10), are characterised. A classification of these forces and moments is (Fossen, 1994):

1. Inertial-Induced Forces:

- added inertia
- hydrodynamic damping
- restoring forces

2. Propulsion Forces:

- Thrust / propeller forces
- Surface control / rudder, fins forces

3. Environmental Forces:

- Ocean current
- Waves
- Wind

In the above classification two different types of force can be distinguished; deterministic forces (types 1 and 2) and probabilistic forces (type 3). The deterministic forces are usually regarded as a polynomial expansion in terms of state variable control action and hydrodynamics coefficients. Hydrodynamic derivative theory can be applied in order to quantify the parameters of the polynomial expansion. On the contrary, the environmental forces, due to their intrinsic random nature, are usually represented as the output of a stocastic process of a known spectral density.

4.3 Hydrodynamic derivatives

The deterministic forces and moments acting on the hull (i.e. propeller thrust, rudder and fins induced forces and moments) can be represented as a function of linear and angular velocity of the ship as well as a function of control surface position (rudder and fins angles). The right hand side of equation (4.10) can be expressed as:

$$\begin{aligned} X &= X(u,v,w,p,q,r,\dot{u},\dot{v},\dot{w},\dot{p},\dot{q},\dot{r},\delta,...) \\ Y &= Y(u,v,w,p,q,r,\dot{u},\dot{v},\dot{w},\dot{p},\dot{q},\dot{r},\delta,...) \\ Z &= Z(u,v,w,p,q,r,\dot{u},\dot{v},\dot{w},\dot{p},\dot{q},\dot{r},\delta,...) \\ K &= K(u,v,w,p,q,r,\dot{u},\dot{v},\dot{w},\dot{p},\dot{q},\dot{r},\delta,...) \\ M &= M(u,v,w,p,q,r,\dot{u},\dot{v},\dot{w},\dot{p},\dot{q},\dot{r},\delta,...) \\ N &= N(u,v,w,p,q,r,\dot{u},\dot{v},\dot{w},\dot{p},\dot{q},\dot{r},\delta,...) \end{aligned} \tag{4.11}$$

It is possible therefore to consider a Taylor series expansion of such forces and moments around an equilibrium point. By limiting attention to the ships motion in the horizontal plane (x-y plane) the linear velocity w and angular velocity p and q can be neglected. Assuming fixed control surface (i.e. $\delta = 0$), equation (4.11) reduces:

$$\begin{aligned} X &= X(u,v,r,\dot{u},\dot{v},\dot{r}) \\ Y &= Y(u,v,r,\dot{u},\dot{v},\dot{r}) \\ N &= N(u,v,r,\dot{u},\dot{v},\dot{r}) \end{aligned} \tag{4.12}$$

Under the hypothesis of stable straight-line course with constant surge speed ($u = u_0$ and $v = \dot{v} = r = \dot{r} = 0$), the Taylor expansion of equations (4.12) limited to the first order terms yields (Mandel, 1967):

$$
\begin{aligned}
X &= \frac{\partial X}{\partial u}\Delta u + \frac{\partial X}{\partial \dot{u}}\dot{u} + \frac{\partial X}{\partial v}v + \frac{\partial X}{\partial \dot{v}}\dot{v} + \frac{\partial X}{\partial r}r + \frac{\partial X}{\partial \dot{r}}\dot{r} \\
Y &= \frac{\partial Y}{\partial u}\Delta u + \frac{\partial Y}{\partial \dot{u}}\dot{u} + \frac{\partial Y}{\partial v}v + \frac{\partial Y}{\partial \dot{v}}\dot{v} + \frac{\partial Y}{\partial r}r + \frac{\partial Y}{\partial \dot{r}}\dot{r} \\
N &= \frac{\partial N}{\partial u}\Delta u + \frac{\partial N}{\partial \dot{u}}\dot{u} + \frac{\partial N}{\partial v}v + \frac{\partial N}{\partial \dot{v}}\dot{v} + \frac{\partial N}{\partial r}r + \frac{\partial N}{\partial \dot{r}}\dot{r}
\end{aligned}
\tag{4.13}
$$

Considering the motion of the ship in the x-y plane with the centre of gravity in its longitudinal plane of symmetry, (y_g=0), the linearisation of the left hand side of equation (4.10) becomes i.e.:

$$
\begin{aligned}
X &= m\dot{u} \\
Y &= m\left(\dot{v} + ru + x_g\dot{r}\right) \\
N &= I_z\dot{r} + mx_g\left(\dot{v} + ru\right)
\end{aligned}
\tag{4.14}
$$

The partial derivatives of equation (4.13) are the so-called hydrodynamic derivatives and are defined as:

$$
\begin{aligned}
X_u &= \left(\frac{\partial X}{\partial u}\right)_{u=u_0} \\
X_{\dot{u}} &= \left(\frac{\partial X}{\partial \dot{u}}\right)_{\dot{u}=0}
\end{aligned}
\tag{4.15}
$$

Combining equations (4.13) and (4.14), the linearised equations of motion of a ship moving in the horizontal plane are rewritten (Abkowitz, 1964):

$$
\begin{aligned}
&\left(X_{\dot{u}} - m\right)\dot{u} + X_u\Delta u + X_{\dot{v}}\dot{v} + X_v v + X_{\dot{r}}\dot{r} + X_r r = 0 \\
&Y_{\dot{u}}\dot{u} + Y_u\Delta u + \left(Y_{\dot{v}} - m\right)\dot{v} + Y_v v + \left(Y_{\dot{r}} - mx_g\right)\dot{r} + \left(Y_r - mu_0\right)r = 0 \\
&N_{\dot{u}}\dot{u} + N_u\Delta u + \left(N_{\dot{v}} - mx_g\right)\dot{v} + N_v v + \left(N_{\dot{r}} - I_z\right)\dot{r} + \left(N_r - mx_g u_0\right)r = 0
\end{aligned}
\tag{4.16}
$$

It is interesting to note that the coefficients of the acceleration terms $\dot{u}$ and $\dot{v}$ have the mass increased by the amounts $X_{\dot{u}}$ and $Y_{\dot{v}}$ respectively. As well the coefficient of angular acceleration $\dot{r}$ has the inertia increased by the amount $N_{\dot{r}}$. These terms, that results from the hydrodynamics forces are called added mass and added inertia respectively. The combination of the added mass and inertia with the mass and inertia of the ship, are called virtual mass and virtual inertia. The name is due to the fact that the ship behaves in water with respect to acceleration as if the mass and inertia had these increased values.

It is important to note that equation (4.16) represents the dynamic of a ship moving in the horizontal plane with a surge velocity u and without considering any control or environmental effects. As will be considered later, these effects (i.e. rudder, fins etc.), will be represented by proper hydrodynamic derivative terms. The determination of the hydrodynamics derivatives can be conducted with different techniques and/or experiments. For simple geometry, for instance, strip theory can be used for the determination of the first order hydrodynamic derivative (Mandel, 1967). Special facilities named rotating arm and planar motion mechanism, are used for the determination of those parameters using a ship model in manoeuvring and towing tank test. An accurate identification of the high order hydrodynamic derivatives, for an accurate model that accounts for the cross-coupling between different motions, requires in general, an expensive test facility and sea trials.

4.4 Stability index and Lateral stability

The ability of a ship to maintain a straight-line course is strictly related to the notion of stability. Figure 4.2 shows the path of a ship, before and after a disturbance occurred

(Mandel, 1967). With respect to this figure, it is possible to distinguish between three types of stability.

Straight-line stability: a ship is straight-line stable when, after the disturbance has occurred, the ship by itself is able to regain a straight course, even though the final direction is different. (Case I in figure 4.2)

Directional stability: A directional stable ship, when the disturbance has disappeared, is able to regain the initial direction of sail. Case II and III of figure 4.2 shows this kind of stability with two different transitions, oscillatory and smooth transition respectively.

Positional stability: With this kind of stability the ship is able to regain the same path, as it would have if the disturbance had not occurred.

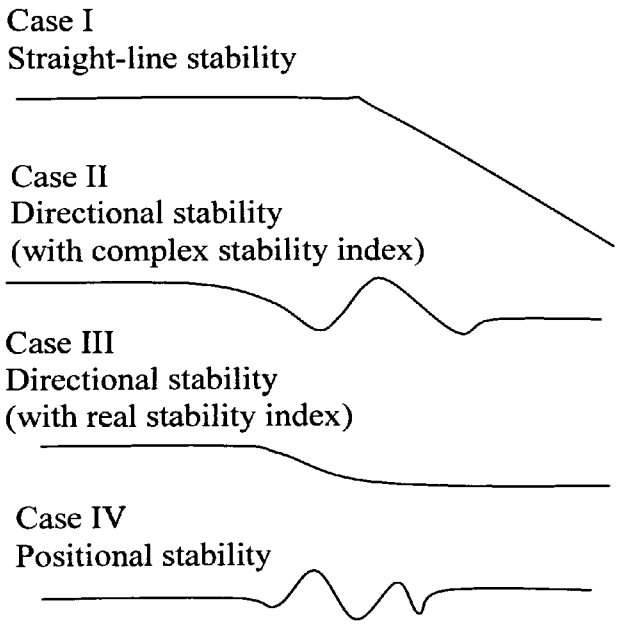

Fig. 4.2: Different kinds of stability

Without automatic control action, the best that can be obtained, for powered vessels, is straight-line stability. Directional stability, is however an intrinsical property of sailing vessels where restoring forces due to the wind blowing on sails maintain the longitudinal orientation of the ship with respect the wind direction. Control surfaces

such as rudder and/or fins are used to guarantee both stability and manoeuvrability. It is important to note in fact, that stability properties and manoeuvrability are two conflicting characteristics. A strong stability attitude implies a poor manoeuvrability characteristics and vice versa. The aim of naval architects and control engineers is to find a good compromise between stability properties and manoeuvrability characteristics for different kind of vessels.

With respect to the simplified equation of motion described by equation (4.16), considering the equilibrium in surge, the equation describing the ship' dynamic reduces to:

$$\begin{aligned}(Y_{\dot v}-m)\dot v + Y_v v + (Y_{\dot r}-mx_g)\dot r + (Y_r - mu_0)r = 0\\ (N_{\dot v}-mx_g)\dot v + N_v v + (N_{\dot r}-I_z)\dot r + (N_r - mx_g u_0)r = 0\end{aligned} \tag{4.17}$$

The standard solution of the system equation (4.17) is of the form:

$$\begin{aligned}v &= v_1 e^{\sigma_1 t} + v_2 e^{\sigma_2 t}\\ r &= r_1 e^{\sigma_1 t} + r_2 e^{\sigma_2 t}\end{aligned} \tag{4.18}$$

Here σ_1 and σ_2 are the so-called stability indexes. According to their values and sign the ship will manifest one of the different stability characteristic mentioned above. It is also possible to relate the solution of equation (4.18) to the value of the hydrodynamic derivative and therefore infer from these values the stability properties of the vessel. In (Abkowitz, 1972) it is proved that if the quantity:

$$C = Y_v(N_r - mx_g) - N_v(Y_r - m) \tag{4.19}$$

is greater then zero, the ship is straight-line stable. Equation (4.19) is also known as the stability criterion from the hydrodynamic derivative theory and is valid in the linear region of operation.

The stability index discussed above, refers to the motion of the ship in the x-y plane. Another important motion for the ship control problem occurs in the y-z plane and is labelled lateral motion (roll and heave motions). The rotation around the longitudinal x-axis (roll motion) and translation along the vertical z-axis are in fact of major concern for the safety and manoeuvrability of the ship. Considering the roll motion uncoupled with the other motions it is possible to define the lateral stability of a ship by simply considering its geometrical properties.

According to figure 4.3, for a body of mass m it is possible to define the centre of gravity (G) as the point where the total force of gravity is applied. Similarly the centre of buoyancy (indicated by C) is defined as the point where the resultant of the buoyancy force is applied. The position of the centre of gravity depends on the body's geometry while the position of the centre of buoyancy depends on the geometry of the wetted body's surface. For a body with a longitudinal symmetry (like that in figure 4.3) the two centres are located in the longitudinal plane of symmetry.

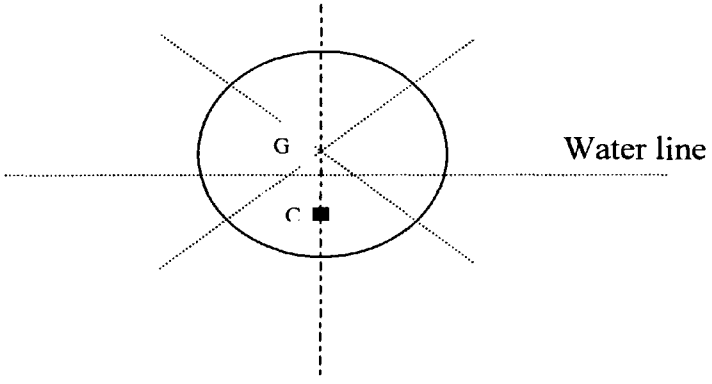

Fig.4.3: Fully symmetric buoy.

A body *is lateral stable* when the centre of gravity is located above the centre of buoyancy (as drawn in figure 4.3). Because of its full symmetry, a ball has its centre of buoyancy always located under the centre of gravity. That is the reason why the ball is completely stable. Figure 4.4, shown a lateral section of a ship heeling over an angle α to starboard. Owing to the non-symmetry from bow to stern of the ship, when it heels over a certain angle the centre of buoyancy goes out of the plane y-z. For small angles of heel (i.e. $< 10^{o}$), it is possible to consider that the new centre of buoyancy is still in the transversal plane (C'). If no change in the load occurs, the centre of gravity does not change its previous position. In this new condition, the two forces (the gravitational force P, due to the displacement of ship, and the buoyancy force S due to Archimedes' principle) generate a righting arm moment proportional to the distance $\overline{GH}$ shown in figure 4.4. The point M, in figure 4.4, is the so-called metacentric point, and it is possible to prove that as long as it is over the centre of gravity the ship is lateral stable, but when it goes below the centre of gravity the ship turns over.

The righting arm formula can be expressed as:

$$M_s = S(r-a)\sin\alpha = Sr\sin\alpha - Sa\sin\alpha \qquad (4.20)$$

Where S=P is the displacement of the ship and $\overline{GH} = (r-a)\sin\alpha$.

The term $(Sr\sin\alpha)$ is the so-called momentum of stability due to the ship's shape. The term $(Sa\sin\alpha)$ because of its sign is the so-called heel momentum. The term S (r-a) is the so-called stability coefficient, and it depends on the distance GM=(r-a) that is defined as the metacentric height.

It is now clear how the dynamics of the roll motion is strictly related to the metacentric height. If a ship has a small metacentric height, the response to a heeling force is slow, and vice versa if the ship has a large metacentric height, its response to a heeling force is fast.

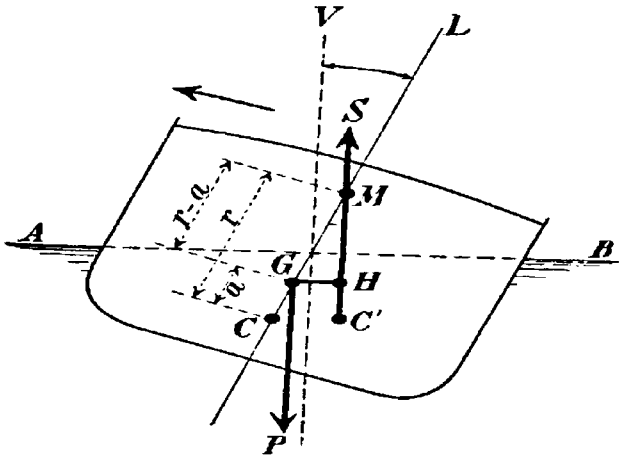

Fig.4.4: Lateral ship's section

Also for the lateral motion, a strong lateral stability implies a poor turning characteristic (high turning radius). Once more a compromise between stability properties and manoeuvrability is needed.

4.5 Models used for control

Considering the ship as a rigid body, the steering equations of motion can be deduced applying Newton's law, (Abkowitz, 1964). With respect the systems frame of figure 4.1, the motion of the ship in the x-y plane can be described by the system equation:

$$\begin{aligned} m\left(\dot{u} - vr - x_g r^2\right) &= X \\ m\left(\dot{v} + ur + x_g \dot{r}\right) &= Y \\ I_z \dot{r} + m x_g \left(\dot{v} + ur\right) &= N \end{aligned} \tag{4.21}$$

The right hand side of equation (4.21) represents the deterministic force and moment produced by the propeller thrust, control action and hydrodynamic effects. It is commonplace to consider an equilibrium situation in surge in which propeller thrust outbalances the hull resistance therefore the first equation in the system (4.21) is usually disregarded in the description of the steering dynamic. The modelling problem then resolves to determine a suitable expression for the force Y and moment N. Under the hypothesis that a linear model is satisfactory, hydrodynamic derivative theory suggests the following series expansion for the terms Y and N respectively:

$$\begin{aligned} Y &= Y_{\dot{v}}\dot{v} + Y_{\dot{r}}\dot{r} + Y_v v + Y_r r + Y_\delta \delta \\ N &= N_{\dot{v}}\dot{v} + N_{\dot{r}}\dot{r} + N_v v + N_r r + N_\delta \delta \end{aligned} \tag{4.22}$$

Substitution of equation (4.22) into (4.21), leads to the well-known linearized equation of motion expressed by equation (4.23):

$$\begin{aligned} (m - Y_{\dot{v}})\dot{v} + (mx_g - Y_{\dot{r}})\dot{r} &= Y_\delta \delta + Y_v v + (Y_r - mu_0)r + Y_0 \\ (mx_g - N_{\dot{v}})\dot{v} + (I_z - N_{\dot{r}})\dot{r} &= N_\delta \delta + N_v v + (N_r - mx_g u_0)r + N_0 \end{aligned} \tag{4.23}$$

Equation (4.23), describe the motion of a ship moving in the horizontal plane, in unrestricted deep water with constant speed.

4.5.1 Nomoto's model

By elimination of $\dot{v}$ and v, equation (4.23) can be transformed in the second order linear differential equation proposed by (Nomoto *et al*, 1957);

$$\dddot{\psi}+\left(\frac{1}{\tau_1}+\frac{1}{\tau_2}\right)\ddot{\psi}+\frac{1}{\tau_1\tau_2}\dot{\psi}=\frac{k}{\tau_1\tau_2}\left(\tau_3\dot{\delta}+\delta\right) \tag{4.24}$$

where $\dot{\psi}=r$, and

$$\begin{aligned}
\frac{k}{\tau_1\tau_2} &= \frac{N_v Y_\delta - Y_v N_\delta}{\left(Y_{\dot{v}}-m\right)\left(N_{\dot{r}}-I_z\right)-\left(Y_{\dot{r}}-mx_g\right)\left(N_{\dot{v}}-mx_g\right)} \\
\tau_3 &= \frac{\left(N_{\dot{v}}-mx_g\right)Y_\delta-\left(Y_{\dot{v}}-m\right)N_\delta}{N_v Y_\delta - Y_v N_\delta} \\
\frac{1}{\tau_1\tau_2} &= \frac{Y_v\left(N_r-mx_g u_0\right)-N_v\left(Y_r-mu_0\right)}{\left(Y_{\dot{v}}-m\right)\left(N_{\dot{r}}-I_z\right)-\left(Y_{\dot{r}}-mx_g\right)\left(N_{\dot{v}}-mx_g\right)} \\
\left(\frac{1}{\tau_1}+\frac{1}{\tau_2}\right) &= \frac{\left(Y_{\dot{v}}-m\right)\left(N_r-mx_g u_0\right)+\left(N_{\dot{r}}-I_z\right)Y_v-\left(Y_{\dot{r}}-mx_g\right)N_v-\left(N_{\dot{v}}-mx_g\right)\left(Y_r-mu_0\right)}{\left(Y_{\dot{v}}-m\right)\left(N_{\dot{r}}-I_z\right)-\left(Y_{\dot{r}}-mx_g\right)\left(N_{\dot{v}}-mx_g\right)}
\end{aligned} \tag{4.25}$$

The coefficients $\left(\frac{1}{\tau_1}+\frac{1}{\tau_2}\right)$, $\frac{k}{\tau_1\tau_2}$ and τ_3 of equation (4.24) for a conventional ship during manoeuvre at a fixed speed remain fairly constant, whereas the coefficient $\frac{1}{\tau_1\tau_2}$ changes resulting in the non-linear nature of the ship dynamics.

4.5.2 Bech's model

(Bech and Wagner-Smitt, 1969), in order to account for the change in the above parameter, proposed to include in equation (4.24) a non-linear term defined as:

$$H(\dot{\psi})=\frac{1}{k}\dot{\psi} \tag{4.26}$$

in such a way that equation (4.24) becomes:

$$\dddot{\psi} + \left(\frac{1}{\tau_1} + \frac{1}{\tau_2}\right)\ddot{\psi} + \frac{k}{\tau_1\tau_2} H(\dot{\psi}) = \frac{k}{\tau_1\tau_2}\left(\tau_3\dot{\delta} + \delta\right) \tag{4.27}$$

In (Bech, 1968) there is also described a practical way to gain some knowledge information about the non linear function expressed by equation (4.26), which led to the well-known Bech's reverse spiral test manoeuvre. In particular, under the hypothesis that the ship can be kept at a nearly constant rate of turn $\dot{\psi}_0$ with relatively small fluctuation of δ and $\dot{\psi}$, the time average of both sides of equation (4.27) gives:

$$\frac{1}{T}\int_0^T\left[\dddot{\psi} + \left(\frac{1}{\tau_1} + \frac{1}{\tau_2}\right)\ddot{\psi} + \frac{k}{\tau_1\tau_2} H(\dot{\psi})\right]dt \to \frac{k}{\tau_1\tau_2} H(\dot{\psi}_0) \quad for, T \to \infty$$

and

$$\frac{1}{T}\int_0^T \frac{k}{\tau_1\tau_2}\left[\tau_3\dot{\delta} + \delta\right]dt \to \frac{k}{\tau_1\tau_2}\delta_0 \qquad for, T \to \infty$$

leading to:

$$H(\dot{\psi}_0) = \delta_0$$

where δ_0 is the mean rudder deflection necessary to steer the ship with a constant rate of turn. The plot of the values δ_0 against the mean rate of turn can result in the two functions reported in figure 4.7 for directionally stable and unstable ships.

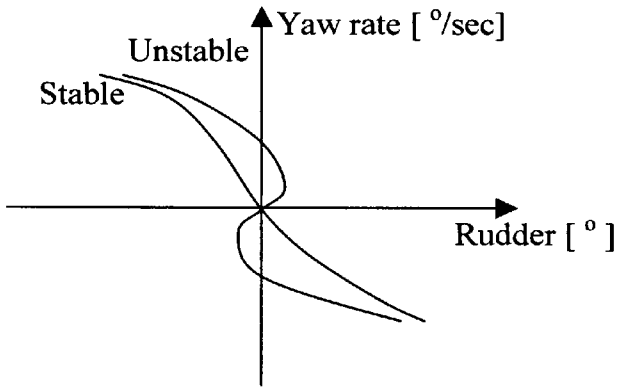

Fig. 4.7: Reversal spiral test for stable and unstable ships

4.5.3 Norrbin's model

Another well-known non-linear model describing the steering dynamics is the one proposed by (Norrbin, 1970) who proposed the following non-linear equation:

$$\tau\ddot{\psi} + H(\dot{\psi}) = k\delta \tag{4.28}$$

where again the non-linear function $H(\dot{\psi})$ describes the non-linear nature of ship dynamics and can be expressed in terms of a polynomial expansion as:

$$H(\dot{\psi}) = \alpha_3\dot{\psi}^3 + \alpha_2\dot{\psi}^2 + \alpha_1\dot{\psi} + \alpha_0$$

Norrbin suggested that, due to hull symmetry the parameter α_0 has zero value, the parameter α_1 can be set equal to unity for course stable ships and equal to (-1) for course unstable. For traditional ships, the parameter α_2 is very small so that the non-linearity of the ship dynamics can describe by the parameter α_3. Therefore equation (4.28), for a course stable ship reduces to:

$$\tau\ddot{\psi} + \dot{\psi} + \alpha_3\dot{\psi}^3 = k\delta \tag{4.29}$$

The justification of the Norrbin's model can be traced to the second-order linear model of Nomoto (equation (4.24)). In fact, Nomoto further reduced the linear model of equation (4.24) to a first-order linear model of the form:

$$\tau\ddot{\psi} + \dot{\psi} = k\delta \tag{4.30}$$

where the time constant τ is defined with respect equation (4.25) as:

$$\tau = \tau_1 + \tau_2 - \tau_3$$

It is clear that equation (4.28) differs from the first-order Nomoto model because the non-linear function $H(\dot{\psi})$, which according to Norrbin tries to describe the nonlinearities of the ship steering dynamics.

The above presented steering models, have some limitations in the description of the ship manoeuvring, due primary to the fact that the ship's dynamics are influenced as well by the forward speed. The Nomoto model, described either by equation (4.24) or

(4.30), is obtained under the assumption of constant ship speed. When the ship is involved in tight manoeuvres, the centripetal force and the rudder movement will introduce an additional drag force that changes the ship speed and therefore the dynamical response. As a consequence a Nomoto model with fixed parameters can describe only the stationary part of a manoeuvre where the speed remains fairly constant. Moreover, the parameters of the model have to be changed for different rudder angles. The model of Norrbin described by equation (4.28), being a first-order model, has the same limitation as the Nomoto model. However, having introduced the non-linear function of the yaw rate it is able to describe, with constant parameters, manoeuvres with different rudder angles. Finally the Bech's model (equation (4.27)), being a second-order model that also uses a non-linear function of the yaw rate, is able to describe non-linear manoeuvres with different rudder angles. However, different parameter settings are necessary for the description of different transition manoeuvre behaviours (i.e. with or without overshoot).

4.6 Summary

In this chapter, the basic mathematical modelling approach for the description of the dynamics of a ship is presented. Considering the ship as a rigid body, the description of the different motions is achieved by applying the Newton's law. Hydrodynamic derivative theory can be used for the inclusion of the deterministic forces and moments produced by the propeller and control surfaces. These have been described in section 4.2 and 4.3 respectively and represent the background material used for the implementation of the mathematical model used for testing the control algorithms in a simulation study. Section 4.4, discussed stability concepts which will characterises the manoeuvrability and the dynamical properties of the ship. For simplicity the discussion

considered the motions in the longitudinal plane (x-z plane) and in the lateral plane (y-z plane) separately. The main observation of this section is that a strong intrinsic stability will imply poor manoeuvrability. The importance of good and effficinet control systems that can guarantee a good balance between motion stability and manoeuvrability is therefore apparent. Finally in section 4.5, mathematical models describing the yaw dynamics used for control design purposes have been discussed. These models will be used during the control design process to describe both, different situation of *a-priori* knowledge about the system as well as to justify the choice about controller and identifier structure.

4.7 Reference List

Abkowitz, M. A. 1964. Lectures on Ship Hydrodynamics Steering and Maneuvrability. *In: Report No. Hy-5.* Hydro- OG Aerodynamisk Laboratorium Lyngby Denmark.

--- 1972. *Stability and Motion Control of Ocean Vehicles.* MIT Press.

Bech, M. I. 1968. The Reversed Spiral Test as Applied to Large Ships. *Shipping World and Shipbuilder,* pp. 1753-1754.

Bech, M. J. and Wagner-Smitt, L., 1969. *Analogue simulation of ship manoeuvres based on full scale sea trials or free sailing model tests.* Report nr. Hy-14. Hydro and aerodynamics laboratory, Lyngby, Denmark.

Fossen, T. I. 1994. *Guidance and Control of Ocean Vehicles.* John Wiley and Sins Ltd.

0-471-94113-1.

Mandel, P. 1967. Ship maneuvering and control. *In:* J. P. Comstock ed. *Principles of Naval Architecture Chapter 8.* The Society of Naval Architects and Marine Engineers.

Nomoto, K. G.,Tagachi, K.,Honda, T., and Hirano, S. 1957. On the steering quality of Ships. *International Shipbuilding Progress,* **4**

Norrbin, N. H. 1970. *Theory and obsarvation on the use of a Mathematical Madel for Ship Maneuvering in Deep and Confined Waters.* 8th Symposium on Naval Hydrodynamics. pp. 807-904, Pasadena, California.

Chapter 5 Non-linear model of a containership

5.1 Introduction

The linear equations of motion presented in chapter 4 are valid, for the description of the ship's dynamics, under the restrictive hypothesis of linearity (small perturbation around the linearisation point). When the dynamics involved in tight manoeuvres are of interest i.e. turning circle or zig-zag manoeuvres or when sailing in rough sea, the mathematical model used for simulation studies, should account for both the non-linearities as well for the cross coupling existing between the different ship's motions. The analytical development of such non-linear mathematical model is based on a Taylor expansion of equation (4.11) given in Chapter 4, which will include high-order terms. Of course equation (4.11) can be extended in order to include terms due to the presence of other control surfaces such as fins or T-foils. However, only the rudder angle is considered as control surface in the development of the mathematical model describing the dynamics of the containership used in this simulation study.

The series expansion of equation (4.11) is usually truncated to third order terms, because experience has shown that accuracy is not significantly improved by inclusion of terms higher than third order. The series expansion is also strongly simplified by exploiting the symmetry of the ship's hull. For instance, with respect the force acting on the x direction and considering the motion of the ship in the x-y plane, equation (4.11) can be rewritten as:

$$X = X(u, v, r, \dot{u}, \dot{v}, \dot{r}, \delta) \tag{5.1}$$

where δ is the rudder angle. Considering the equilibrium point characterised by a constant surge velocity ($u=u_0$) and zero for the other linear and angular velocities and accelerations ($v = r = \dot{v} = \dot{r} = 0$), the complete Taylor expansion, up to the third order terms of equation (5.1) is:

$$X = X_0 + \left[X_u \Delta u + X_v v + X_r r + X_{\dot{u}} \dot{u} + X_{\dot{v}} \dot{v} + X_{\dot{r}} \dot{r} + X_\delta \delta\right] +$$
$$\frac{1}{2!}\left[X_{uu}\Delta u^2 + X_{vv}v^2 + X_{rr}r^2 + X_{\dot{u}\dot{u}}\dot{u}^2 + ... + X_{\delta\delta}\delta^2 + 2X_{uv}\Delta uv + 2X_{ur}\Delta ur + ... + 2X_{\dot{r}\delta}\dot{r}\delta\right] +$$
$$\frac{1}{3!}\left[X_{uuu}\Delta u^3 + X_{vvv}v^3 + ... + X_{\delta\delta\delta}\delta^3 + 3X_{uuv}\Delta u^2 v + ... + 6X_{uvr}\Delta uvr + 6X_{uv\dot{r}}\Delta uv\dot{r} + ...\right] \tag{5.2}$$

where X_0 is the force in the x-direction at the equilibrium condition.

It is possible to prove that due to the geometrical symmetry of the ship along the x-z plane, the relationship between X and v, must correspond to one of the three curves shown in figure 5.1 (Mandel, 1967).

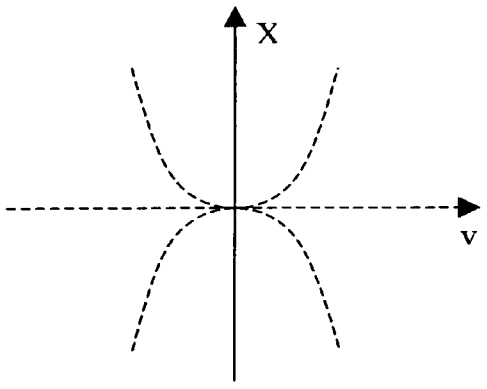

Fig. 5.1: Three possible relationships between X and v
(Mandel 1967)

All the three curves of figure 5.1, are symmetrical to the X axis, which implies that in the Taylor expansion only the even terms are different from zero while the odd terms

are all equal to zero. (Abkowitz, 1972) has showed that as a result of symmetry about x-z plane, X is also an even function of $r, \delta, \dot{v}$ and $\dot{r}$. With the above consideration, equation (5.2) simplifies to:

$$X = X_0 + X_u \Delta u + \frac{1}{2} X_{uu} \Delta u^2 + \frac{1}{6} X_{uuu} \Delta u^3 + \frac{1}{2} X_{vv} v^2 + \frac{1}{2} X_{rr} r^2 + \frac{1}{2} X_{\delta\delta} \delta^2 + \frac{1}{2} X_{vvu} v^2 \Delta u + \frac{1}{2} X_{rru} r^2 \Delta u + \frac{1}{2} X_{\delta\delta u} \delta^2 \Delta u + X_{vr} vr + X_{v\delta} v\delta + X_{r\delta} r\delta + X_{vru} vr\Delta u + X_{v\delta u} v\delta\Delta u + X_{r\delta u} r\delta\Delta u \quad (5.3)$$

This way of proceeding (exploiting the symmetry of ship's hull) simplifies the Taylor expansion and therefore the formulation of the forces (X, Y and Z) and moments (N, M and K) acting on the hull. It also reduces considerably the number of model parameters (hydrodynamics derivatives) that have to be identified. In the next section the non-linear model of a containership, used in this thesis for the simulation study of the proposed controllers, is presented.

5.2 Non-linear model of a containership

The identification study of a fast containership, the main parameters of which are given in Table I of appendix A, is described in detail in (Blanke and Jensen 1997) and (Tiano and Blanke, 1997). During the identification study, the heave and pitch motions were neglected in comparison with the others principle four motions. This is a common assumption for the identification of large tanker. In fact, due to their size, these ships will manifest a negligible coupling between heave and pitch motions with the others four principle motions. Equation 5.4 represents the non-linear equation describing the ship's dynamics in four degrees of freedom, deduced from Newton's law.

$$
\begin{aligned}
m\left(\dot{u} - vr - x_g r^2 + z_g pr\right) &= X + X_w \\
m\left(\dot{v} + ur - z_g \dot{p} + x_g \dot{r}\right) &= Y + Y_w \\
I_{zz}\dot{r} + mx_g\left(ur + \dot{v}\right) &= N + N_w \\
I_{xx}\dot{p} - mz_g\left(ur + \dot{v}\right) &= K + K_w - \rho g D R_z(\varphi)
\end{aligned}
\tag{5.4}
$$

The above equations with reference to the co-ordinate system shown in figure 4.1 of Chapter 4, describes the coupled surge, sway, yaw and roll motions, where D is the displacement, g the gravity constant, ρ the water mass density, $R_z(\varphi)$ is the action of the rightening arm that depends on the roll angle φ, while (x_G,0,z_G) are the co-ordinates of the mass centre. The mass is denoted by m whereas *Ixx* and *Izz* are the inertial moments about x and z, respectively. The linear velocity of surge and sway are u and v and the angular ones of yaw and roll are respectively r and p. The rightening arm function can be expressed as:

$$
R_z(\varphi) = \sin\varphi\left(GM + \frac{BM}{2}\tan^2\varphi\right) \tag{5.5}
$$

where GM is the ship metacentric height and BM is the distance from the centre of buoyancy to the metacentre.

5.2.1 Deterministic forces and moments

In equation (5.4), terms *X*, *Y* denote the deterministic forces acting along x and y while *N* and *K* are the deterministic moments around z and x, which take into account the hydrodynamic effects from the hull movements and forces exerted on the ship by the rudder and by the propulsion system.

By combining physical insight with hydrodynamic consideration and experience in ship modelling, (Blanke and Jensen, 1997) proposed the following expansion for the forces and moments:

Surge equation:

$$(m - X_{\dot{u}})\dot{u}_a = X_u u_a + X_{uu} u_a u_a + X_{uuu} u_a^3 + (m + X_{vr})vr + (mx_g + X_{rr})r^2 + X_\delta \delta + X_{\delta\delta}\delta^2 + X_{\delta u}\delta u_a + X_{\delta uu}\delta u_a^2 + X_v v + X_{vv}v^2 + X_{\delta v}\delta v + X_{\delta vv}\delta v^2 + X_{v\varphi} v\varphi + X_\varphi \varphi + X_{\varphi\varphi}\varphi^2 + X_{pp}p^2 + X_{ppu}p^2 u_a + X_w \tag{5.5}$$

Sway equation:

$$(m - Y_{\dot{v}})\dot{v} + (mx_g - Y_{\dot{r}})\dot{r} - (mz_g + Y_{\dot{p}})\dot{p} = -mur + Y_\delta \delta + Y_{\delta\delta}\delta^2 + Y_{\delta\delta\delta}\delta^3 + Y_v v + Y_{vv}v^2 + Y_{v|v|}v|v| + Y_{v|r|}v|r| + Y_{vrr}vr^2 + Y_r r + Y_{r|r|}r|r| + Y_{rrr}r^3 + Y_{r|v|} + Y_{rvv}rv^2 + Y_{\delta v}\delta v + Y_{\delta vv}\delta v^2 + Y_{\delta u}\delta u_a + Y_{\delta\delta u}\delta^2 u_a + Y_{\delta\delta\delta u}\delta^3 u_a + Y_p p + Y_{ppp}p^3 + Y_{pu}pu_a + Y_{pu|pu|}pu_a|pu_a| + Y_\varphi \varphi + Y_{v\varphi} v\varphi + Y_{v\varphi\varphi} v\varphi^2 + Y_{\varphi vv}\varphi v^2 + Y_0 + Y_{0u}u_a + Y_w \tag{5.6}$$

Yaw equation:

$$(mx_g - N_{\dot{v}})\dot{v} + (I_{zz} - N_{\dot{r}})\dot{r} - N_{\dot{p}}\dot{p} = -mx_g ur + N_\delta \delta + N_{\delta\delta}\delta^2 + N_{\delta\delta\delta}\delta^3 + N_v v + N_{vv}v^2 + N_{v|v|}v|v| + N_{v|r|}v|r| + N_{vrr}vr^2 + N_r r + N_{r|r|}r|r| + N_{rrr}r^3 + N_{rvv}rv^2 + N_{r|v|}r|v| + N_{\delta v}\delta v + N_{\delta vv}\delta v^2 + N_{\delta u}\delta u_a + N_{\delta\delta u}\delta^2 u_a + N_{\delta\delta\delta u}\delta^3 u_a + N_p p + N_{ppp}p^3 + N_{pu}pu_a + N_{pu|pu|}pu_a|pu_a| + N_\varphi \varphi + N_{v\varphi}v\varphi + N_{v\varphi\varphi}v\varphi^2 + N_{\varphi vv}\varphi v^2 + N_0 + N_{0u}u_a + N_w \tag{5.7}$$

Roll equation:

$$(I_{xx} - K_{\dot{p}})\dot{p} - (mz_g + K_{\dot{v}})\dot{v} - K_{\dot{r}}\dot{r} = K_v v + K_{vv}v^2 + K_{v|v|}v|v| + K_{v|r|}v|r| + K_{vrr}vr^2 + mz_g ur + K_r r - \rho g \nabla G_z(\varphi) + K_{r|r|}r|r| + K_{rrr}r^3 + K_{rvv}rv^2 + K_{r|v|}r|v| + K_\delta \delta + K_{\delta\delta}\delta^2 + K_{\delta\delta\delta}\delta^3 + K_{\delta v}\delta v + K_{\delta vv}\delta v^2 + K_{\delta u}\delta u_a + K_{\delta\delta u}\delta^2 u_a + K_{\delta\delta\delta u}\delta^3 u_a + K_p p + K_{p|p|}p|p| + K_{ppp}p^3 + K_{pu}pu_a + K_{pu|pu|}pu_a|pu_a| + K_{v\varphi}v\varphi + K_{v\varphi\varphi}v\varphi^2 + K_{\varphi vv}\varphi v^2 + K_0 + K_{0u}u_a + K_w \tag{5.8}$$

The values of the hydrodynamic derivatives are given in Table II of appendix A in non-dimensional form, according to which, the ship length L is the linear measure unit while the time unit is U/L (the time required for travelling a distance equal to the ship length). The normalised velocity u_a is defined as:

$$u_a = \frac{U - U_{cruise}}{U} \tag{5.9}$$

where $U = \sqrt{u^2 + v^2}$ is the ship's absolute velocity vector and U_{cruise} is the nominal cruise speed. The normalised velocity u_a can become negative for a non-zero sway velocity v. This condition will correspond to a decreasing in the longitudinal speed. Forces and moments are made non-dimensional by:

$$\begin{bmatrix} X' \\ Y' \\ N' \\ K' \end{bmatrix} = \frac{1}{0.5\rho U^2 L^2} \begin{bmatrix} X \\ Y \\ (1/L)N \\ (1/L)K \end{bmatrix} \tag{5.10}$$

Linear and angular velocity and acceleration are made non-dimensional by:

$$v' = \frac{v}{U}, \quad \dot{v}' = \dot{v}\frac{L}{U^2}, \; r' = r\frac{L}{U}, \; \dot{r}' = \dot{r}\frac{L^2}{U^2} \text{ where } U = \sqrt{u^2 + v^2} \neq 0 \tag{5.11}$$

The values of the above hydrodynamic derivatives were identified in the RPMM (Roll Planar Motion Mechanism) towing tank test facilities of the Danish Maritime Institute (DMI) by the authors of the original paper. Cross validation and fine-tuning of the model parameters were carried out by identification study (Tiano and Blanke, 1997) and by full scale and model scale sea trials. During model validation in sea trial tests, some differences between the model predictions and sea results were reported. For instance, the ship was found marginally stable in heading while the model was unstable and the roll damping factor of the ship was higher than predicted. It was reported that these discrepancies, between the model and the ship's response are mainly due to scale effects and some small changes in the appendages between the model and the real ship. To fit the full scale measurements to the model predicted, a re-tuning of some of the model parameters was necessary. Table III of appendix A gives the set of adjusted parameters. However, as mentioned in the original paper, these parameter adjustments cannot be taken as unique due to the fact that the multifrequency test, adopted for validation, only allowed for the adjustment of the high frequency part of the manoeuvre. The low frequency part of the sea trial manoeuvres, responsible for estimating the steady state motion, had to be adopted without change. As a consequence, validity of the model in describing manoeuvring regime cannot be guaranteed, while the dynamical response,

which is essentially for the control system design can be considered as being quite accurate.

The above equations have been implemented within the Matlab package and solved with a modified Euler method for [u,v,r,p]. The roll and yaw angles are obtained by the relations $r = \dot{\psi}$ and $p = \dot{\phi}$ while the position of the ship in the x-y plane is obtained from the relations $u = \dot{x}$ and $v = \dot{y}$. The inclusion of the disturbances and the steering dynamics is described next.

5.2.2 Disturbances modelling

The external disturbances, i.e. wind and waves, are represented by the terms X_w, Y_w, N_w, K_w in the corresponding right hand parts of equation (5.4). Such terms, owing to their intrinsically random nature, are generally quite difficult to be characterised through explicit mathematical relations. For example, as to the waves, they should be calculated by integrating the wave pressure over the immersed surface of the hull, on the assumption that the pressure within the waves is unaffected by the presence of the ship. As it has been shown in (Lewis, 1967), a reasonable simplifying assumption consists in applying a linear superposition principle, which makes it possible to separate the ship motion due to the environment from the motion induced by the rudder and by the propeller thrust.

As described in Appendix B, the wave effects have been modelled using the response operator approach, by which it is possible to reconstruct the motion of the ship induced by the waves. Response operator for different speed ($U = [0,10,15,20,22]\, m/\sec$) and

different encounter angles ($\chi = [0^o, 45^0, 90^0, 135^0, 180^0]$) were available for surge, sway roll and yaw. The induced yaw rate and roll rate can be computed by noting that from equation (B.21) of appendix B:

$$S_{zz}(\omega_n, \beta, U) = \left|R_{z\zeta}(\omega_n, \beta, U)\right|^2 S_\zeta(\omega_n, \beta) \tag{5.12a}$$

follows:

$$S_{\dot{z}\dot{z}}(\omega_n, \beta, U) = \left|R_{\dot{z}\zeta}(\omega_n, \beta, U)\right|^2 S_{\dot{\zeta}}(\omega_n, \beta) = s\left|R_{z\zeta}(\omega_n, \beta, U)\right|^2 S_\zeta(\omega_n, \beta) \tag{5.12b}$$

therefore the response operator for the rate of change can be calculated as:

$$\left|R_{\dot{z}\zeta}(\omega_n, \beta, U)\right| = \omega\left|R_{z\zeta}(\omega_n, \beta, U)\right| \tag{5.13a}$$

$$\arg\left(R_{\dot{z}\zeta}(\omega_n, \beta, U)\right) = \frac{\pi}{2} + \arg\left(R_{z\zeta}(\omega_n, \beta, U)\right) \tag{5.13b}$$

The sea spectrum formula used for this simulation study is the Pierson-Moskowitz spectrum reported in equation (B.16) of appendix B. Equation (B.27) therefore becomes:

$$\sigma_\omega^2(\omega_1, \omega_2) = \int_{\omega_1}^{\omega_2} S_\zeta(\omega_n, \beta) d\omega_n = \frac{h_{1/3}^2}{16}\left(\exp\left[-691/\omega_2^4 T^4\right] - \exp\left[-691/\omega_1^4 T^4\right]\right) \tag{5.14}$$

The tabulated response operators are interpolated each sample time according to the actual velocity and encounter angle. Equation (B.25) of appendix B can be used therefore in order to reconstruct the motion of the ship induced by the waves.

The wave induced ship's state so reconstructed (denoted by $x_{wave} = [u, v, r, p, \varphi, \psi, x, y]$) is then added to the state vector deduced by solving the differential equation (5.5), (5.6), (5.7) and (5.8). Applying the superposition principle, the motion of the ship in waves is then represented by the state vector $x_{tot} = x_{wave} + x_{\det.}$. Where $x_{\det}$ is the state produced from the deterministic forces and moments (expressed from equations 5.5 to 5.8).

It is clear, from equation (B.21) of appendix B, that when the response operators are all set equal to unity, the induced ship motion spectrum reconstructed by equation (B.25) should be equal to the sea spectrum. Figure 5.2 shows the theoretical Pierson-Moskowitz spectrum expressed by equation (B.16) (in solid line) and the spectrum reconstructed using the above approach (with circle), when the response operators are set to unity. This figure is an indirect verification of the approach's validity.

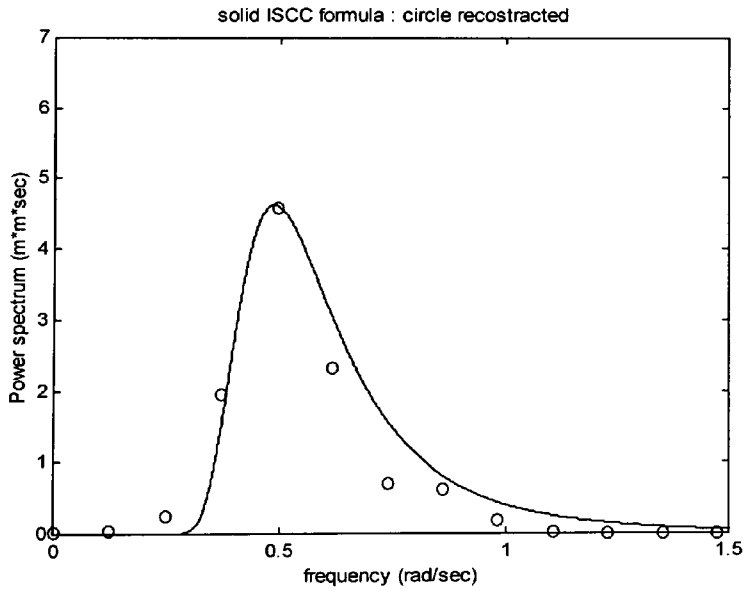

Fig.5.2: Solid Pierson-Moskowitz spectrum. With circle reconstructed from response operators

With respect the wind effects, this can be modelled using equations (B.34) and (B.35) of appendix B. The forces and moments so calculated are added to the deterministic ones

expressed in equation (5.5), (5.6), (5.7) and (5.8). The values for the coefficients C_X, C_Y and C_N of equation (5.34) are reported in table IV of appendix A. Finally the shallow water effects is described by equations (B.44). Although being a not complete model of the shallow water effects, equation (B.44) are used to test the performances of the proposed control algorithm with respect parameter's uncertanty.

The rudder actuator dynamics, can be included in the simulation by considering the simplified model given in (Amerongen, 1982). A block diagram showing the rudder dynamics is shown in figure 5.3.

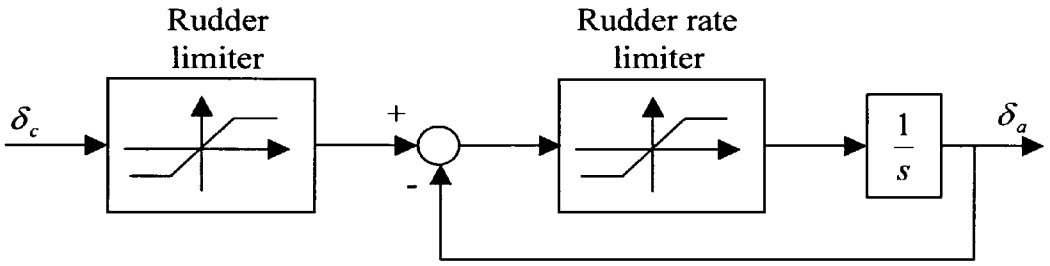

Fig.5.3: steering machine dynamic

The two rudder limits (on the maximum values and the maximum rate of change) can be implemented by two if-then statements in the main loop of the simulation algorithm. The rudder angle is then considered as part of the state vector.

5.2.3 The overall system

Figure 5.4 summarise the block diagram of the overall non-linear system used for testing the proposed control algorithms. Here the wind effects enter as external forces and moments on the right hand side of equation (5.4). The wave effects are modelled as

output disturbances and the induced ship state is added to the state vector representing the low-frequency hull motion, obtained by solving equations (5.5), (5.6), (5.7) and (5.8) with inputs rudder angle and surge velocity. The shallow water effects will produce a change in the values of some hydrodynamic derivatives according to equation (B.44) of appendix B.

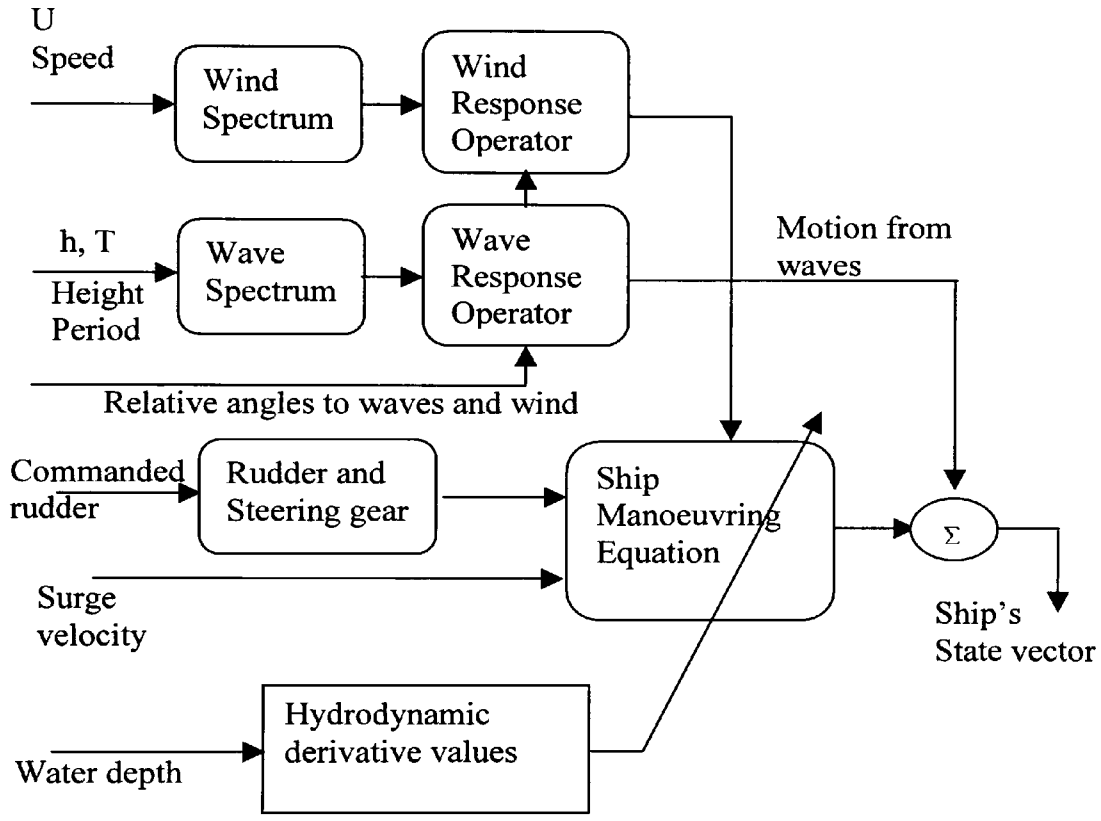

Fig.5.4: Block diagram of the complete simulated system

5.3 Manoeuvring characteristics

The manoeuvring characteristics of a ship are determined in sea trials by performing standard manoeuvres. From these manoeuvres, naval architects, can infer about the efficiency of the control surfaces (rudders and fins) and about the performance and limitation of the ship control systems. The most used manoeuvres for this purpose are the turning circle manoeuvre, the zig-zig manoeuvre and the Bech's reverse spiral test.

The turning circle manoeuvre is mainly used to identify the steady turning radius of the ship and how well the steering machine performs for course-changing manoeuvre. The turning circle manoeuvre is performed by deflecting the rudder of a certain amount (typically 15^0 to 30^0) while the ship is sailing in a straight course with constant speed. Figure 5.5 shown a simulated 30^0 turning circle manoeuvre for the containership discussed earlier. The yaw rate (shown in fig 5.5d) after about 250 seconds, ends its transition. At this point the manoeuvre is in its steady state phase. In figure 5.5b, the longitudinal speed is plotted against time, as a consequence of the drag introduced by the rudder deflection, the initial speed from 12.5 m/sec decrees to 6.5 m/sec. Figure 5.5c shows the roll angle during the manoeuvre where it is possible to appreciate the inverse response. In linear theory this effect is described by a zero in the right half s-plane of the roll-rudder transfer function. The presence of this zero, which produces a delay in the rudder/roll response, is a problem when the rudder is used for roll damping. In fact the non-exact compensation of a positive zero can compromise the stability of the overall system.

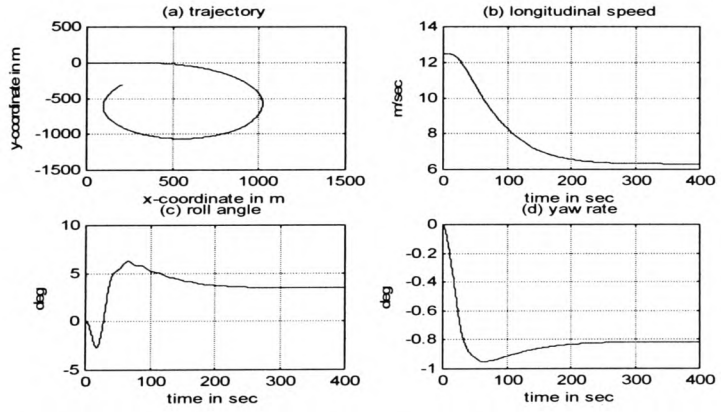

Fig.5.5: 30^0 course changing manoeuvre

Different papers have shown the effectiveness of the rudder roll damping system for a particular application (Klugt, 1987) however, it has been shown that the resultant control system suffers from poor robustness property (Blanke and Christiansen, 1993).

The zig-zag manoeuvre consists of deflecting the rudder of a certain amount i.e. 15^0 to starboard from an initial straight course with a constant speed. When the ship's head angle has changed of an amount equal to the rudder angle (15^0 for the previous example), the rudder is moved on the other side of the same amount (15^0 to port) until the ship's head angle has reached the same angle in the opposite direction (15^0 for the previous example). Figure 5.6 shown the rudder sequence and the yaw angle against time for a $15^0/15^0$ zig-zag manoeuvre. Figure 5.7 shown the yaw and roll, for the same manoeuvre. It can be seen that under this condition the motion of the ship became periodic.

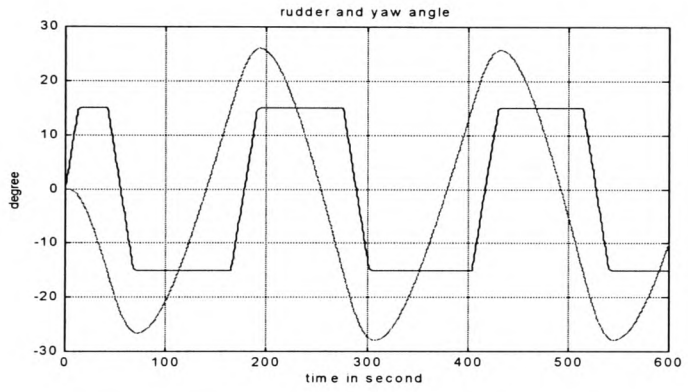

Fig.5.6: $15^0/15^0$ zig-zag manoeuvre

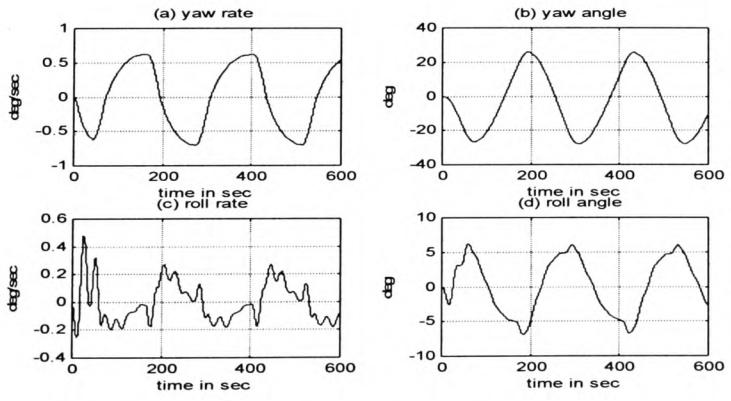

Fig.5.7: $15^o/15^o$ zig-zag manoeuvre

The Bech's reverse spiral manoeuvre is a modification of the Dieudonne's spiral test, which aim to describe the non-linear relationship between rudder angle and yaw rate. The spiral manoeuvre is also used to determine the validity range of linear approximation. The reverse spiral manoeuvre consists in steering the ship in such a way that the rate of turn is nearly constant. Figure 5.8 shows the simulated spiral manoeuvre for the course-stable containership described earlier. As pointed out by (Abkowitz, 1964), the non zero rudder angle for the zero rate of turn can be justified by asymmetries introduced by the single screw propeller. This is also in accordance with the identification study presented in the original paper of (Blanke and Jenssen 1997) where is pointed out that the ship under study is marginally stable.

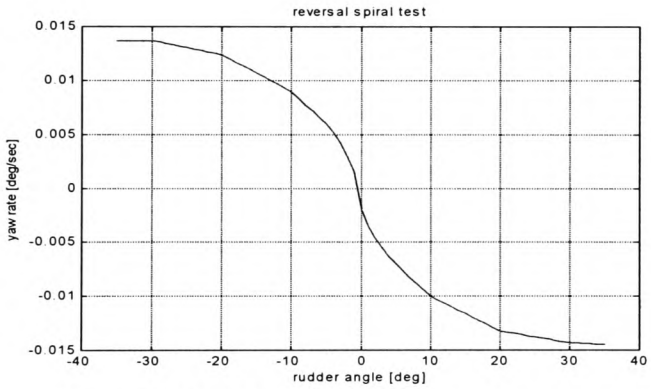

Fig 5.8: Bech's reverse spiral manoeuvre

A series of the above manoeuvres can be used for the identification of the model parameters, presented in chapter 4 for the autopilot design. The turning-circle manoeuvre is essentially a step response of the system. The data collected from this manoeuvre can be used for the characterisation of the dynamical part of the ship response. The parameters of a Nomoto model can be obtained by different identification techniques (Astrom and Kallstrom C.G., 1976) (Tiano and Volta, 1978). The reversal spiral test can be used for the identification of the static characteristic of the yaw dynamic. The non-linear function of the Norrbin model (equation (4.28)) can be

identified by a series of turning circle manoeuvre. However, in general the problem of model identifiability has to be considered. Astrom and Kollstrom investigated the identification problem and have shown that the transfer function given by the second-order model of Nomoto it is always identifiable (provided there is not pole-zero cancellation). However, the state space representation can be properly identified if the sway velocity measurement is also available. (Astrom and Kallstrom, 1976)

5.4 Summary

In this chapter the mathematical model of a containership is described in some detail. The identification study of the above containership has been done by (Blanke and Jensen, 1997) and all the data are fully available in the literature. For the sake of completeness these data are added in appendix A while appendix B give the description of the environmental disturbances. The way in which the complete mathematical model is implemented in simulation has also been described. Manoeuvring tests are briefly described at the end of the chapter. These manoeuvres are used to gain some knowledge on the dynamical response of the system which can be exploited during the control design process. For instance, appendix A describes how from a turning circle manoeuvre a second-order transfer function of the yaw rate to the rudder angle can be obtained and how the main time constant of the containership can be calculated.

5.5 Reference List

Abkowitz, M. A. 1964. Lectures on Ship Hydrodynamics Steering and Maneuvrability. *In: Report No. Hy-5.* Hydro- OG Aerodynamisk Laboratorium Lyngby

Benmark.

--- 1972. *Stability and Motion Control of Ocean Vehicles.* MIT Press.

Amerongen, J. van 1982. *Adaptive Steering of Ships: A model-reference approach to improved manoeuvring and economical course keeping.* Husdrukkerij, Delft University of Technology. Ph.D. Thesis.

Astrom, K. J., and Kallstrom C.G. 1976. Identification of Ship Steering Dynamics. *Automatica,* **12** (9), pp. 9-22.

Blanke M. and Christensen A. 1993. *Robustness of Rudder-Roll Damping course control.* Proc. 10th Ship Control Systems Symposium. Addendum 93-119. Ottawa Canada

Blanke M. and Jensen A.G. 1997. Dynamic properties of container vessel with low metacentric height. *Transactions of The Institute of Measurement and Control,* **19** (2), pp. 78-93.

Klugt, P. G. M. van 1987. *Rudder Roll Stabilization.* Delft University of Technology. Ph.D. Thesis.

Lewis, E. V. 1967. The motion of ships in waves. *In:* J. P. Comstock ed. *Principles of Navav Architecture. (Chapter 9).* New York: The Society of Naval Archotects and Marine Engineers, pp. 605-717.

Mandel, P. 1967. Ship maneuvering and control. *In:* J. P. Comstock ed. *Principles of*

Naval Architecture Chapter 8. The Society of Naval Architects and Marine Engineers.

Tiano, A., and Blanke, M. 1997. Multivariable identification of ship steering and roll motions. *Trans. Inst. Measurement and Control,* **19** (2), pp. 63-77.

Tiano, A., and Volta, E. 1978. *Application of identification techniques to ship systems.* Proc. 7th. IFAC World Congress. pp. 1583-1588, Helsinki.

Chapter 6 Autopilots designed with fuzzy set theory

6.1 Introduction

The importance of being able to exploit heuristic knowledge about the system for the achievement of better control system performances has been already pointed out in Chapter 1 section 2, about the pioneering work of Sperry. In his Metal-Mike, Sperry captured the fundamental characteristic of the helmsmen to anticipate the ship yaw motion. His engineering genius allowed him to design a commercial mechanical system that could reproduce the anticipative behaviour of the helmsmen. Nowadays, when the control system is implemented in digital computers in the form of an algorithm, fuzzy logic represents a major component in the design of a controller based on a cognitive model. In fact, when the control design process is based on cognitive models of the process to be controlled, the aim is to formulate a set of rules that can be representative of the behaviours of an expert operator, rather then to specify a set of differential equations that characterises the control system.

With respect to the course-changing problem, the steering actions of the helmsman are aimed to reduce as quick as possible the course error, without too much overshoot and with a not too large rate of turn (to keep in acceptable values the heeling angle). He or she, will base the control action on heuristic judgement of the following information:

1) the new desired heading angle, given by the officer of the watch,

2) the actual heading angle, given by the compass,

3) the ship turning rate, judged from the compass or from observing fixed points in the shore or clouds.

Based on the above observations a reasonable choice for a fuzzy course-changing controller is the PD-like fuzzy controller. In fact, the inputs of the PD-like fuzzy controller are the error and the change in the error while the output is the commanded rudder angle. A block diagram of the PD-like fuzzy controller is shown in figure 6.1.

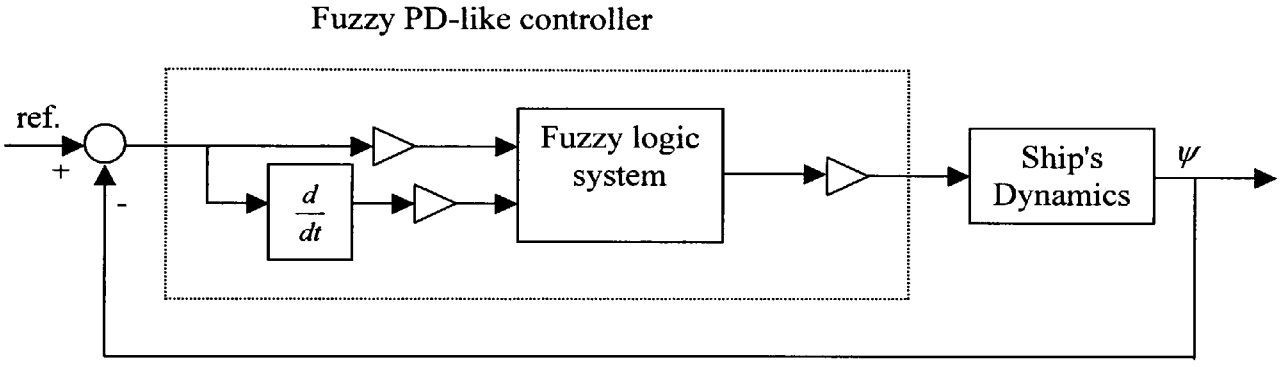

Fig.6.1: Fuzzy PD-like controller

The course-keeping problem is in general more difficult to formulate. The aim of the helmsmen is to keep the course error as small as possible, and at the same time minimising the number of rudder calls in order to reduce the induced drag force and consequent loss of speed. A possible strategy is to produce a sequence of rudder pulses with period and amplitude which are dependent on a suitable compromise between precision and loss of speed. Figure 6.2 shows a possible rudder sequence during course keeping.

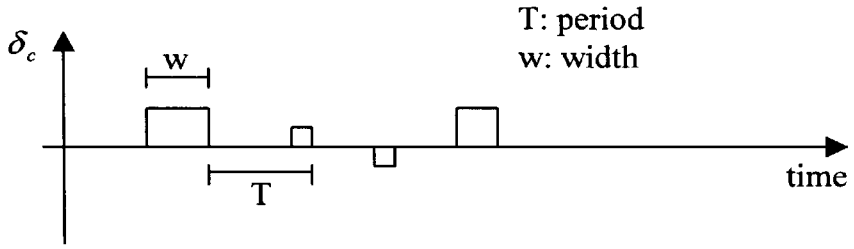

Fig.6.2: Rudder sequence during course-keeping

In the following sections of this chapter, fuzzy logic systems will be used in order to exploit the above mentioned heuristic description of the course-keeping and course-changing manoeuvres. Simulation results are reported in each of the sections while conclusions are summarised at the end of the chapter.

6.2 Fuzzy course-keeping controller

As mentioned in section 6.1 of this Chapter, a possible control strategy for the course-keeping problem is to produce a sequence of rudder pulses with period and amplitude determined by a suitable compromise between induced drag and course precision. For the determination of the period of the rudder calls, the low-pass nature of the yaw dynamics has to be considered. Too fast a rudder sequence must be avoided. Provided that the course error is in acceptable bound, the control action produced by the rudder movement should be aimed at compensating the yaw acceleration induced by the external disturbances (mainly the wave's effects). A rudder angle which is proportional and in counter phase with the yaw rate is then a possible solution.

The above control strategy can be expressed by the following set of rules:

1) IF course_error is Small and yaw_rate is Positive_Big THEN rudder=-K_y*(yaw rate) and width is Big
2) IF course_error is Small and yaw_rate is Positive THEN rudder=-K_y*(yaw rate) and width is Normal
3) IF course_error is Small and yaw_rate is Zero THEN rudder=0
4) IF course_error is Small and yaw_rate is Negative THEN rudder=-K_y*(yaw rate) and width is Normal
5) IF course_error is Small and yaw_rate is Negative_Big THEN rudder=-K_y*(yaw rate) and width is Big
6) IF course_error is Big and yaw_rate is Any THEN rudder=-K_p*(error)

Rules from one to five produces rudder angles which are proportional and in counter phase with the yaw rate and at the same time specifies the duration of the pulse (width). The action of these first five rules, is aimed to produce a control action which respond as quickly as possible to deviation from the straight course. These rules apply when the course error is in an acceptable bound. When the course error increases rule six takes over and the rudder angle is determined by a proportional type controller. In such a case, if the external disturbances are particularly strong, the control action can degenerate into a bang-bang controller. The period of each sequence in the above strategy is considered fixed and only the width is determined (see figure 6.2), however a set of rules can be introduced in order to determine this variable too.

An interpretation of the above control strategy can be attempted by considering the series expansion of the pulses sequence. Equation (6.1) and (6.2) express the Fourier transformation and its coefficients respectively.

$$\delta(t) = \frac{1}{T}\sum_{n=-\infty}^{\infty} F_n e^{jn\omega t} \tag{6.1}$$

$$F_n = \int_{-T/2}^{T/2} \delta(t) e^{-jn\omega t} dt = 2\delta_{\max} w \frac{\sin(n\omega w)}{n\omega t} \tag{6.2}$$

From equation (6.2) it is clear that the amplitude of the Fourier coefficients is proportional to the width (w) of the pulses while the number of harmonic in the first lobe are inversely proportional to w. Increasing w therefore will increase the amplitude of the harmonics while the number of the significant harmonics will be reduced. For a fixed period T this is equivalent to increasing the low frequency contribution. On the contrary if roll damping is attempted, higher frequencies of the control signal are of interest. The value of w therefore should be reduced. However, this will reduce the amplitude of each harmonics that can be re-amplified by increasing the value of $\delta_{\max}$. This is why, for roll damping faster and larger rudder movements are needed. The constrains on the steering machine dynamics therefore play a major role for the achievement of this objective (Klugt, 1987).

In order to guarantee that phase lags between the rudder angle and the yaw rate signal are not introduced by the limited rudder speed, the rudder angle has to be limited to a maximum value. It has been suggested (Amerongen and Naute Lemke, 1980) that in order to avoid the saturation of the rudder rate the following inequality must hold:

$$\frac{\delta_{max}}{\dot{\delta}_{max}} < 0.2\tau \tag{6.3}$$

where τ is the main time constant of the ship. For a value of $\tau \approx 15$ seconds and $\dot{\delta}_{max} = 2.5$ deg/sec the maximum allowed rudder angle is approximately 7.5^{o}.

The membership functions associated to the linguistic variables course_error, width and yaw_rate are represented in figure 6.3, figure 6.4 and figure 6.5 respectively. As pointed out in Chapter 2, a two outputs fuzzy system can be implemented by two single output fuzzy systems. This is due to the fact that the output of rule one is equivalent to the outputs of the two rules implemented by two different fuzzy systems i.e.:

1.a)IF course_error is Small and yaw_rate is Positive_Big THEN rudder=-K_y*(yaw rate)

1.b) IF course_error is Small and yaw_rate is Positive_Big THEN width is Big

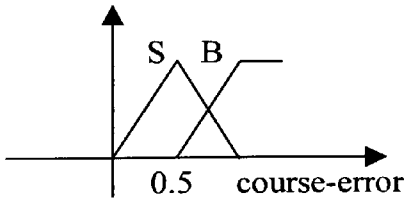

Fig.6.3: Membership functions for the absolute value of the course error

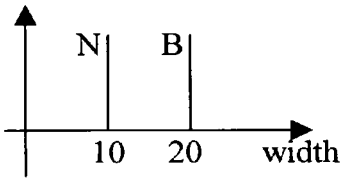

Fig.6.4: Membership functions for the pulse width

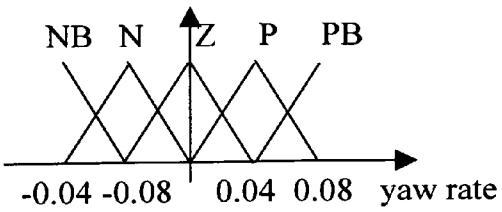

Fig.6.5: Membership functions for the yaw rate

Two Takagi-Sugeno fuzzy systems, with singleton fuzzification, product inference and centre average defuzzification, are used for implementing the control strategy expressed by the above rules. For simplicity the value of K_p is set equal to unity while K_y is determined heuristically from the following considerations. From the reversal spiral curve, shown in Chapter 5 section 5.3, it is seen that a steady rudder angle of 10^o will produce a steady turning rate of about 0.5 degree/sec. There is therefore a gain of approximately 20 seconds between the rudder angle and the rate of turn. However, this applies to steady conditions only, and to have an effective response to the rudder angle, the gain has to be increased by a factor which is proportional to the main time constant of the yaw dynamic. A factor of 5 can be chosen for the containership used in this study, leading to values of K on the order of one hundred. Figures 6.6 and 6.7 show the surge speed with the yaw angle, and the rudder angle with the yaw rate for a course-keeping manoeuvre.

The disturbances are defined, with respect the Pierson-Moskowitz spectral density, by an average period of 9 seconds and a significant wave height of 5 meters. The angle of attack for the waves is 90^o (beam sea). From these figures it is possible to appreciate the effectiveness of the controller in terms of loss of speed and course error.

The controller described above was tested for a change in the ship speed and for different angles of attack. While in head sea at cruise speed the performances were still acceptable, in following sea conditions the course-keeping controller performed poorly. Figures 6.8 and 6.9 shown the surge velocity with the yaw angle, and the rudder angle with the yaw rate respectively for the course-keeping manoeuvre when the angle of attack is 30^o.

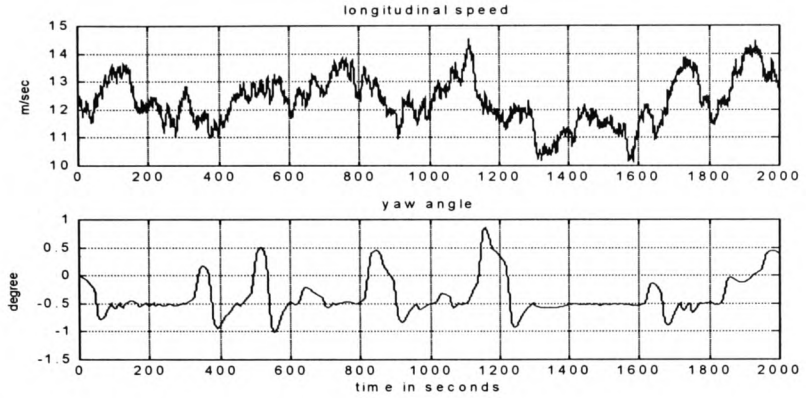

Fig.6.6: Surge velocity and yaw angle for a course-keeping in beam sea

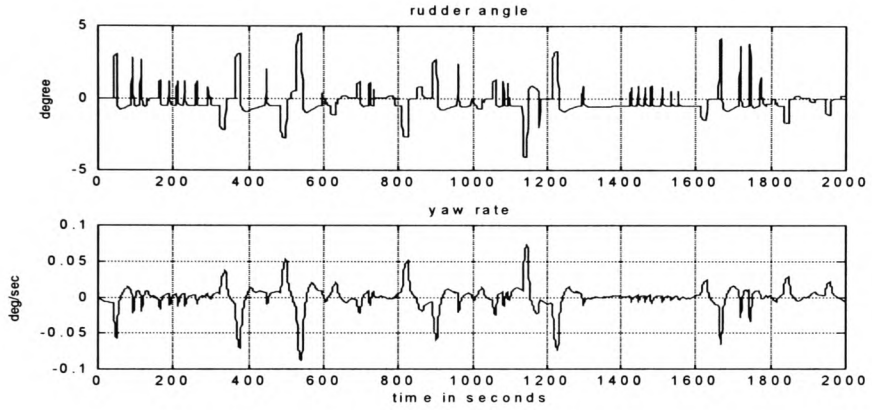

Fig.6.7: Rudder angle and yaw rate for a course-keeping in beam sea

The performances of the course-keeping autopilot can be improved by further adjustment of the controller parameters as well as by expanding the rule base knowledge. However, the final performances of such a control system will be much dependent upon the skill and experience of the designer. Therefore, an automatic procedure to deal with the above mentioned problems is desirable and can be achieved by exploiting the adaptive and learning properties of the adaptive networks discussed in Chapter 3.

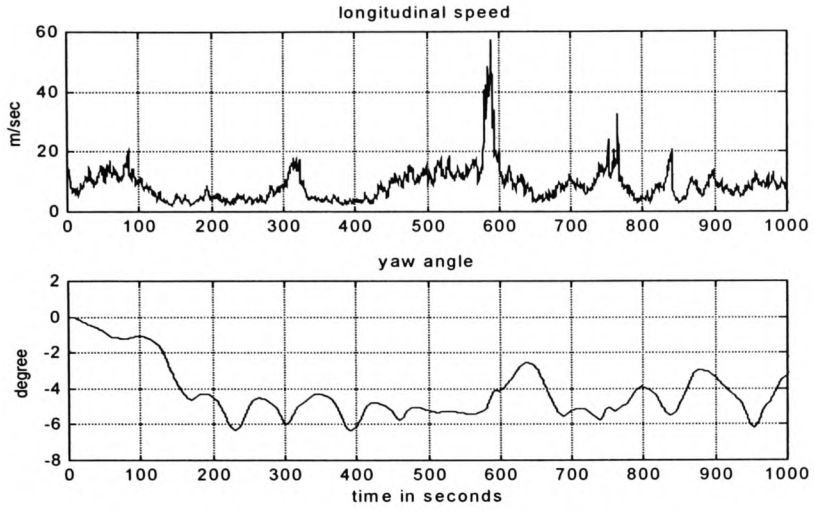

Fig.6.8: Surge velocity and yaw angle for course-keeping in following sea

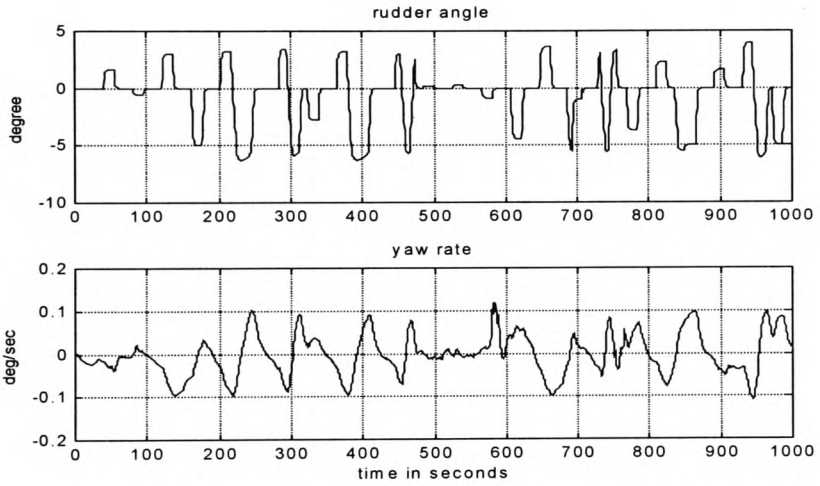

Fig.6.9: Rudder angle and yaw rate for a course-keeping in following sea

6.3 Fuzzy course-changing controller

As discussed in the previous section, a fuzzy PD-like controller, for implementing the course-changing autopilot, represents a viable choice for the controller structure. In order to simplify the parameters setting of the fuzzy controller, a normilised universe of discourse for the inputs and output variables is chosen. To re-scale the inputs and output of the fuzzy controller, to the proper domain, inputs and output gains are used. When no

a-priori knowledge, on the dynamics of the system to be controlled are assumed, the input and output universe of discourse are uniformely divided in different regions. To each of these regions a fuzzy membership function is associated. In the particular case of the fuzzy course-changing autopilot, seven linguistic variables have been defined such as "Zero", "Positive-Small", "Positive", "Positive-Big", "Negative-Small", "Negative" and "Negative-Big". Each linguistic variable is described by a triangular membership function, with centres uniformely distributed in the interval [-1, +1] and width such that a 50% overlapping is achieved.

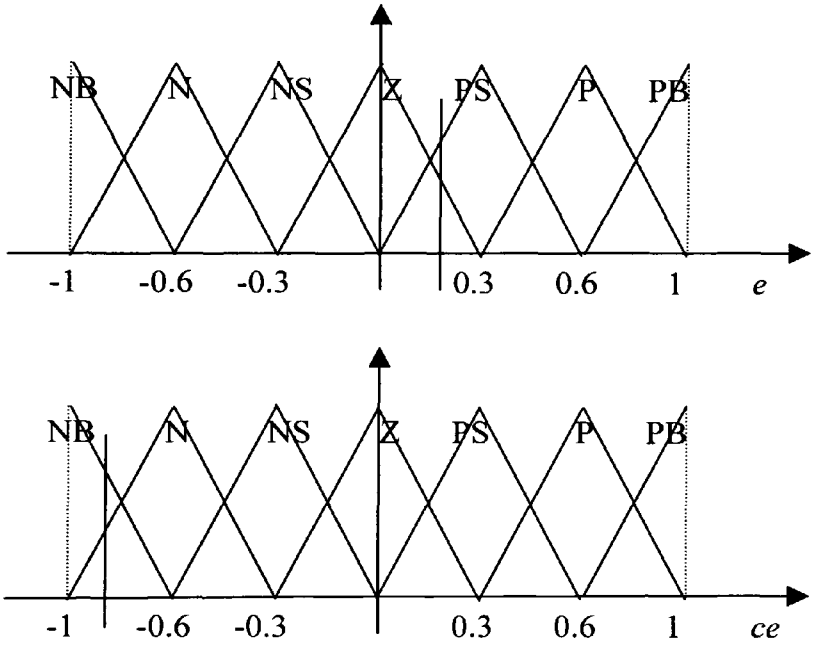

Fig.6.10: Input membership functions fired for $e(t)$=0.2 and $ce(t)$=-0.8

Figure 6.10 shown the seven triangular membership functions in the normilised universe of discourse for both the error and the change in the error. With two inputs and seven linguistic variables the number of rules in the base-knowledge are 49. In order to implement the PD-like fuzzy controller, a zero-order Takagi-Sugeno fuzzy system is used so that the output controller parameters are reduced to 49. The PD-like fuzzy

controller described above with singleton fuzzification, product inference and centre average defuzzification is described by equation (6.4):

$$y(\bar{x}) = \frac{\sum_{i=1}^{m} \delta_i \left(\prod_{j=1}^{n} \mu_{A_j}(x_j) \right)}{\sum_{i=1}^{m} \left(\prod_{j=1}^{n} \mu_{A_j}(x_j) \right)} \tag{6.4}$$

where m=49 and n=2. The complete rule-base knowledge is given in table I when the output membership functions are uniformly distributed in the normalised output universe of discourse.

Table I (49 rules base knowledge for the fuzzy controller)

Error / **C_error**	**NB**	**N**	**NS**	**Z**	**PS**	**P**	**PB**
NB	-1	-1	-0.6	-0.6	-0.3	-0.3	0
N	-1	-0.6	-0.6	-0.3	-0.3	0	0.3
NS	-0.6	-0.6	-0.3	-0.3	0	0.3	0.3
Z	-0.6	-0.3	-0.3	0	0.3	0.3	0.6
PS	-0.3	-0.3	0	0.3	0.3	0.6	0.6
P	-0.3	0	0.3	0.3	0.6	0.6	1
PB	0	0.3	0.3	0.6	0.6	1	1

In order to optimise the performance of the resultant fuzzy controller the learning techniques discussed in Chapter 3 can be used. An alternative, described in the following, is to attempt the optimisation of the fuzzy controller based on the heuristic knowledge of the system to be controlled. (Procyk and Mamdani, 1979) were the first to use the linguistic information of the controlled process to perform the optimisation of the controller parameters. (Layene and Passino, 1998), subsequently extended this idea to the model reference adaptive approach, the structure of which is represented in figure 6.11.

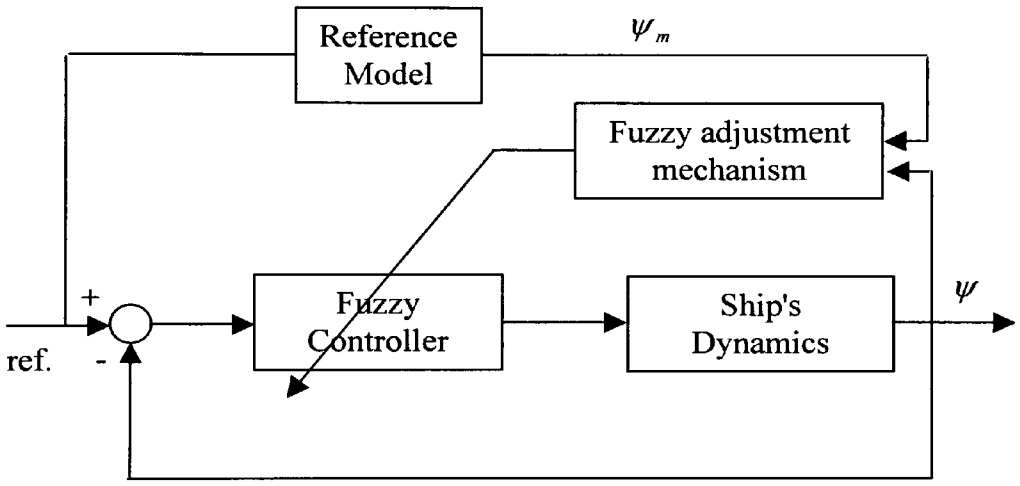

Fig.6.11: Model reference adaptive fuzzy autopilot

The objective in the model reference adaptive fuzzy autopilot, is to design a fuzzy logic system that can infer about the changes upon certain controller parameters in order to improve the performance of the closed loop system. Similarly to the adaptive control framework, where the adaptation is produced by the so-called adjustment mechanism, here the block that produces the adaptation is referred to as the fuzzy-adjustment-mechanism.

For the design of such a fuzzy adjustment mechanism, knowledge of the dynamic system to be controlled is needed. For instance, in the particular case of a course-changing autopilot it is possible to define the following adaptation strategy.

Suppose that with the input $\delta(kT)$ the tracking error at time T $(e_i(kT) = \psi(kT) - \psi_m(kT))$ is positive. If the input at time kT would have been $\delta(kT) + \varepsilon$, where ε represents an extra effort from the controller, it is expected that the error at that time would have been less. Therefore ε represents the correction that the controller has to produce in its output as a consequence of the adaptation. In others words, ε can be seen as a measure of the correction (adaptation) that has to be produced by the fuzzy adaptation mechanism. A rule that can represent this situation is:

IF tracking error is Positive THEN ε is Positive

In principle the fuzzy adjustment mechanism can also include rules which account for saturation of the rudder angle or rules which account for the coupling between yaw and roll motion. However, in this case the design of the overall system will be complicated.

For the fuzzy system described by equation (6.4), in order to increase the output value (by the amount ε) it is sufficient to increase the value of δ_i. By changing δ_i into $\delta_i + \varepsilon$ the output of the fuzzy controller will increase of an amount proportional to ε. It is possible therefore to use a fuzzy logic system in order to infer about the amount of change to be made on the output parameters of the PD-like fuzzy controller. Using a fuzzy logic system with the same structure as the PD-like fuzzy controller, described by equation (6.1), with inputs the tracking error and the change in the tracking error and

output the amount of change in the controller parameters, with the same seven linguistic variables defined before, the 49 rules describing the adaptation strategy are as follows:

$$\text{IF } e_t \text{ is Z and } ce_t \text{ is Z THEN } \varepsilon = \varepsilon_1$$

$$\vdots$$

$$\text{IF } e_t \text{ is P and } ce_t \text{ is P THEN } \varepsilon = \varepsilon_{49}$$

where e_t and ce_t are the error and change in the tracking error respectively. The input and output membership functions of the fuzzy adjustment mechanism are uniformily distributed in the normilised universe of discourse. However, for the tuning of the inputs and output gains there are not explicit guidelines and the tuning is based entirely on heuristic judgement of the system performance (Layene and Passino, 1998).

It is important to note, that at each time (kT) with inputs e(kT) and ce(kT) the output of the fuzzy controller is mainly determined by those rules with the antecedent part described by membership functions with centre close to the inputs value. This is shown schematically in figure 6.10, for input values defined as $e(t) = 0.2$ and $ce(t) = -0.8$.

For the condition expressed by figure 6.10, the subset of rules which will contribute to the output are:

If e is PS and ce is NB **Then** u is $\delta_6 = -0.3$

If e is PS and ce is N **Then** u is $\delta_7 = -0.3$

If e is Z and ce is NB **Then** u is $\delta_{11} = -0.6$

If e is Z and ce is N **Then** u is $\delta_{12} = -0.3$

It is possible to consider this local behaviour of the system in order to speed up the adaptation process by changing only the parameters that belong to those rules for which the actual contribution to the output is greater then a certain threshold. The subset of controller parameters that will be adjusted in the above example is represented therefore by $\{\delta_6, \delta_7, \delta_{11}, \delta_{12}\}$. If in the system to be controlled a time delay is present, (i.e. the actual output is produced by previous input values), it is important that the parameter adjustment is referred to those rules that contributed to the present output. In the particular case of the ship's dynamics, motivated by the Norrbin or Bech's model, a time delay of one time step has to be considered. In other words, the amount of change inferred by the fuzzy adjustment mechanism refers to the set of rules which were fired in the previous time step. With this approach, the optimisation of the system's performances is achieved by a non-linear equation defined through a set of linguistic rules.

The above control algorithm was tested in simulations involving the containership described in Chapter 5. Different environmental conditions, as described in Appendix B, as well as different initial conditions for the controller parameters were tested, i.e. all the output controller parameters being set to zero or uniformly distributed in the output universe of discourse. Figure 6.12 shows a 30° course-changing manoeuvre performed with wave conditions defined, with respect the Pierson-Moskowitz spectral density (equation (B.16)), by a significant wave height of 3 metres, average period of 8 seconds and starting angle of attack of 60°. The dotted line represents the reference manoeuvre while the solid line represents the ship's heading angle. The time history of the rudder angle is shown on the right side of the figure. Figure 6.13 shows the time history of some of the state variables (yaw rate, roll rate and roll angle) as well as (top left corner) the output of the fuzzy adjustment mechanism.

Trial and error adjustment to the gains of both the controller and fuzzy adjustment mechanism resulted in the manoeuvre shown in figure 6.12. However, when the same set up was used to perform a different sequence of course-changing manoeuvres for different surge velocities, the controller performed poorly.

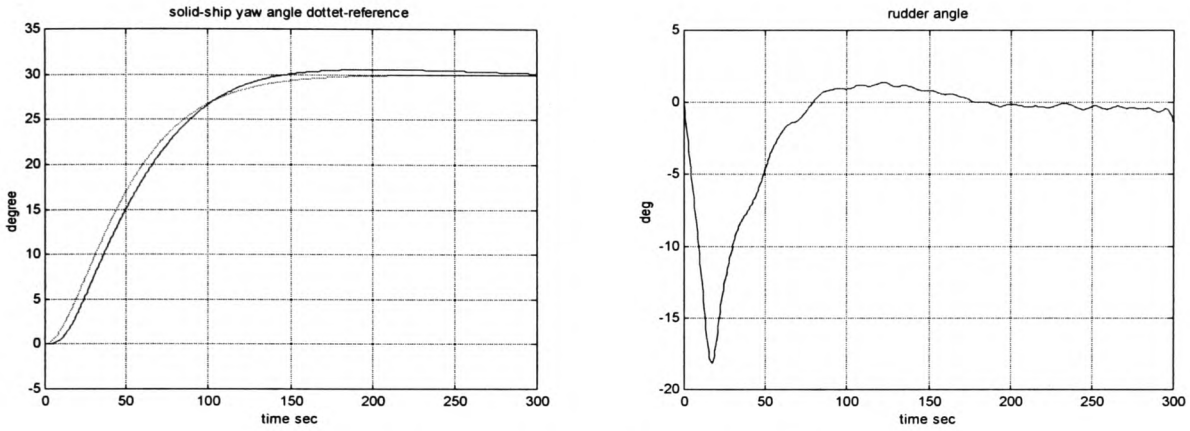

Fig.6.12: 30° course-changing manoeuvre

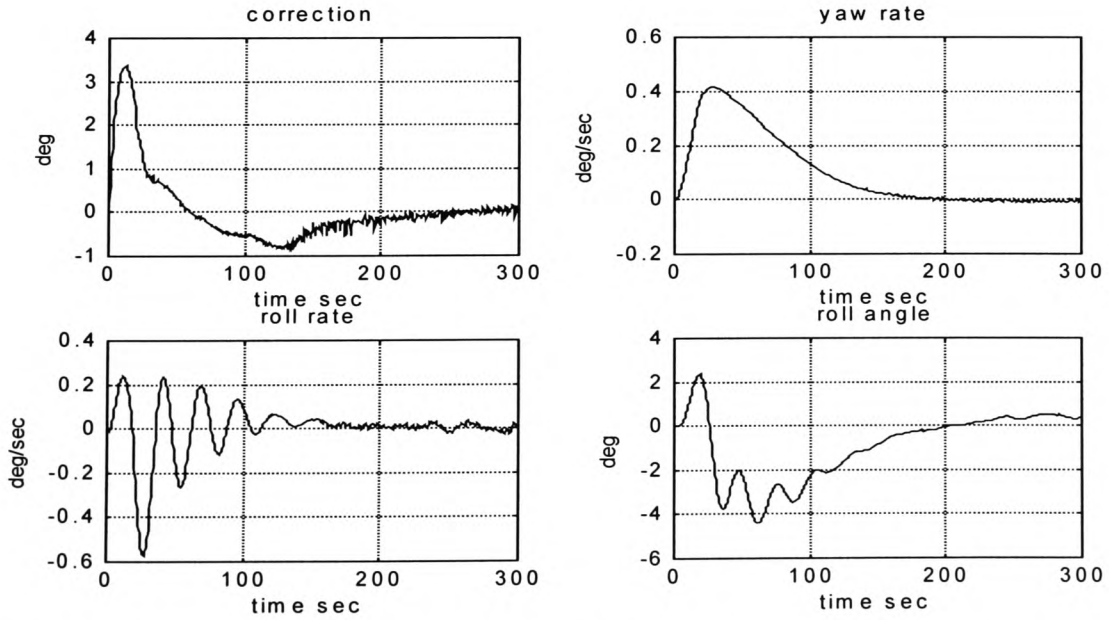

Fig.6.13: State variables and correction signals for the 30° course-changing manoeuvre

A significant improvement of the controller performances was achieved by increasing the number of rules in the knowledge base. Considering eleven linguistic variables such as "Negative-very-big", "Negative-big", "Negative", "Negative-small", "Negative-very-small", "Zero", "Positive-very-small", "Positive-small", "Positive", "Positive-big" and "Positive-very-big", the total number of rules becomes 121 which are shown in Table II. For the zero-order Takagi-Sugeno controller (given in equation (6.4)) the output adjustable parameters are also 121.

Table II (121 rules base knowledge for the fuzzy controller)

Error / **C_error**	**NVB**	**NB**	**N**	**NS**	**NVS**	**Z**	**PVS**	**PS**	**P**	**PB**	**PVB**
NVB	-1	-1	-0.8	-0.8	-0.6	-0.6	-0.4	-0.4	-0.2	-0.2	0
NB	-1	-0.8	-0.8	-0.6	-0.6	-0.4	-0.4	-0.2	-0.2	0	0.2
N	-0.8	-0.8	-0.6	-0.6	-0.4	-0.4	-0.2	-0.2	0	0.2	0.2
NS	-0.8	-0.6	-0.6	-0.4	-0.4	-0.2	-0.2	0	0.2	0.2	0.4
NVS	-0.6	-0.6	-0.4	-0.4	-0.2	-0.2	0	0.2	0.2	0.4	0.4
Z	-0.6	-0.4	-0.4	-0.2	-0.2	0	0.2	0.2	0.4	0.4	0.6
PVS	-0.4	-0.4	-0.2	-0.2	0	0.2	0.2	0.4	0.4	0.6	0.6
PS	-0.4	-0.2	-0.2	0	0.2	0.2	0.4	0.4	0.6	0.6	0.8
P	-0.2	-0.2	0	0.2	0.2	0.4	0.4	0.6	0.6	0.8	0.8
PB	-0.2	0	0.2	0.2	0.4	0.4	0.6	0.6	0.8	0.8	1
PVB	0	0.2	0.2	0.4	0.4	0.6	0.6	0.8	0.8	1	1

The above controller was then tested for a sequence of course changing manoeuvres. Figure 6.14 shows a typical sequence of such reference angles performed with

disturbances as defined for the previous manoeuvre, while figure 6.15 shows some of the corresponding state variables and the adjustment signals. Finally, figures 6.16 and 6.17 shows the course-changing manoeuvre, when at time 500 seconds the surge velocity is changed from 12.5 m/sec to 7 m/sec. The tracking error shown in the last two course changes is due mainly to the fact that at this speed the ship is unable to follow the desired manoeuvre. In fact, although the rudder angle is saturated the corresponding yaw rate is lower than the values achieved in the previous turning.

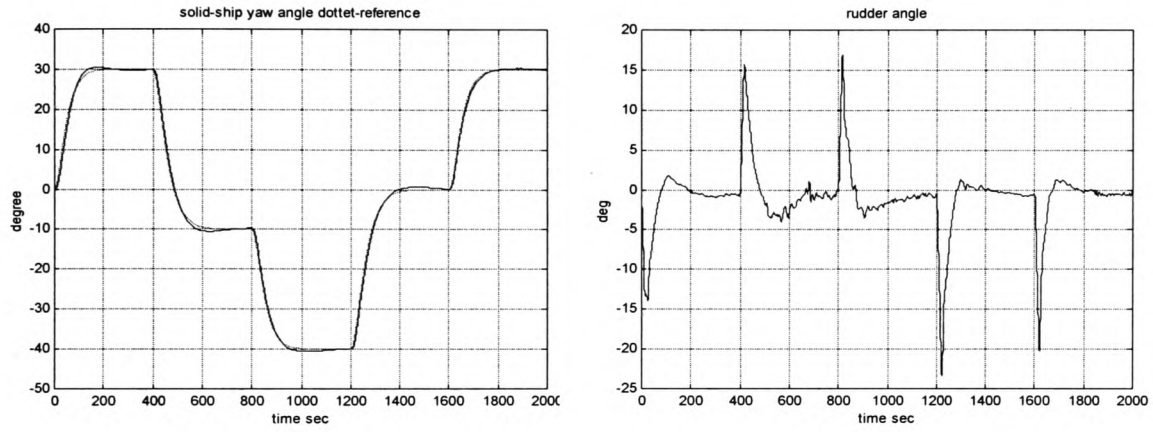

Fig.6.14: Sequence of course-changing manoeuvres

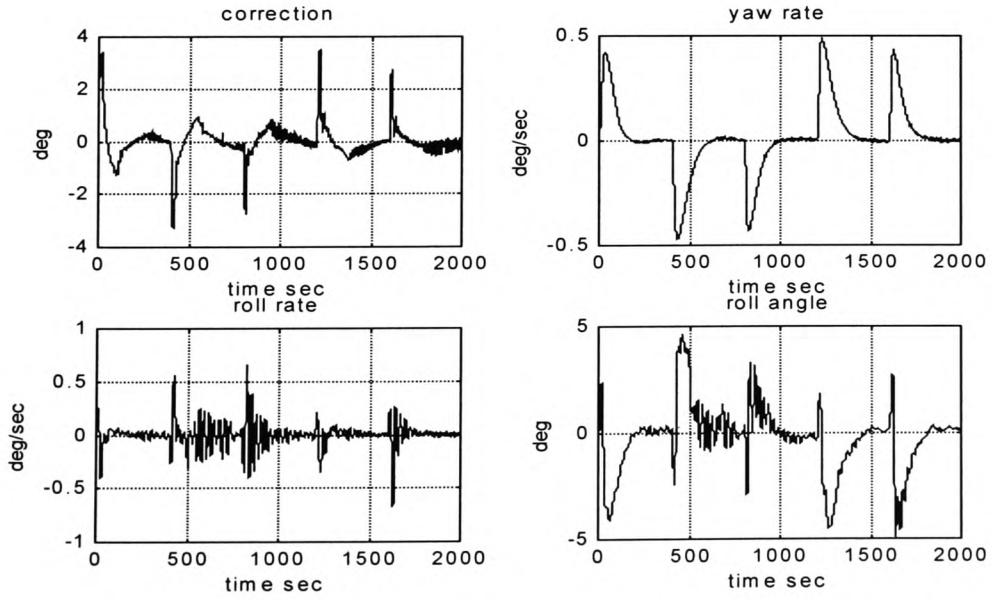

Fig.6.15: State variables and correction signals for the sequence of course-changing manoeuvres

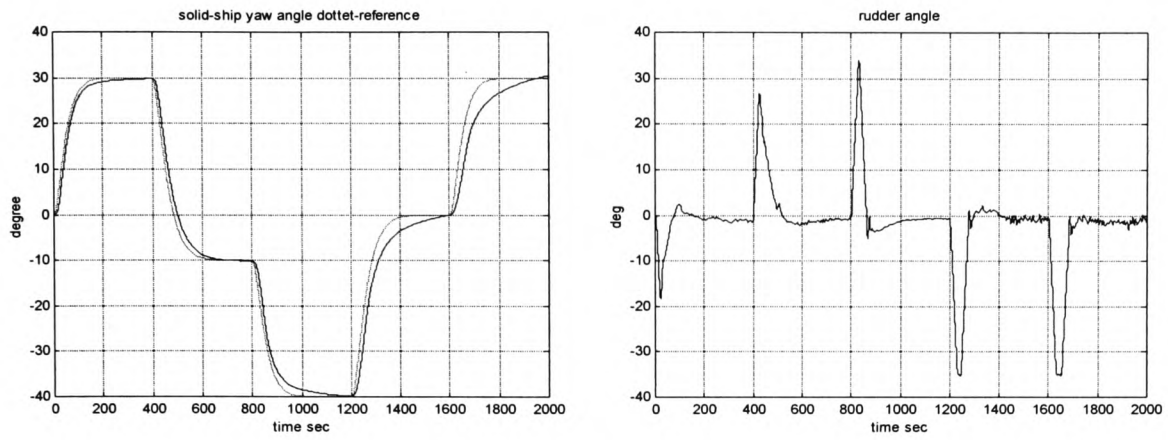

Fig.6.16: Heading and rudder angle for a step change in the surge velocity

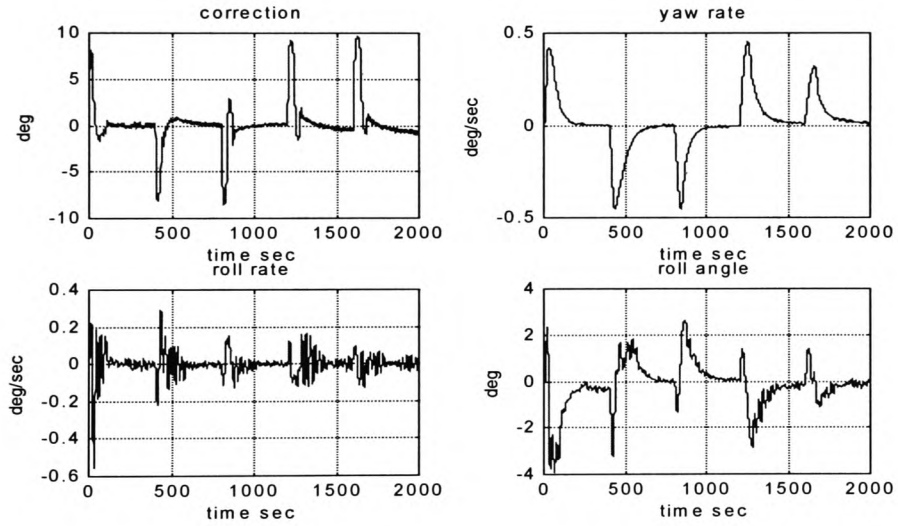

Fig.617: State variables and correction signals for a step change in the surge velocity

6.4 Conclusions

In this chapter, fuzzy logic systems have been used for the design of autopilots based on the heuristic information of the ship. It is seen that the ability to exploit heuristic knowledge, which can be easily embedded in the controller design process is the major advantage that fuzzy logic systems present over neural networks and any other kinds of

approximator. However, the performances of the controller, achieved with this kind of control design approach, are unlikely to be optimal and are dependent on the experience of the designer. In fact, a simple PID controller can easily obtain the same (if not better) performances than the course-keeping controller presented in section 6.2. Moreover the design process becomes more complex when the multivariable nature of the ship dynamics are considered and in any case the resultant controller does not posses neither adaptive nor learning ability.

The controller obtained with this approach can therefore be considered as a first attempt to solve the control problem. Further adjustment of the controller parameters can be done either by exploiting heuristic knowledge, as in the course-changing autopilot presented in section 6.3, or by any of the learning algorithms used for training neural networks. The latter is where the effort of the research community has been concentrated recently (Jang, 1993) (Sutton *et al*, 1996) (Sutton and Marsden, 1997) (Sutton *et al* 1997). However, it is important to note that the implementation of this control design technique has shown good results in problems difficult to control by other means. The pioneering work of Mamdani is the major reference in this content.

6.5 Reference List

Amerongen, van J., and Naute Lemke, van H. R. 1980. *Criteria for optimum steering of ships.* Proc. Ship Steering Automatic Control. pp. 3-22, Genova.

Jang, J. S. R. 1993. ANFIS: Adaptive-Network-Based Fuzzy Inference Systems. *IEEE Transactions on Systems, Man and Cybernetics,* **23** (3), pp. 665-684.

Klugt, P. G. M. van 1987. *Rudder Roll Stabilization.* Delft University of Technology. Ph.D. Thesis.

Layene, J. R., and Passino, K. M. 1998. Fuzzy Model Reference Learning Controller. *In:* Dimiter Driankov and Rainer Palm ed. *Advances in Fuzzy Control.* New York ISBN 3-7908-1090-8: Physica-Verlag Heidelberg, pp. 263-282.

Mamdani, E. H., and Assilian, S. 1975. An experiment in linguistic synthesis with a fuzzy logic controller. *International journal of Man-Machine Studies,* **7** (1), pp. 1-13.

Procyk, T. J., and Mamdani, E. H. 1979. A linguistic self-organising process controller. *Automatica,* **15**, pp. 15-30.

Sutton, R., and Marsden, G. D. 1997. A fuzzy autopilot optimised using a genetic algorithm. *Journal of Navigation,* **Vol 50** (No 1), pp. pp 120-131.

Sutton, R., Taylor, S.D.H. and Roberts, G. N. 1997. Tuning Fuzzy ship autopilot using artificial neural networks. *Transactions of The Institute of Measurement and Control,* **19** (2), pp. 94-106.

Sutton, R.,Taylor, S. D. H., and Roberts, G. N. 1996. Automatic ship steering system based on neurofuzzy algorithms. *Proc. MMAR 16 Mcezcdouzdroje, Poland,*

Chapter 7 Intelligent Autopilots

7.1 Introduction

As mentioned in Chapter 1, the adaptive properties of a system constitute the fundamental characteristic of an intelligent controller. The design of such adaptive control system can be divided into two main steps. First the structure of a controller is chosen and then the parameters of the controller are adjusted in such a way that a suitable performance criteria is met. For the selection of the controller structure *a-priori* knowledge, if available either in terms of mathematical models or in terms of linguistic rules, can be exploited. On the other hand, the choice of the adaptive algorithm, for the adjustment of the controller parameters, is determined both by the numerical tractability and the selected controller structure. Different possibilities and a vast literature exist where controller structures (i.e. MPN, RBFN, FLS etc.) and adaptation algorithms (back-propagation, least mean square etc.) are combined in an attempt to solve a particular control problem (Miller *et al*, 1990). Some of these structures have been also discussed in Chapter 2 and in the particular case of autopilots design for ships, the majority of these architecture employs multilayer perceptron networks with direct adaptation and back-propagation algorithm (Hearn *et al* 1997).

In the following sections, controllers based on neural networks are proposed for solving the course-keeping and course-changing control problem. According to the description of adaptive networks given in Chapter 3, it is clear that the following controller can also be implemented by means of fuzzy logic systems which should be preferred when a cognitive model of the system is available.

The choice on the controller structure, of the proposed intelligent autopilots, is motivated by making some assumption on the ship's dynamics, while the selection of the training algorithm is motivated by numerical problems. In particular, in sections 7.2 and 7.3 MPNs are used to employ the controller structure therefore the back-propagation algorithm is mandatory. On the contrary in section 7.4, for the proposed stable adaptive autopilot, RBFN with fixed input parameters is used, therefore more general adaptive laws can be employed, thereby facilitating the analytical analysis of the overall system.

7.2 Model-reference neural autopilots

A generalisation of the Bech and Norrbin model describing the ship's yaw dynamics, is represented by the non-linear auto regressive model of equation (7.1):

$$\psi(k+1) = f[\psi(k),...,\psi(k-n+1)] + g[\delta(k),...,\delta(k-d-m+1)] \tag{7.1}$$

If the non-linear functions f and g are known, the model-following control problem can be solved by the control law:

$$[\delta(k),...,\delta(k-m+1)] = g^{-1}\{\psi_m(k+1) - f[\psi(k),...,\psi(k-n+1)]\} \tag{7.2}$$

where ψ_m is the output of a reference model. In general, the functions f and g are unknown or slowly time variant. It is possible therefore, to formulate the control problem (the implementation of equation (7.2)) in the framework of adaptive control

theory, where neural network can be used to approximate the control mapping expressed by equation (7.2).

Both methods, the direct and indirect adaptive approach can be considered. Figure 7.1, shows the block diagram of a direct adaptive approach.

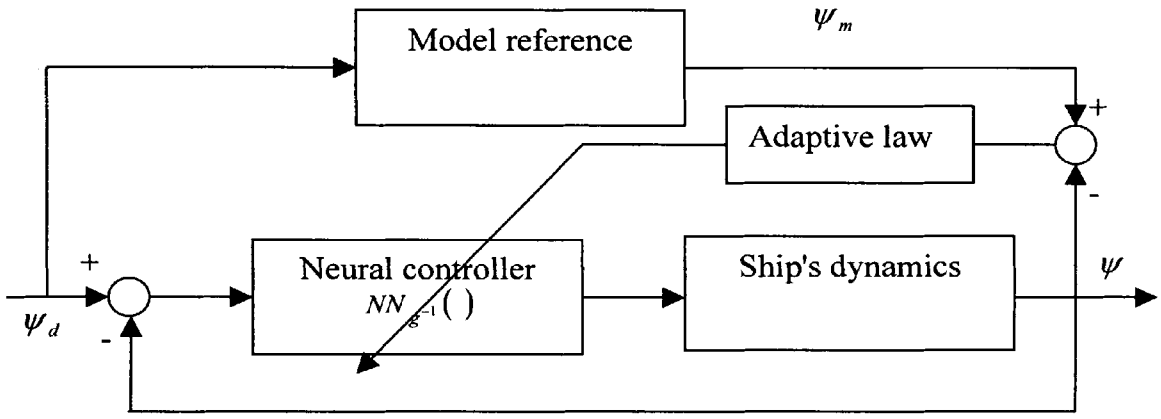

Fig.7.1: Direct adaptive neural controller

The neural network $NN_{g^{-1}}(\ )$, in figure 7.1, tries to implement an approximation of the control law expressed by equation (7.2). When the backpropagation algorithm is used to implement the adaptive law, the Jacobian of the ship's dynamics is needed. However, this is not always available therefore, different approximation have to be considered (Saerens and Soquest, 1991) (Tiano *et al*, 1994). On the contrary, the indirect adaptive approach does not rely on this particular information and is therefore considered next.

With the indirect approach, the system parameters are first identified and then used in turn to implement the control law. For this purpose, two neural networks are used to identify the functions f and g of equation (7.1) and then used to implement the

control law expressed by equation (7.2). Figure 7.2 shown the block diagram of the indirect neural controller.

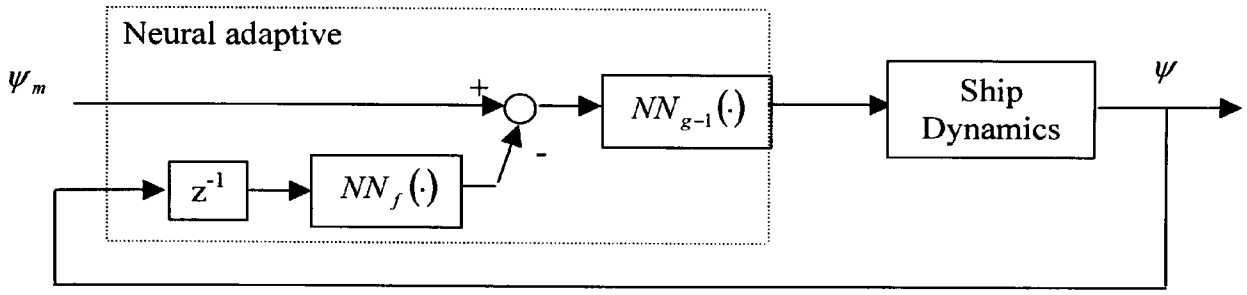

Fig. 7.2: The indirect neural controller

The identification of the functions f and g, achieved by neural networks, represents an important stage during the controller design process. Due to their universal approximation capabilities neural networks are good candidates for solving this identification task. A possible architecture representing the identification structure is represented by the block diagram of figure 7.3. Since the input of the network NN_f is fed with the previous output of the ship $\psi(k)$, instead of the estimated output $\hat{\psi}(k)$, algebraic loops are avoided in the neural network and the back-propagation algorithm can be used.

Two feedforward neural networks with one non-linear hidden layer of 25 nodes were trained with the backpropagation algorithm to approximate the function f and g. The availability of the non-linear model makes the training of the two networks easier, since a significant collection of data can be measured. Figure 7.4 shows both the output of the identified neural model (in dotted line) and the output of the non-linear model (in solid line) for a 20°/20° zig-zag manoeuvre, when in equation (7.1) d=0, n=2 and m=1. The

two signals are practically indistinguishable, confirming the validity of the above identifier.

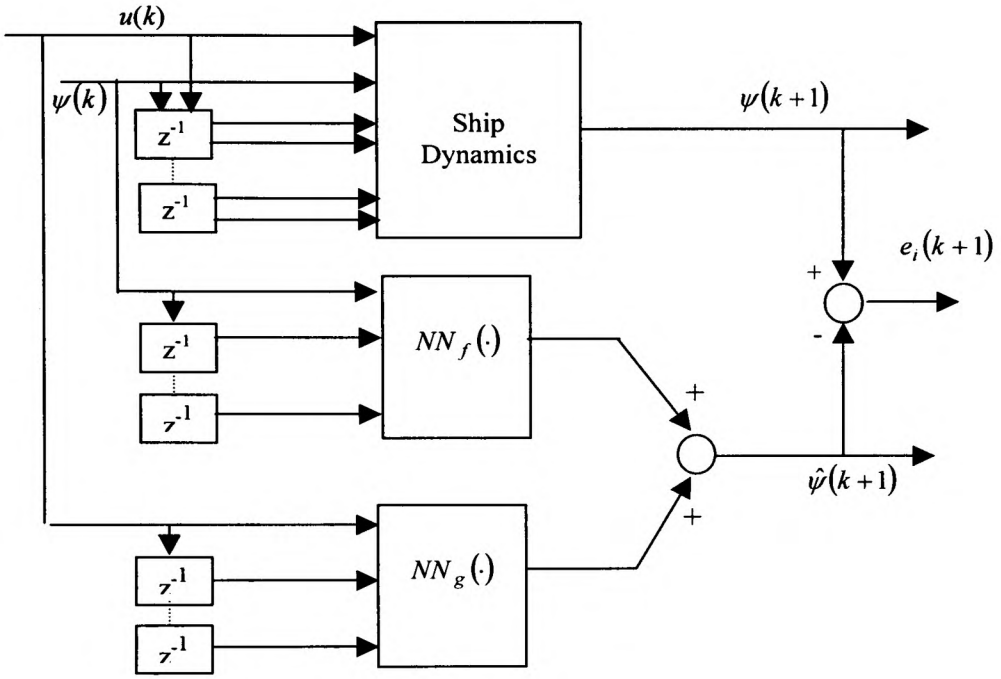

Fig.7.3: Series-parallel identification block diagram

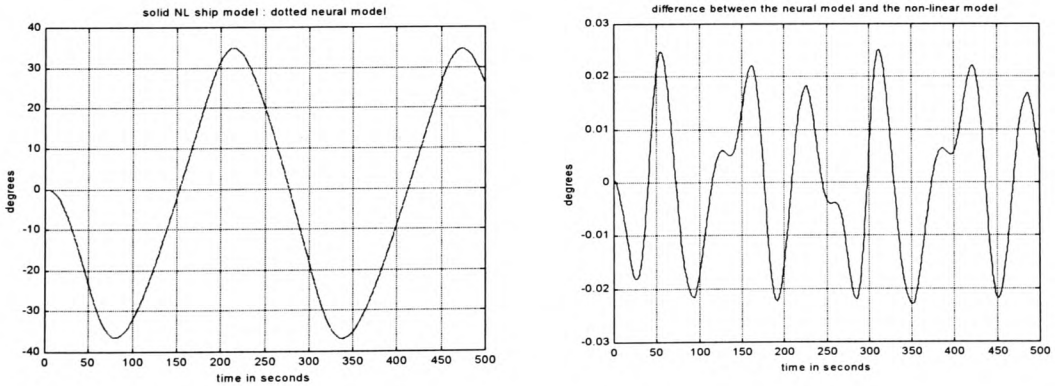

Fig.7.4: $20^o/20^o$ zig-zag manoeuvre. (Solid line ship's non-linear model. Dotted line neural networks model). Right figure, difference between the two signals.

For the implementation of the control law (equation (7.2)), the inverse of the estimated mapping NN_g is calculated from a random input/output collection of data uniformily distributed in the interval $\left]-35^0;+35^0\right[$ where the function g is defined, in such a way that $NN_g\left(NN_{g^{-1}}\right)=1$. Figure 7.5 shows a plot of the mapping NN_g in the domain of interest. From this figure it is possible to infer the invertibility of this mapping which is shown in figure 7.6.

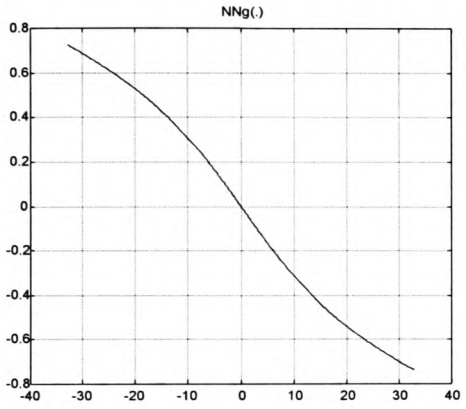

Fig. 7.5; NN_g mapping

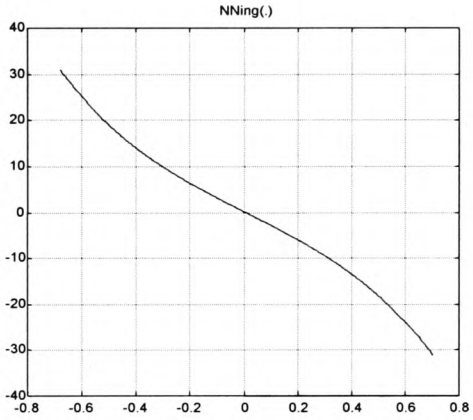

Fig. 7.6: $NN_{g^{-1}}$ mapping

According to equation (7.1), the mapping NN_g, represents the relationship between the actual rudder angle and the next yaw angle. Considering the Bech's model, this function can be either one of the two functions illustrated in Chapter 4 (figure 4.7) for course stable and course unstable ships. From this figure, it is possible to conclude that for course-stable ship, the mapping NN_g is always invertible. However, for course-unstable ships, the same result does not hold. It is important to note that in order to ensure that zero is mapped into zero, the biases of the networks are set equal to zero, reducing the overall number of parameters to be trained.

Finally, in order to implement the control law expressed by equation (7.2), the reference manoeuvre has to be specified. As discussed in Chapter 1 section 1.3, concerning the steering criteria, (Amerongen, 1984) suggested a second order transfer function of the form:

$$\frac{\psi_m(s)}{\psi_d(s)} = \frac{K_{pm}/\tau_{pm}}{s^2 + s/\tau_m + K_{pm}/\tau_m}$$

The time constant τ_m is chosen approximately 2 to 3 times smaller than the dominating time constant of the ship at cruise speed and must be such that the process is able to follow the model. If the rate-of-turn limiter is neglected, K_{pm} follows from the desired damping ratio (ξ) of the system:

$$K_{pm} = 1/(4\xi^2\tau_m)$$

Possible values of ξ are between ξ=1 which corresponds to a zero overshoot condition, to ξ=0.7 which corresponds to an overshoot of approximately 5% of the desired final value (which may be considered acceptable in open sea). The selection of τ_m results from the following consideration: a reasonable course controller will have a rate-feedback gain which makes the time constant of the ship 2 to 3 times smaller with respect to the case of the open-loop system (without controller). By choosing a similar time constant for the model reference this guarantees that the process can follow the model.

Due to the heavy computation involved in training the two mapping $NN_{g^{-1}}$ and NN_f the algorithm was tested off-line. Figure 7.7 and 7.8 shows a 10° and a 30° course-changing manoeuvre respectively. The waves disturbance were characterised, with respect the Pierson-Moskowitz spectral formula, by an average period of 8 sec and a significant wave height of 3 meters. The starting angle of attack was equal to 90° leading the second manoeuvre to a quartering sea condition. The oscillations on the rudder angle are due to the effects of the wave disturbances, however also in this critical condition the heading angle is properly maintained.

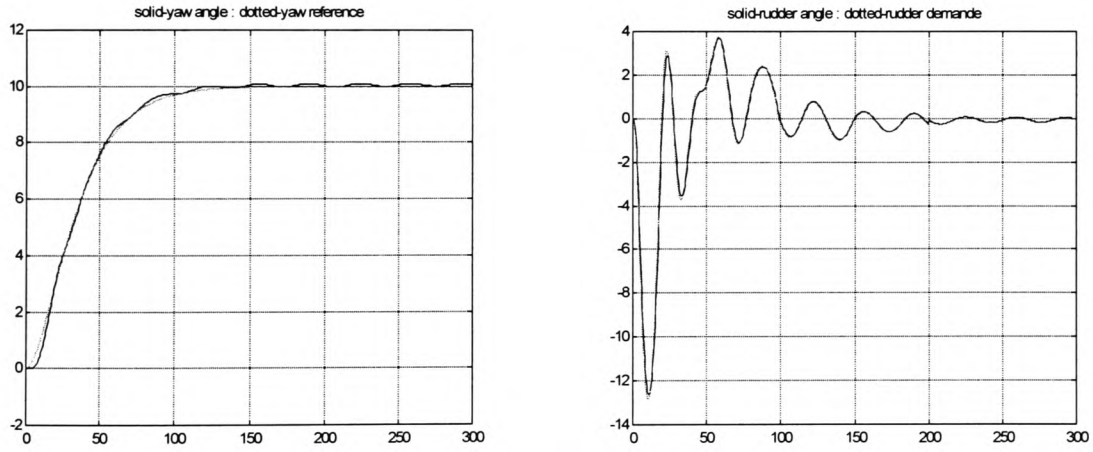

Figure 7.7: A 10° course-changing manoeuvre. (x-axis time in seconds, y-axis degree)

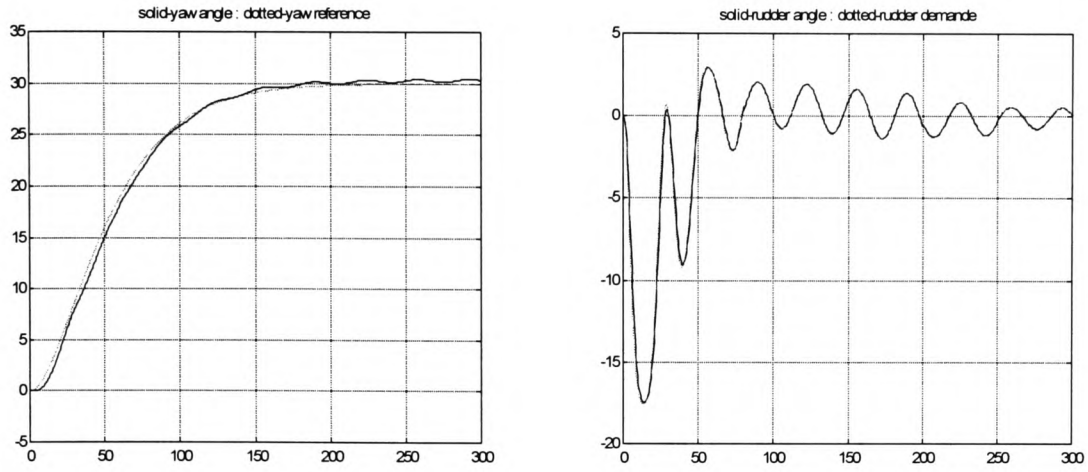

Figure 7.8: A 30° course-changing manoeuvre. (x-axis time in seconds, y-axis degrees)

The difficulty in implementing on-line the above control algorithm, rely on the assumption concerning the ship's model stated in equation (7.1). Although this represents a generalisation of the yaw dynamics, the numerical tractability of the indirect adaptive approach is compromised.

7.3 Course-keeping autopilots

As mentioned in the Chapter 1 section 3, concerning the definition of steering criteria, the design of a course-keeping autopilot can be formulated in the framework of Linear Quadratic optimal control. Different papers have shown the applicability of this technique for steering large tankers in different sailing conditions with a proper choice of the weighting matrices. However, in order to analytically solve the optimal control problem, the assumption that a linear model represents the ship's dynamics around an operating point is postulated. Such a linear model can be either represented by the first-order Nomoto model, (or second-order in the case of course unstable ships), or can be

obtained by considering the first-order truncation of the power series expansion of the ship's equations of motion. The assumption that the rudder angle is "small" (does not exceed approximately 8/10 degree) therefore has to be fulfilled.

A different way to approach this problem is represented by the feedback linearisation theory. The problem of feedback linearisation of a non-linear system can be stated as follows: given the non-linear system expressed by equation (7.3a):

$$x(k+1) = f[x(k), \delta(k)] \tag{7.3a}$$

where $x \in \Re^n$ is the state, $\delta \in \Re$ is the control input and $f[\ ]$ being a smooth vector field in $\Re^n$. The system expressed by equation (7.3a) is said input-state linearizable if there exist a region $\Omega \subset \Re^n$, a diffeomorphism $\phi : \Omega \to \Re^n$ and a non-linear feedback control law:

$$u = \alpha[x(k), v(k)] \tag{7.3b}$$

such that the new state variable $z = \phi(x)$ and the new input v satisfy a linear time-invariant relation:

$$z(k+1) = \phi[x(k+1)] = \phi[f(x(k), \alpha(x(k), v(k)))] = Az(k) + Bv(k) \tag{7.4}$$

In other words, the problem is to find a suitable change of co-ordinates in the state space $z = \phi(x)$ and a feedback law $u(k) = \alpha[x(k), v(k)]$, such that the feedback system with new input $v(k)$ and state $z(k)$ is equivalent to a linear one. The problem whether or not

the two mapping $\phi(\ )$ and $\alpha(\ )$ exists for a particular non-linear system, has been studied extensively and it is a well-established subject in the non-linear system analysis (Isidori, 1985), (Slotine and Li, 1992). Figure 7.9 shows the block diagram of a feedback linearised system.

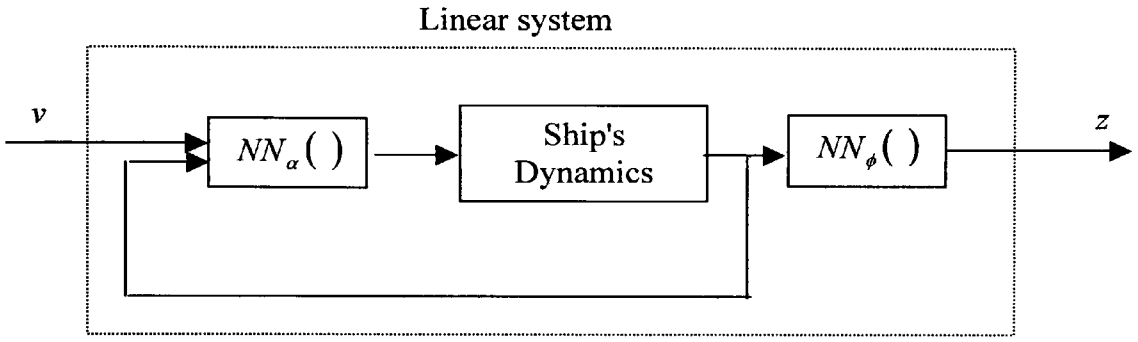

Fig.7.9: Feed-back linearised system

For the simplified case where the ship is considered as a single input single output system, the yaw motion can be described either by the Bech or Norrbin non-linear model. For a course-stable ship with a completely symmetric hull the Norrbin model reduce to equation (4.29) i.e. $\tau\ddot{\psi} + \dot{\psi} + \alpha_3\dot{\psi}^3 = k\delta$.

From a straightforward analysis of this equation it is clear that with the control law:

$$k\delta = \alpha_3\dot{\psi}^3 + v \tag{7.5}$$

the non-linear equation of motion (4.29) in term of the new input v became:

$$\tau\ddot{\psi} + \dot{\psi} = v \tag{7.6}$$

which is a first-order Nomoto linear model. In other words the idea of feedback linearisation is to find a suitable control law (i.e. equation (7.5)) and possibly a state co-ordinate change, such that the non-linearity of the system can be compensated for and the resultant system is described by a linear equation.

The problem of finding the two mapping $\phi(\ )$ and $\alpha(\ )$, is substantially complicated when the non-linear function f in unknown. However, provided that the two mappings exist, that is the system is feedback linearisable, (Levin and Narendra, 1993) have shown how two neural networks can be trained to approximate those mappings. In other words, two neural networks (or in principle any kind of approximators) can be trained in order to compensate for the unknown or slowly time variant non-linearity. Figure 7.10 shows the block diagram where two neural networks NN_α and NN_ϕ are trained in such a way that the overall system fits the input/output data collected from a linear approximation of the original non-linear system. In the particular case of the course-keeping autopilot, motivated by equation (7.5), the network NN_ϕ can be omitted. Once the system is feedback linearised, with respect the new system, from v to ψ, it is possible to design any kinds of linear controller.

The linear model, from where the data for training the neural network are collected, can be obtained either from a Nomoto model or from a straightforward linearisation of the non-linear equation of motion (both are described in appendix A). In order to allow the use of the back-propagation algorithm, a neural model of the ship dynamics has been trained off-line. This model can be considered as an additional but not modifiable layer

of the neural network NN_α. The dynamic loop of the system, shown in figure 7.10, is considered by expanding the input vector in order to include past output values. Therefore, algebraic loops in the neural networks are avoided and the back-propagation algorithm can be used for training the transformation mapping NN_α.

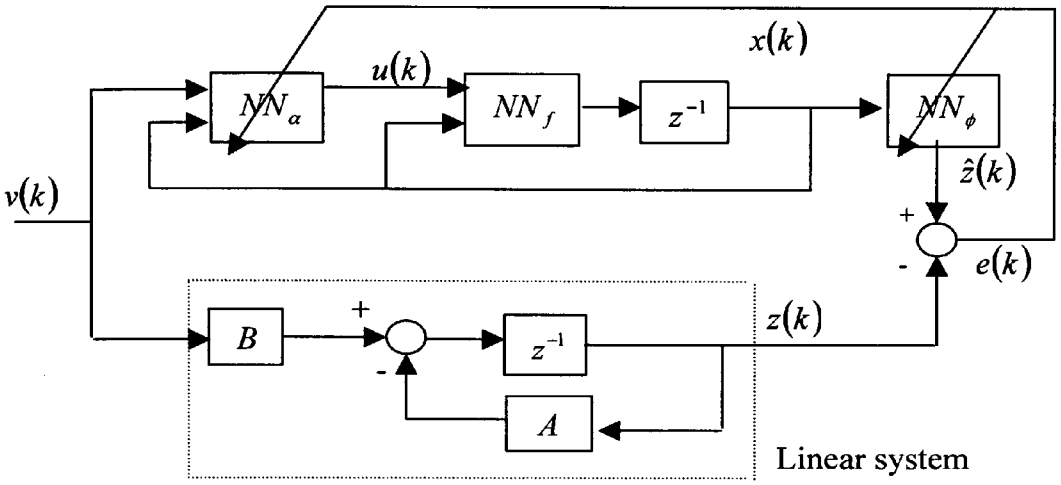

Fig. 7.10: Architecture for feedback linearisation

The linear model of the ship's dynamics has been obtained for a surge velocity of 12.5 m/sec and a zero value for the others state variables. With respect to the linearised model, a linear quadratic controller was designed and tested with respect the non-linear system and the feedback linearised system. Figure 7.11 and 7.12 shows a course-keeping manoeuvre for both the linear controller and the non-linear controller (LQ plus NN_α).

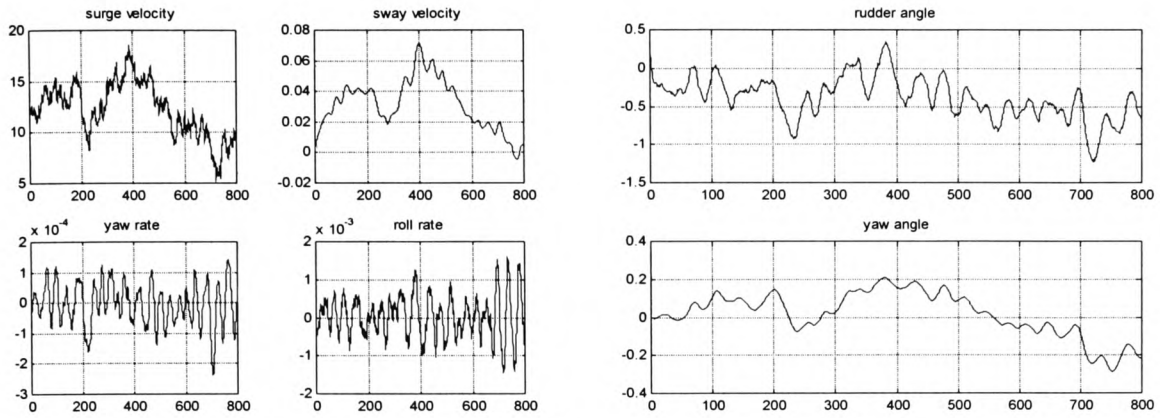

Fig.7.11: Course-keeping with the linear quadratic controller (x-axis time in seconds

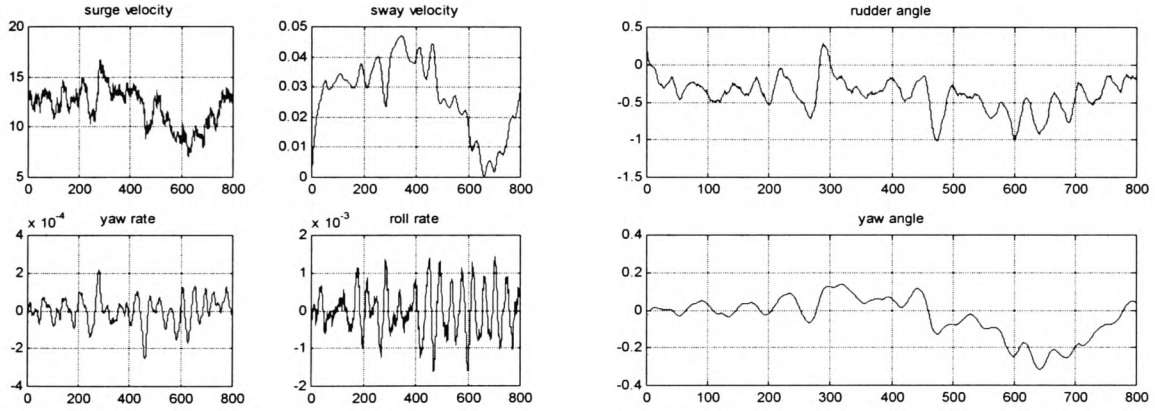

Fig.7.12: Course-keeping with the non-linear controller (x-axis time in seconds)

From a comparison of the two responses, it is possible to say that when the initial state of the system is equal (or close) to the linearisation point, the two controllers (linear and non-linear) perform both acceptably well. However, when the initial point of the system is different from the linearisation point, the non-linear controller performs better then the linear one.

Figure 7.13 and figure 7.14 shows the response of the two controllers for an initial yaw rate of 0.02 rad/sec and a surge velocity of 5 m/sec. Although the linear controller is still able to maintain the course of the ship, the non-linear controller in terms of rudder signal performs better. The simulations were done with disturbances characterised by a significant wave height of 5 metres and an average period of 10 sec. The ship was sailing in quartering sea (angle of attack 30^{o}).

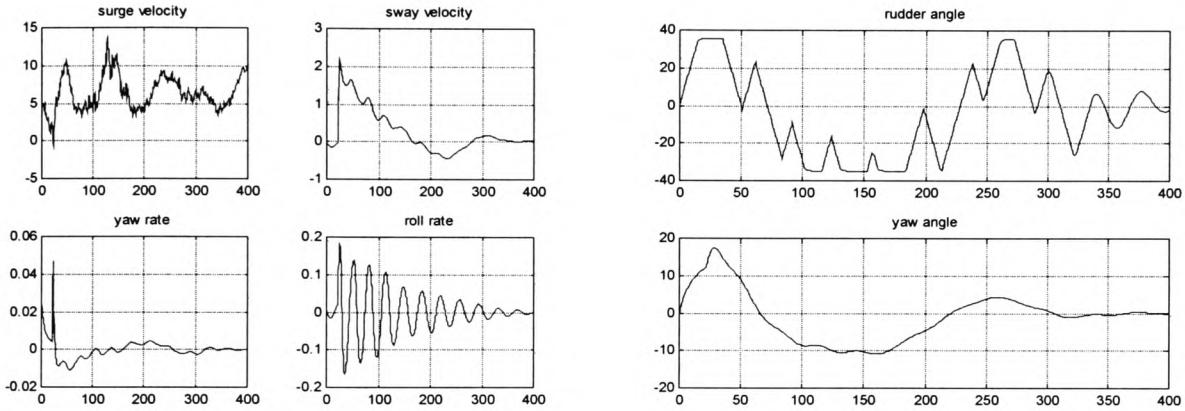

Fig.7.13: Linear quadratic controller for initial surge velocity of 5 m/sec

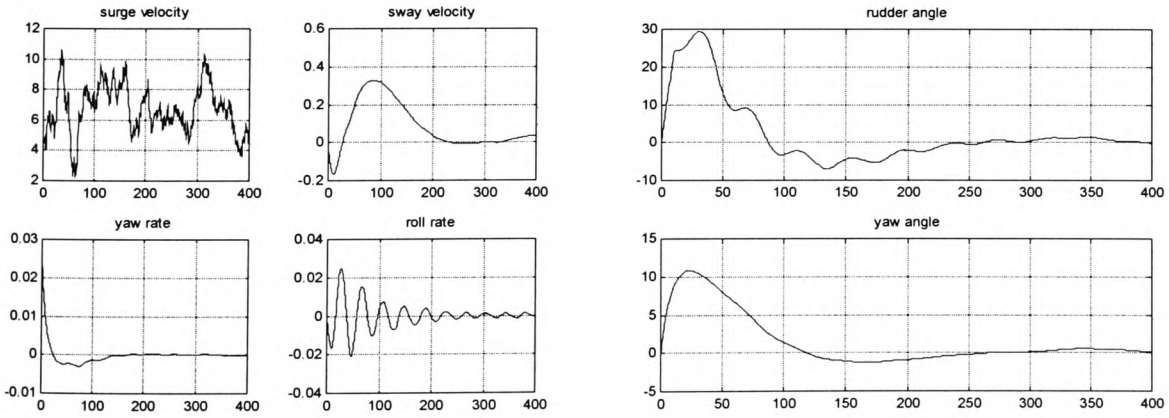

Fig.7.14: Non-linear controller for initial surge velocity of 5 m/sec

Finally figures 7.15 and 7.16 shows the response of the two controllers when the initial roll rate is sets equal to 0.2 rad/sec. In this situation the responses of the linear controller in terms of control signal is more critical.

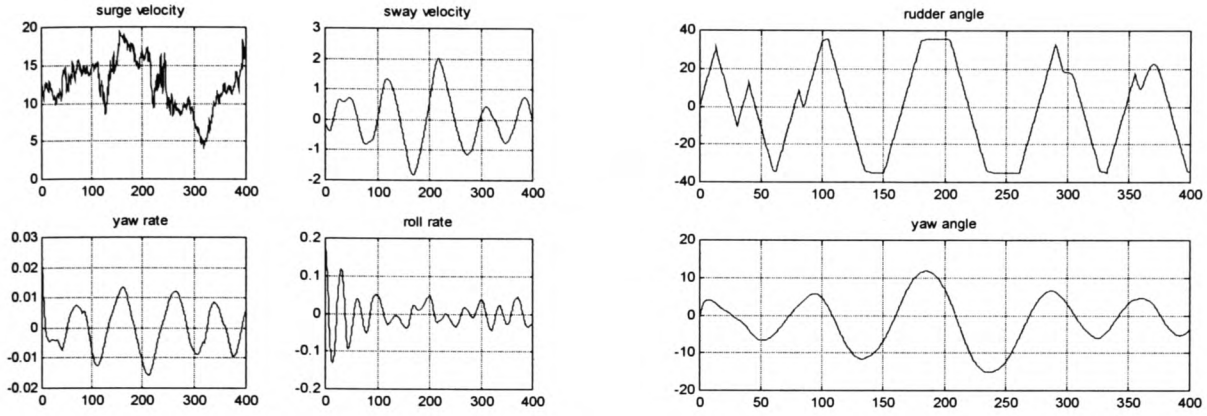

Fig.7.15: Linear controller for initial roll rate of 0.2 deg/sec

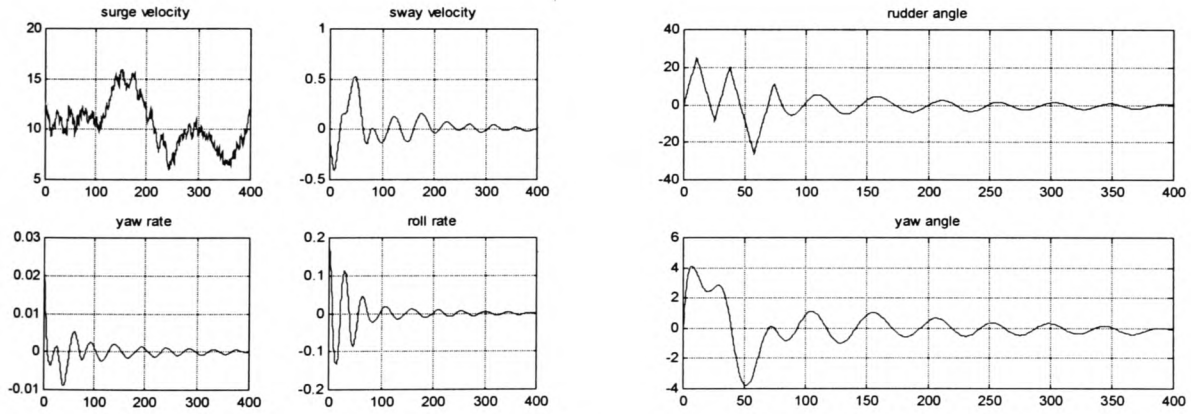

Fig.7.16: Non-linear controller for the initial roll rate of 0.2 deg/sec

To draw some preliminary conclusions, it is important to note that a fundamental assumption was that the state of the system was available for measurement. When this is not the case, the use of state observer may complicate the training of the networks for the feedback linearisation. Moreover, in order to allow the use of the backpropagation algorithm, a neural network model of the ship's dynamics was necessary. In this

simulation study, the neural model of the ship was trained off-line, however especially in the adaptive approach this may not be always possible.

7.4 Stable adaptive autopilots

In the previous paragraph some adaptive autopilots based on neural networks were discussed. The effectiveness of the proposed control algorithms was tested by simulation study, where different conditions of disturbances were considered.

Bearing in mind the definition of adaptivity given by Zadeh, (reported in Chapter 1 section 1.4), it is reasonable to state that under all the simulated conditions, (represented by the set W in Zadeh's definition), the proposed algorithms showed adaptive properties with respect the tracking error, (represented by the set P in Zadeh's definition), for both the course-changing and course-keeping manoeuvres. In this respect, it is also possible to infer about the stability of the controller algorithms, in the sense that no unbounded response was measured for all the different simulated conditions. Of course, these results are valid only for the conditions tested in simulation and nothing can be inferred about the conditions that were not tested.

A different approach than the one based on simulation tests, to guarantee the performance of the adaptive control algorithm, is to attempt an analytical analysis of the system. Due to the non-linear time variant nature of the adaptive algorithm, at the present this is a very challenging task. However, the design of stable adaptive systems has been solved analytically if certain restrictive conditions on the system to be controlled apply (Narendra *et al*, 1980), (Morse, 1980), (Goodwin *et al*, 1980). In the

following subsections, the design of a stable adaptive autopilot based on neural networks is discussed.

7.4.1 Statement of the problem

A possible representation of the yaw dynamics, motivated by the discussion about the models used for control in Chapter 4, is as follows:

$$\psi(k+1)=\sum_{i=1}^{N}\alpha_i f_i[\psi(k),\psi(k-1),...,\psi(k-n+1)]+\sum_{j=0}^{m-1}\beta_j\delta(k-d-j+1) \qquad (7.7)$$

In equation (7.7) the yaw angle is expressed as a linear combination of (possibly) non linear function of the past yaw angle plus a linear combination of past and actual rudder angle (the last is the main difference with respect the model proposed in equation (7.1) for the indirect model reference approach of Chapter 7 section 2). Equation (7.7) represents a generalisation of the Norrbin and the Bech model. This representation of the yaw dynamics is particular interesting for control purposes, because if the parameters α_i, β_j and the function f_i are known and the parameter $1/\beta_0$ is well defined, the control action, for the model following problem, can be computed by the equation:

$$\delta(k-d+1)=\frac{1}{\beta_0}\left[\psi_m(k+1)-\sum_{i=1}^{N}\alpha_i f_i-\sum_{j=1}^{m-1}\beta_j\delta(k-d-j+1)\right] \qquad (7.8)$$

where $\psi_m(k+1)$ is the desired heading angle produced by a reference model. In the adaptive control approach, the dynamic of the ship is supposed to be either unknown or

slowly time variant. Using an indirect approach, the unknown parameters can be estimated and used to implement the control law (equation (7.8)), based on the certainty equivalence principle. The identification of the unknown parameters can be done by using a model with the same structure of the plant (represented by equation (7.7)) as:

$$\hat{\psi}(k+1)=\sum_{i=1}^{N}\hat{\alpha}_i f_i[\psi(k),\psi(k-1),...,\psi(k-n+1)]+\sum_{j=0}^{m-1}\hat{\beta}_j\delta(k-d-j+1) \qquad (7.9)$$

In equation (7.9) the unknown parameters appear linearly and linear adaptive theory can be applied. It is possible to prove, that under certain assumption on the function f_i, with the normilised adaptive law:

$$\hat{\theta}(k+1)-\hat{\theta}(k)=-\eta(k)\frac{e(k+1)\omega(k)}{1+\|\omega(k)\|^2} \qquad (7.10)$$

the non-linear adaptive system expressed by equation (7.7) with the control law expressed in equation (7.8), results in all the signals uniformily bounded with the tracking error and the identification error approaching asymtotically to zero which is:

$$\lim_{k\to\infty}(\hat{\psi}(k)-\psi(k))=\lim_{k\to\infty}(\psi(k)-\psi_m(k))=0 \qquad (7.11)$$

In equation (7.10), $\hat{\theta}=\left[\hat{\alpha}_1,\hat{\alpha}_2,...,\hat{\alpha}_N,\hat{\beta}_0,\hat{\beta}_1,...,\hat{\beta}_{m-1}\right]^T$ is the parameter estimation vector, η is the adaptation gain, $e=\hat{\psi}-\psi$ is the estimation error and :

$$\omega(k)=[f_1[Y(k)],...,f_N[Y(k)],\delta(k-d+1),...,\delta(k-d-m+2)]^T \qquad (7.12)$$

with:

$$Y(k)=[\psi(k),\psi(k-1),...,\psi(k-n+1)] \tag{7.13}$$

the signals vector. (Narendra and Annaswamy, 1989)

In practical situations however, not only the parameters of the model are unknown but also the non-linear function *f*. Due to their universal approximation property, neural networks and fuzzy logic systems are good candidates for performing the estimation of the functions *f*. The universal approximation property of these systems will gurantee that any smooth non-linear function *f* can be approximated with any degree of accurancy over a compact region *D*. This is expressed by equation (7.14):

$$\left\| f[Y(k)]-\hat{f}[Y(k)] \right\| \le \varepsilon \qquad \forall Y(k)\in D, and \varepsilon > 0 \tag{7.14}$$

The error ε introduced by the approximation can be treated as a state dependent bounded disturbance. Hence a modification of the adaptive law expressed in equation (7.10), in order to guarantee robustness in the presence of bounded disturbances, has to be considered. One such modification proposed by (Peterson and Narendra, 1982), is the inclusion of a dead-zone in the adaptive law. Equation (7.10) is rewritten as:

$$\hat{\theta}(k+1)=\begin{cases} \hat{\theta}(k) & if \left|e(k+1)\right| \le \varepsilon_{\max} \\ \hat{\theta}(k)-\eta(k)\dfrac{e(k+1)\omega(k)}{1+\left\|\omega(k)\right\|^2} & otherwise \end{cases} \tag{7.15}$$

Once both parameters and non-linear functions are identified, the control law becomes:

$$\delta(k-d+1)=\frac{1}{\hat{\beta}_0}\left[\psi_m(k+1)-\sum_{i=1}^{N}\hat{\alpha}_i\hat{f}_i-\sum_{j=1}^{m-1}\hat{\beta}_j\delta(k-d-j+1)\right] \tag{7.16}$$

and provided that $1/\hat{\beta}_0$ is well defined, the adaptation law expressed by equation (7.15) can be implemented.

According to the circumstances, the identification of the unknown non-linear function f_i can be performed either on-line or off-line. However, if on-line identification is attempted, in order to extend the stability result of (Peterson and Narendra, 1982), it is important that the parameters of the approximator $\hat{f}_i$ appear as well linearly in the control law. This in turn constrains the kinds and structures of approximators to be used. As described in Chapter 2, radial basis function networks with fixed centres and deviation and adjustable output parameters or fuzzy logic systems with fixed input membership functions fulfil this requirement and can be used for the design of stable adaptive law.

7.4.2 Controller design

Due to the relatively high sampling rate that can be chosen in comparison to the ship's dominant time constant, the Bech's model expressed by equation (4.27) can be rewritten in the equivalent discrete time form as:

$$\psi(t+1)=\alpha_1\psi(t)+\alpha_2 H(\psi(t-1))+\beta_0\delta(t-1)+\beta_1\delta(t-2) \tag{7.17}$$

where t is the time step and $\alpha_1 = -\left(\frac{1}{\tau_1} + \frac{1}{\tau_2}\right)$, $\alpha_2 = -\frac{k}{\tau_1\tau_2}$, $\beta_0 = \frac{k\tau_3}{\tau_1\tau_2}$, $\beta_1 = \frac{k}{\tau_1\tau_2}$ and $H(\,)$ is the non-linear function defined by the reversal spiral test. The identifier expressed by equation (7.9) becomes:

$$\hat{\psi}(t+1) = \hat{\alpha}_1\psi(t) + \sum_{i=1}^{N}\hat{\gamma}_i R_i(\psi(t-1)) + \hat{\beta}_0\delta(t-1) + \hat{\beta}_1\delta(t-2) \tag{7.18}$$

where the unknown non-linear function $\alpha_2 H(\psi(t-1))$ is approximated by a RBFN ($\sum_{i=1}^{N}\hat{\gamma}_i R_i$ equation (2.5) of Chapter 2) with basis functions R_i defined as:

$$R_i = e^{-\frac{\|\psi(t-1)-c_i\|^2}{\sigma_i^2}} \tag{7.19}$$

where c_i and σ_i are the centre and the deviation of each basis functions and are considered fixed. The parameter vector to be adjusted by equation (7.15) is now defined as $\hat{\theta} = \left[\hat{\alpha}_1, \hat{\gamma}_i, \hat{\beta}_0, \hat{\beta}_1\right]$. If no a-priori knowledge on the function to be approximated is available, it is commonplace to divide the domain of definition of the non-linear function in i uniformly distributed points. In order to guarantee good generalisation properties of the approximator, the deviation parameters σ_i of each basis functions are chosen such that a sufficient overlapping between the basis functions is ensured. For this particular application the range of the simulated manoeuvre has been sampled uniformly with steps of 5°. Therefore, for a manoeuvring range of 70° the total number of centres is $i = 15$ while the deviation is assumed to be the same for each basis function and equal to $\sigma^2 = -(2.5)^2/\ln 0.5$. From equation (7.18) it is clear that a total

number of 18 parameters has to be estimated in order to implement the identifier, the structure of which is shown by figure 7.17.

Once the parameters of equation (7.18) have been identified with the adaptive law expressed by equation (7.10) or (7.15), the control law, based on the certainty equivalence principle, described by equation (7.20) can be implemented:

$$\delta(t)=\frac{1}{\hat{\beta}_0(t)}\left\{\psi_m(t+2)-\hat{\alpha}_1(t)\psi(t+1)-\sum_i\hat{\gamma}_i(t)R_i(\psi(t))-\hat{\beta}_1(t)\delta(t-1)\right\} \tag{7.20}$$

Because the delay of the system is d=2, the reference heading angle at time (t+2) must be available. In other words, in order to implement the above control law, the heading angle two steps ahead is needed. The overall control structure is shown in figure 7.18. The model reference from where the desired heading angle $\psi_m(t+2)$ is computed, is the same as discussed in the previous section.

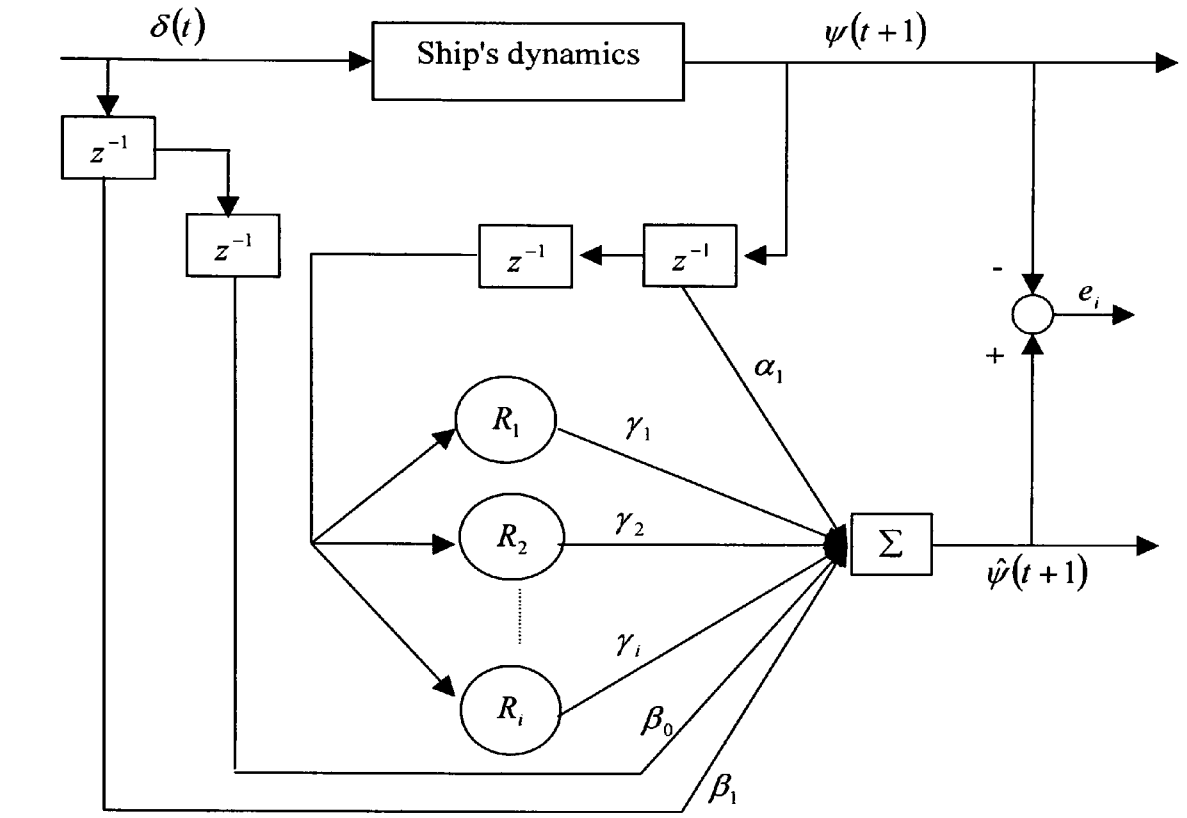

Fig. 7.17: Structure of the identifier using radial basis network

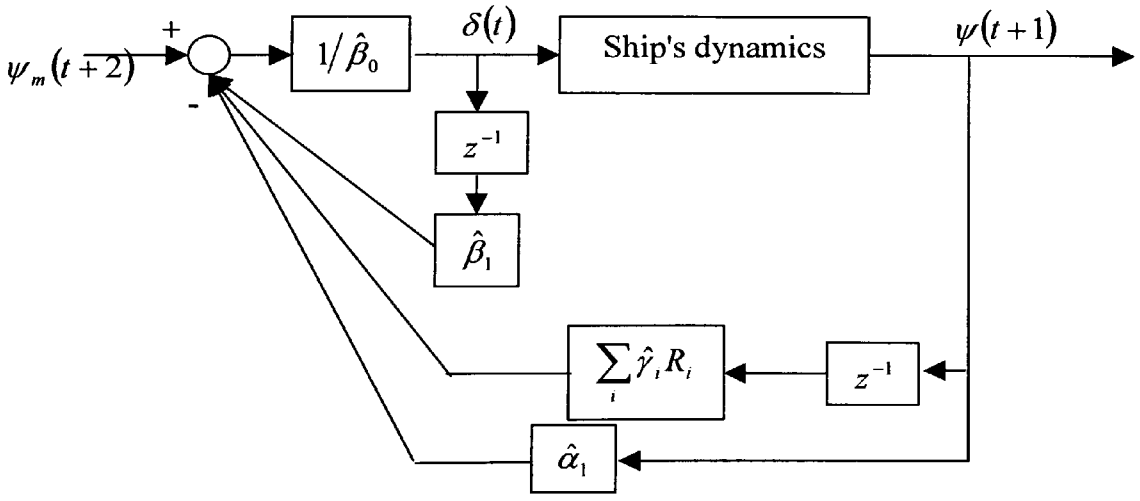

Fig.7.18: Controller structure based on radial basis function network

7.4.3 Simulation results

The control algorithm presented above was tested in a simulation study involving the containership model described in Chapter 5 with the disturbance effects as described in Appendix B. Appendix C gives the stability analysis of the proposed intelligent controller.

The shallow water effects, described by equation (B.44) of appendix B, were tested both by a constant change and a step change in the water depth. Figure 7.19 shows the depth of water at each time instant (left up corner) and the relative hydrodynamics parameter values as expressed by equation (B.44) of appendix B. Note that the shallow water effect begins to take effect at water depth from 3 to 4 times T. With respect to figure B.3, equation (B.44) and (B.45), when H=T the ship is running aground F will be zero and the coefficients K_i will diverge to infinity. Therefore, in the simulations a minimum value for the water depth was set as, $H_{final} = T + \varepsilon$ with $\varepsilon > 0$.

The wave conditions are defined, with respect the Pierson-Moskowitz spectral density (equation (B.16)), with a significant wave height $h_{1/3}$ of 3 metres and an average period T of 8 seconds. Figure 7.20 shown the heading and the rudder angle for a sequence of course-changing manoeuvres with wave disturbances and shallow water effects defined as above and starting angle of attack of 60°. Figure 7.21 shows the parameter values during the adaptation with the tracking and estimation error. All parameters, of equation (7.18) where initialised to zero, except for β_0 which in order to avoid unbounded control signal is constrained to be $|\beta_0| \geq 0.1$.

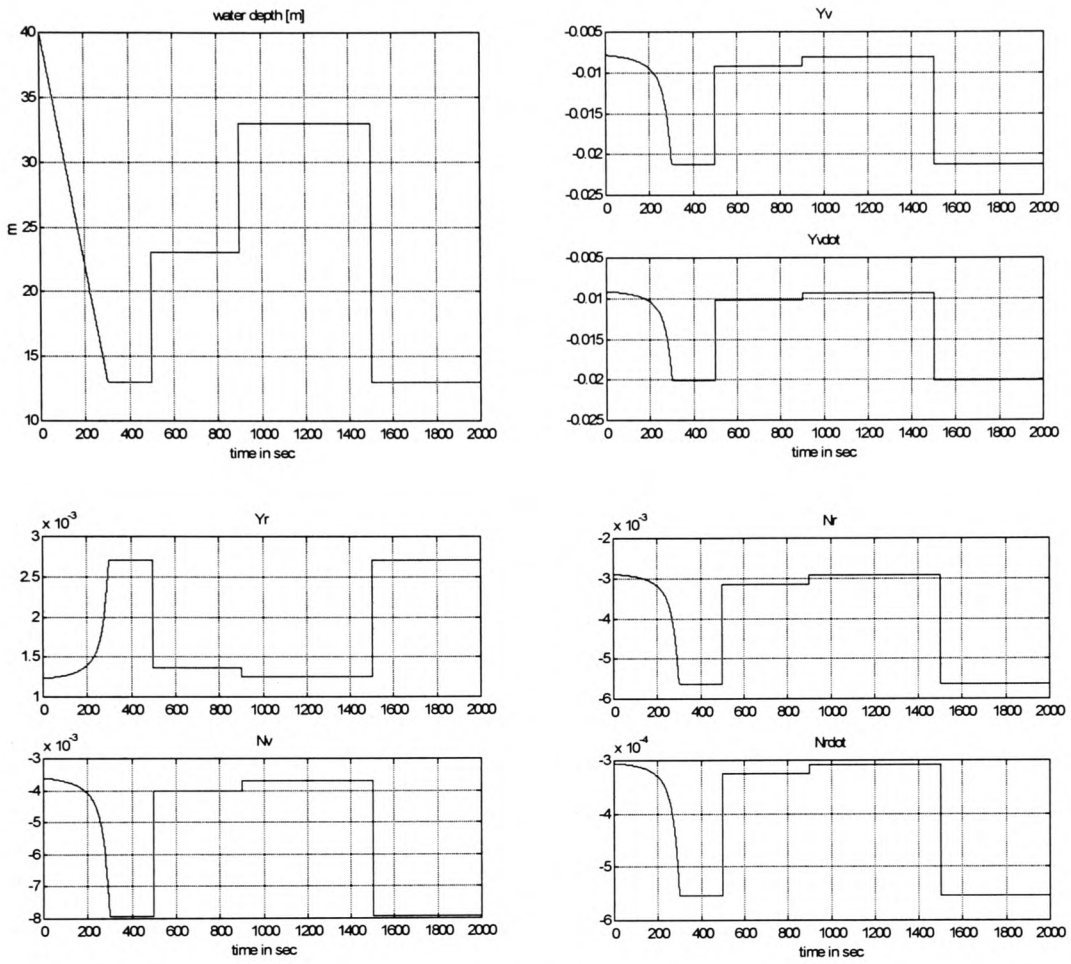

Fig. 7.19: Water's depth and hydrodynamics parameters

From the simulated change of water depth, shown in figure 7.19, it is seen that the step changes occur at time 500, 900 and 1500 seconds. While in correspondence to the two first steps, the heading angle shown in figure 7.20 presents a marked oscillatory behaviour the response of the adaptive controller to the third step is clearly better. This is due to the fact that the first two step changes in water depth occur in a transition phase of the manoeuvre while the controller is still learning. The third step disturbance occur when the transition of the manoeuvre is completed and the controller has already experienced a series of course-changing manoeuvres. This learning ability is shown better in figure 7.22 where the same sequence of course-changes as shown in figure

7.20 is performed, with the controller parameters initialised with values inherited from the previous manoeuvre.

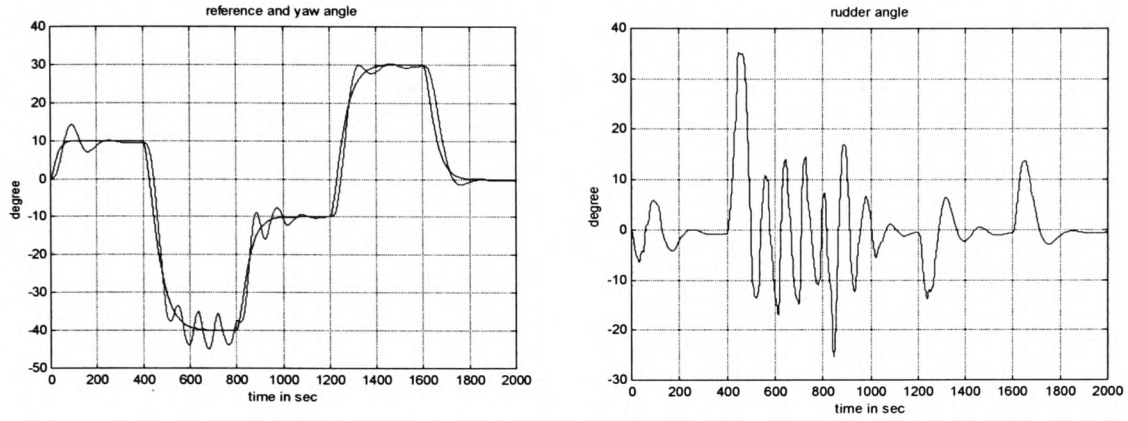

Fig. 7.20: Heading and rudder angle for course-changing

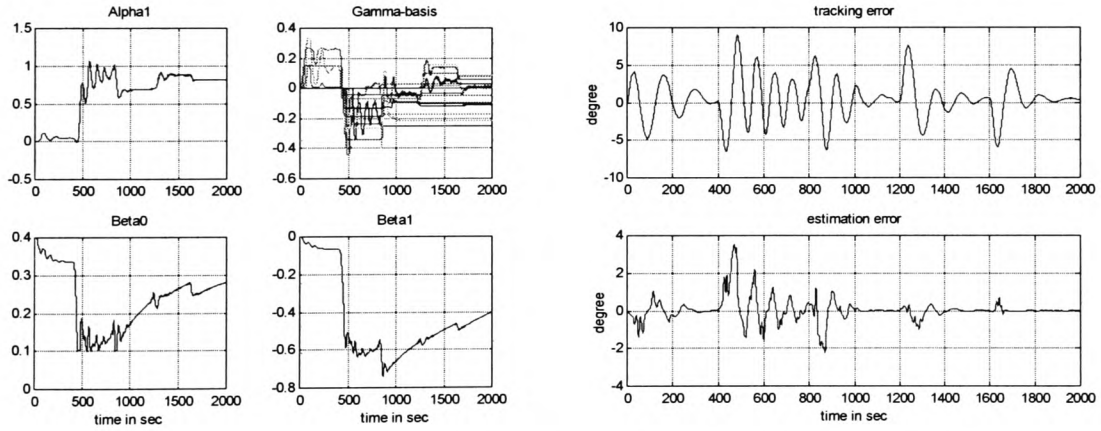

Fig. 7.21: Controller parameters, tracking and estimation error for the course changing manoeuvre

The oscillatory behaviours of the heading angle is related to the robustness properties of the adaptive algorithm. As discussed in section 7.4.1 it is possible to consider a dead-zone in the adaptive law to prevent adaptation when the identification error is below a certain threshold. The dead-zone of the adaptation law is set proportional to the

approximation error introduced by the RBFN and as well proportional to the effects of the external disturbances.

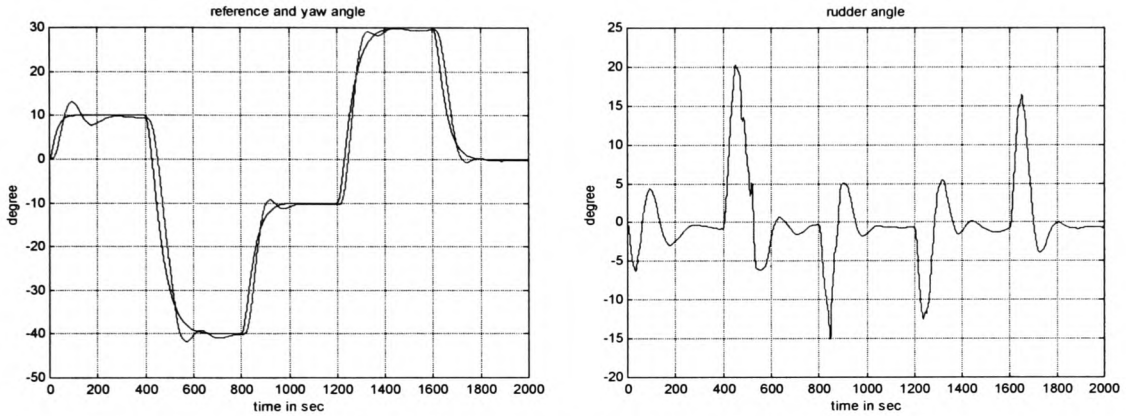

Fig.7.22: Heading and rudder angle for the course-changing

Figures 7.23 and 7.24 shown the same course-changing manoeuvre as defined above with a dead-zone in the adaptive law (equation (7.15)). Due to the presence of the dead-zone in the adaptive law, it is not guaranteed that the tracking error will converge to zero. This is shown in the Appendix C where the stability of the overall system it is also proved.

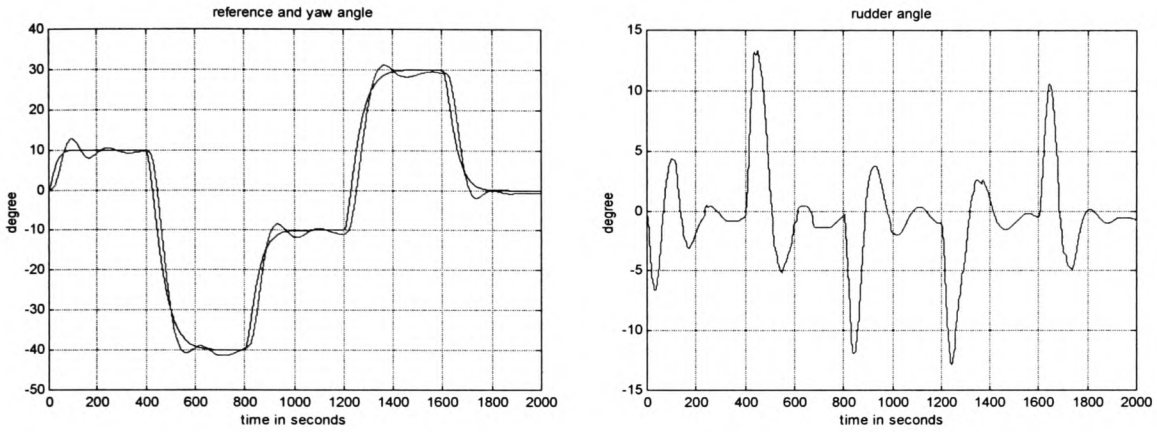

Fig. 7.23: Heading and rudder angle for a dead-zone in the adaptive law

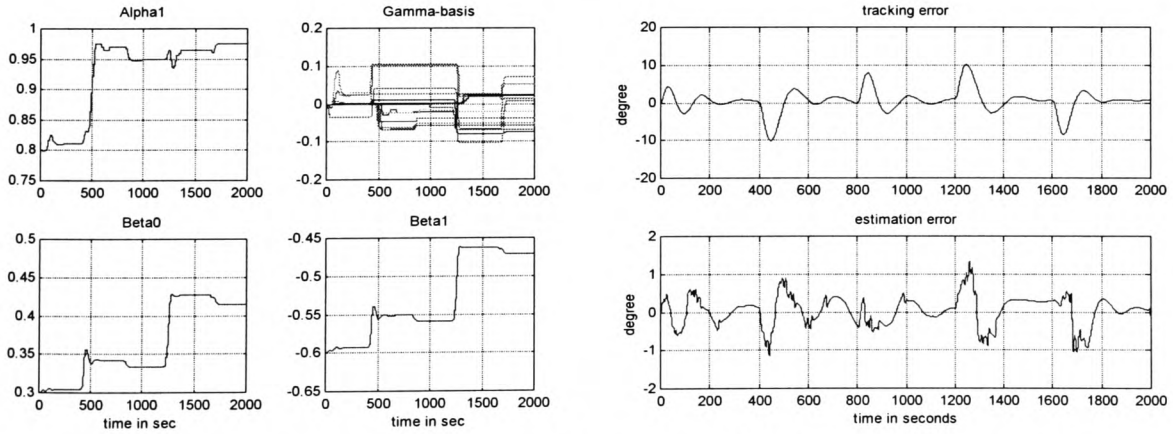

Fig. 7.24: Controller parameters, tracking and estimation error for the dead-zone in the adaptive law

A fundamental aspect of this approach is therefore the initialisation of the controller parameters. A good initialisation of the controller parameters will clearly enhance the transient response of the controller. With respect to this problem of adaptive controllers, the application of multiple models and switching criteria is worth considering. For instance, (Narendra and Balakrishnan, 1997), propose different switching and tuning schemes combining fixed and adaptive model where the stability of the overall system is still guaranteed. However, all simulation results showed that the proposed controller is able to deal with the dynamic changes that a ship will encounter due to different sailing conditions.

Figures 7.25 and 7.26 shown the same manoeuvre defined above where the controller parameters are initialised from the previous manoeuvre and when at time 500 seconds the surge velocity is changed from 12.5 m/sec to 7 m/sec. Although the adaptive autopilot is still able to steering the ship along the entire manoeuvre, the transient response of the ship's heading angle can be improved by considering a proper re-initialisation of the controller parameters. Gain scheduling with respect to the speed of the ship can be considered as a simplified alternative to the multiple models with switching criteria already mentioned. However, it is important to remind that as a consequence of the change in the dynamical response of the ship, the reference manoeuvre should be adjusted too.

Finally figures 7.27 and 7.28 shown the complete course-changing manoeuvre performed with a surge speed of 7 m/sec after the controller parameters have been trained for two complete manoeuvres. Figures 7.29 and 7.30 shown the course-changing manoeuvre for a surge velocity of 12.5 m/sec in the conditions of no disturbances and

with only three basis functions which lead to a total number of six adjustable parameters. These last figures shown clearly that the design of intelligent autopilots for ships can be solved on-line with an indirect adaptive approach by mean of RBFN for which the analytical analysis of stability properties is also achieved.

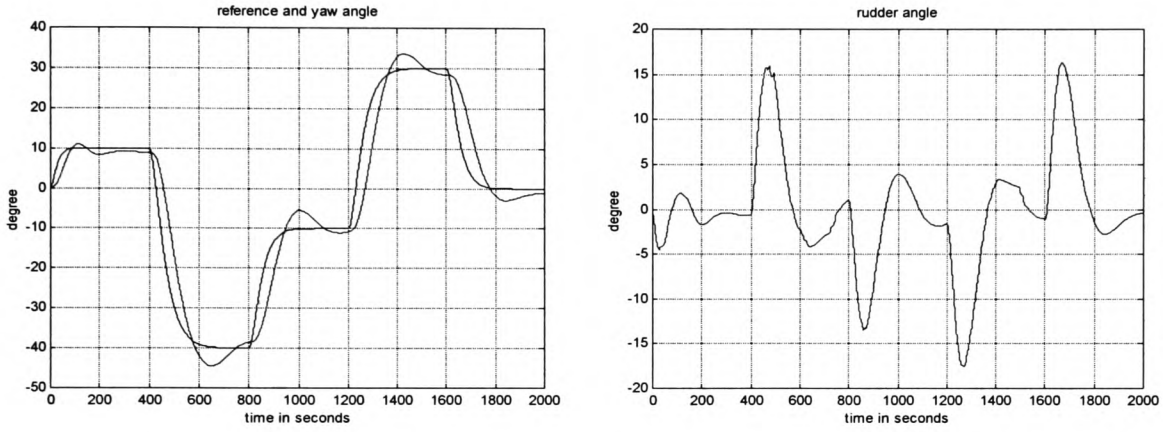

Fig. 7.25: Heading and rudder angle for the step change in the surge velocity

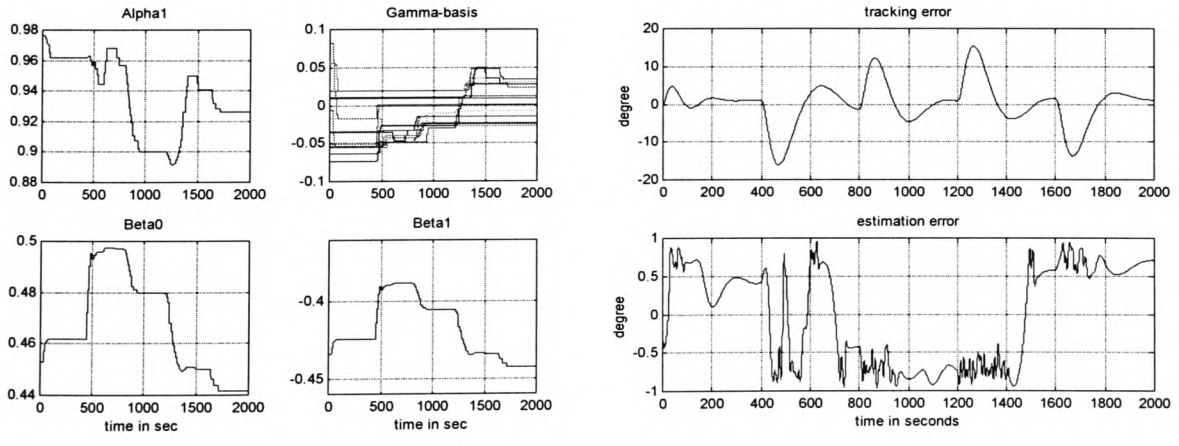

Fig.7.26: Controller parameters, tracking and estimation error for the step change in the surge velocity

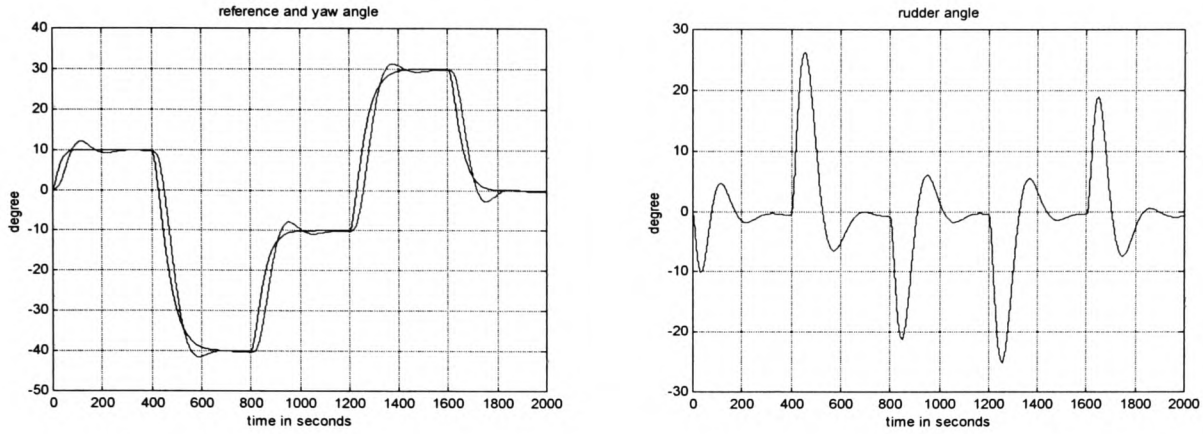

Fig.7.27: Heading and rudder angle for a surge velocity of 7 m/sec

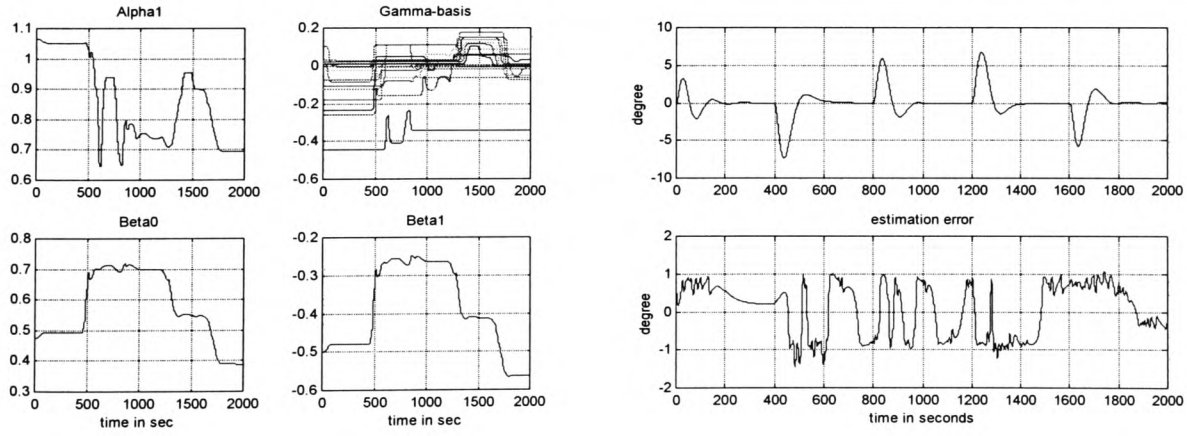

Fig.7.28: Controller parameters, tracking and estimation error for a surge velocity of 7 m/sec

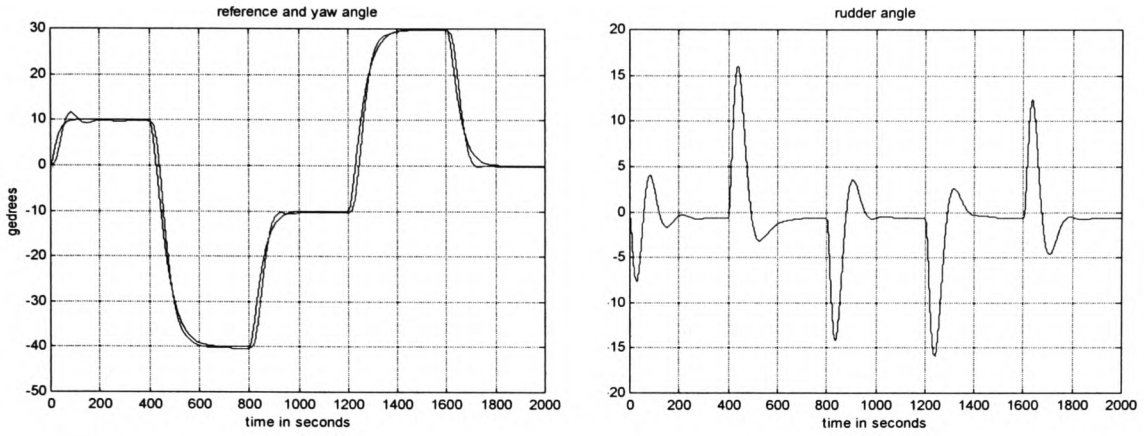

Fig.7.29: Heading and rudder angle for the course change manoeuvre without disturbances

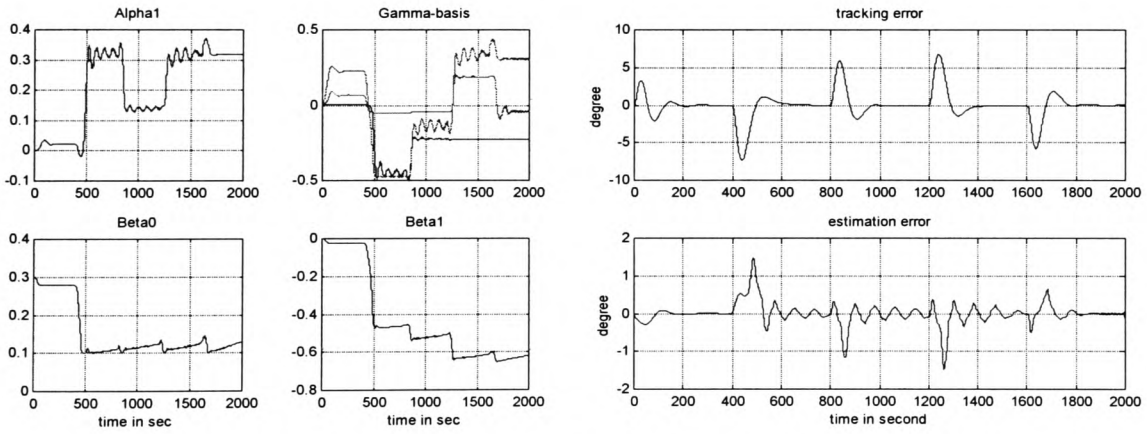

Fig.7.30: Controller parameters, tracking and estimation error foe the course change without disturbances

7.5 Conclusions

In this chapter, autopilots based on neural networks for the course-keeping and course-changing problem have been presented. Within the framework of adaptive networks the

results achieved using neural networks can be extended to the fuzzy counterpart. The latter should be used when heuristic information of the system to be controlled is available.

The majority of the papers presented in the literature proposes a solution for the intelligent ship autopilot design, based on the direct adaptive approach based on the back-propagation algorithm. Although the motivation for this controller structure is based on the need to guarantee on-line implementation of the proposed algorithm, the proper implementation of the back-propagation requires the knowledge of the Jacobian of the ship system equation. When the Jacobian is not available a simplification is to consider the sign of the unknown partial derivative (Saerens and Soquest, 1991). However, as pointed out in (Tiano *et al*, 1994) when the sign of the partial derivative is not properly determined, convergence of the adaptation algorithm may be compromised. As a consequence, in section 7.2 the indirect model reference adaptive approach was proposed for the course-changing problem. Moreover, in the attempt to generalise the result, the ship's dynamics were represented by a non-linear auto regressive model. With this choice on the model structure, the numerical computation involved during the identification step increased, rendering the proposed control algorithm not suitable for on-line implementation. The on-line implementation of the algorithm is moreover complicated due to the requested identification of the ship dynamics in closed loop.

For the course-keeping manoeuvre, the feedback linearisation technique has been investigated. In (Levin and Narendra, 1993), it is shown how the feedback-linearisation of a non-linear plant can be achieved with the use of neural networks. However the problem is only addressed when the state of the system is available for measurement.

Due to the non-linear time variant nature of the proposed autopilots based on MPNs trained with the back-propagation algorithm, the performance (in terms of tracking error and control signal) can be tested only in simulations. Prompted by this limitation, in the final section, it is shown how an analytical solution to the stability problem of the indirect adaptive systems can be formulated, when neural networks are used for the approximation of unknown non-linear function. When the adjustable parameters of the neural network appear linearly, well-known results of linear adaptive theory can be applied and the control algorithm can be implemented on-line. This in turn pose some constrains in the kinds of approximator structure that has to be used. It has been shown that Radial basis function networks with fixed parameters in the input non-linear layer are suitable for this task. However, with this approach the transient response of the adaptive algorithm cannot be guaranteed being the optimal in all the possible situations. Further enhancement of the intelligent controller can include multiple models with switching criteria or a simpler gain scheduling. This is also in accordance with the discussion given in Chapter 1, where the design of intelligent controller have been defined as a combination of different techniques for the purpose of achieving more sophisticated and reliable control systems.

It is believed that the lacking of experimental results concerning intelligent controllers is partially due to the difficulty in finding an analytical solution for the stability analysis of the overall system. Radial basis function networks and fuzzy inference systems with fixed input membership functions have been proved to be advantageous in this respect. However, until now the design of ship autopilots using this architecture have received little attention.

7.6 Reference List

Amerongen, J. van 1984. Adaptive steering of ships- A model reference approach. *Automatica,* **20** (1), pp. 3-14.

Goodwin, G. C.,Ramadge, P. J., and Caines, P. E. 1980. Discrete-Time Multivariable Adaptive Control. *IEEE Transactions on Automatic Control,* **AC-25** (3), pp. 449-461.

Hearn, G. E.,Zhang, Y., and Sen, P. 1997. *Alternative designs of neural network based autopilots: A comparative study.* 4th IFAC Conference on MCMC '97. pp. 54-59, Brijuni, Croatia.

Isidori, A. 1985. *Nonlinear Control Systems: An Introduction.* Berlin: Springer-Verlag. 3-540-15595-3.

Levin, A. U., and Narendra, K. S. 1993. Control of Nonlinear Dynamical Systems Using Neural Networks: Controllability and Stabilization. *IEEE Transactions on Neural Networks,* **4** (2), pp. 192-206.

Miller, W. T. III,Sutton R.S., and Werbos P.J. 1990. *Neural Networks for Control.* U.S.A.: The MIT Press. 0-262-13261-3.

Morse, A. S. 1980. Global Stability of Parameter-Adaptive Control Systems. *IEEE Transactions on Automatic Control,* **AC-25** (3), pp. 433-439.

Narendra, K. S., and Annaswamy, A. M. 1989. *Stable Adaptive Systems.*

Narendra, K. S.,Lin, Y. H., and Valavani, L. S. 1980. Stable Adaptive Controller Design, Part II: Proof of Stability. *IEEE Transaction on Automatic Control* , **AC-25** (3), pp. 440-448.

Narendra, K., and Balakrishnan, S. 1997. Adaptive control using multiple models. *IEEE Transaction on Automatic Control,* (AC-42), pp. 171-187.

Peterson, B. B., and Narendra, K. S. 1982. Bounded error adaptive control. *IEEE Transactions on Automatic Control,* (27), pp. 1161-1168.

Saerens, M., and Soquest, A. 1991. Neural controller based on back-propagation algorithm. *IEE Proceedings Radar and Signal,* **138** (1), pp. 56-62.

Slotine, J. J. E., and Li, W. 1992. *Applied Nonlinear Control.* Prentice Hall.

Tiano, A.,Mort, N.,Derradji, D. A.,Cuneo, M.,Ranzi, A., and Zhou, W. W. 1994. *Rudder Roll Stabilisation by Neural Network-Based Control Systems.* Proc. 3rd Int. MCMC '94. pp. 33-44

Chapter 8 Conclusions and further recommendations

8.1 Review

In this thesis the problem of designing autopilots for ships based on intelligent control approaches has been investigated. The motivation for this and the challenges have been briefly addressed in the introductory chapter where also a pragmatic viewpoint that intelligent control theory is the discipline that involves both intelligence and control theory is presented.

The motivation for considering this control design approach for solving the ship motion control problem, is based on an attempt to produce control systems that can guarantee acceptable performance in a wide range of operating conditions. This control design problem is traditionally defined in the framework of robust and adaptive control theory. In the robust approach, the aim is to design a controller with fixed parameters which perform acceptably well in different sailing conditions while in the adaptive approach the controller parameters are constantly varied in an attempt to seek the optimum of a suitable performance function.

Control algorithms that possess the ability to learn about and adapt to the disturbances and the different operating conditions represents a very appealing alternative solution for the control design problem. Prompted by advances in computing technology, algorithms with some of the above mentioned characteristic can run on-line in standard computer systems and can be used for an efficient solution of the intelligent control problem. However, to fulfil the computational requirements, according to the particular control problem, some assumptions on the controller structure and the learning algorithm has to be assessed.

Chapter two introduces the two main system structures used for implementing intelligent control paradigms developed in this thesis, namely artificial neural networks and fuzzy logic systems. When focusing on the functional evaluation, it is shown that these two systems can be described in the common framework of adaptive networks. In this framework, a synergistic comparison between neural networks and fuzzy logic systems is made.

Chapter three briefly describes adaptive networks with their universal approximation capability and some of the most traditional control architecture structures. The universal approximation capability of these networks will guarantee that a solution to the problem of approximating the control mapping does exist. This essentially has motivated the use of such systems in different conditions of uncertainty as learning or adaptive systems. Two of the most popular and standard learning algorithms, namely the least mean square and the back-propagation algorithms, are presented at the end of this chapter.

Chapters four, and five describes in some detail the system to be controlled, namely the ship. In particular, chapter four introduces the Newton equations of motion used for the mathematical description of the different motions of a ship. Hydrodynamic derivatives and stability criteria for the lateral and vertical motions have been also discussed, the latter characterises the manoeuvrability and the dynamical properties of a ship. In the final section of chapter four, mathematical models describing the yaw dynamics used for control design purposes have been discussed. These models have been used for the description of different situations of *a-priori* knowledge and for the justification of the proposed controller and identifier structures.

Chapter five describes the particular containership used in the simulation study, the main parameters of which are reported in Appendix A. This chapter describes the way the non-linear equations of motion are implemented and the disturbances accounted for to make the simulation of the overall systems. Standard manoeuvres are also described at the end of the chapter. Appendix A describes how from these manoeuvres, knowledge on the dynamical response of the systems can be gained while Appendix B describes the formulation of the environmental disturbances. The quality of the mathematical model used for testing in simulation the proposed controllers facilitate the extension of the achieved results to practical applications.

Chapter six introduces control algorithms that are motivated by a description which an expert would give about the manoeuvre. In this context, fuzzy logic systems represents a very powerful tool where heuristic knowledge in terms of if-then rules can be easily incorporated in the control design process. Examples of the course-changing and the course-keeping autopilots have been shown in section 6.2 and 6.3 respectively. The difficulty of this control design approach is that the performances of the resultant controller will depend on the experiences of the designer. Therefore, the control system performances cannot be guaranteed to be optimal. Further adjustment of some or all of the controller parameters is needed. This successive adjustment can be achieved by any of the learning algorithms introduced in the framework of adaptive networks or by exploiting heuristic knowledge through the use of another fuzzy logic system. As a consequence, the control system designed with this approach can be seen as a first attempt to solve the control problem based on which further optimisation can be applied.

Chapter seven describes the proposed intelligent control algorithms. For the solution of the course-changing control problem, an indirect model reference adaptive approach has been proposed. In this approach, the assumption on the ship dynamics is made more general by assuming a non-linear regressive model of known order. The unknown non-linear functions are approximated by means of neural networks and then used in turn to implement the controller. Although the indirect approach does not rely on the information of the system's Jacobian, it suffers from excessive computational effort. Moreover the on-line implementation of the algorithm is complicated by the fact that the unknown non-linear function describing the ship's dynamics has to be identified in closed-loop.

The course-keeping control problem has been formulated in the framework of feedback linearisation theory. Although the proposed algorithm showed better performances when compared with a traditional linear quadratic controller, an on-line implementation has not been attempted.

In the last section of chapter six a stable adaptive autopilot based on neural networks is presented. In this context the aim is to extend results of linear adaptive theory to the case where unknown or time variant non-linearity characterises the system's response. The choice on the structure of the approximator as well as the learning algorithm are motivated both by the need to guarantee an analytical solution for the stability analysis and also to guarantee an on-line implementation of the control algorithm. It has been shown that the design of an intelligent autopilot can be posed in the framework of adaptive theory where the analytical analysis of the control system can be attained. The performances of the resultant controller have been tested with respect a non-linear

model of a containership and it has been shown that the proposed controller responded satisfactory to all the dynamic changes for which it has been tested.

8.2 Discussion and Conclusions

Continuous development in computing technology will clearly move the computational barrier further, allowing more general control algorithm to be implemented. A field of control system that is strictly related to the computing technology is the field of intelligent control. Here, peculiar characteristics of intelligent species are emulated and translated in algorithms in order to design advantageous and efficient control systems.

The most used control system structures for the design of intelligent autopilot for ships, is the feedforward networks trained with the back-propagation algorithm. The motivation for this structure is based on the universal approximation capability of this system which will guarantee the existence of the approximation mapping.

At the present time, the use of the direct adaptive approach compared to the indirect approach is mainly motivated from the less computational effort involved in training the controller parameters. However, due to the non-linear nature of the overall system, analytical analysis of stability properties are not addressed. When focusing on the functional evaluation of the network nodes, neural networks and fuzzy logic systems are comparable. Therefore, the difficulties encountered in the analytical analysis of such systems are the same. At the present, major effort in the research community has been concentrated on developing training algorithms to guarantee the successful learning of the proposed neural and fuzzy based autopilots.

Sections 7.2 and 7.3 of Chapter 7, describes respectively the indirect adaptive approach for the design of course-changing autopilots and the feedback linearisation technique for the design of a course-keeping autopilot both implemented with feedforward neural networks and back-propagation algorithm. It may be argued, that the difficulty in implementing the above control algorithms on-line may be overcome by using a more powerful computing system. However, research in the field of artificial intelligence and learning systems, has to be focused on developing new learning algorithms for an efficient training of dynamical networks. At the present time, this problem is mainly solved with the use of dynamical filter, whereby by expansion of the input vector to include past values of the input and output signals, algebraic loops in the network are avoided allowing the use of the back-propagation algorithm. The need for a neural network model of the system to be controlled also represents a computational drawback which is usually overcome by considering a fixed neural model of the plant trained off-line. In this case the truly adaptive properties of the systems are not achieved.

It is important to notice that all the systems discussed herein, are non-linear and time variants. Therefore, following the historical evolution of control theory, another important field of research is represented by the non-linear control theory. A better understanding of non-linear systems can advise in different aspect, i.e. how many parameters are necessary in the controller, which of them can be considered fixed and which are adjustable. An example where analytical results of adaptive control theory can be used advantageously for the design of stable intelligent controller is given in Chapter 7 section 7.4. Here, both the structure and the adaptive law are motivated by the need to guarantee on-line implementation and stability analysis of the overall system

and are driven by the theory of adaptive linear systems. An efficient adaptive autopilot based on neural networks is then achieved.

It has been already mentioned, that an important characteristic of fuzzy logic systems, is their ability to incorporate heuristic knowledge expressed in terms of if-then rules. This characteristic, which differentiate fuzzy logic systems from any other approximators can be used advantageously during the control design process. This has been shown in the particular case of the ship autopilots, in Chapter six. The investigation of the non-singleton fuzzification as a way to pre-process and pre-filter noisy measurements following heuristic information is another area of future investigation that deserves some attention.

Finally, the question whether intelligent control design techniques should be used in place of conventional approaches for the design of autopilots for ships, especially in practical applications, is of particular interest. Although the full advantages of these control techniques can be appreciated better when the multivariable control design approaches are considered, it has been shown that indeed it is possible to design efficient autopilots for ships based on an intelligent control approach. However at the present time the on-line implementation is not always guaranteed for a general structure of the approximator. Moreover, to be able to solve analytically the stability analysis of the resultant system some constraint on the approximator structure as well as on the adaptive law has to be fulfilled.

The main contribution of the thesis is to address the design of intelligent autopilots for which an analytical analysis of the overall system can be attempted. Following the historical development of adaptive systems, it is believed that one of the reasons why

intelligent autopilots are not yet widespread in practical applications is the lack of theoretical results concerning the stability analysis of these systems. By carefully choosing the controller structure it has been shown how an analytical analysis of the system's performance can be achieved and at the same time the on-line implementation of the control algorithm is guaranteed.

Appendix A

This appendix reports the main data of the containership used in the simulation study described in Chapter five.

A.1 Geometrical data and hydrodynamics coefficients

Table I: Containership main data

Length	231	m
Beam	32	m
Draught	10.81	m
Mass	$47\ 10^6$	Kg
Displacement	46000	m^3
Metacentric height	0.83	m
Block coefficient	0.56	
Propeller diameter	8	m
Rudder area	60	m^2
Rudder rate (one pump)	2.3	deg/sec
Cruising speed	12.7	m/sec
Transverse area of superstructure (A_Y)	5200	m^2
Transverse area of superstructure (A_X)	1100	m^2

Table II: Hydrodynamic coefficients for the containership

X-Coefficients * 10^5	Y-Coefficients* 10^5	N-Coefficients * 10^5	K-Coefficients *10^5
X_v=-24	Y_v=-725	N_v=-300.0	K_v=25.0
X_{vv}=-1	Y_{vv}=98.6	N_{vv}=-109.6	K_{vv}=0.0
	$Y_{v\|v\|}$=-5801.5	$N_{v\|v\|}$=-712.9	$K_{v\|v\|}$=99.2
X_{δ}=-1.4	Y_{δ}=248.1	N_{δ}=-128.9	K_{δ}=-6.5
$X_{\delta\delta}$=-116.8	$Y_{\delta\delta}$=13.4	$N_{\delta\delta}$=-11.9	$K_{\delta\delta}$=-0.8
X_u=-226.2	$Y_{\delta\delta\delta}$=-193	$N_{\delta\delta\delta}$=101.4	$K_{\delta\delta\delta}$=4.1
X_{uu}=-64.5	$Y_{\delta u}$=-379.4	$N_{\delta u}$=196.9	$K_{\delta u}$=8.9
X_{uuu}=-137.2	$Y_{\delta\delta u}$=55.6	$N_{\delta\delta u}$=12.8	$K_{\delta\delta u}$=1.3
	$Y_{\delta\delta\delta u}$=232.3	$N_{\delta\delta\delta u}$=-125.4	$K_{\delta\delta\delta u}$=-4.8
X_0=0	Y_0=4.7	N_0=-0.6	K_0=-0.1
$X_{v\delta}$=124.5	Y_{0u}=-5.3	N_{0u}=6.5	K_{0u}=1.1
$X_{v\delta\delta}$=341	$Y_{\delta v}$=-100	$N_{\delta v}$=24.6	$K_{\delta v}$=5.4
$X_{vv\delta}$=0	$Y_{\delta vv}$=189/2	$N_{\delta vv}$=-349.1	$K_{\delta vv}$=-0.9
$X_{\delta u}$=-17.2	$Y_{\delta\|v\|}$=0	$N_{\delta\|v\|}$=0	$K_{\delta\|v\|}$=0
$X_{\delta\delta u}$=224.9			
X_{φ}=-5.9	Y_{φ}=37.7	N_{φ}=-17.9	
$X_{\varphi\varphi}$=-42.2	$Y_{\varphi\varphi}$=0	$N_{\varphi\varphi}$=0	
$X_{v\varphi}$=108.1	$Y_{v\varphi}$=144.9	$N_{v\varphi}$=17.8	$K_{v\varphi}$=-14.7
$X_{v\varphi\varphi}$=0	$Y_{v\varphi\varphi}$=2459.3	$N_{v\varphi\varphi}$=-0.9	$K_{v\varphi\varphi}$=-103.9
$X_{\varphi vv}$=0	$Y_{\varphi vv}$=177.2	$N_{\varphi vv}$=-933.9	$K_{\varphi vv}$=-6.2
X_r=43.1	Y_r=118.2	N_r=-280.0	K_r=8
X_{rr}=4.4	$Y_{r\|r\|}$=0	$N_{r\|r\|}$=0	$K_{r\|r\|}$=-20.0
	Y_{rrr}=-158	N_{rrr}=-224.5	K_{rrr}=0
X_{rv}=607.2	$Y_{r\|v\|}$=-409.4	$N_{r\|v\|}$=-778.8	$K_{r\|v\|}$=41.1
	Y_{rvv}=-994.6	N_{rvv}=-1287.2	K_{rvv}=-34.6
	$Y_{v\|r\|}$=-1192.7	$N_{v\|r\|}$=--174.4	$K_{v\|r\|}$=10.4
	Y_{vrr}=-1107.9	N_{vrr}=36.8	K_{vrr}=22.2
$X_{\dot{u}}$=-124.4	$Y_{\dot{r}}$=-48.1	$N_{\dot{r}}$=-30	$K_{\dot{r}}$=-1
	$Y_{\dot{v}}$=-878	$N_{\dot{v}}$=42.3	$K_{\dot{v}}$=0
	Y_p=-3.4	N_p=-8	K_p=-3.0
X_{pp}=7.2	$Y_{p\|p\|}$=0	$N_{p\|p\|}$=0	$K_{p\|p\|}$=-1.0
	Y_{ppp}=-9.3	N_{ppp}=-5	K_{ppp}=0.8
X_{ppu}=3.9	Y_{pu}=23.6	N_{pu}=12.8	K_{pu}=0
	$Y_{pu\|pu\|}$=-52.5	$N_{pu\|pu\|}$=-12.4	$K_{pu\|pu\|}$=-1.4
	$Y_{\dot{p}}$=23.3	$N_{\dot{p}}$=0.2	$K_{\dot{p}}$=-0.7

Table III
(Hydrodynamics parameters re-tuned to match the full scale experiments)

Hydrodynamic derivative	RPMM model * 10^{-5}	Tuned to full scale test *10^{-5}
N_r	-282.3	-280.0
N_v	-356.0	-300.0
K_v	35.6	24.0
K_r	-44.7	8.0
$K_{r\|r\|}$	0.0	-20.0
K_{rrr}	15.9	0.0
K_{vv}	-4.6	0.0
$K_{\dot{p}}$	-2.7	-0.7
K_p	-2.0	-3.0
$K_{p\|p\|}$	0.0	-1.0
K_δ	-5.1	-6.5

Table IV

(Wind coefficients)

χ_w	C_X	C_Y	C_N
0	-0.778	0	0
20	-0.852	-0.297	-0.0518
40	-0.482	-0.52	-0.11
60	-0.111	-0.93	-0.11
80	-0.222	-0.93	-0.03
100	-0.185	1	0.006
120	0	-0.93	0.155
140	0.556	-0.52	0.1703
160	0.963	-0.297	0.11
180	0.815	0	0

200	0.963	0.297	-0.09
220	0.556	0.52	-0.163
240	0	0.93	-0.145
260	-0.185	1	-0.0518
280	-0.222	0.93	0.0037
300	-0.111	0.93	0.126
320	-0.482	0.52	0.126
340	-0.852	0.297	0.006
360	-0.778	0	0

A.2 Linear model

A multivariable linear model, in state space representation, can be obtained from a straightforward linearisation of the non-linear equation (6.4) considering only the first-order terms in the Taylor expansion (equation (6.5), (6.6), (6.7) and (6.8)). The following state vector representation:

$$\dot{x} = Ax + B\delta$$

with state $x = [v, r, p, \varphi, \psi]$, is obtained for: $A = (M)^{-1} N$ and $B = (M)^{-1} b$, where:

$$M = \begin{bmatrix} (m - Y_{\dot{v}}) & (mxg - Y_{\dot{r}}) & -(mzg + Y_{\dot{p}}) & 0 & 0 \\ (mxg - N_{\dot{v}}) & (Izz - N_{\dot{r}}) & -N_{\dot{p}} & 0 & 0 \\ -(mzg + K_{\dot{v}}) & -K_{\dot{r}} & (I_{xx} - K_{\dot{p}}) & 0 & 0 \\ 0 & 0 & 0 & 1 & 0 \\ 0 & 0 & 0 & 0 & 1 \end{bmatrix} \quad \text{(A.1)}$$

$$N\begin{bmatrix} Y_v & (Y_r - mu) & Y_p & Y\varphi & 0 \\ N_v & (N_r - mxgu) & N_p & N\varphi & 0 \\ K_v & (K_r + mzgu) & K_p & (k_\varphi - mxgGM) & 0 \\ 0 & 0 & 1 & 0 & 0 \\ 0 & 1 & 0 & 0 & 0 \end{bmatrix} \tag{A.2}$$

$$b = \begin{bmatrix} Y_\delta \\ N_\delta \\ K_\delta \\ 0 \\ 0 \end{bmatrix} \tag{A.3}$$

For a ship speed of 12.5 m/sec and GM=83 cm the parameters of the state space equations re-tuned to meet the full scale measurement are (Blanke & Jensen, 1997):

$$\begin{bmatrix} \dot{v} \\ \dot{r} \\ \dot{p} \\ \dot{\varphi} \\ \dot{\psi} \end{bmatrix} = \begin{bmatrix} -0.0115 & -3.2325 & -0.1112 & -0.0694 & 0 \\ -0.0010 & -0.2216 & -0.0066 & -0.0010 & 0 \\ 0.0037 & 0.0960 & -0.0752 & -0.0552 & 0 \\ 0 & 0 & 1 & 0 & 0 \\ 0 & 1 & 0 & 0 & 0 \end{bmatrix} \begin{bmatrix} v \\ r \\ p \\ \varphi \\ \psi \end{bmatrix} + \begin{bmatrix} 0.1217 \\ -0.0050 \\ -0.103 \\ 0 \\ 0 \end{bmatrix} \delta \tag{A.4}$$

Figure A.1 and A.2 shown the Bode plot for the turning rate and the roll angle respectively for the model of equation (A.4).

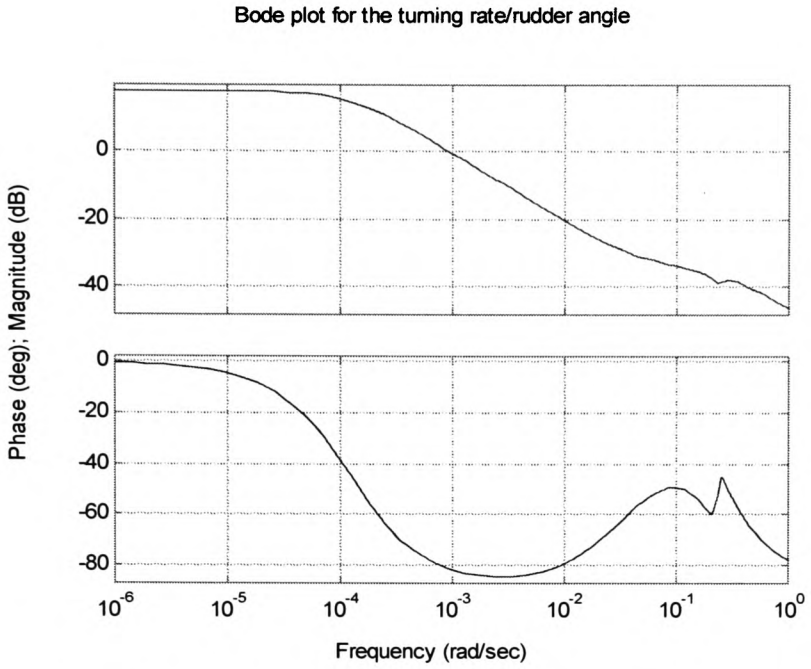

Fig.A.1: Bode plot, turning rate/rudder angle

Fig. A.2: Bode plot, roll angle/rudder angle

Note the different scale in the two figure above.

Figure A.3 and A.4 shows the state variables for a 5°/5° and 15°/15° zig-zag manoeuvre respectively. In dotted line is the response of the linearised model while in solid line is the non-linear model response. The error of the linear model increase as the manoeuvre becomes more tight.

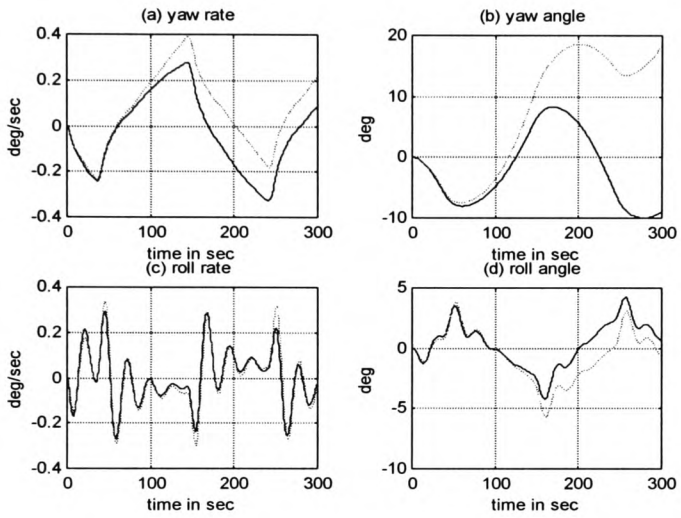

Fig.A.3: 5°/5° zig-zag manoeuvre. Dotted linear model, solid non-linear model

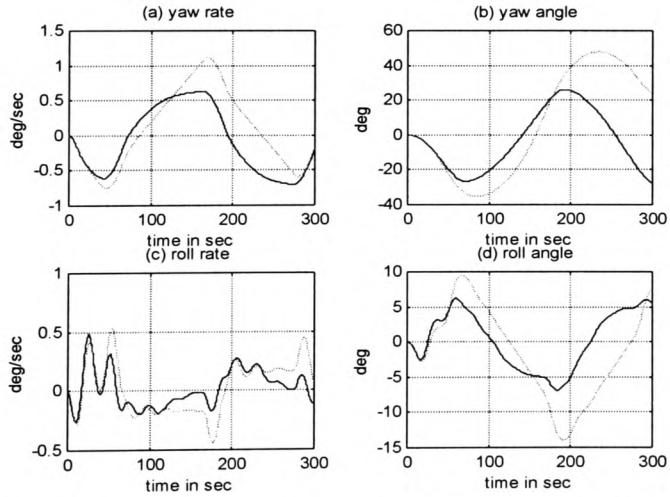

Fig.A.4: 15°/15° zig-zag manoeuvre. Dotted linear model, solid non-linear model

A linear model of the yaw dynamics, from the knowledge of the hydrodynamic derivatives, can be obtained from equations (4.24) and (4.25). However, a different way to proceed is to consider the response of standard manoeuvres briefly described in Chapter 6. Figure A.5, shows the time sequence of the rudder angle and the turning rate for a 10^{o} course-changing manoeuvre.

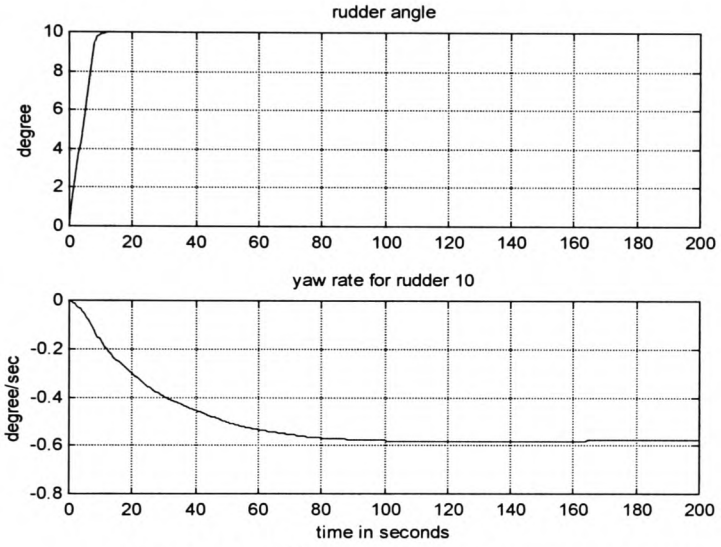

Fig.A.5: 10^{o} course-changing manoeuvre

By inspection of figure (A.5) it is clear that a first-order system with time constant $\tau \approx 18$ seconds, can describe such response. However, when the manoeuvre becomes more tight as in the case of a 30^{o} course-changing manoeuvre a second-order system is more precise.

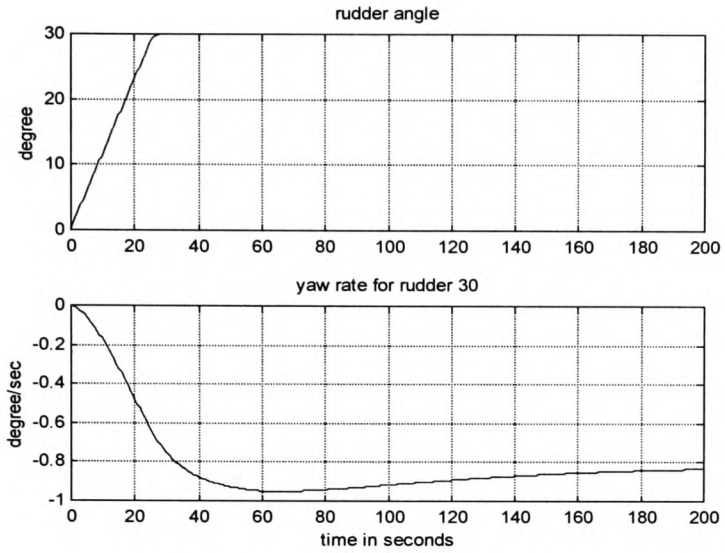

Fig.A.6: 30° course-changing manoeuvre

Figure A.6 shows a 30° course-changing manoeuvre, where it is possible to appreciate the overshoot of the yaw rate. By writing the second-order system in the general form of equation A.5:

$$\frac{\dot{\psi}(s)}{\delta(s)} = k\frac{\omega_n^2}{s^2 + 2\xi\omega_n s + \omega_n^2} \tag{A.5}$$

and applying well-known results of linear theory, from figure A.6, the parameters of equation (A.5) can be deduced as follows:

$$k = \frac{-0.82}{30} = 0.027; \qquad S_{\%} = 0.12\frac{100}{0.82} = 14.6\%; \qquad \xi = 0.5;$$

$$\omega_n = \frac{\pi}{\sqrt{1-\xi^2}}\frac{1}{60} = 0.06 rad/\sec$$

Figure A.7 shows the response of the linear model of equation A.5 with the above parameters (in dotted line) and the response of the non-linear model (in solid line). The main time constant of equation A.5 is:

$$\tau = \frac{1}{2\xi\omega_n} \approx 17 \text{ seconds.}$$

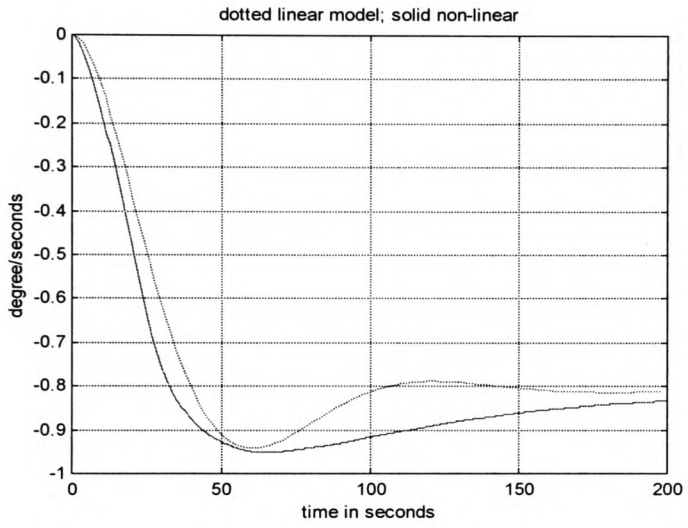

Fig.A.7: 30° step response of the linear (dotted line) and non-linear (solid line) model

A.3 Reference List

Blanke, M., & Jensen, A. G. 1997. Dynamic properties of container vessel with low metacentric height. *Transactions of The Institute of Measurement and Control,* **19** (2), pp. 78-93.

Appendix B Disturbances Modelling

B.1 Introduction

The motion exhibited by a sailing vessel is the result of different factors some of which are produced by the environmental conditions (i.e. wind, waves, current, water depth). In general all the factors that have an effect on the ship's motion and are not voluntarily determined by any control systems are labelled disturbances. For modelling purposes, it is possible to distinguish between two main categories of disturbances that are relevant for the control system design:

Additive disturbances: Environmental effects (i.e. wind, waves and current) can be considered as additive input signals to the process. Usually for modelling purposes, the superposition principle is applied in order to separate the ship motions induced by environmental effects from the motions produced by propeller thrust and control surfaces (i.e. rudder, fins etc.). Despite the non-linear nature of the ship's dynamics, the superposition principle allows a quite accurate and numerically reliable simulation of the environmental induced ship's motions (Lewis, 1967).

Multiplicative disturbances: These disturbances (i.e. depth of water, load and speed change), will affect the transfer function of the process making the overall system time variant.

There are different ways to account for the above mentioned disturbances during a simulation study. In this Appendix, sections B.2, B.3 and B.4, will discuss the effects induced by the waves, wind and current respectively. It will be shown how these effects can be modelled and accounted for during the control system design process. Section B.5 briefly describes the shallow water effects. However, due to its dominant effects on

the ship's dynamics, the waves induced disturbances will be described in more detail (Lewis, 1967).

B.2 Waves effects

(This section is mostly paraphrased from (Lewis, 1967))

Wave effects on ship motions are of great importance for naval architects in terms of safety and the overall system performance. A vessel sailing in a rough sea will manifest an undesirable acceleration that can lead to critical situations. For instance, an aircraft carrier in order to fulfil its mission of safely launching and landing aeroplanes must maintain a minimum speed into the wind, while at the same time the amplitudes of vertical motion or acceleration at the catapult or in the landing area must not exceed acceptable values. The ship's acceleration induced by the wave motion ultimately will affect the manoeuvrability therefore the safety of the ship. For these reasons the modelling of wave motion is of particular importance during the control system design process.

The method to describe how waves are generated is very complex, it is related to many different conditions like wind, sea depth and fetch (distance over which the wind blows). Two methods for wave motion modelling are reported in naval literature. The trochoidal method that is basically a geometrical approach for the description of the waves propagation, and the theory of simply gravity waves, where the sea motion is seen as a simple two-dimensional sinusoidal wave train over an infinite water surface with infinite depth. Although the trochoidal wave theory is the earlier approach, the theory of simply gravity waves is more suitable for statistical interpretation of waves motion and can be easily extended to the description of the irregular sea waves.

B.2.1 Simply Gravity Waves Theory (Regular waves)

The fundamental hypothesis under the simply gravity waves theory is that the waves in a fully developed sea have a strong periodic component. It is also assumed that the crests are straight, infinitely long, parallel and equally spaced, and the wave heights are constant. Under these hypothesis the wave profile can be described by a cosine function as in equation (B.1):

$$\zeta_0 = \zeta_a \cos k(x - V_w t) \tag{B.1}$$

where ζ_a is the surface wave amplitude (half-height from crest to trough), x is the direction of wave propagation. V_w is the wave velocity sometimes referred as celerity to emphasise that it is the wave form rather then the water particles that advances. Finally, k is the wave number defined as:

$$k = \frac{2\pi}{\lambda_w} \tag{B.2}$$

where λ_w is the wave length. The expression for the wave celerity can be obtained by energy considerations of the water mass. In shallow water $(\text{roughly } h \le \lambda_w/25)$, and deep water $(h \ge \lambda_w/25)$ such expressions are respectively reported in equations (B.3) and (B.4):

$$V_w^2 = gh \tag{B.3}$$

$$V_w^2 = \frac{g}{h} = \frac{g\lambda_w}{2\pi} \tag{B.4}$$

where h is the water depth and g is gravity acceleration. A more convenient form for the equation of a simple harmonic wave (equation (B.1)), can be obtained by using the circular frequency defined as:

$$\omega = \frac{2\pi}{T_w} \tag{B.5}$$

The period T_w is the time required for the wave to travel one wave length and hence the relationship between wave length and period in deep water can be derived from equation (B.4) as:

$$T_w = \frac{\lambda_w}{V_w} = \left(\frac{2\pi\lambda_w}{g}\right)^{1/2} \tag{B.6}$$

Equation (B.1) describing the wave profile become:

$$\zeta_0 = \zeta_a \cos(kx - \omega t) \tag{B.7}$$

When the wave is observed at a fixed point, with $x = 0$ equation (B.7) yields:

$$\zeta_0 = \zeta_a \cos(-\omega t) = \zeta_a \cos(\omega t) \tag{B.8}$$

Alternatively, if the wave profile is studied at $t = 0$, equation (B.7) yields:

$$\zeta_0 = \zeta_a \cos(kx) \tag{B.9}$$

The slope of the wave surface is obtained by differentiation:

$$\frac{d\zeta_0}{dx} = k\zeta_a \sin kx \tag{B.10}$$

The slope is maximum when sin(kx)=1, then:

$$Max\frac{d\zeta_0}{dx} = k\zeta_a = \frac{2\pi\zeta_a}{\lambda_w} \tag{B.11}$$

This maximum slope occurs midway between a crest and a hollow.

The observation that real waves have sharper crest and flatter hollows than the simple cosine wave described by equation (B.7) can be accounted for by the inclusion of a second-order term into a series expansion. The wave profile represented as a function of x at fixed time $t=0$, in deep water can be expressed with the so-called Stokes equation:

$$\zeta_0 = \zeta_a \cos(kx) + \pi\frac{\zeta_a^2}{\lambda_w}\cos 2kx \tag{B.12}$$

In other words, the simple cosine curve is modified by a harmonic that is half the length of the fundamental. The velocity of the harmonic wave, however must be the same as for the fundamental.

B.2.2 Harmonic waves theory (Irregular waves)

The Stokes equation is a good approximation for describing regular waves in fully developed sea under the assumptions of the simple gravity wave theory. Irregular waves, however are more complex. Generally produced by a combination of different factors, like limited fetch, influence of a different storm, abrupt change in water depth etc. A possible description of the irregular sea waves derives from the application of generalised harmonic analysis. The fundamental idea is to represent the irregular sea surface by the superposition of a very large number (theoretically infinite) of small-amplitude (infinitesimal) sine waves of different periods, amplitude and directions. Each of the individual components following the simple harmonic wave theory regarding wave length, period and speed. The elevation of the sea surface, ζ, as a function of time can be expressed by equation (B.13).

$$\zeta(t) = \lim_{\substack{\omega_n \to \infty \\ \partial\omega \to 0}} \Sigma \cos[\omega_n t + \varepsilon(\omega_n)][2S_\zeta(\omega_n)\partial\omega]^{1/2} \qquad \text{(B.13)}$$

In equation (B.13) $\varepsilon(\omega_n)$ is a random phase between $[0,2\pi]$, while $S_\zeta(\omega_n)$ is the spectral density of the sea and represents the energy carried from the n^{th} harmonic. In practice the summation in equation (B.13) is limited to the first 10 to 15 components. Different spectral formulae have been proposed for the statistical description of sea states. Earlier formulation of the spectral density included wind speed as a parameter. The spectral formulation due to Neumann (1952) and described by equation (B.14) is one of these examples.

$$S_\zeta(\omega_n) = C\omega^{-6} e^{2\left(\frac{-g}{\omega V}\right)^2} \tag{B.14}$$

where C is an empirical constant and V is the wind speed. Bretschneirder (1959), who considered the spectral density formulation as a function of the significant waves height ($h_{1/3}$), proposed a more sophisticated spectrum described by equation (B.15).

$$S_\zeta(\omega_n) = \frac{1.25\omega_0^4}{4\omega^5} h_{1/3} e^{-1.25\left(\frac{\omega_0}{\omega}\right)^4} \tag{B.15}$$

At present, the modified Pierson-Moskowitz spectrum is the formulation more widely used for prediction of responses of marine vehicles and offshore structures in open sea. It is also recommended by the International Towing Tank Conference (ITTC) and the International Ship and Offshore Structures Congress (ISSC) and the formula is given in equation (B.16):

$$S_\zeta(\omega_n) = \frac{173 h_{1/3}^2}{\omega_n^5 T_n^4} e^{\left(\frac{-691}{T_n^4 \omega_n^4}\right)} \tag{B.16}$$

where T_n is the average period between successive crests while $h_{1/3}$ (the significant waves height) is defined as the average of the 1/3 highest waves measured in a fixed period of observation.

Figure B.1 shows the spectral density for different significant wave height and average period calculated using equation (B.16). As the significant wave height increases the bulk of energy is shifted to a lower frequency.

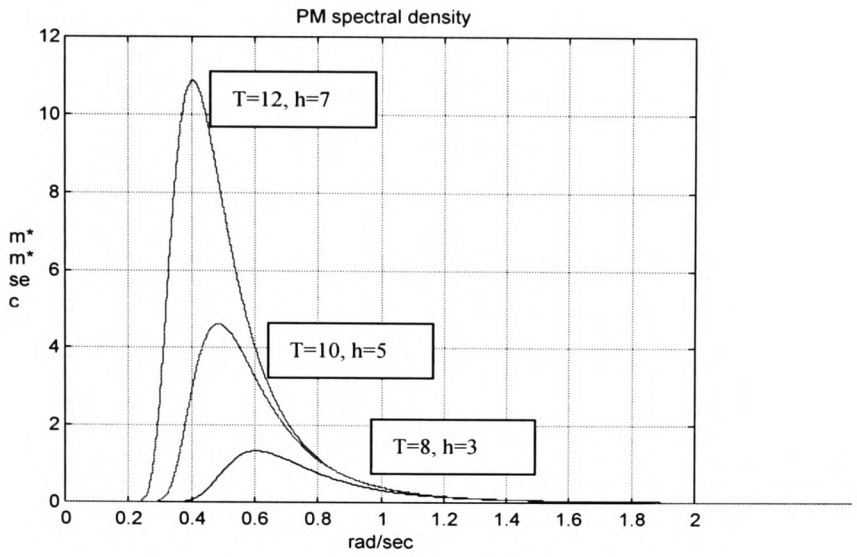

Fig.B.1: Pierson-Moskowitz spectral density for different values of T and $h_{1/3}$

B.2.3 Waves forces and moments

To derive the expressions for the forces and moments induced by the waves pressure on the ship's hull, a set of simplifying assumptions should be specified:

1. The forces and moments acting on the hull, result from the water pressure acting on the wetted surface,
2. The wave field is not affected by the presence of the ship's hull,

For a ship where the wetted part is a rectangular parallelepiped with length L, breadth B and draft T, Kallstrom proposed the following formulae (from (Fossen, 1994)):

$$X_{wave}(t) = \sum_{i=1}^{N} \rho g B L T \cos\beta s_i(t)$$
$$Y_{wave}(t) = \sum_{i=1}^{N} -\rho g B L T \sin\beta s_i(t) \qquad \text{(B.17)}$$
$$N_{wave}(t) = \sum_{i=1}^{N} \frac{1}{24} \rho g B L (L^2 - B^2) \sin 2\beta s_i^2(t)$$

where β is the angle of encounter defined as the angle between the travelling direction of the wave and ship. $s_i(t)$ is the wave slope calculated by differentiation of the wave profile and N is the number of harmonic considered for the description of the irregular wave (typically 10 to 15). When a fixed point of observation is assumed (x=0 for simplicity) the i^{th} component of the irregular wave can be described by equation (B.8), its derivative become:

$$s_i(t) = \zeta_{a,i} \sin \omega_{n,i} t \qquad \text{(B.18)}$$

When the ship has a velocity different from zero, it experiences the wave effects with a different frequency and a different power. The spectral density therefore has to be modified according to the actual ship's velocity and angle of encounter as defined above. Equation (B.18) is modified as follows:

$$s_i(t) = \zeta_{a,i} \sin \omega_{e,i} t \qquad \text{(B.19)}$$

where ω_e is the frequency of encounter defined by equation (B.20).

$$\omega_e = \omega_n \left(1 - \omega_n \frac{U}{g} \cos\beta\right) \qquad \text{(B.20)}$$

Applying the superposition principle the forces and moment expressed in equation (B.17) are added to the right hand side of the Newton's equation describing the dynamics of a ship.

B.2.4 Response operators

A different way to simulate the environmental effects, is to regard directly to the response of the ship at a certain wave conditions. The purpose is to reconstruct the motion of the ship induced by the waves in terms of the state variables. The spectral density of the ship's induced motion can be calculated from the wave spectral density by the use of the so-called receptance operator. Figure B.2 and equation (B.21) illustrate this idea.

$$S_{zz}(\omega_n, \beta, U) = \left|R_{z\zeta}(\omega_n, \beta, U)\right|^2_{U=0} S_{\zeta}(\omega_n, \beta) \tag{B.21}$$

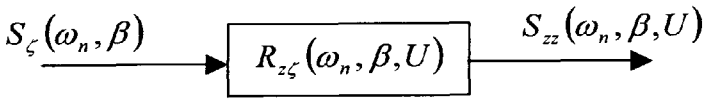

Fig.B.2: Spectral density of the ship's induced motion

The receptance operator or response operator $R_{z\zeta}$, represents the relationship between wave height ζ to the ship's motion z. The spectral density for the moving vessel in term of its frequency of encounter ω_e is obtained by observing that wave energy in a frequency interval is unaffected by the observer speed. This is expressed by equation (B.22):

$$S_{zz}(\omega_n,\beta,U)d\omega_n = S_{zz}(\omega_e,\beta,U)d\omega_e \tag{B.22}$$

From equation (B.20) follows:

$$\frac{d\omega_e}{d\omega_n} = 1 - 2\omega_n \frac{U}{g}\cos\beta \tag{B.23}$$

therefore from (B.21) and (B.22) the spectral density as a function of the encounter frequency can be expressed as:

$$S_{zz}(\omega_e,\beta,U) = \frac{\left|R_{z\zeta}(\omega_n,\beta,U)\right|^2 G_\zeta(\omega_n,\beta)}{1 - 2\omega_n \frac{U}{g}\cos\beta} \tag{B.24}$$

The problem with equation (B.24) is that in a following sea ($0^o < \beta < 90^0$) the denominator can be zero, (when $\omega_n = \frac{g}{2U\cos\beta}$), introducing infinite peaks in the spectral density of the ship's induced motion S_{zz}. This problem can be avoided by considering an approximation of the sea spectrum by a finite sum of sinusoids with random initial phase:

$$z(t) = \sum_{i=1}^{n} a_i \sin(\omega_{e,i} t + \varphi_i + \varphi_{init}) \tag{B.25}$$

For a different response operator, *z(t)* will be a particular induced motion (surge, sway or roll). The coefficients a_i can be calculated from the relation between the power spectrum as:

$$\frac{1}{2}a_i^2 = \int_{\omega_1}^{\omega_2} S_{zz}(\omega_e,\beta,U)d\omega_e = \int_{\omega_1}^{\omega_2} \left|R_{z\zeta}(\omega_n,\beta,U)\right|^2 S_\zeta(\omega_n,\beta)d\omega_n \qquad \text{(B.26)}$$

Using the variance definition:

$$\sigma_\omega^2(\omega_1,\omega_2) = \int_{\omega_1}^{\omega_2} S_\zeta(\omega_n)d\omega_n \qquad \text{(B.27)}$$

from equation (B.26) the sine amplitude can be computed as:

$$a_i = \sqrt{2}\left|R_{z\zeta}(\omega_{n,i},\beta,U)\right|\sqrt{\sigma_\omega^2(\omega_2,\omega_3)} \qquad \text{(B.28)}$$

Applying the superposition principle, the induced motion z(t) can be added to the state vector computed from the Newton's equation.

B.3 Wind effects

(This section is mostly paraphrased from (Fossen, 1994))

The wind induced forces and moments on a ship can be described by a combination of a mean wind speed and a turbulent component describing the effect of gusting. The mean component of wind exposes the ship to a quasi-steady force although non-stationary in a

long period of time. The turbulent component is random in magnitude and direction, and can be characterised by an appropriate spectrum. One of the most popular formulations for the wind gust is the Davenport spectrum:

$$S_w(\omega) = k\frac{916700\omega}{\left[1+(191\omega/V_w(10))^2\right]^{4/3}} \tag{B.29}$$

where:

k is the turbulent factor ≈ 0.05

$V_w(10)$, is the average wind speed, expressed in knots, at a level of ten metres above the water surface,

ω is the frequency of the wind oscillations expressed in rad/sec.

Another formulation for the wind gust is the so-called Harris spectrum:

$$S_w(\omega) = k\frac{5286V_w(10)}{\left[1+(286\omega/V_w(10))^2\right]^{5/6}} \tag{B.30}$$

In order to calculate the local velocity of the wind at a certain height z of the sea surface, it is possible to apply the boundary-layer profile given the formula:

$$V_w(z) = V_w(10)\cdot\left(z/10\right)^{1/7} \tag{B.31}$$

The spectrum formula, used by the Danish Maritime Institute, describing the high wind speeds over the North Sea is for the surge component (Blanke M. and Jensen A.G., 1997) and is given by:

$$G_{uu}(\omega)=\frac{zV_w^2(10)}{V_w}\cdot\frac{32.2}{\left(1+\omega\left(\frac{110z}{2\pi V_w}\right)\right)^{5/3}} \tag{B.32}$$

while for the sway component, the Kailman formula is:

$$G_{vv}(\omega)=\frac{zV_w^2(10)}{V_w}\cdot\frac{1.113}{\left(1+\omega\left(\frac{9.5z}{2\pi V_w}\right)\right)^{5/3}} \tag{B.33}$$

The forces and moment on the ship due to the wind effect, can be expressed as (Isherwood, 1972):

$$\begin{aligned} X_w &= \frac{1}{2}\rho_{air}C_X(\chi_w)V_w^2A_X \\ Y_w &= \frac{1}{2}\rho_{air}C_Y(\chi_w)V_w^2A_Y \\ N_w &= \frac{1}{2}\rho_{air}C_N(\chi_w)V_w^2A_YL_{pp} \end{aligned} \tag{B.34}$$

where V_w is the local wind velocity in knots, ρ_{air} is the air density in k_g/m^3, A_X and A_Y are the transverse and lateral projected areas in m^2, C_X C_Y and C_N are the forces and moment coefficients which are a function of the relative angle of attack (χ_w) and L_{pp} is the overall length of the ship. The forces and moment coefficients are calculate by experimental tests. Due to the difficulty in determine the coefficient C_K from experimental test, the roll moment induced by the wind can be expressed by the empirical formula:

$$K_w = Y_w z_{ayc} \tag{B.35}$$

where z_{ayc} is the distance from the water surface to the geometrical centre of the cross section. When the ship is moving with surge speed u and sway speed v, the components of the relative wind are:

$$u_w = (V_w + u_g)\cos(\psi_w - \psi) - v_w \sin(\psi_w - \psi) - u + u_c \tag{B.36}$$

$$v_w = (V_w + v_g)\sin(\psi_w - \psi) + v_w \cos(\psi_w - \psi) - v + v_c \tag{B.37}$$

where u_c and v_c are current velocity components, u_g and v_g are the gust velocity components, ψ_w and ψ are the wind and ship direction respectively. The relative angle of attack can be computed thus:

$$\chi_w = \arctan\left(\frac{v_w}{u_w}\right) \tag{B.38}$$

and the square of relative wind speed, which is used for calculation of forces, is:

$$V_w^2 = u_w^2 + v_w^2 \tag{B.39}$$

Note that in calculating the gust components, the apparent frequencies of the turbulent components are affected by the Doppler effect. The encounter frequencies are then:

$$\omega_{ue} = \frac{V_w + U\cos(\psi_w - \psi)}{V_w}\omega \tag{B.40}$$

$$\omega_{ve} = \frac{V_w - U\sin(\psi_w - \psi)}{V_w}\omega \tag{B.41}$$

Since the energy contained in a certain interval of wavelengths of the turbulence is not dependent on the velocity of the observer:

$$dG(\omega_e)d\omega_e = dG(\omega)d\omega \tag{B.42}$$

the Doppler effect is just a linear compression or expansion of the spectrum, with an associated change in spectral density to give unchanged total power.

B.4 Ocean Current

Ocean currents can be generated by many phenomena, such as wind blowing to the sea surface, isotherms (regions with different water temperature), Coriolis acceleration due to the earth rotation, tidal current due to gravitational effects. In any case the ocean currents have a strong steady component, that allow its modelling by considering the relative velocity between the ship and current. The modified velocity vector due to the presence of current is therefore expressed as:

$$\vec{v}_r = \vec{v} - \vec{v}_c \tag{B.43}$$

where $\vec{v}$ is the ship velocity vector and $\vec{v}_c$ is the current velocity vector. For simulation purposes it is sufficient therefore to compute the new surge and sway component of the ship velocity according to equation (B.43) and substitute these new component in the Newton equation of motion.

B.5 Shallow water effects

When a ship sails in open sea, the lines of the flow water goes not only around the sides of the ship but also down and along the bottom of the ship. However, when the water is shallow, the flow under the hull is restricted, causing more flow along the sides. This in turn changes the forces and moments distribution acting on the ship and hence the values of the hydrodynamic derivatives describing those forces. In order to properly account for these effects it is therefore necessary to perform apposite trial tests in shallow water. The new hydrodynamic derivatives values, identified in this condition, are then used for the simulation of the ship dynamics sailing in shallow water.

Although specific of hydrodynamic derivative values exist for a particular ship model, (Sheng, 1981) and further (Clarke, 1983) proposed, the correction of the following hydrodynamic derivatives based on the geometry of the ship's hull to account for shallow water effects.

$$\frac{Y'_{\dot{v}}}{Y'_{\dot{v}_\infty}} = K_0 + \frac{2}{3}K_1\frac{B}{T} + \frac{8}{15}K_2\left(\frac{B}{T}\right)^2 \qquad \frac{N'_{\dot{r}}}{N'_{\dot{r}_\infty}} = K_0 + \frac{2}{5}K_1\frac{B}{T} + \frac{24}{105}K_2\left(\frac{B}{T}\right)^2$$

$$\frac{Y'_{v}}{Y'_{v_\infty}} = K_0 + K_1\frac{B}{T} + K_2\left(\frac{B}{T}\right)^2 \qquad \frac{N'_{v}}{N'_{v_\infty}} = K_0 + \frac{2}{3}K_1\frac{B}{T} + \frac{8}{15}K_2\left(\frac{B}{T}\right)^2 \qquad \text{(B.44)}$$

$$\frac{Y'_{r}}{Y'_{r_\infty}} = K_0 + \frac{2}{3}K_1\frac{B}{T} + \frac{8}{15}K_2\left(\frac{B}{T}\right)^2 \qquad \frac{N'_{r}}{N'_{r_\infty}} = K_0 + \frac{1}{2}K_1\frac{B}{T} + \frac{1}{3}K_2\left(\frac{B}{T}\right)^2$$

where

$$K_0 = 1 + \frac{0.0775}{F^2} - \frac{0.0110}{F^3}; \quad K_1 = -\frac{0.0643}{F} + \frac{0.0724}{F^2} - \frac{0.0113}{F^3}; \quad K_2 = \frac{0.0342}{F};$$

and

$$F = \left(\frac{H}{T} - 1\right)$$

In the above formulae the subscript ∞ refers to the hydrodynamic derivative's values in depth water. The parameters H, B and T are specified in figure B.3.

The correction proposed by Sheng and Clarke and reported in equation (B.44) are based on linear theory and clearly are not an exhaustive model of the shallow water effects. Nevertheless, because of their generality they represent an easy and general way to account for the shallow water effects for control systems simulation purposes.

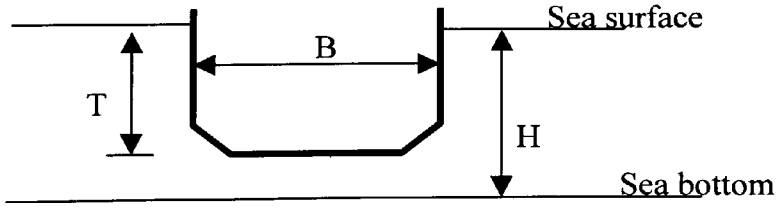

Figure B.3: The ship in shallow water

B.6 Summary

In this Appendix the environmental effects on the dynamics of a ship are described. Waves, wind, current and shallow water effects have been described in section B.2, B.3, B.4 and B.5 respectively. The former three disturbances are considered as additive while the latter will affect the parameters of transfer function making the overall system time variant. Due to its major effects for the control systems performances, the modelling of wave effects has been considered in more details. The proposed control algorithm will be tested with respect different of disturbances and sailing conditions.

B.7 Reference List

Blanke M. and Jensen A.G. 1997. Dynamic properties of container vessel with low metacentric height. *Transactions of The Institute of Measurement and Control,* **19** (2), pp. 78-93.

Clarke, D. 1983. The Application of Manoeuvring Criteria in Hull Design Using Linear Theory. *Transactions of Royal Institution of Naval Architects,* **125**, pp. 45-68.

Fossen, T. I. 1994. *Guidance and Control of Ocean Vehicles.* John Wiley and Sins Ltd. 0-471-94113-1.

Isherwood, R. M. 1972. Wind Resistence of Merchant Ships. *RINA Transc.*, **115**, pp. 327-338.

Lewis, E. V. 1967. The motion of ships in waves. *In:* J. P. Comstock ed. *Principles of*

Navav Architecture. (Chapter 9). New York: The Society of Naval Archotects and Marine Engineers, pp. 605-717.

Sheng, Z. Y. 1981. *Contribution to the discussion of the Manoeuvrability Committee Report.* Proceeding of 16th ITTC. pp. 170-173, Leningrad.

Appendix C

In this appendix the stability proof of the adaptive autopilot based on neural networks presented in section 7.4 of Chapter 7 is presented.

C.1 Stability proof

The adaptive law expressed by equation (7.15) is motivated by the linear adaptive theory, in which it has been proved that if:

1. the relative degree d, of the system is known,
2. the non-linear functions f satisfy a global Lipschitz condition and
3. the output of the system does not grow faster than the input,

then the non-linear system expressed by the equation (7.7), with the adaptive law expressed by equation (7.15) and the control law (7.16) results in all the signals being uniformly bounded and there exist an integer K_t and a non-negative constant C such that:

$$|\hat{\psi}(k)-\psi(k)| \le \varepsilon_{\max} \quad \text{and} \quad |\psi(k)-\psi_m(k)| \le C \quad \text{for all} \quad k \ge K_t .$$

A detailed proof of this result can be found in the original paper (Peterson and Narendra, 1982) or in chapter 8 of (Narendra and Annaswamy, 1989). Here the main steps involved are briefly highlighted.

Step 1.

Considering a bounded disturbance ε, equation (7.7) can be rewritten:

$$\psi(k+1)=\theta^T\omega(k)+\varepsilon(k) \tag{C.1}$$

the identification error becomes:

$$e(k+1)=\hat{\psi}(k+1)-\psi(k+1)+\varepsilon(k)=\phi^T(k)\omega(k)+\varepsilon(k) \tag{C.2}$$

where $\phi(k)=\hat{\theta}(k)-\theta$ is the parameter error. Using the direct method of Lyapunov it is proved that:

i) the parameter error $\phi(k)=\hat{\theta}(k)-\theta$ is bounded,

ii) the identification error either does not grow faster then the signal vector $\omega(k)$ or is bounded $|e(k)|\le\varepsilon_{\max}$ and

iii) the parameter error converge $\lim_{k\to\infty}\|\Delta\phi(k)\|=0$.

This can be done by choosing the Lyapunov candidate function $V(k)=\phi^T(k)\phi(k)$. The time derivative evaluated along equation (7.15) is:

$$V(k+1)-V(k)=\phi^T(k+1)\phi(k+1)-\phi^T(k)\phi(k)=$$

$$=-\frac{\eta(k)e^2(k+1)}{1+\|\omega(k)\|^2}\left[2-\eta(k)\frac{\|\omega(k)\|^2}{1+\|\omega(k)\|^2}\right]+\frac{2\eta(k)e(k+1)\varepsilon(k)}{1+\|\omega(k)\|^2} \tag{C.3}$$

If $e(k+1)>\varepsilon_{\max}$, with $0<\eta(k)<2$ the first term of the right hand side of equation (C.3) dominates the second term therefore $\Delta V(k)\le 0$. If on the contrary $e(k+1)\le\varepsilon_{\max}$

the parameter vector is not updated therefore $\Delta V(k)=0$. Hence in any case for all k is $\Delta V(k)\leq 0$.

i) Because the sequence $V(k)$ is bounded and non-increasing, it must converge as $k\to\infty$ therefore $\|\phi(k)\|$ is bounded.

ii) Since $\lim_{k\to\infty}\Delta V(k)=0$, either K_t exist such that for $k>K_t$ $|e(k)|\leq\varepsilon_{\max}$, or the sequence $e(t_k+1)$, with t_k defined as $t_k\{i:e(i+1)>\varepsilon_{\max}\}$ are the time instants where the identification error is greater then $\varepsilon_{\max}$, cannot grow faster then the signal vector at the time t_k:

$$e(t_k+1)=o[\|\omega(t_k)\|]$$

which implies:

$$e(k+1)=o\left[\sup_{t\leq k}\|\omega(t)\|\right] \tag{C.4}$$

Equation (C.4) can be rewritten $e(k+1)=\sigma(k)\|\omega(k)\|$ where $\lim_{k\to\infty}\sigma(k)=0$.

iv) From the adaptive law equation (7.15) it follows that:

$$\|\Delta\phi(k)\|=\eta(k)\frac{\sigma(k)\omega(k)}{1+\|\omega(k)\|^2}$$

which leads to $\lim_{k\to\infty}\|\Delta\phi(k)\|=0$.

Step 2.

Using arguments based on the input-output relationships, it is shown that the state vector of the non-linear systems (7.7) is bounded and the tracking error converges.

This is achieved first considering hypothesis three, for which the output of the system $\psi(k)$ cannot grow faster then the input $\delta(k)$, this is expressed by the order relation:

$$\delta(k) = O\left[\sup_{t \le k+d} \psi(t)\right] \tag{C.5}$$

For hypothesis two and equation (C.5) the output cannot grow faster then the vector signal $\omega(k)$ which is:

$$\omega(k) = O\left[\sup_{t \le k+d} \psi(k)\right] \tag{C.6}$$

Because of the use of the dead-zone in the adaptive law, the estimated parameter vector is bounded. Hence, to conclude the proof, it is necessary to show that the output $\psi(k)$ and the estimated output $\hat{\psi}(k)$ are also bounded.

The control law (7.15) based on the certainty equivalence principle has to satisfy:

$$\psi_m(k) = \hat{\theta}(k)\omega(k+d-1)$$

Now studying the tracking error:

$$\psi(k+d)-\psi_m(k+d)=\theta^T\omega(k+d-1)-\hat{\theta}^T(k)\omega(k+d-1)+\varepsilon=$$
$$\left[\theta-\hat{\theta}(k+d-1)+\sum_{j=k}^{k+d-2}\Delta\hat{\theta}(j)\right]^T\omega(k+d-1)+\varepsilon=-e(k+d)+\left[\sum_{j=k}^{k+d-2}\Delta\hat{\theta}(j)\right]^T\omega(k+d-1)+\varepsilon$$

For equations (C.4) and (C.6) it is possible to infer that the tracking error grows more slowly than the output:

$$|\psi(k+d)-\psi_m(k+d)|=o\left[\sup_{t\le k+d}\psi(t)\right]+C \tag{C.7}$$

where C is a non-negative constant depending on ε. Since $\psi_m(k)$ is a bounded signal, $\psi(k)$ cannot grow in an unbounded fashion and this implies that

$$\lim_{k\to\infty}|\psi(k)-\psi_m(k)|=C$$

The estimation error also converges to:

$$\lim_{k\to\infty}|\hat{\psi}(k)-\psi(k)|=\varepsilon_{\max}$$

Finally since $\psi(k)$ is bounded from (C.2) also $\delta(k)$ is bounded.

The knowledge on the relative degree d, required by hypothesis 1, is fulfilled by the analysis outlined in section 4.5 of Chapter 4. Hypothesis 2, is guaranteed by the choice on the radial basis function, while hypothesis 3, implies that the ship is directionally stable. Based on the above argument, it is possible to conclude that the control law

described by equation (7.16) with the adaptive law of equation (7.15), guarantees that all the signals in the adaptive loop are bounded and that the tracking and estimation error converges.

C.2 Reference List

Narendra, K. S., and Annaswamy, A. M. 1989. *Stable Adaptive Systems.*

Peterson, B. B., and Narendra, K. S. 1982. Bounded error adaptive control. *IEEE Transactions on Automatic Control,* (27), pp. 1161-1168.

Appendix D Published papers

The following papers relate directly with the work presented in this thesis and they have been or are accepted for publication.

D.1 List of journal paper

A. Zirilli, G.N. Roberts, A. Tiano and R. Sutton, "Adaptive Steering of a containership based on Neural Networks". Accepted for publication in International Journal of Adaptive Control and Signal Processing, January 2001

D.2 List of conference papers

ZIRILLI, A., ROBERTS, G., TIANO, A. and SUTTON, R. 1999. A model-reference neural autopilot for ships. IMarE Conference: Computers and Ships, London. pp 25-35

ZIRILLI, A., ROBERTS, G.N., TIANO, A. and SUTTON, R. 1999. A Neuro-Fuzzy Model Reference Autopilot for Ships. Twelfth ship control systems symposium. The Hague, Netherlands.

ZIRILLI, A., ROBERTS, G.N., TIANO, A. and SUTTON, R. 2000. An adaptive autopilot for ships based on neural networks controller. International Conference & Exhibition on Gearing, Transmissions and Mechanical Systems. 3-6 July 2000, Nottingham, UK. Pp.493-502

ZIRILLI, A., ROBERTS, G.N., TIANO, A. and SUTTON, R. 2000. An adaptive Fuzzy autopilot for a containership. 5th IFAC Conference on Manoeuvring and Control of Marine Craft. 24-27 August 2000 Aalborg University, Denmark. pp 317-322

ZIRILLI, A., ROBERTS, G.N., TIANO, A. and SUTTON, R. 2000. Feedback-linearisation controller based on neural networks for the course-keeping problem of a containership. UKACC International Conference, Control 2000, 4-7 September University of Cambridge, UK.

Adaptive Steering of a containership based on Neural Networks

A. Zirilli[1*], G.N. Roberts[1], A. Tiano[2] and R. Sutton[3]
[1]*Mechatronics Research Centre, University of Wales College, Newport Allt-yr-yn Campus, P.O. Box 180, Newport, NP20 5XR, UK*
[2]Department of Information and Systems, University of Pavia, Pavia, Italy Via Ferrata 1, I-27100 Pavia, Italy. Also: Institute of Ship Automation C.N.R Via de Marini 6, I-16149 Genoa, Italy.
[3]Department of Mechanical and Marine Engineering, University of Plymouth, Drake's Circus, Plymouth, PL4 8AA, UK.

*Corresponding author. Tel.: +44 (0)1633 432487; Fax: +44 (0)1633 432442
E-mail address: **antonio.zirilli@newport.ac.uk**

Summary

This paper describes the design of an adaptive autopilot for a containership. Well-known results of linear adaptive theory are extended trough the use of neural network to the case where the plant dynamic is described by a non-liner equation. The desired behaviour of the containership during course-changing manoeuvre is defined by the response of a reference model. Using an indirect approach, the controller parameters are adjusted based on the definition of an estimation error. The proposed adaptive controller is tested by a simulation study based on a non-linear model, describing the dynamics of a containership in four degrees of freedom. In order to take into account the wave effects, a stochastic model of the ship wave induced motion is considered. Shallow water effect is also considered by changing some of the hydrodynamics parameters.

1. Introduction

The introduction of automatic autopilot for steering a ship can be traced back to the 1922 with the pioneering work of Sperry and Minorsky. The simple proportional autopilot, suggested in Sperry[1] and Minorsky[2], was supplying a corrective signal to the rudder proportional to the heading error. Subsequent enhancements were the inclusion of a derivative term for the heading error and a further integrating term leading to the more sophisticated PID controller. Due to its relatively simplicity, these kinds of controller dominated the scenario until the early 1970s. The need to move from fixed PID controller, to more sophisticated adaptive autopilot, can be explained by the fact that the ship's dynamics is influenced by factors such as load and trim conditions, weather conditions and deep of water. Moreover, the optimal achievement of the two main steering modes of an autopilot, namely course-keeping and course-changing, can be properly defined only with respect a particular sailing conditions. For instance, with respect the course-keeping mode of operation, the autopilot has to select the best trade-off between precision (which will minimise the elongation of the sailed distance) and control effort (rudder movement, which will produce additional drag force and consequent loss of speed). However this trade-off is not always the same. In different sailing conditions, different priority (or weight) is assigned to the precision and control effort. When the ship is sailing in restricted water precision is of main concern, while in open sea fuel consumption is of major interest.

The most popular approach for dealing with the above mentioned autopilot demands, was the Linear Quadratic (LQ) Controller, in which the controller parameters are selected in order to satisfy certain optimal criteria expressed as a quadratic cost function. Different cost functions taking into account yaw and rudder deviation, fuel consumption, etc., were proposed Norrbin[3], and Broome[4] et al. Although the LQ

technique fits very nicely in the formulation of the ship's course-keeping control problem and appeared to be robust for parameter changes, other researchers were investigating the applicability of adaptive control techniques such as model reference Honderd and Winkelman[5], Amerongen and Udink Ten Cate[6] or self-tuning adaptive controller Kallstrom[7] et al, Brink[8] et al, which are much appropriate for the formulation of the ship's course changing problem.

In this paper the design of an adaptive autopilot based on neural networks concept is described. Because of the excellent approximation capability of neural networks such kinds of approximator can be used to account for the non-linear nature of ship dynamics. The paper is organised as follows: section 2 describes the non-linear mathematical model of a containership used in this simulation study. The waves and shallow water effects are also described. Section 3 reviews some well-known steering models used for control design purposes. These models are used to motivate the choice on the controller structure. In section 4, three neural networks structures used for control purposes are briefly introduced and discussed. In section 5, the adaptive control problem as introduce in linear adaptive theory is discussed and extended to the case where the system is described by non-linear unknown functions. The adaptive law and the design of a model reference is also described. In section 6, the design of the ship's autopilot is considered while in section 7 simulation results are presented. Finally section 8 concludes the paper with some remarks.

2. Mathematical Model of a Containership

The mathematical model of a container ship used in this study is described in detail in Blanke and Jessen[10] and Tiano and Blanke[11]. Equation 1 represent the non-linear equation describing the ship's motion in four degree of freedom, deduced by the Newton's law.

$$\begin{aligned} m\left(\dot{u} - vr - x_g r^2 + z_g pr\right) &= X + X_w \\ m\left(\dot{v} + ur - z_g \dot{p} + x_g \dot{r}\right) &= Y + Y_w \\ I_{zz}\dot{r} + mx_g\left(\dot{ur} + \dot{v}\right) &= N + N_w \\ I_{xx}\dot{p} - mz_g\left(\dot{ur} + \dot{v}\right) &= K + K_w - \rho g D R_z(\varphi) \end{aligned} \tag{1}$$

The above equations with reference to the co-ordinate system shown in figure 1, describe the coupled surge, sway, yaw and roll motions, where D is the displacement, g the gravity constant, ρ the water mass density, $R_Z(\varphi)$ is the action of the rightening arm that depends on the roll angle φ, while $(x_G,0,z_G)$ are the co-ordinates of the mass centre. The mass is denoted by m whereas Ixx and Izz are the inertial moments about x and z, respectively. The linear velocity of surge and sway are u and v and the angular ones of yaw and roll are respectively r and p. The rightening arm function can be expressed as:

$$R_z(\varphi) = \sin\varphi\left(GM + \frac{BM}{2}\tan^2\varphi\right) \tag{2}$$

where GM is the ship metacentric height and BM is the distance from the centre of buoyancy to the metacentre.

Terms X, Y denote the deterministic forces acting along x and y while N and K are the deterministic moments around z and x, which take into account the hydrodynamic effects from the hull movements and forces exerted on the ship by the rudder and by the propulsion system. Such forces and moments are usually described by regarding X, Y, N and K as polynomial expansion in terms of state variables, control actions and hydrodynamic coefficients Lewis[12].

The external disturbances, i.e. wind and waves, are represented by the terms X_w, Y_w, N_w, K_w in the corresponding right hand parts of equation (1). Such terms, owing to their intrinsically random nature, are generally quite difficult to be characterised through explicit mathematical relations: for example, as to the waves, they should be calculated by integrating the wave pressure over the immersed surface of the hull, on the assumption that the pressure within the waves is unaffected by the presence of the ship. As it has been shown in Lewis[12] and Price and Bishop[13], a reasonable simplifying assumption consists in applying a linear superposition principle, which makes it possible to separate the ship motion due to the environment from the motion induced by the rudder and by the propeller thrust. According to this modelling approach, waves and wind are regarded as finite order linear realisations of stochastic processes characterised by known spectral densities.

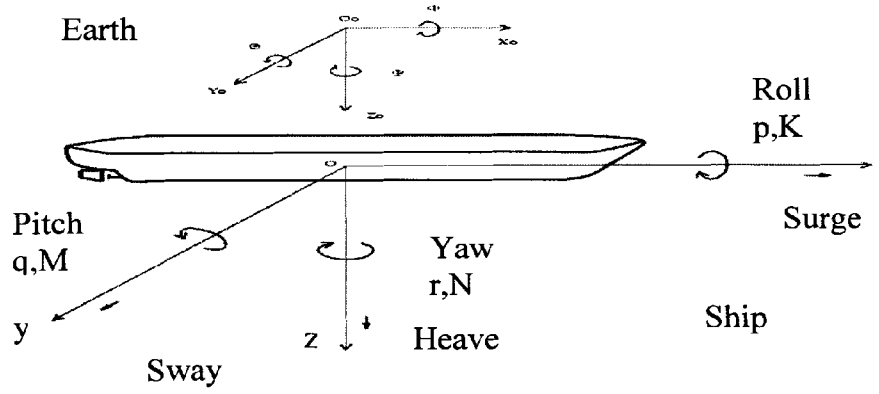

Figure:1 Ship's system frame

By limiting attention to sea waves, which are by far the dominant disturbance, it is possible to regard a long crested irregular sea height $\zeta(t)$, at time t, as described by a one-dimensional amplitude spectrum, the main parameters of which are the significant wave height, h and the average wave period T. This spectrum, accepted by the International Ship Structure Congress (ISSC) is given by:

$$G_\zeta(\omega) = \frac{173h^2}{\omega^5 T^4} \exp\left(\frac{-691}{T^4\omega^4}\right) \tag{3}$$

The relation between the response of each individual component of the wave induced ship state vector $x_w = [u_w\ v_w\ r_w\ p_w]^T$, can be obtained in terms of the spectrum:

$$G_{x_w'}(\omega,\chi,U) = \left|R_{x_w'}(\omega,\chi,U)\right|^2 G_\zeta(\omega) \qquad i=1,..4 \tag{4}$$

where χ is the angle of encounter between ship and waves, U is the ship velocity and $R_{x_w^{(i)}}$ is the receptance operator, which is assumed to be known from experimental tests, describing the response of the ship i^{th} motion to the waves, Blanke and Jessen[10]. In order to obtain the corresponding spectrum relative to the ship centre of mass, it is finally necessary to express the spectrum given by equation (4) as a function of the frequency of encounter between ship and waves $\omega_e = \omega\left(1 - \frac{\omega U}{g}\cos(\chi)\right)$. Once the waves induced ship state vector x_w is computed the total ship state vector is represented by:

$$x_{tot}=x_w+x$$

According to this approach, it is possible to implement an accurate and numerically reliable simulation of sea wave induced ship motions.

As suggested in Sheng[14] and Clarke[15], the shallow water effects can be represented by the correction of the following hydrodynamic derivative:

$$\frac{Y'_{\dot{v}}}{Y'_{\dot{v}_\infty}} = K_0 + \frac{2}{3}K_1\frac{B}{T} + \frac{8}{15}K_2\left(\frac{B}{T}\right)^2 \qquad \frac{N'_{\dot{r}}}{N'_{\dot{r}_\infty}} = K_0 + \frac{2}{5}K_1\frac{B}{T} + \frac{24}{105}K_2\left(\frac{B}{T}\right)^2$$

$$\frac{Y'_{v}}{Y'_{v_\infty}} = K_0 + K_1\frac{B}{T} + K_2\left(\frac{B}{T}\right)^2 \qquad \frac{N'_{v}}{N'_{v_\infty}} = K_0 + \frac{2}{3}K_1\frac{B}{T} + \frac{8}{15}K_2\left(\frac{B}{T}\right)^2 \quad (5)$$

$$\frac{Y'_{r}}{Y'_{r_\infty}} = K_0 + \frac{2}{3}K_1\frac{B}{T} + \frac{8}{15}K_2\left(\frac{B}{T}\right)^2 \qquad \frac{N'_{r}}{N'_{r_\infty}} = K_0 + \frac{1}{2}K_1\frac{B}{T} + \frac{1}{3}K_2\left(\frac{B}{T}\right)^2$$

where

$$K_0 = 1 + \frac{0.0775}{F^2} - \frac{0.0110}{F^3}; \quad K_1 = -\frac{0.0643}{F} + \frac{0.0724}{F^2} - \frac{0.0113}{F^3}; \quad K_2 = \frac{0.0342}{F};$$

and

$$F = \left(\frac{H}{T} - 1\right)$$

In the above formulae the subscript ∞ refers to the hydrodynamic derivative's values in depth water. The parameters H, B and T are specified in figure 2. The correction suggested by Sheng and reported in equation (5) do not completely describe the effect of the shallow water, they are in fact limited to few hydrodynamic derivatives. However, these corrections are related to the geometry of the hull ship, therefore the above formulae represent a quite general model of the shallow water effects that is used in this simulation study to simulate parameters uncertainties.

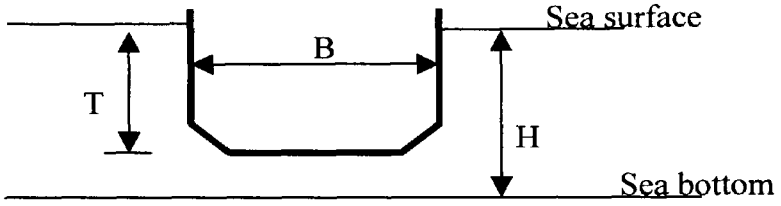

Figure 2: The ship in shallow water

3. Steering Dynamics

Broadly speaking, there are two main control design approaches termed; model-based and model-free control design techniques. In the model based control design technique it is assumed that a model of the plant to be controlled is available. However, because the model can describe only the main futures of the system dynamics, adaptive or robust techniques are used in order to guarantee acceptable performance of the overall system with respect the unmodelled dynamics and parameter uncertainties. Model-free design techniques are based on the assumption that a model of the plant to be controlled is not necessary. In the following of this section some ship mathematical models used for the control design of autopilot based on the former technique are introduced. These models will be used in order to justify the structure of the identifier and controller used in the proposed adaptive controller.

Considering the ship as a rigid body, the steering equations of motion can be deduced applying Newton's law, Abkowitz[16]. With respect the systems frame of figure 1, the motion of the ship in the x-y plane can be described by the system equation:

$$\begin{aligned} m\left(\dot{u} - vr - x_g r^2\right) &= X \\ m\left(\dot{v} + ur + x_g \dot{r}\right) &= Y \\ I_z \dot{r} + m x_g \left(\dot{v} + ur\right) &= N \end{aligned} \tag{6}$$

The right hand side of equation (6) represents the deterministic force and moment produced by the propeller thrust, control action and hydrodynamic effects. It is commonplace to consider an equilibrium situation in surge in which propeller thrust outbalances the hull resistance therefore the first equation in the systems (6) is usually disregarded in the description of the steering dynamic. The modelling problem then resolves to determine a suitable expression for the force Y and moment N. Under the hypothesis that a linear model is satisfactory, hydrodynamic derivative theory suggests the following series expansion for the terms Y and N respectively:

$$\begin{aligned} Y &= Y_{\dot{v}}\dot{v} + Y_{\dot{r}}\dot{r} + Y_v v + Y_r r + Y_\delta \delta \\ N &= N_{\dot{v}}\dot{v} + N_{\dot{r}}\dot{r} + N_v v + N_r r + N_\delta \delta \end{aligned} \tag{7}$$

Substitution of equation (7) into (6), leads to the well-known linearized equation of motion expressed by equation (8):

$$\begin{aligned} \left(m - Y_{\dot{v}}\right)\dot{v} + \left(m x_g - Y_{\dot{r}}\right)\dot{r} &= Y_\delta \delta + Y_v v + \left(Y_r - m u_0\right) r + Y_0 \\ \left(m x_g - N_{\dot{v}}\right)\dot{v} + \left(I_z - N_{\dot{r}}\right)\dot{r} &= N_\delta \delta + N_v v + \left(N_r - m x_g u_0\right) r + N_0 \end{aligned} \tag{8}$$

Equation (8), describe the motion of a ship moving in the horizontal plane, in unrestricted deep water with constant speed.

By elimination of $\dot{v}$ and v, equation (8) can be transformed in the second order linear differential equation proposed by Nomoto[17] et al;

$$\dddot{\psi}+\left(\frac{1}{\tau_1}+\frac{1}{\tau_2}\right)\ddot{\psi}+\frac{1}{\tau_1\tau_2}\dot{\psi}=\frac{k}{\tau_1\tau_2}\left(\tau_3\dot{\delta}+\delta\right) \tag{9}$$

where $\dot{\psi}=r$, and

$$\frac{k}{\tau_1\tau_2}=\frac{N_vY_\delta-Y_vN_\delta}{(Y_{\dot{v}}-m)(N_{\dot{r}}-I_z)-(Y_{\dot{r}}-mx_g)(N_{\dot{v}}-mx_g)}$$

$$\tau_3=\frac{(N_{\dot{v}}-mx_g)Y_\delta-(Y_{\dot{v}}-m)N_\delta}{N_vY_\delta-Y_vN_\delta}$$

$$\frac{1}{\tau_1\tau_2}=\frac{Y_v(N_r-mx_gu_0)-N_v(Y_r-mu_0)}{(Y_{\dot{v}}-m)(N_{\dot{r}}-I_z)-(Y_{\dot{r}}-mx_g)(N_{\dot{v}}-mx_g)}$$

$$\left(\frac{1}{\tau_1}+\frac{1}{\tau_2}\right)=\frac{(Y_{\dot{v}}-m)(N_r-mx_gu_0)+(N_{\dot{r}}-I_z)Y_v-(Y_{\dot{r}}-mx_g)N_v-(N_{\dot{v}}-mx_g)(Y_r-mu_0)}{(Y_{\dot{v}}-m)(N_{\dot{r}}-I_z)-(Y_{\dot{r}}-mx_g)(N_{\dot{v}}-mx_g)}$$

(10)

The coefficients $\left(\frac{1}{\tau_1}+\frac{1}{\tau_2}\right)$, $\frac{k}{\tau_1\tau_2}$ and τ_3 of equation (9) for a conventional ship during manoeuvre at a fixed speed remain fairly constant, whereas the coefficient $\frac{1}{\tau_1\tau_2}$ changes resulting in the non-linear nature of the ship dynamics. Bech and Wagner-Smitt[18], in order to account for the change in the above parameter, proposed to include in equation (9) a non-linear term defined as:

$$H(\dot{\psi})=\frac{1}{k}\dot{\psi} \tag{11}$$

in such a way that equation (9) became:

$$\dddot{\psi}+\left(\frac{1}{\tau_1}+\frac{1}{\tau_2}\right)\ddot{\psi}+\frac{k}{\tau_1\tau_2}H(\dot{\psi})=\frac{k}{\tau_1\tau_2}\left(\tau_3\dot{\delta}+\delta\right) \tag{12}$$

In Bech[19] there is also described a practical way to gain some knowledge information about the non linear function expressed by equation (11), which led to the better-known Bech's reverse spiral test manoeuvre. In particular, under the hypothesis that the ship can be kept at a nearly constant rate of turn $\dot{\psi}_0$ with relatively small fluctuation of δ and $\dot{\psi}$, the time average of both sides of equation (12) gives:

$$\frac{1}{T}\int_0^T\left[\dddot{\psi}+\left(\frac{1}{\tau_1}+\frac{1}{\tau_2}\right)\ddot{\psi}+\frac{k}{\tau_1\tau_2}H(\dot{\psi})\right]dt\rightarrow\frac{k}{\tau_1\tau_2}H(\dot{\psi}_0)\quad for,T\rightarrow\infty$$

and

$$\frac{1}{T}\int_0^T\frac{k}{\tau_1\tau_2}\left[\tau_3\dot{\delta}+\delta\right]dt\rightarrow\frac{k}{\tau_1\tau_2}\delta_0\qquad for,T\rightarrow\infty$$

leading to:

$$H(\dot{\psi}_0)=\delta_0$$

where δ_0 is the mean rudder deflection necessary to steer the ship with a constant rate of turn. The plot of the values δ_0 against the mean rate of turn can result in the two functions reported in figure 3 for directionally stable and unstable ships. In practice, as stated above, the non-linear function $H(\dot{\psi})$ can be obtained from the reversed spiral test.

The non-linear differential equation describing the steering dynamic expressed by equation (12) can be rewritten in the form:

$$\ddot{\psi} = \frac{k}{\tau_1\tau_2}\left[\left(\tau_3\dot{\delta}+\delta\right)-H(\dot{\psi})\right]-\left(\frac{1}{\tau_1}+\frac{1}{\tau_2}\right)\ddot{\psi} \tag{13}$$

Due to the relatively high sampling rate that can be chosen in comparison to the ship's dominant time constant, equation (13) can be rewritten in the equivalent discrete time form as:

$$\psi(t+3) = \frac{k}{\tau_1\tau_2}\left[\left(\tau_3\delta(t+1)+\delta(t)\right)-H(\psi(t+1))\right]-\left(\frac{1}{\tau_1}+\frac{1}{\tau_2}\right)\psi(t+2)$$

or,

$$\psi(t+1) = \frac{k}{\tau_1\tau_2}\left[\left(\tau_3\delta(t-1)+\delta(t-2)\right)-H(\psi(t-1))\right]-\left(\frac{1}{\tau_1}+\frac{1}{\tau_2}\right)\psi(t)$$

finally,

$$\psi(t+1) = \alpha_1\psi(t)+\alpha_2 H(\psi(t-1))+\beta_0\delta(t-1)+\beta_1\delta(t-2) \tag{14}$$

where t is the time step and:

$$\alpha_1 = -\left(\frac{1}{\tau_1}+\frac{1}{\tau_2}\right) \quad ; \quad \alpha_2 = -\frac{k}{\tau_1\tau_2} \quad ; \quad \beta_0 = \frac{k\tau_3}{\tau_1\tau_2} \text{ and } \beta_1 = \frac{k}{\tau_1\tau_2}.$$

Equation (14) represents a particular parameterisation of the ship steering dynamics. This parameterisation, as will be shown later, can be used in the indirect adaptive control problem in order to justify the structure of the identifier for the estimation of the unknown parameters.

Another well-known non-linear model describing the steering dynamics is the one proposed by Norrbin[20] in 1970. Norrbin proposed the following non-linear equation:

$$\tau\ddot{\psi}+H(\dot{\psi}) = k\delta \tag{15}$$

where again the non-linear function $H(\dot{\psi})$ describes the non-linear nature of ship dynamics and can be expressed in terms of a polynomial expansion as:

$$H(\dot{\psi}) = \alpha_3\dot{\psi}^3+\alpha_2\dot{\psi}^2+\alpha_1\dot{\psi}+\alpha_0$$

Norrbin suggested that, due to hull symmetry the parameter α_0 has zero value, the parameter α_1 can be set equal to unity for course stable ships and equal to -1 for course unstable. Finally the parameter α_3 can describe the non linearity of the ship dynamics. Therefore equation (15), for course stable ship reduce to:

$$\tau\ddot{\psi} + \dot{\psi} + \alpha_3\dot{\psi}^3 = k\delta \tag{16}$$

The justification of the Norrbin's model can be traced to the second-order linear model of Nomoto (equation (9)). In fact, Nomoto further reduced the linear model of equation (9) to a first-order linear model of the form:

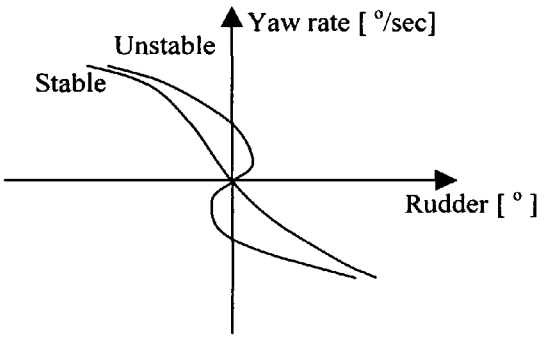

Fig. 3: Reversal spiral test for stable and unstable ships

$$\tau\ddot{\psi} + \dot{\psi} = k\delta \tag{17}$$

where the time constant τ is defined with respect equation (10) as:

$$\tau = \tau_1 + \tau_2 - \tau_3$$

It is clear that equation (15) differs from the first-order Nomoto model because the non-linear function $H(\dot{\psi})$, which according to Norrbin tries to describe the nonlinearities of the ship steering dynamics. Following the same parameterisation of the Bech's model, equation (16) can be rewritten as:

$$\psi(t+2) = -\frac{1}{\tau}\psi(t+1) - \frac{\alpha_3}{\tau}\psi^3(t+1) + \frac{k}{\tau}\delta(t)$$

or equivalently:

$$\psi(t+1) = \alpha_1\psi(t) + \alpha_2\psi^3(t) + \beta_0\delta(t-1) \tag{18}$$

where:

t is the time step, $\alpha_1 = \frac{1}{\tau}$; $\alpha_2 = -\frac{\alpha_3}{\tau}$ and $\beta_0 = \frac{k}{\tau}$.

Equation (18) could also be used to justify the parameterisation of the identifier for the adaptive control problem.

It can be observed that, equation (14) and equation (18) are quite similar. In particular, in both equations the delay is equal to 1, the heading angle at time (t+1) will be affected by the rudder angle at time (t-1) and both contain a non-linear function, which in the Norrbin model is expressed by a polynomial expansion while in the Bech's model is defined by the reverse spiral test.

4. Neural networks for control

The last twenty years have witnessed a growing increase in the use and study of neural networks for control applications Hunt[21] et al. The primary characteristic that rendered these systems attractive, is the fact that under certain conditions, the parameters of the network can be adjusted from input-output data. This has led to the use of such systems, under different conditions of uncertainties, as adaptive or learning systems. Mainly

inspired by biological systems, different types of neural network architectures have been proposed. Multilayer Perceptron Networks (MPN), Radial basis Function Networks (RBFN) and Cerebellar Model Articulation Controller (CMAC) are few examples that share the ability to be universal approximator Cybenko[22], Hornick[23] et al. In the framework of control system theory, the feature to be a universal approximator, is strictly related to adaptation and learning ability of the network. In fact, the problem of learning a mapping from an input to an output space, using a set of data, can be formulated as the problem to find an associative memory that retrieves the appropriate output when presented with the input and generalises when presented with different input. The problem of learning as formulated above is dealt with in the framework of approximation theory and related fields such as system identification and system estimation. In general, the problem to approximate a multivariate function $f(\bar{x})$ by an approximating function $NN(\theta,\bar{x})$ rarises three main questions:

1) What kind of approximator has to be used. In other words, what classes of functions $f(\bar{x})$ can be approximated by the selected approximator $NN(\theta,\bar{x})$.
2) What kind of algorithm has to be used for finding the optimal parameters θ^* for a given choice of $NN(\theta,\bar{x})$.
3) Is the selected approximator with the selected algorithm realisable in practice?

The proper answers to the above questions are application dependent. However, the above questions motivate the choice of the particular controller structure and adaptation algorithm. They also represent a systematic procedure to find the most suitable combination of different identification and control design techniques. In the context of neural networks, the first question refers primarily to the problem of choosing a particular neural network, (i.e. MPN, RBFN, CMAC etc.), while the second question is related to the particular parameterisation that can be achieved. Finally, the last question dictates the hardware specification and whether or not the adaptation can be performed on line. To measure the quality of the approximation, the idea of distance between the function to be approximated $f(\bar{x})$ and the approximator $NN(\theta,\bar{x})$ is used. A function ρ is defined in order to quantify such distance. A common choice for the function ρ is the Euclidean norm. Once the function ρ has been defined and the approximator $NN(\theta,\bar{x})$ has been chosen, the approximation problem reduce to finding the parameter θ^* for which:

$$\rho\left[NN(\theta^*,\bar{x}), f(\bar{x})\right] \leq \rho\left[NN(\theta,\bar{x}), f(\bar{x})\right] \tag{19}$$

for any θ belonging to the set of admissible values. A solution to this problem, if it exist, is said to be the best approximation. It is clear that the existence of the best approximation depends ultimately on the class of the functions to which $NN(\theta,\bar{x})$ belongs to. Next three classes of approximator functions corresponding to different neural networks architectures are defined.

Linear networks: The classical linear network approximator is described by the linear equation:

$$NN(\bar{\theta},\bar{x}) = \theta \cdot \bar{x} \tag{20}$$

where θ and $\bar{x}$ are n+1-dimensional vectors. A representation of the neural network implementing equation (20) is shown in figure 4.

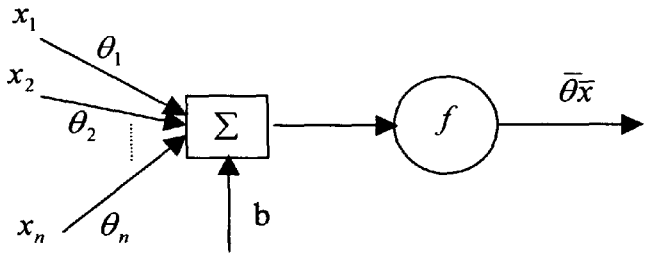

Fig. 4: Linear network

Where f, also called neuron activation function, is a linear function, $\bar{\theta} = [\theta_1, \theta_2 ..., \theta_n, b]^T$ are the weights and bias parameters and $\bar{x} = [x_1, x_2, ..., x_n, 1]$ is the input vector.

Radial Basis Function networks: This class of approximation scheme is linear with respect to a suitable choice of basis functions of the original input space $\{\Phi_j\}$ with $j = 1,..,n$. The RBFN is represented by equation (21) and shown schematically in figure 5.

$$NN(\bar{\theta}, \bar{x}) = \sum_{j=1}^{n} \theta_j \Phi_j(\bar{x}) \tag{21}$$

The basis functions can be Spline, Gaussian or orthogonal polynomial.

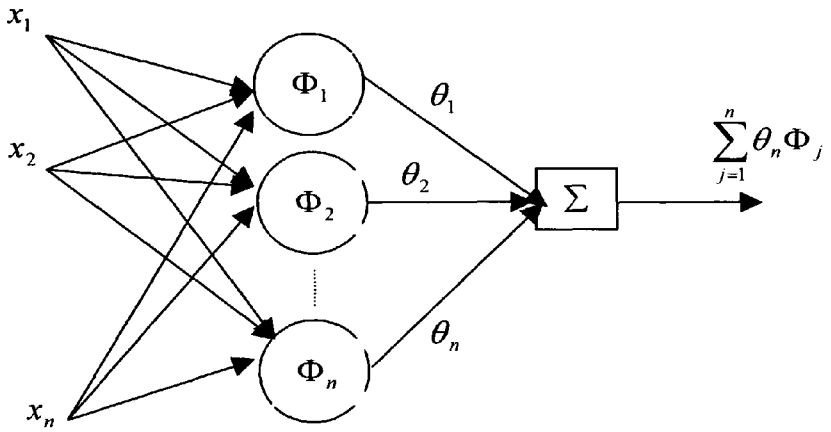

Fig. 5: Radial Basis Network

In equation (21), $\bar{x} = [x_1, x_2, ..., x_n]^T$ is the input vector, $\bar{\theta} = [\theta_1, \theta_2, ..., \theta_n]^T$ is the parameter vector and Φ_j are the basis functions.

Multilayer Perceptron networks are of the nested sigmoid type. They are represented by equation (22).

$$NN(\bar{\theta}, \bar{x}) = f\left(\sum_n \theta_n f\left(\sum_j \theta_j f\left(\cdots f\left(\sum_i \theta_i \bar{x}\right)\cdots\right)\right)\right) \tag{22}$$

where f are non-linear functions. In the particular case of one hidden non-linear layer, the network can be represent by figure 4, where the function f is now a non-linear function. It is clear therefore that the class of linear neural networks is included in the class of MPN.

A brief comparison of MPN and RBFN can be made, considering some advantages and disadvantages of both. From equation (22) it is clear that the parameters of a MPN are related in a non-linear fashion with respect the output. Hence, derivative based algorithms are mandatory for the adjustment of the parameters. This, in turn, implies that the parameters can converge to local minima unless other derivative-free methods are used which in general due to their low speed of convergence, are not well suited for on-line implementation. Moreover, the adjustment of a single parameter of the network affects the output globally. For this reason, all the weights have to be adjusted simultaneously for each training data set, reducing the effect of previous learning and slowing down the convergence rates of the algorithm. On the contrary, in the RBFN, once the parameters defining the basis functions are fixed, the adjustable parameters are related in a linear fashion to the output. This allows the use of the Least Mean Square algorithm which is considerably faster then the derivative based algorithms. Moreover, when the input vector is close to the centre of the ith basis function, the response of this is large while it is virtually zero when the input vector is very far from the centre. It is possible to consider this local behaviour of the network in order to speed up the learning and to retain previous learned patterns. However the overall behaviour of the network is highly affected by the choice of the basis function parameters. Same heuristic methods exist in order to ensure good approximation properties of the network and a good rule is to ensure a sufficient overlapping of the basis function in the input domain. Others non-heuristic methods based on cluster analysis can be used only if a significant amount of data can be collected. As a consequence of this, for a high dimensional input space the number of the basis functions that are needed to ensure good approximation properties may became numerically intractable.

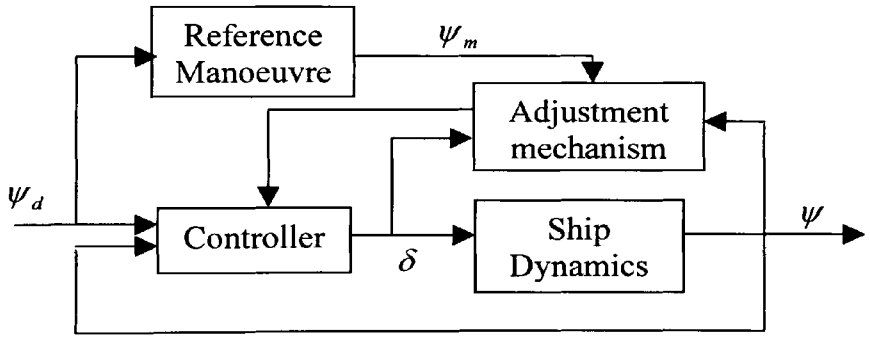

Figure 6: Model reference adaptive system

5. Adaptive Control Problem

Adaptive control deals with the problem of controlling the output of a plant in the presence of parametric or structural uncertainty. In conventional adaptive control theory, to make the problem analytically tractable, the plant is assumed to be linear with unknown parameters. A suitable controller structure is chosen, and the parameters of the controller are adjusted using an adaptive law, so that the output of the plant follows the output of a reference model asymptotically. Assuring that a set of fixed parameters in the controller can achieve the desired response makes the problem well-posed and represent the algebraic part of the problem, while the generation of stable adaptive laws constitutes the analytic part. A general block diagram representing such an adaptive system is shown in figure 6. Here the controller can be thought of as consisting of two loops. The inner loop is an ordinary feedback loop composed of the process and the controller. The outer loop adjusts the controller parameters in such a way that the error, which is the difference between process output and model output is small.

Two distinct approaches, named direct and indirect adaptive approach, have been proposed for the design of adaptive controllers. In the indirect approach, the parameters of the plant to be controlled are estimated and the parameters of the controller are adjusted based on these estimates. In the direct approach, the control parameters are directly adjusted based on the observed output error.

5.1 Statement of the problem

As mentioned above, a stable reference model with input-output pair $\{\psi_d(k), \psi_m(k)\}$ can be chosen so that $\psi_m(k)$ represents the desired output behaviours for the unknown plant represented by the input-output pair $\{\delta(k), \psi(k)\}$. The object is to determine a bounded control input $\delta(\cdot)$ so that the error $e(k) = \|\psi_m(k) - \psi(k)\|$, is bounded and tends to zero asymptotically. To makes the problem analytically tractable some assumptions on the non-linear plant dynamics must be done. In particular, it is assumed that, in the domain of interest the plant is identifiable with a finite input-output sequence and it is of known relative degree.

A possible representation of the non-linear ship's dynamics, motivated by the previous section is expressed by equation (23):

$$\psi(k+1) = \sum_{i=1}^{N} \alpha_i f_i[\psi(k), \psi(k-1), ..., \psi(k-n+1)] + \sum_{j=0}^{m-1} \beta_j \delta(k-d-j+1) \tag{23}$$

This representation is particular interesting for control purposes, because if the parameters α_i, β_j and the function f_i are known and $1/\beta_o$ is well defined, the control action can be computed by the equation:

$$\delta(k-d+1) = \frac{1}{\beta_0}\left[\psi_m(k+1) - \sum_{i=1}^{N} \alpha_i f_i - \sum_{j=1}^{m-1} \beta_j \delta(k-d-j+1)\right] \tag{24}$$

where $\psi_m(k+1)$ is the desired heading angle produced by the reference model. However, in the adaptive control problem, the ship dynamics are unknown. Using an indirect approach, the unknown parameters can be estimated and used to implement the control law (equation 24), based on the certainty equivalence principle.

Defining therefore, an identification model with the same structure of the plant as:

$$\hat{\psi}(k+1) = \sum_{i=1}^{N} \hat{\alpha}_i f_i[\psi(k), \psi(k-1), ..., \psi(k-n+1)] + \sum_{j=0}^{m-1} \hat{\beta}_j \delta(k-d-j+1) \tag{25}$$

since the unknown parameters appears linearly, it is known that under certain assumptions on the function f, with the normalised adaptive law:

$$\hat{\theta}(k+1) - \hat{\theta}(k) = -\eta(k)\frac{e(k+1)\omega(k)}{1 + \|\omega(k)\|^2} \tag{26}$$

the non-linear system (23) results in all the signals uniformly bounded and

$$\lim_{k\to\infty} \hat{\psi}(k) - \psi(k) = \lim_{k\to\infty} \psi(k) - \psi_m(k) = 0 \tag{27}$$

In equation (26), $\hat{\theta} = [\hat{\alpha}_1, \hat{\alpha}_2, ..., \hat{\alpha}_N, \hat{\beta}_0, \hat{\beta}_1, ..., \hat{\beta}_{m-1}]^T$ is the parameter estimation vector, η is the adaptation gain, $e = \hat{\psi} - \psi$ is the estimation error and

$$\omega(k) = [f_1[Y(k)], ..., f_N[Y(k)], \delta(k-d+1), ..., \delta(k-d-m+2)]^T$$

with:

$$Y(k) = [\psi(k), \psi(k-1), ..., \psi(k-n+1)]$$

is the signals vector. Narendra and Annaswamy[24]

In practical situations however, not only the parameters of the model are unknown but also the non-linear function *f*. Due to their universal approximation property discussed in the previous section, neural network are good candidate for performing the estimation of the functions *f*. The universal approximation property of these systems will gurantee that any smooth non-linear function *f* can be approximated with any degree of accurancy over a compact region *D*. This is expressed by equation (28):

$$\left\| f[Y(k)] - \hat{f}[Y(k)] \right\| \leq \varepsilon \qquad \forall Y(k) \in D, and \varepsilon > 0 \tag{28}$$

The error ε introduced by the neural network approximation can be treated as a state dependent bounded disturbance. Hence a modification of the adaptive law expressed in equation (26), in order to guaranty robustness in the presence of bounded disturbances, has to be considered. One such modification proposed by Peterson and Narendra[25], is the inclusion of a dead-zone in the adaptive law. Equation (26) is rewritten as:

$$\hat{\theta}(k+1) = \begin{cases} \hat{\theta}(k) & if \left| e(k+1) \right| \leq \varepsilon_{\max} \\ \hat{\theta}(k) - \eta(k) \dfrac{e(k+1)\omega(k)}{1 + \left\| \omega(k) \right\|^2} & otherwise \end{cases} \tag{29}$$

Once identified both parameters and non-linear functions, the control law:

$$\delta(k-d+1) = \frac{1}{\hat{\beta}_0} \left[\psi_m(k+1) - \sum_{i=1}^{N} \hat{\alpha}_i \hat{f}_i - \sum_{j=1}^{m-1} \hat{\beta}_j \delta(k-d-j+1) \right] \tag{30}$$

provided that $1/\hat{\beta}_0$ is well defined, with the adaptation law expressed by equation (29) can be implemented.

5.2 Reference Model

It is import that the dynamic behaviour of the reference model matches the dynamics of the ship regardless of the magnitude of the demanded change of yaw angle. A reference model that is too sluggish cannot produce optimal performance since the ship cannot reach the required heading in the minimum time. On the contrary, a reference model that is too fast compared with the ship response characteristics should not be used because this may cause rudder actuator saturation and consequent performance degradation.

As suggested by van Amerongen[26] a course-changing manoeuvre can be easily described by the step response of a second-order system. From this response, as shown in figure 7, it is possible to identify three different phases: 1) a start of the turn, 2) a steady turning, and 3) an end of the turn. The turn should have a start, which clearly indicates to other ships the intention of the manoeuvre. The stationary part is determined both by limiting the rudder angle and by controlling the rate of turn. The end of the turn, for safety reason, should be completed without overshoot of the heading angle. In terms of the Laplace operator such a reference model can be represented by equation (31):

$$\frac{\psi_m(s)}{\psi_d(s)} = \frac{K_{pm}/\tau_{pm}}{s^2 + s/\tau_m + K_{pm}/\tau_m} \tag{31}$$

The time constant τ_m is chosen approximately 2 to 3 times smaller than the dominating time constant of the ship at cruise speed and must be such that the process is able to follow the model. If the rate-of-turn limiter is neglected, K_{pm} follows from the desired damping ratio (ξ) of the system:

$$K_{pm} = 1/(4\xi^2\tau_m) \tag{32}$$

Possible values of ξ are between ξ=1 which corresponds to a zero overshoot condition, to ξ=0.7 which corresponds to an overshoot of approximately 5% of the desired final value (which may be considered acceptable in open sea). The selection of τ_m results from the following consideration: a reasonable course controller will have a rate-feedback gain which makes the time constant of the ship 2 to 3 times smaller with respect to the case of the open-loop system (without controller). By choosing a similar

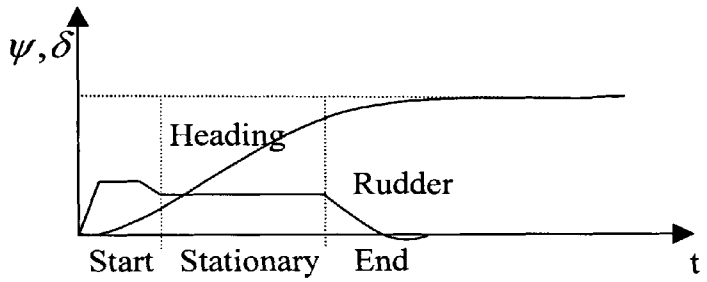

Figure 7: Course changing manoeuvre

time constant for the model reference this guarantees that the process can follow the model.

The choice of the reference model represented by equation (31) can be also motivated by the steering dynamic expressed by equation (17). With this choice of the reference model, it is ensured that at least in the linear range of application, the reference model has the same relative degree of the ship's dynamics.

6. Controller Design

As stated above the indirect adaptive control approach is considered for the steering control problem. The structure of the identifier is motivated from the discussion of section 3 and the non-linear model proposed by Bech is considered. The non-linear model is therefore represented by equation (14) for which with respect equation (23), d=2 and n=m=2 while the identifier is expressed by equation (33):

$$\hat{\psi}(t+1) = \hat{\alpha}_1\psi(t) + \sum_{i=1}^{N}\hat{\gamma}_i R_i(\psi(t-1)) + \hat{\beta}_0\delta(t-1) + \hat{\beta}_1\delta(t-2) \tag{33}$$

where, the unknown non-linear function $\alpha_2 H(\psi(t-1))$ defined by the reversal spiral test manoeuvre can be approximate by the Gaussian basis functions R_i defined as:

$$R_i = e^{-\frac{\|\psi(t-1)-c_i\|^2}{\sigma_i^2}} \tag{34}$$

where c_i and σ_i are the centre and the deviation of each basis functions. If a priori knowledge on the non-linear function $\alpha_2 H(\psi(t-1))$ is available in terms of data measurements, well-known clustering methods can be applied in order to determine the number and values of the parameters c_i and σ_i. If no a priori knowledge is available for the choice of the centre c_i it is commonplace to divide the domain of definition of the non-linear function in i uniformly distributed points. In order to guarantee good generalisation properties of the approximator, the deviation parameters σ_i of each basis functions are chosen such that a sufficient overlap between the basis functions is ensured. For this particular application the range of the simulated manoeuvre has been sampled uniformly with steps of 5°. Therefore with respect the manoeuvre reported in figure 11 the total number of lattice centre is $i = 15$ while the deviation is assumed to be the same for each basis function and equal to $\sigma^2 = 2.5/\ln 0.5$. From equation (33) it is clear that a total number of 18 parameters has to be estimated in order to implement the identifier, the structure of which is shown by figure 8.

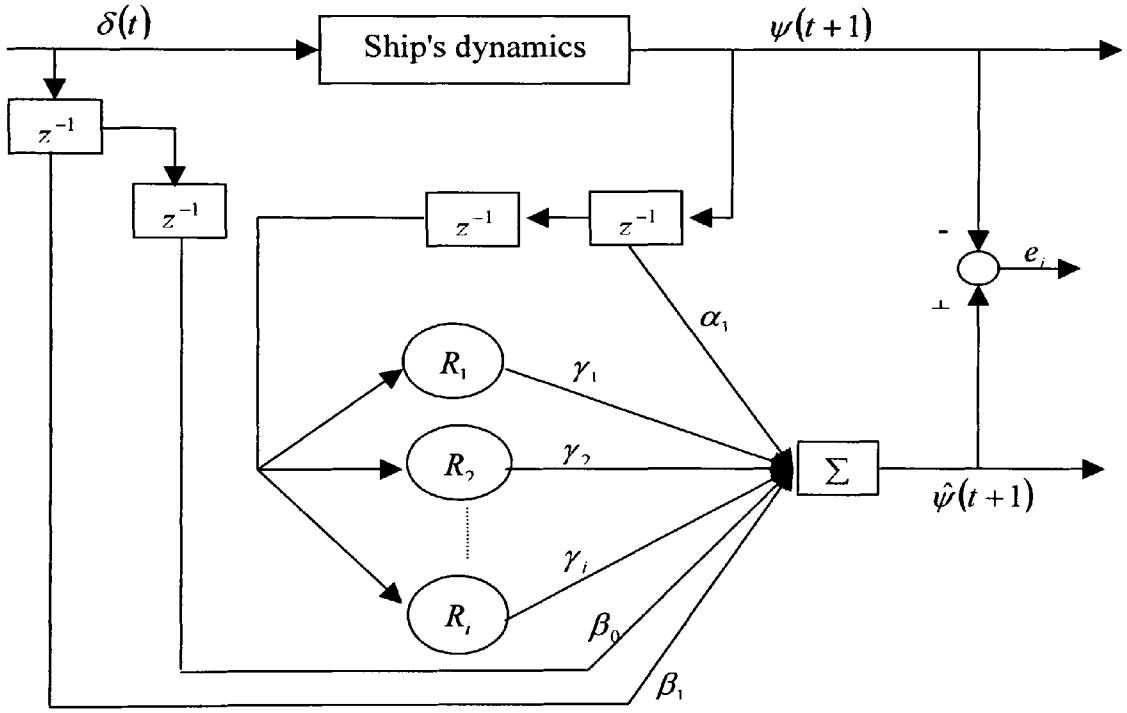

Fig. 8: Identifier structure

The advantage in using this kind of approximator represented by equation (21) relies on the fact that the parameters to be estimated appear linearly, preserving therefore the validity of well known stability results obtained in linear adaptive theory when equation (29) is used as adaptive law. Finally, the parameters estimated in equation (33) with the adaptive law expressed in equation (29) are used in turn to implement the control law based on the certainty equivalence principle defined by the equation (35):

$$\delta(t) = \frac{1}{\hat{\beta}_0(t)}\left\{\psi_m(t+2) - \hat{\alpha}_1(t)\psi(t+1) - \sum_i \hat{\gamma}_i R_i(\psi(t)) - \hat{\beta}_1(t)\delta(t-1)\right\} \tag{35}$$

where $\psi_m(t+2)$ is the output of the reference model defined by equation (31). The overall controller structure is shown in figure 9. Because d=2 the reference heading

angle at time (t+2) must be available. In other words the reference heading angle two steps ahead is needed in order to implement the above control law.

7. Simulation Results

The adaptive controller presented above was evaluated by a simulation study involving the containership model described in section 2. Due to the presence of external disturbance and the approximation introduced by the radial basis network, in the adaptive law represented by equation (29) the dead-zone was sets to a value proportional to the wave induced state vector x_w. In order to avoid unbounded control output the parameter β_0 is constrained to be outside the interval [-0.1;+0.1]. The wave conditions are defined with respect to equation (3) by an average period of T=8 sec and a significant wave height of h=3 meters.

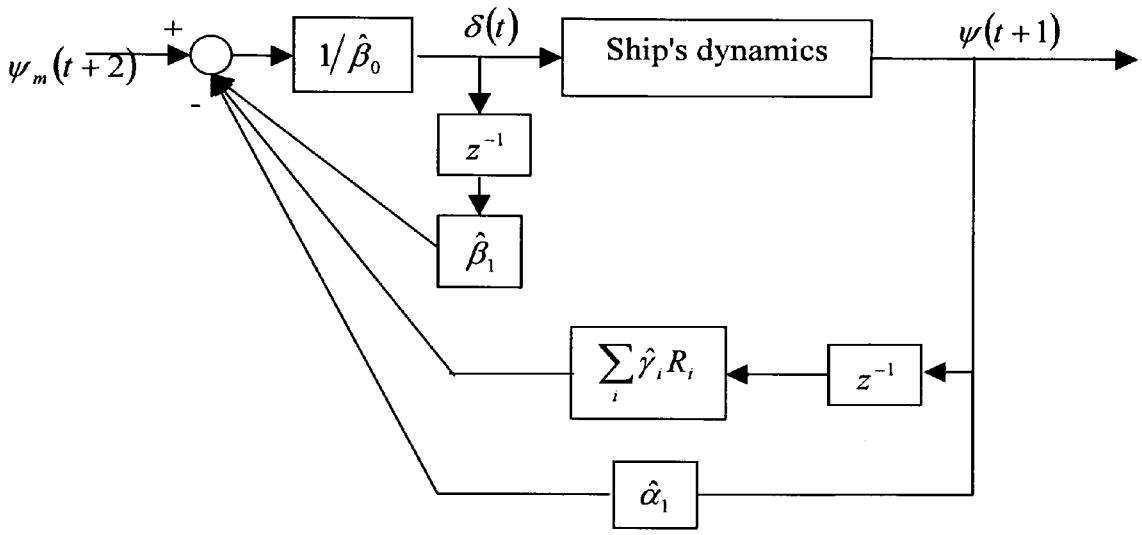

Fig. 9: Adaptive controller structure

The shallow water effect has been tested both by a constant change and a step change in the water depth. Figure 10 shows the depth of water at each time instant and the relative hydrodynamic parameter values as expressed by equation (5). With respect to figure (2) the coefficients are:

B=32; % Breadth [m]
T=10.7; % mean draft [m]

The shallow water effect begins to take effect at water depth from 3 to 4 times T. Note that when H=T the ship is running aground, F will be zero and the coefficients K_i will diverge to infinity. Therefore, in the simulations was set a minimum value for the water depth as, $H_{final} = T + \varepsilon$ with $\varepsilon > 0$.

Figure 11 shown the heading and the rudder angle for a sequence of course-changing manoeuvres with wave disturbances and shallow water effects defined as above and starting angle of attack of 60°. All parameters, of equation (33) except for β_0, where initialised to zero. Figure 12 shows the parameter values during the adaptation and the tracking and estimation error. Due to the presence of the dead-zone in the adaptive law, it is not guaranteed that the tracking error will converge to zero. This is shown in the appendix where it is also proved the stability of the overall system. Finally, figure 13

shows the same sequence of course-changes as shown in figure 11, with the controller parameters initialised with values different than zero. From this figure it is possible to understand how a good initialisation of the controller parameters will enhance the transient response of the controller. For this instance the application of multiple models and switching criteria suggested in Narendra and Balakrishnan[27] is worth considering.

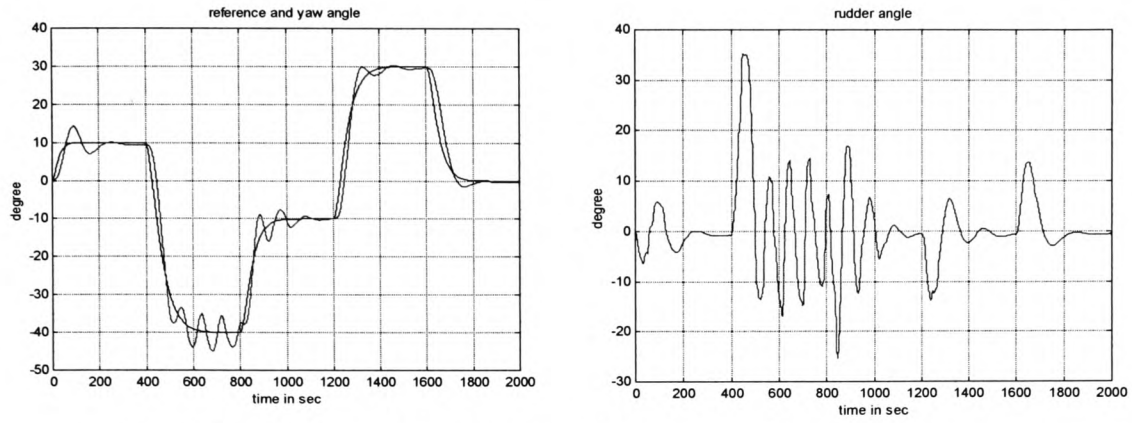

Fig. 11: Heading and rudder angle for course-changing manoeuvre

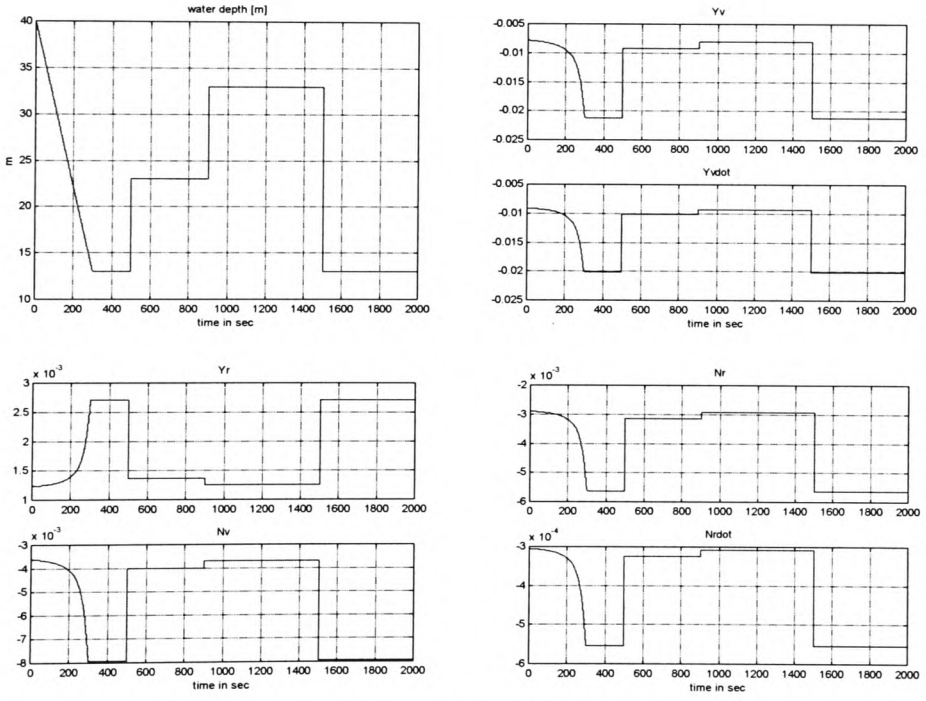

Fig. 10: Water's depth and hydrodynamics parameters

8. Concluding Remarks

In this paper the problem of designing an adaptive autopilot for a containership is addressed. Non-linear models describing the steering dynamic are introduced in order to justify the choice of the controller and identifier structure. Based on the certainty equivalence principle an indirect adaptive controller is designed and evaluated by

simulation study. The adaptive control law is motivated by well-known results in linear adaptive theory. During the controller design in order to take into account the non-linear nature of the ship's dynamics, a radial basis function neural networks is used to approximate the non-linear function defined by the Bech's reversal spiral test. The choice of the radial basis neural network upon the multilayer perceptron neural network is also motivated. Due to the presence of external disturbance induced by the waves and the approximation introduced by the neural network, a dead-zone in the adaptive law is introduced. As shown in the simulation results, the transient response of the adaptive autopilot can be enhanced by a proper choice of the initial values for the controller parameters. However all simulation results showed that the proposed controller is able to deal with the dynamics changes that a ship can encounter due to different sailing conditions.

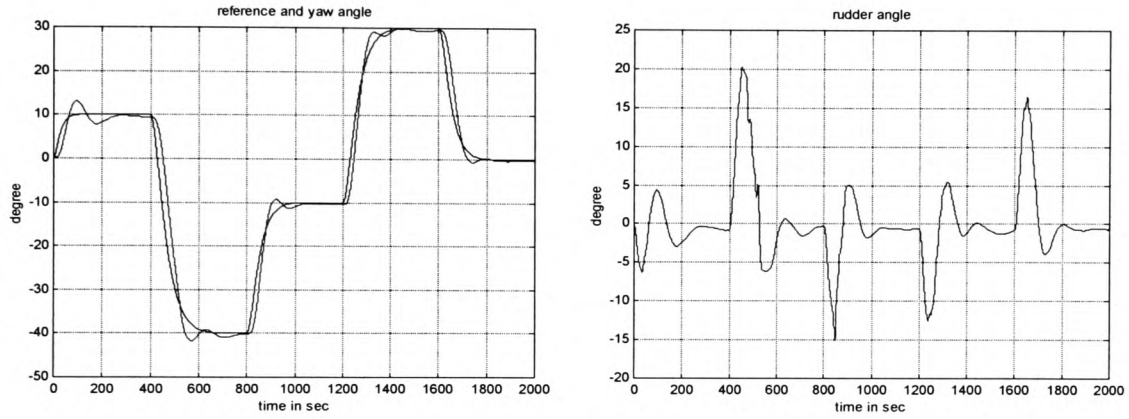

F Fig.13: Heading and rudder angle for the course-changing manoeuvre
changing manoeuvre

Appendix

The adaptive law expressed by equation (29) is motivated by the linear adaptive theory, in which it has been proved that if:
the relative degree d, of the system is known,
the non-linear functions f satisfy a global Lipschitz condition and
the output of the system does not grow faster then the input,
then the non-linear system expressed by the equation (23), with the adaptive law expressed by equation (29) and the control law (30) results in all the signals being uniformly bounded and there exist an integer K_t and a non-negative constant C such that:

$|\hat{\psi}(k)-\psi(k)| \le \varepsilon_{\max}$ and $|\psi(k)-\psi_m(k)| \le C$ for all $k \ge K_t$.

A detailed proof of this result can be found in the original paper Peterson and Narendra[25] or in chapter 8 of Narendra and Annaswamy[24] or in the books of Astrom and Wittenmark[28], Ioannou and Sun[29]. Here the main steps involved are briefly highlighted.

Step 1.

Considering a bounded disturbance ε, equation (23) can be rewritten:

$$\psi(k+1)=\theta^T\omega(k)+\varepsilon(k) \tag{A.1}$$

the identification error became:

$$e(k+1)=\hat{\psi}(k+1)-\psi(k+1)+\varepsilon(k)=\phi^T(k)\omega(k)+\varepsilon(k) \tag{A.2}$$

where $\phi(k)=\hat{\theta}(k)-\theta$ is the parameter error. Using the direct method of Lyapunov it is proved that

the parameter error $\phi(k)=\hat{\theta}(k)-\theta$ is bounded,

the identification error either does not grow faster then the signal vector $\omega(k)$ or is bounded $|e(k)|\le\varepsilon_{\max}$ and

the parameter error converge $\lim_{k\to\infty}\|\Delta\phi(k)\|=0$.

This can be done by choosing the Lyapunov candidate function $V(k)=\phi^T(k)\phi(k)$. The time derivative evaluated along equation (29) is:

$$\begin{aligned}V(k+1)-V(k)&=\phi^T(k+1)\phi(k+1)-\phi^T(k)\phi(k)=\\&=-\frac{\eta(k)e^2(k+1)}{1+\|\omega(k)\|^2}\left[2-\eta(k)\frac{\|\omega(k)\|^2}{1+\|\omega(k)\|^2}\right]+\frac{2\eta(k)e(k+1)\varepsilon(k)}{1+\|\omega(k)\|^2}\end{aligned} \tag{A.3}$$

If $e(k+1)>\varepsilon_{\max}$, with $0<\eta(k)<2$ the first term of the right hand side of equation (A.3) dominates the second term therefore $\Delta V(k)\le 0$. If on the contrary $e(k+1)\le\varepsilon_{\max}$ the parameter vector is not updated therefore $\Delta V(k)=0$. Hence in any case for all k is $\Delta V(k)\le 0$.

i) Because the sequence $V(k)$ is bounded and non-increasing, it must converge as $k\to\infty$ therefore $\|\phi(k)\|$ is bounded.

ii) Since $\lim_{k\to\infty}\Delta V(k)=0$ either K_1 exist such that for $k>K_1$ $|e(k)|\le\varepsilon_{\max}$, or the sequence $e(t_k+1)$, with t_k defined as $t_k\{i:e(i+1)>\varepsilon_{\max}\}$ are the time instants where the identification error is greater then $\varepsilon_{\max}$, cannot grow faster then the signal vector at the time t_k:

$$e(t_k+1)=o[\|\omega(t_k)\|]$$

which implies:

$$e(k+1)=o\left[\sup_{t\le k}\|\omega(t)\|\right] \tag{A.4}$$

Equation (A.4) can be rewritten $e(k+1)=\sigma(k)\|\omega(k)\|$ where $\lim_{k\to\infty}\sigma(k)=0$.

iii) From the adaptive law equation (29) it follows that

$$\|\Delta\phi(k)\|=\eta(k)\frac{\sigma(k)\omega(k)}{1+\|\omega(k)\|^2}$$

which leads to $\lim_{k\to\infty}\|\Delta\phi(k)\|=0$.

Step 2.

Using arguments based on the input-output relationships, it is shown that the state vector of the non-linear systems (23) is bounded and the tracking error converges.

This is achieved first considering hypothesis three, for which the output of the system $\psi(k)$ cannot grow faster then the input $\delta(k)$, this is expressed by the order relation:

$$\delta(k) = O\left[\sup_{t \le k+d} \psi(t)\right] \tag{A.5}$$

For hypothesis two and equation (A.5) the output cannot grow faster then the vector signal $\omega(k)$ which is:

$$\omega(k) = O\left[\sup_{t \le k+d} \psi(k)\right] \tag{A.6}$$

Because the use of the dead-zone in the adaptive law, the estimated parameter vector is bounded. Hence, to conclude the proof, it is necessary to show that the output $\psi(k)$ and the estimated output $\hat{\psi}(k)$ are also bounded.

The control law (29) based on the certainty equivalence principle has to satisfy:

$$\psi_m(k) = \hat{\theta}(k)\omega(k+d-1)$$

Now studying the tracking error:

$$\psi(k+d) - \psi_m(k+d) = \theta^T \omega(k+d-1) - \hat{\theta}^T(k)\omega(k+d-1) + \varepsilon =$$

$$\left[\theta - \hat{\theta}(k+d-1) + \sum_{j=k}^{k+d-2} \Delta\hat{\theta}(j)\right]^T \omega(k+d-1) + \varepsilon = -e(k+d) + \left[\sum_{j=k}^{k+d-2} \Delta\hat{\theta}(j)\right]^T \omega(k+d-1) + \varepsilon$$

For equations (A.4) and (A.6) it is possible to infer that the tracking error grows slowly than the output

$$\left|\psi(k+d) - \psi_m(k+d)\right| = o\left[\sup_{t \le k+d} \psi(t)\right] + C \tag{A.5}$$

where C is a non-negative constant depending on ε. Since $\psi_m(k)$ is a bounded signal, $\psi(k)$ cannot grow in an unbounded fashion and this implies that

$\lim_{k\to\infty} \left|\psi(k) - \psi_m(k)\right| = C$

The estimation error also converges to:

$$\lim_{k\to\infty} \left|\hat{\psi}(k) - \psi(k)\right| = \varepsilon_{\max}$$

Finally since $\psi(k)$ is bounded from (A.2) also $\delta(k)$ is bounded.

The knowledge on the relative degree d, required by hypothesis 1, is fulfilled by the analysis outlined in section 3. Hypothesis 2, is guaranteed by the choice on the radial basis function, while hypothesis 3, implies that the ship is directionally stable. Based on the above argument, it is possible to conclude that the control law described by equation (30) with the adaptive law of equation (29), guarantee that all the signals in the adaptive loop are bounded and that the tracking and estimation error converges.

Reference List

1. Sperry E. Automatic steering. Trans. Society of Naval Architects and Marine Engineers. 1922; 53-61.

2. Minorsky N. Directional Stability of Automatically Steered Bodies. Journal of American Society of Naval Engineers. 1922; 34:280 309.

3. Norrbin N.H. On the added resistance due to steering on a straight course. Proc. 13th International Towing Tank ; Berlin. 1972: Vol.1 p282-408.

4. Broome D.R., Keane A. J. and Marshall L. The effect of variations in ship operations on an adaptive autopilot. Proc. Ship Steering and Automatic Control; Genova. 1980: 77-95.

5. Honderd G. and Winkelman J.E. An Adaptive Autopilot for Ships. Proc. 3rd ship Control Systems SymposiumBath; 1972: Vol.2.

6. Amerongen J. van and Udink Ten Cate A.J. Model reference adaptive autopilots for ships. Automatica. 1975; Vol.11:441-449.

7. Kallstrom C.G., Astrom K. J. Thorell N. E. Eriksson J. and Sten L. Adaptive autopilots for tankers. Automatica. 1979; Vol. 15:254-284.

8. Brink A.W., Baas G. E. Tiano A. and Volta E. Adaptive automatic course-keeping control of a supertanker and a container ship: a simulation study. Proc. 5th Ship Control Systems Symposium; Annapolis. 1978: Vol 4.

9. Astrom K.J. Why Use Adaptive Techniques for Steering Large Tankers. Int. J. Control. 1980; Vol.32, No4:689-708.

10. Blanke M. and Jessen A.G. Dynamic properties of container vessel with low metacentric height. Transactions of The Institute of Measurement and Control. 1997; 19(2):78-93.

11. Tiano A. and Blanke M. Multivariable identification of ship steering and roll motions. Trans. Inst. Measurement and Control. 1997; 19(2):63-77.

12. Lewis E.W. Principles of Naval Architecture. Society of Naval Architecture and Marine Engineers, New York. 1988.

13. Price W.G. and Bishop R. Probabilistic Theory of Ship Dynamic. London: Chapman and Hall; 1974.

14. Sheng Z. Y. Contribution to the discussion of the Manoeuvrability Committee Report. Proceeding of 16th ITTC; Leningrad. 1981: 170-173.

15. Clarke D. The Application of Manoeuvring Criteria in Hull Design Using Linear Theory. Transactions of Royal Institution of Naval Architects. 1983; 125:45-68.

16. Abkowitz M.A. Lectures on ship hydrodynamics, steering and manoeuvrability. Hydro and Aerodynamics Laboratory, Lyngby, Denmark; 1964; Report nr. Hy-5.

17. Nomoto K.G., Tagachi K. Honda T. and Hirano S. On the steering quality of Ships: International Shipbuilding Progress; 1957; Vol. 4.

18. Bech M.J. and Wagner-Smitt L. Analogue simulation of ship manouvres based on full scale sea trials or free sailing model tests. Hydro and aerodynamics laboratory, Lyngby, Denmark; 1969; Report nr. Hy-14.

19. Bech M.I. The Reversed Spiral Test as Applied to Large Ships. Shipping World and Shipbuilder. 1968; 1753-1754.

20. Norrbin N.H. Theory and obsarvation on the use of a MAthematical MOdel for Ship Maneuvering in Deep and Confined Waters. 8th Symposium on Naval Hydrodynamics; Pasadena, California. 1970.

21. Hunt K.J., Sbarbaro D. Zbikowsky R. and Gawthrop P. J. Neural Networks for Control Systems - A survey. Automatica. 1992; 28(6):1083-1112.

22. Cybenko G. Approximation by superposition of sigmoidal functions. Mathematics of Cotrol, Signals and Systems. 1989; 2:183-192.

23. Hornick K., Stinchcombe M. and White H. Multilayer Feedforward Networks are Universal Approximators. Neural Network. 1989; 2:359-366.

24. Narendra K.S. and Annaswamy A.M. Stable Adaptive Systems.: Englewood Cliffs, N.J. : Prentice-Hall; 1989.

25. Peterson B.B and Narendra K.S. Bounded error adaptive control. IEEE Transactions on Automatic Control. 1982 Dec; (27):1161-1168.

26. Amerongen J. van. Adaptive steering of ships- A model reference approach. Automatica. 1984; 20(1):3-14.

27. Narendra K. and Balakrishnan S. Adaptive control using multiple models. IEEE Transaction on Automatic Control. 1997; (AC-42):171-187.

28. Astrom K.J. and Wittenmark B. Adaptive Control . second ed. Addison-Wesley; 1995. ISBN: 0-201-55866-1.

29. Ioannou P.A. and Jing Sun. Robust Adaptive Control.: Prentice Hall; 1996. ISBN: 0 13 439100 4.

A model-reference neural autopilot for ships

A. G. M. Zirilli[1], G. N. Roberts[1], A.Tiano[2] and R. Sutton[3]

[1]University of Wales College, Newport Allt-yr-yn Campus, PO Box 180, Newport, NP9 5XR, U.K.

[2]Department of Information and Systems, University of Pavia, Via Ferrata 1, I-27100 Pavia, Italy. Also: Institute of Ship Automation C.N.R, Via de Marini 6, I-16149 Genova, Italy.

[3]University of Plymouth, Drake's Circus Plymouth, PL4 8AA, UK.

SYNOPSIS

This paper describes the development of a new autopilot for ships, which is based upon the well-known model-reference approach, the optimum performance of which is achieved through the use of artificial neural networks. The system's behaviour is defined by the model reference through a setting of specific parameters, while the neural controller is properly trained in order to comply with the desired performances. So for sailing in restricted water, where the manoeuvre precision is the most important feature, it will be tuned to give a zero overshoot in the ship heading angle response, in order to avoid the risk of a dangerous path. A high value for the initial yaw rate can also be selected in order to clearly show the intention of the manoeuvre to others ships. On the contrary during navigation in open water, a more relaxed performance can be selected, in order to minimise fuel consumption and drag force due to the rudder motion. The algebraic part of the adaptive control design is formulated using the assumptions that the ship's dynamics can be represented by a Auto-Regressive-Moving-Average model, and that the neural network chosen for the controller can approximate the control law with any degree of accuracy. Finally, the analytical part of the controller design, is accomplished using the back-propagation algorithm which in this application is able to adapt on-line the network's controller parameters in order to guarantee the closed loop performances as specified by the model reference. A series model is also introduced in order to take into account the non-linearity in the ship's rudder dynamics.

Author's Biography

Antonio Zirilli was born in Milazzo Sicily, Italy on March 21st, 1970. He achieved a high technical school degree in Electronics on July 1988, at I.T.I.S: "G.Marconi" of Messina and a graduation as Electronics Engineer in 1996, from the University of Pavia Italy presenting a thesis on "Multivariable Control of Ship Motion in Rough Sea". After graduation he served in the Italian Navy till January 1998. During this period he achieved on July 1997 a degree of Captain for the Merchant Navy at the Technical Nautical Institute "C. Duilio" of Messina On December 1997 he became a chartered electronic engineer. In January 1998 he was awarded a scholarship as a Ph.D. student at the Mechatronics Research Centre, University of Wales College of Newport, U.K., developing a research project on "Intelligent Ship Motion Control".

Professor Geoff Roberts is Director of the Mechatronics Research Centre at the University of Wales College Newport, UK. He joined Newport as a Reader in Mechatronics in 1994 following a seventeen year commission in the Royal Navy, most of which was served at the Royal Naval Engineering College (RNEC). He was promoted to Lieutenant Commander and Senior Lecturer in 1981, to Principal Lecturer in 1990 and to Head of Control Engineering and Reader in Marine Control Systems in 1993. Professor Roberts holds an honours degree in electrical engineering, A MSc in marine engineering and a PhD in control engineering, he is a Chartered Engineer, a Fellow of the IMarE, the Institution of Electrical Engineers and the Institute of Measurement and Control. He is Chairman of the IEE Control Division, Chairman of the IFAC Technical Committee on Marine Applications and is a member of the Editorial Advisory Panel of the Computing and Control Engineering Journal.

Professor Antonio Tiano was born in Genova, Italy, on December 11, 1943. He received the degree of Doctor in Applied Mathematics from Genova University in 1969. Since 1972 he is scientific researcher at the Institute of Ship Automation of the Italian National Council of Researchers in Genova. Since 1987 until 1991 he was associate professor of system theory at the University of Modena, Italy. Since 1991 he is Associate Professor of Automatica at the University of Pavia, faculty of engineering, Italy. His current interests include, modelling identification and control of dynamic systems, with a particular reference to marine vehicles. More recently his two particular fields of interests are, chaos in dynamic systems and application of AI methods to control.

Dr Robert Sutton, holds a degrees of BEng (Tech) in Engineering Production, and Meng and PhD in Control Engineering from the University of Wales. During his 16 years in the Royal Navy, he spent 10 years at the Royal Naval Engineering undertaking research work into warship control systems in the posts of Senior Lecturer and College Reader. On completion of his service in 1992, Dr Sutton took up an appointment with the University of Plymouth in the Institute of Marine studies (IMS) as a Senior Lecturer. In 1994 he became a Principal Lecturer and the Head of the Marine Technology Division within the IMS. In 1998, he was promoted to Reader in Control Systems Engineering. He is a member of the Advisory Board and Publications Committee of the Underwater Technology Journal. In addition, he is a member of the ImechE's Machine Systems, Computing and Control Executive Committee and Vice-Chairman of its Control Technical Activities Sub-Committee.

INTRODUCTION

Historically the first ship control system was introduced by Sperry [20] and Minorsky in 1922 [14]. The aim of this autopilot was to maintain the course of the ship using a simple proportional action on the heading error angle. The implementation and use of such a simple autopilot demonstrated that thanks to a better course keeping there was also a reduction in propulsion losses and therefore a saving in fuel costs. A further improvement of the control law was the inclusion of a derivative term for the heading error and a further integrating term leading to the better known PID autopilot. Due to the relatively simplicity in the implementation of PID autopilot, this kind of controller dominated the scenario until the early 1970s.

Because of the increasing cost of fuel, controlling the ship motion became a problem of major interest. The new challenge was to develop and put into operation new ship's control systems, which could perform the desired task in a safe and economical way. For this purpose the coupling between the different motions could not be neglected. The most popular approach was the Linear Quadratic (LQ) Controller, in which the controller parameters are selected in order to satisfy certain optimal criteria expressed as a quadratic cost function. Different cost functions taking into account yaw and rudder deviation, fuel consumption, etc., were proposed [16], [6], and [12]. Although the LQ technique appeared robust for parameter changes, other researchers were investigating the applicability of adaptive control techniques such as model reference [9], [1] or self-tuning adaptive controller [11], [5], in order to take into account the non-linearity in steering dynamics. Adaptive control is also needed to maintain optimal performances, even when the process characteristics change due to the changing in forward speed, load condition, water deep etc.

The fast development of small and inexpensive microcomputers and advances in computing technology have fuelled the so-called 'Intelligent Control' theory, in which control algorithms are developed by emulating certain characteristics of intelligent biological systems. The foundation of such systems can be found at the intersection of disciplines like cybernetics, artificial intelligence and informatics [23]. The ship autopilot presented herein is based on the well-known theory of model reference adaptive systems. In general, the design based on stability theory methods requires that either the process and reference model be linear. The solution adopted in this paper in order to deal with certain class of non-linearity due to the ship steering machine, is based on the work of van Amerongen (1984) [2], then the design of a intelligent non-linear adaptive controller based on model reference theory and neural network concepts is presented.

SHIP MATHEMATICAL MODEL

The mathematical model of a container ship used in this study is described in detail in [21] and [4]. It is herein considered a stochastic extension of such models capable to describe the ship response in irregular sea waves, which is expressed by the following non-linear equations:

$$\begin{aligned} m\left(\dot{u} - vr - x_g r^2 + z_g pr\right) &= X + X_w \\ m\left(\dot{v} + ur - z_g \dot{p} + x_g \dot{r}\right) &= Y + Y_w \\ I_{zz}\dot{r} + mx_g\left(\dot{ur} + \dot{v}\right) &= N + N_w \\ I_{xx}\dot{p} - mz_g\left(\dot{ur} + \dot{v}\right) &= K + K_w - \rho g D R_z(\varphi) \end{aligned} \tag{1}$$

The above equations with reference to the co-ordinate system shown in figure 1, describe the coupled surge, sway, yaw and roll motions, where D is the displacement, g the gravity constant, ρ the water mass density, $R_Z(\varphi)$ is the action of the rightening arm that depends on the roll angle φ, while $(x_G,0,z_G)$ are the co-ordinates of the mass centre. The mass is denoted by m whereas Ixx and Izz are the inertial moments about x and z, respectively. The linear velocity of surge and sway are u and v and the angular ones of yaw and roll are respectively r and p. The rightening arm function can be expressed as:

$$R_z(\varphi) = \sin\varphi\left(GM + \frac{BM}{2}\tan^2\varphi\right) \tag{2}$$

where GM is the ship metacentric height and BM is the distance from the centre of buoyancy to the metacentre.

Terms X, Y denote the deterministic forces acting along x e y while N and K are the deterministic moments around z and x, which take into account the hydrodynamic effects from the hull movements and forces exerted on the ship by the rudder

and by the propulsion system. Such forces and moments are usually described [13] by regarding X,Y,N,K as polynomial expansion in terms of state variables, control actions and hydrodynamic coefficients.

The effects of external disturbances, i.e. wind and waves, consist of related forces X_w, Y_w and moments N_w, K_w acting as perturbation terms in the corresponding right hand parts of eq. (1). Such terms, owing to their intrinsically random nature, are generally quite difficult to be characterised through explicit mathematical relations: for example, as to the waves, they should be calculated by integrating the wave pressure over the immersed surface of the hull, on the assumption that the pressure within the waves is unaffected by the presence of the ship [13]. As it has been shown in [13] and [17], a reasonable simplifying assumption consists in applying a linear superposition principle, which makes it possible to separate the ship motion due to the environment from the motion induced by the rudder and by the propeller thrust. According to this modelling approach, waves and wind are regarded as finite order linear realisations of stochastic processes characterised by known spectral densities.

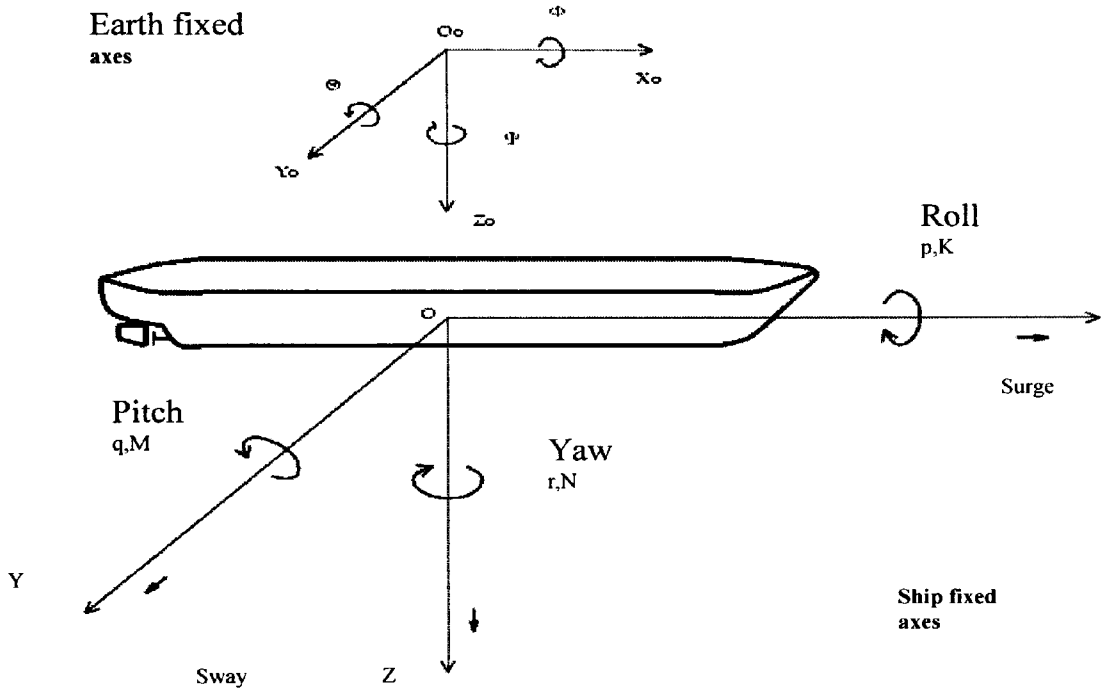

Fig:1 Co-ordinate system

By limiting attention to sea waves, which are by far the dominant disturbance, it is possible to regard a long crested irregular sea height $\zeta(t)$, at time t, as described by a one-dimensional amplitude spectrum, the main parameters of which are the significant wave height, h and the average wave period T. This spectrum, accepted by the International Ship Structure Congress (ISSC) is given by:

$$G_\zeta(\omega) = \frac{173h^2}{\omega^5 T^4} \exp\left(\frac{-691}{T^4\omega^4}\right) \tag{3}$$

The relation between the response of each individual component of the wave induced ship state vector $\mathbf{x_w} = [u_w\ v_w\ r_w\ p_w]^T$, can be obtained in terms of the spectrum:

$$G_{x_w^i}(\omega,\chi,U) = \left|R_{x_w^i}(\omega,\chi,U)\right|^2 G_\zeta(\omega) \qquad i=1,4 \tag{4}$$

where χ is the angle of encounter between ship and waves, U is the ship velocity and $R_{x_w^i}$ is the receptance operator, which is assumed to be known from experimental tests, describing the response of the ship i^{th} motion to the waves [4]. In order to obtain the corresponding spectrum relative to the ship centre of mass, it is finally necessary to express the spectrum

given by eq(4) as a function of the frequency of encounter between ship and waves $\omega_e = \omega\left(1 - \frac{\omega U}{g}\cos(\chi)\right)$. Once the waves induced ship state vector x_w is computed the total ship state vector is represented by:

$x_{tot}=x_w+x$

According to this approach, it is possible to implement an accurate and numerically reliable simulation of sea wave induced ship motions.

MODEL REFERENCE

The *model reference adaptive system* was originally proposed to solve a problem in which the performance specifications are given in terms of a reference model [3]. This model specified how the process output should ideally respond to the command signal. A block diagram of the system is shown in figure2. The controller can be thought of as consisting of two loops. The inner loop is an ordinary feedback loop composed of the process and the controller. The outer loop adjusts the controller parameters in such a way that the error, which is the difference between process output and model output is small. Because of the model reference represents the desired plant output with respect to the specified command input, it is important that the dynamics of the reference model match the dynamics of the controlled ship with respect to the magnitude of the demanded change of reference yaw angle. A reference model, which is too sluggish, cannot produce an optimal performance since the ship cannot reach the required heading in the minimum time. Conversely, it should not be used a reference model which is too fast compared with the ship response characteristics because this may cause rudder actuator saturation and performance degradation.

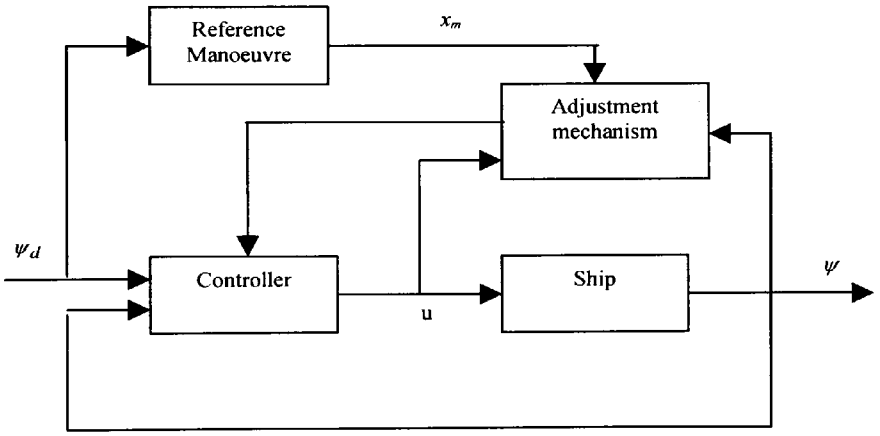

Figu. 2: Block Diagram of a Model Reference Controller

As suggested by [2] a course changing manoeuvre can be easily described by the step response of a second order system. From this response, as shown figure 3, it is possible to identify three different phases: 1) a start of the turn, 2) a steady turning, and 3) an end of the turn. The turn should have a start, which clearly indicates to other ships the intention of the manoeuvre. The stationary part is determined both by limiting the rudder angle and by controlling the rate of turn. The end of the turn for safety reasons, should be completed without overshoot of the heading angle. In terms of Laplace transfer function such a model reference can be represented by equation (5):

$$\frac{\psi_m(s)}{\psi_r(s)} = \frac{K_{pm}/\tau_m}{s^2 + s/\tau_m + K_{pm}/\tau_m} \tag{5}$$

where s is the Laplace operator and ψ_r is the new requested head angle. The time constant τ_m is chosen approximately 2-3 times smaller than the dominating time constant of the ship at cruise speed and must be such that the process is able to follow the model. If the rate-of-turn limiter is neglected, K_{pm} follows from the desired damping ratio (ξ) of the system:

$$K_{pm} = 1/\left(4\xi^2\tau_m\right) \tag{6}$$

Possible values of ξ are between ξ=1 which corresponds to a zero overshoot condition, to ξ=0.7 which corresponds to an overshoot of approximately 5% of the desired value. The selection of τ_m results from the following consideration: a reasonable course controller will have a rate-feedback gain which makes the time constant of the ship 2-3 times smaller with respect to the case of the open-loop system (without controller). By choosing a similar time constant for the model reference this guarantees that the process can follow the model. In order to include the effect of the steering machine, mainly the rudder saturation and limited rate of change, such a second-order model is extended to a third order in which the gain factor K_{pm} is replaced by

$$\frac{K_{pm} f}{s\tau_\delta + 1} \tag{7}$$

where f and τ_δ are computed on-line and are defined as

$$f = \frac{\delta_{\max}}{|\delta_r|} \qquad \text{and} \qquad \tau_\delta = \frac{|\delta_r - \delta|}{\dot{\delta}_{\max}}$$

where $\delta_{\max}$ is the maximum available rudder angle, $\dot{\delta}_{\max}$ is the maximum rudder speed and δ_r is the requested rudder angle from the controller.

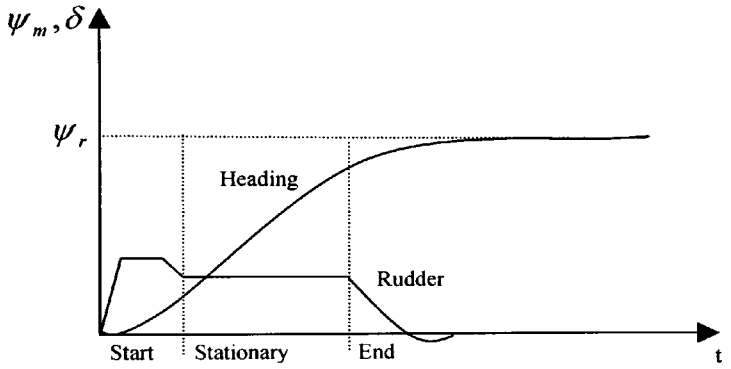

Fig. 3: Course changing manoeuvre

The third order model reference equation will then be:

$$\dddot{\psi}_m + \left(\frac{1}{\tau_\delta} + \frac{1}{\tau_m}\right)\ddot{\psi}_m + \frac{1}{\tau_\delta \tau_m}\dot{\psi}_m + \frac{K_{pm} f}{\tau_\delta \tau_m}\psi_m = \frac{K_{pm} f}{\tau_\delta \tau_m}\psi_r \tag{8}$$

Such a model can be seen as a pre-filter which drives the desired heading angle, in order to avoid steering machine saturation related to large rudder demands. With such a pre-filtering the model reference can be easily designed as a linear second-order transfer function in which the parameters are exactly τ_m and K_{pm}. [2]

CONTROLLER DESIGN

Neural Networks for control and system analysis have been intensively investigated during the last ten years, not only in terms of the research being carried out, but perhaps more importantly in terms of the potential range of applications. The main characteristics of neural networks for control applications can be summarised as: they can be used to approximate any continuos mapping [10], they perform this approximation through learning, [7] parallel processing and fault tolerance are easily accomplished. One of the most popular and commonly used algorithms for learning in neural networks is error back propagation. This algorithm is based mainly on a combination of least-mean square and gradient descent methods [18].

Generally speaking there are two main approach to the synthesis of a Model Reference Adaptive Controller (MRAC), [8], the first one is based on the minimisation of a predefined performance index, and the second one is based on the definition of a Lyapunov function. In this paper the authors present an adaptive based model reference controller through the use of

artificial neural network by means of a minimisation of a predefined performance function through the use of the back-propagation algorithm.

Back-propagation algorithm

The back-propagation algorithm, is a generalisation of the Least Mean Square (LMS) algorithm, used to train multilayer networks. As with the LMS learning law, back-propagation is an approximate steepest descent algorithm, in which the performance index is the mean square error. The only difference between the LMS algorithm and back-propagation algorithm is given by the way in which the derivatives are calculated. As mentioned above, a neural network can be used to approximate any continuos function [10], the structure of such network is shown in figure 4, and it can be summarised in: an input layer with linear neurons, at least one hidden layer of non-linear neurons and an output layer. The output of one layer becomes the input of the following layer, the equation that describes this operation is:

$$a^{m+1} = f^{m+1}\left(W^{m+1}a^{m} + b^{m+1}\right) \qquad \text{for m=0,1,...,M-1} \tag{9}$$

where M is the number of layers in the network, W and b are respectively the weight and bias matrix and f is the neurons function. The neurons in the first layer receive external inputs, which provide the starting point of equation (9), the outputs of the neurons in the last layer are considered the network outputs.

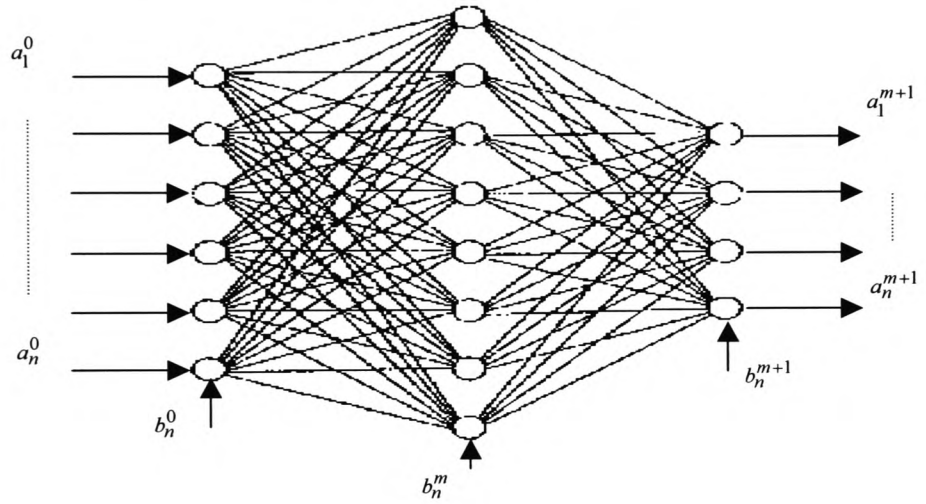

Fig.4: Neural network diagram

The back-propagation algorithm adjusts the network parameters (the neurons' weight and bias) in order to minimise the mean square error:

$$F(x) = E\left[e^2\right] = E\left[(t-a)^2\right] \tag{10}$$

where x is the vector of network parameters, t is the desired output (or target) and a is the actual output from the network. Substituting the expectation of the squared error by the squared error at iteration k, the performance function to be minimised can now be written :

$$F(x) = E = \tfrac{1}{2}\sum_{k}(t_k - a_k)^2 \tag{11}$$

The error is minimised by starting with any set of weights and biases and repeatedly changing each weight by an amount proportional respectively to $\frac{d(E)}{d(W)}$ for the weight and $\frac{d(E)}{d(b)}$ for the biases as follows:

$$w_{i,j}^{m}(k+1) = w_{i,j}^{m}(k) - \alpha\frac{d(E)}{d\left(w_{i,j}^{m}\right)} \tag{12}$$

$$b_i^m(k+1) = b_i^m(k) - \alpha \frac{d(E)}{d(b_i^m)} \tag{13}$$

where α is the learning rate. For practical purposes, in [18] there is proposed a way to increase the learning rate without leading to undesired oscillations. A momentum term is added to equations (12) and (13) to give:

$$\Delta w_{i,j}^m(k) = -(1-\gamma)\alpha \frac{d(E)}{d(w_{i,j}^m)} + \gamma \Delta w_{i,j}^m(k-1) \tag{14}$$

$$\Delta b_i^m(k) = -(1-\gamma)\alpha \frac{d(E)}{d(b_i^m)} + \gamma \Delta b_i^m(k-1) \tag{15}$$

where the momentum parameter is sandwiched between $0 \le \gamma < 1$.

Adaptive Controller

The overall structure of the adaptive system proposed in this paper to control the non-linear ship dynamic is shown in figure 5.

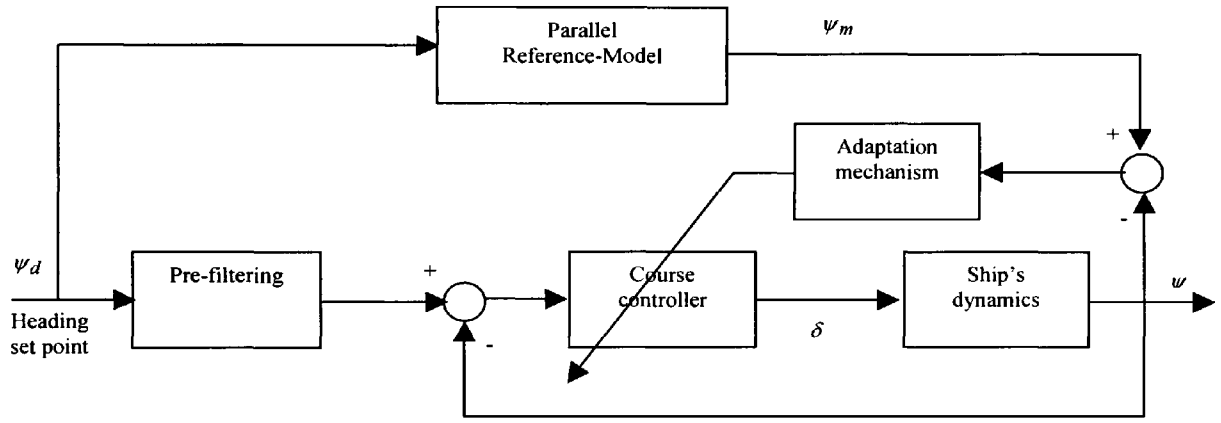

Fig. 5: Block diagram of the Model-reference neural Autopilot

Because of the assumptions made in the above mentioned model reference section, about the third-order pre-filtering, the non-linearity in the control action due to the rudder saturation and the limited rate-of-turn can be disregarded and the non-linear ship dynamics can be represented by equation (16), where the heading angle at time *(k+1)* depends on the past value of ψ and the control action $\delta(k)$:

$$\psi(k+1) = f[\psi(k),....,\psi(k-n+1)] + g[\delta(k)] \tag{16}$$

This equation is a particular generalisation of the Auto-Regressive-Moving-Average (ARMA) model, particularly useful for control purposes since the output depends linearly on the control action $\delta(k)$. With respect to such a model, if the non-linear functions f and g are known, the input $\delta(k)$ at any instant can be computed as:

$$\delta(k) = g^{-1}\{\psi_m(k+1) - f[\psi(k),....,\psi(k-n+1)]\} \tag{17}$$

where ψ_m is the desired output at time *(k+1)* imposed by the model reference.

A neural network in parallel with the ship model, as shown in figure 6, can perform an on-line identification of the function f of equation (16). Here the error at time *k+1*, *e(k+1)* will be back-propagate through the ship neural model and then through the neural controller. As suggested by Narendra [15], the neural ship model, also known as the *sensitivity model*, is used in order to back-propagate the error for the upgrading of the controller's parameters while the neural controller performs the identification of the function g, which is supposed to be invertible. The neural controller is constituted by an input layer of two neurons, an hidden layer of ten non-linear neurons and an output layer of one linear neuron. The controller inputs are the desired yaw angle at time *k+1* and the actual yaw angle at time *k*, the output is the rudder angle at

time k, which should drive the ship's heading to the desired yaw angle at time $k+1$. The adaptation law, as discussed above, is based on the error defined as the difference between the desired and the actual ship heading as follows:

$$e(k+1)=\psi_m(k+1)-\psi(k+1) \tag{18}$$

The weights and biases changes should be proportional to:

$$\frac{d\left(e(k+1)^2\right)}{d\left(w_{i,j}\right)}=2(e(k+1))\frac{d(\psi(k+1))d(\delta(k))}{d(\delta(k))d\left(w_{i,j}\right)} \tag{19}$$

$$\frac{d\left(e(k+1)^2\right)}{d\left(b_i\right)}=2(e(k+1))\frac{d(\psi(k+1))d(\delta(k))}{d(\delta(k))d\left(b_i\right)} \tag{20}$$

The unknown part of equation (19) and (20), in order to solve the adaptation problem is the derivative $d(\psi(k+1))/d(\delta(k))$. In fact the error $e(k+1)$ is known as well the changes $d(\delta(k))/d\left(w_{i,j}\right)$ and $d(\delta(k))/d\left(b_i\right)$, which can be calculated by the back-propagation algorithm trough the neural controller. Although Saerens et al [19] suggested the use of the $sign\left(d(\psi(k+1))/d(\delta(k))\right)$ instead of $d(\psi(k+1))/d(\delta(k))$, the authors preferred to identify on-line the function f as above mentioned, in such a way to mimic the ship behaviour in order to back-propagate the error $e(k+1)$ through the model and then through the controller in order to upgrade the weights and bias of the controller network according to equations (14) and (15). This choice is motivated by the fact that, especially when the model is a non-linear, multivariable and strongly coupled system, it is difficult to properly determine the $sign\left(d(\psi(k+1))/d(\delta(k))\right)$ and a wrong sign can cause ambiguity in training the network.

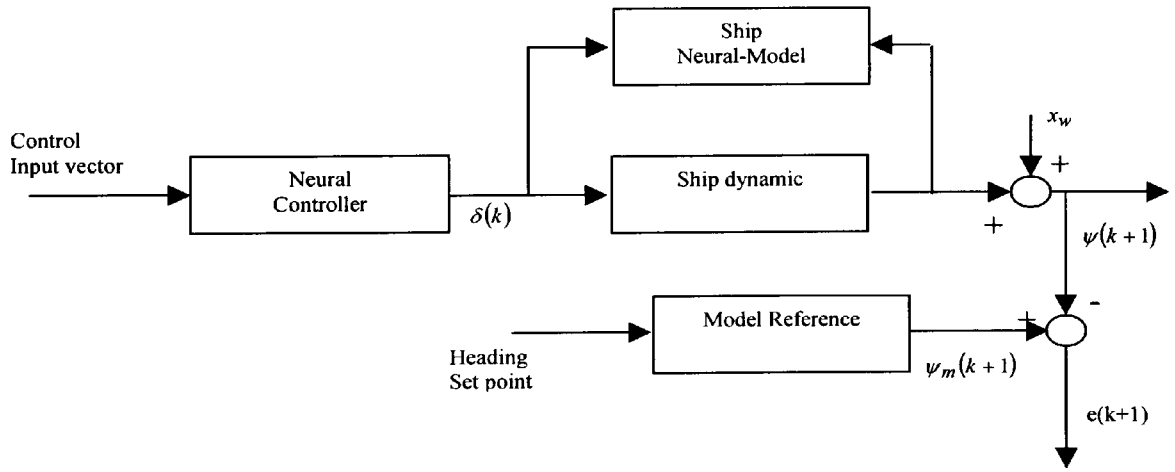

Fig.6: Block diagram showing the adaptive neural controller.

Ambiguity in training the network means that the neural controller establishes a "cause and effect" relationship, between input and output, which is contrary to what would be expected from a clear understanding of the situation being investigated. For instance, controlling a ship with a large inertia and subject to environmental excitation can lead to the particular ambiguity of learning the incorrect result that "to turn the ship to port the controller needs to instruct the rudder to be turned to starboard". The choice to identify a neural model of the ship in order to compute the derivative $d(\psi(k+1))/d(\delta(k))$, is also consistent with what is suggested in [22], in which a state space model of the ship is assumed to be available.

SIMULATIONS AND RESULTS

The model reference neural controller presented above was tested by simulation experiments involving the containership described in [21]. The control algorithm can be summarised as:

Choice of the interim reference head angle from the third order series model,
Upgrade the neural ship model from the measured actual input/output,
Back-propagate the actual ship head error, in order to adapt the neural controller,
Apply the neural controller output to the ship mathematical model presented in equation (1),
Go back to step 1).

In order to improve the performance of the neural adaptive controller, only in terms of algorithm time response, an off-line training of the controller was performed without including the external wave disturbances. The purpose of the off-line training was to find the appropriate initial values of the weights and biases of the adaptive controller, which then could be adapted on-line with a fewer numbers of steps with respect to the case in which the off-line training was not performed. Although in training neural networks it is advisable to include the disturbances in the training data, it is the authors' opinion that in this particular case the inclusion of disturbances can not clearly demonstrate the real adaptability nature of the controller. In this case, off-line training was used to help the back-propagation algorithm overcome the drawback of local minima.

In figures 7 and 8, simulations results for a 10 degree and a 30 degree course manoeuvres are shown. The external waves disturbance is characterised by a significant wave height of h=3 m and a period of T=8 sec. The 10 degree manoeuvre is simulated with a starting angle of attack (the angle between the longitudinal ship axis and the mean waves direction) of 45 degree while the 30 degree manoeuvre has an initial angle of attach of 60 degree, leading to a final situation of beam sea. Also in this critical condition, as it can be appreciated from the simulation response, the model-reference neural autopilot is able to maintain properly the ship course. In the figures, the dashed lines represents the model reference output, while the solid line represents the actual ship response. From these figures is possible to appreciate the excellent tracking performance of the model reference neural autopilot.

The parameters τ_m and k_{pm} of the series model for those particular manoeuvres were identified by simulating the ship's response with a conventional PID controller. The aim was to find those parameters values, which did not cause saturation in the rudder machine. An example of these values are shown in table I.

Table I. Model reference parameters

Manoeuvre Degree	K_{pm} *(5% overshoot)*	τ_{pm} *(5% overshoot)*	K_{pm} *(0% overshoot)*	τ_{pm} *(0% overshoot)*
5	0.0728	7	0.041	6
10	0.05	10	0.035	7
20	0.03	15	0.025	10
30	0.027	18	0.019	13
40	0.023	21	0.016	15

As a final observation the authors would like to mention that although artificial neural networks have been shown to perform well as controllers for course-changing applications and the generalisation properties have provided robust performances for a range of magnitudes of reference step, much further work remains to be done. The inclusion of others factors in the controller design, such as water depth and load condition that clearly affect the ship dynamic, is part of the ongoing research. Also some insight on stability analysis will be carried out.

CONCLUSIONS

In this paper the authors presented a way for the synthesis of a model reference adaptive autopilot for a containership through the use of neural networks. The more relaxed assumptions on the ship's dynamic, made during the controller design, led to the characterisation of a controller able to dial with non-linearity produced by the environmental disturbances and in principal with all non-linearity that are reflected in a change in the ship's dynamics. However, the gain in generalisation is paid for with a lack in stability analysis and the good qualitative performance of the controller are only showed through simulations. In all the simulations carried out the model-reference neural autopilot was able to follow the desired response specified by a model reference, the parameters of which were properly settled in order to observe the ship's dynamics.

As a final remark, is possible to say that this paper address a quite promising technique for the design of adaptive non-linear controllers. However for the implementation of such technique, in the real world, it is still necessary first to prove the generalisation of the simulation results showed herein. Therefore investigation of stability, persistent excitation and robustness of such systems is mandatory in order to guarantee the success.

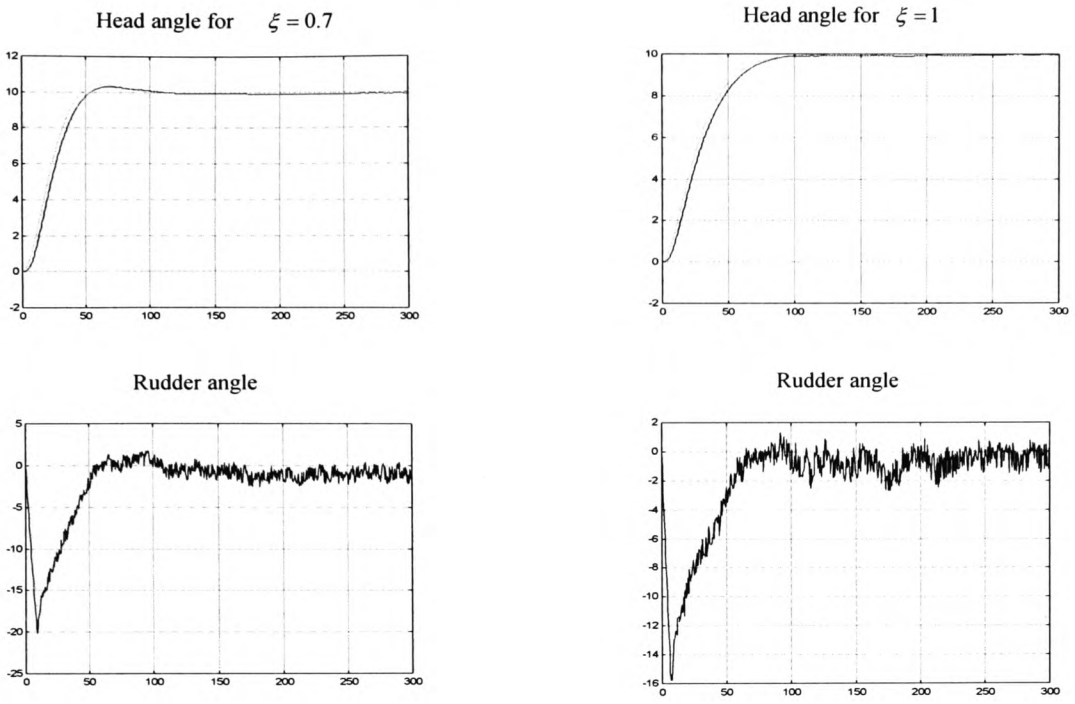

Fig.7: A 10 degree course changing with a significant waves height of h=3 meters and periodo of T=8 sec.

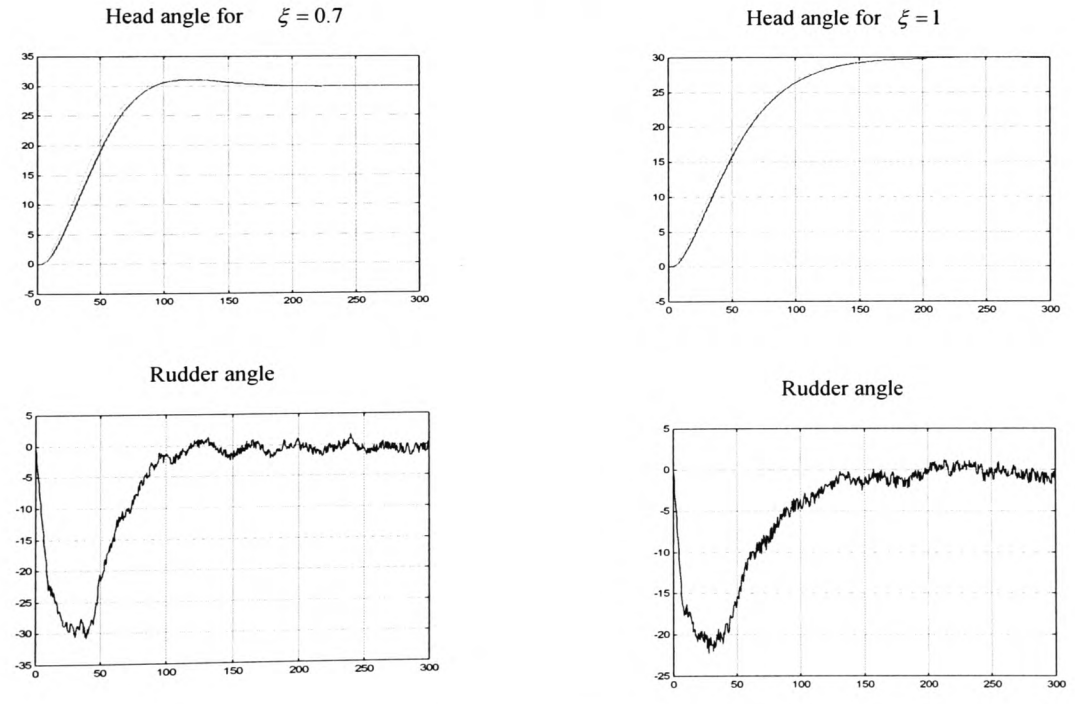

Fig.8: A 30 degree course changing with a significant waves height of h=3 meters and period of T=8 sec.

REFERENCES

1. Amerongen J. van and Udink Ten Cate A.J. Model reference adaptive autopilots for ships. Automatica. 1975; Vol.11:441-449.
2. Amerongen Van J. Adaptive steering of ships- A model reference approach. Automatica. 1984; 20(1):3-14.
3. Astrom K.J. and Wittenmark B. Adaptive Control . second edition, Addison-Wesley; 1995.
4. Blanke M. and Jessen A.G. Dynamic properties of container vessel with low metacentric height. Transactions of The Institute of Measurement and Control. 1997; 19(2):78-93.
5. Brink A.W., Baas G. E. Tiano A. and Volta E. Adaptive automatic course-keeping control of a supertanker and a container ship: a simulation study. Proc. 5th Ship Control Systems Symposium; Annapolis. 1978.
6. Broome D.R., Keane A. J. and Marshall L. The effect of variations in ship operations on an adaptive autopilot. Proc. Ship Steering and Automatic Control; Genova. 1980.
7. Hagan, M. T. Demuth H. B. and M. H. Beale. Neural Network Design. Boston: PWS Publishing; 1996.
8. Hang C.C. and Parks P.C. Comparative studies of Model Reference Adaptive Control Systems. IEEE Transc. on Automatic Control. 1973 Oct; AC-18(5):419-28.
9. Honderd G. and Winkelman J.E. An Adaptive Autopilot for Ships. Proc. 3rd ship Control Systems SymposiumBath; 1972.
10. Hornick K., Stinchcombe M. and White H. Multilayer Feedforward Networks are Universal Approximators. Neural Network. 1989; 2.
11. Kallstrom C.G., Astrom K. J. Thorell N. E. Eriksson J. and Sten L. Adaptive autopiltos for tankers. Automatica. 1979; Vol. 15:254-284.
12. Katebi M.R., Johnson M. A. Grimble M. J. The design of Rudder Roll Stabilisation Control System using LQ control approach. International Symposium on Marine Manoeuvring Craft; Southampton (U.K.). 1993.
13. Lewis E.W. Principles of Naval Architecture. Society of Naval Architecture and Marine Engineers, New York. 1988.
14. Minorsky N. Directional Stability of Automatically Steered Bodies. Journal of American Society of Naval Engineers. 1922; 34:280 309.
15. Narendra K.S. Adaptive Control of Dynamical Systems Using Neural Networks. Handbook of Intelligent Control. New York: Van Nostrand Reinhold; 1992; pp. 141-183.
16. Norbin N.H. On the added resistance due to steering on a straight course. Proc. 13th International Towing Tank ; Berlin. 1972.
17. Price W.G. and Bishop R. Probabilistic Theory of Ship Dynamic. London: Chapman and Hall; 1974.
18. Rumelhart D., James L. Mcclelland and the PDP Research Group. Parallel Distributed Processing. Eighth edition 1988 ed. USA: The Massachusetts Institute of Technology; 1986.
19. Saerens M. and Soquest A. Neural controller based on back-propagation algorithm. IEE Proc. Vol. 138 pp.55-62; 1991 Feb.
20. Sperry E. Automatic steering. Trans. Society of Naval Architects and Marine Engineers. 1922; 53-61.
21. Tiano A., Blanke M. Multivariable identification of ship steering and roll motions. Trans. Inst. Measurement and Control. 1997; 19(2):63-77.
22. Tiano A., Mort N. Derradji D. A. Cuneo M. Ranzi A. and Zhou W. W. Rudder Roll Stabilisation by Neural Network-Based Control Systems. Proc. 3rd int. conference Manoeuvring and Control of Marine Craft; 1994: 33-44.
23. Zi-Xing Cai. Intelligent Control: Principles, Techniques and Applications. Singapore: World Scientific Publishing Co. Pte. Ltd.; 1997. ISBN: 981-02-2564-4.

A Neuro-Fuzzy Model Reference Autopilot for Ships

A.G.M. Zirilli[1], G.N. Roberts[1], A. Tiano[2] and R Sutton[3]

[1]Mechatronics Research Centre, University of Wales College, Newport Allt-yr-yn Campus, P.O.Box 180, Newport, NP20 5XR, UK

[2]Department of Information and Systems, University of Pavia, Pavia, Italy Via Ferrata 1, I-27100 Pavia, Italy. Also: Institute of Ship Automation C.N.R Via de Marini 6, I-16149 Genoa, Italy.

[3]Department of Mechanical and Marine Engineering, University of Plymouth, Drake's Circus, Plymouth, PL4 8AA, UK.

Biographies

Antonio Zirilli was born in Milazzo Sicily, Italy on March 21st, 1970. He achieved a high technical school degree in Electronics on July 1988, at I.T.I.S: "G.Marconi" of Messina and a graduation as Electronics Engineer in 1996, from the University of Pavia Italy presenting a thesis on "Multivariable Control of Ship Motion in Rough Sea". In January 1998 he was awarded a scholarship as a Ph.D. student at the Mechatronics Research Centre, University of Wales College of Newport, U.K., developing a research project on "Intelligent Ship Motion Control".

Professor Geoff Roberts is Director of the Mechatronics Research Centre at the University of Wales College Newport, UK. Professor Roberts holds an honours degree in electrical engineering, a MSc in marine engineering and a PhD in control engineering, he is a Chartered Engineer, a Fellow of the Institute of Marine Engineers, the Institution of Electrical Engineers and the Institute of Measurement and Control. He is Chairman of the IEE Control Division, Chairman of the IFAC Technical Committee on Marine Applications and is a member of the Editorial Advisory Panel of the Computing and Control Engineering Journal.

Professor Antonio Tiano was born in Genova, Italy, on December 11, 1943. He received the degree of Doctor in Applied Mathematics from Genova University in 1969. Since 1991 he is Associate Professor of Automatica at the University of Pavia, faculty of engineering, Italy. His current interests include, modelling identification and control of dynamic systems, with a particular reference to marine vehicles. More recently his two particular fields of interests are, chaos in dynamic systems and application of AI methods to control.

Dr Robert Sutton, holds a degrees of BEng (Tech) in Engineering Production, and MEng and PhD in Control Engineering from the University of Wales. He is currently Reader in Control Systems Engineering at the University of Plymouth in the Department of Mechanical and Marine Engineering. He is also a member of the Advisory Board and Publications Committee of the Underwater Technology Journal. In addition, he is a member of the IMechE's Machine Systems, Computing and Control Executive Committee and Vice-Chairman of its Control Technical Activities Sub-Committee.

Abstract

This paper describes the development of an autopilot for a ship which is based upon the well-known model-reference approach, the optimum performance of which is achieved through a combination of an artificial neural network and fuzzy logic. The system's behaviour is defined by the model reference through a setting of specific parameters, while the neural controller is properly trained in order to comply with the desired performances. For sailing in restricted water, where the manoeuvring precision is the most important target, the model reference is tuned to give a zero desired-overshoot in the ship's heading angle response, in order to avoid the risk of a dangerous path. Whilst during navigation in open water, a more relaxed performance can be selected, in order to minimise fuel consumption and drag force due to the rudder motion. Moreover, the dynamic behaviour of the reference model should be matched to the dynamics of the ship regardless of the magnitude of the demanded change of yaw angle. A reference model, which is too sluggish, cannot produce an optimal

performance since the ship cannot reach the required heading in the minimum time: On the other hand a reference model which is too fast compared with the ship response characteristics should not be used because this may cause rudder actuator saturation and a consequent performance degradation.

The data for training the neural network are generated from simulations based on a non-linear ship equations. In order to provide more realistic conditions a stochastic model of the environment is considered both during the training period and during the simulation tests. The effects of the shallow water on the ship's dynamics are also considered by changing some of the hydrodynamic derivatives of the mathematical model.

1 Introduction

Historically the first generation of ship control systems were introduced by Sperry[1] and Minorsky[2] in 1922. The aim of these autopilots was to maintain the course of the ship using a simple proportional action on the heading error angle. The implementation and use of such a simple autopilot demonstrated that thanks to a better course keeping there was also a reduction in propulsion losses and therefore a saving in fuel costs. A further improvement of the control law was the inclusion of a derivative term for the heading error and a further integrating term leading to the better known PID autopilot. Due to the relatively simplicity in the implementation of PID autopilot, this kind of controller dominated the scenario until the early 1970s.

Owing to the increasing cost of fuel, controlling the ship motion became a problem of major interest. The new challenge was to develop and put into operation new ship's control systems, which could perform the desired task in a safe and economical way. For this purpose the coupling between the different motions could not be neglected. The most popular approach was the Linear Quadratic (LQ) Controller, in which the controller parameters are selected in order to satisfy certain optimal criteria expressed as a quadratic cost function. Different cost functions taking into account yaw and rudder deviation, fuel consumption, etc., were proposed Norbin[3], Katebi[4] et al, and Broome[5]et al. Although the LQ technique fits very nicely in the formulation of the ship's course-keeping control problem and appeared to be robust for parameter changes, other researchers were investigating the applicability of adaptive control techniques such as model reference Honderd & Winkelman[6], Amerongen & Udink Ten Cate[7] or self-tuning adaptive controller Kallstrom[8]et al, Brink[9]et al, which are much appropriate for the formulation of the ship's course changing problem. Adaptive control is also needed to maintain optimal performances, even when the process characteristics change due to the changing in forward speed, load condition, water deapth etc. Astrom[10].

The ship's autopilot presented herein is based on the well-known theory of model reference adaptive systems. In general, the design based on stability theory methods requires that either the process and reference model be linear. The solution adopted in this paper is based on the assumption that an Auto-Regressive-Moving-Average model can describe the ship's dynamics. The structure of the neural controller is thus obtained indirectly from the estimation of the ARMA model parameters. As will be discussed further, this indirect approach has different advantages with respect the direct adaptive approach, especially when the back-propagation algorithm is used for the controller's parameter adaptation.

2 Mathematical model

The mathematical model of a container ship used in this study is described in detail in Blanke & Jessen[11] and Tiano and Blanke[12]. It is herein considered a stochastic extension of such models capable to describe the ship's response in irregular sea waves, which is expressed by the following non-linear equations:

$$
\begin{aligned}
m\left(\dot{u}-vr-x_g r^2+z_g pr\right) &= X+X_w \\
m\left(\dot{v}+ur-z_g\,\dot{p}+x_g\,\dot{r}\right) &= Y+Y_w \\
I_{zz}\,\dot{r}+mx_g\left(\dot{ur}+\dot{v}\right) &= N+N_w \\
I_{xx}\,\dot{p}-mz_g\left(\dot{ur}+\dot{v}\right) &= K+K_w-\rho gDR_z(\varphi)
\end{aligned}
\qquad (1)
$$

The above equations with reference to the co-ordinate system shown in figure 1, describe the coupled surge, sway, yaw and roll motions, where D is the displacement, g the gravity constant, ρ the water mass density, $R_Z(\varphi)$ is the action of the rightening arm that depends on the roll angle φ, while $(x_G,0,z_G)$ are the co-ordinates of the mass centre. The mass is denoted by m whereas Ixx and Izz are the inertial moments about x and z, respectively. The linear velocity of surge and sway are u and v and the angular ones of yaw and roll are respectively r and p. The rightening arm function can be expressed as:

$$
R_z(\varphi)=\sin\varphi\left(GM+\frac{BM}{2}\tan^2\varphi\right) \qquad (2)
$$

where GM is the ship metacentric height and BM is the distance from the centre of buoyancy to the metacentre.

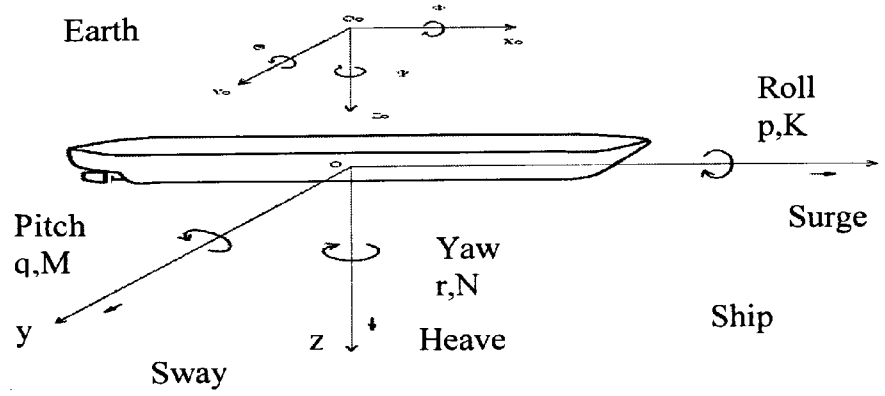

Figure:1 Ship's system frame

Terms X, Y denote the deterministic forces acting along x and y while N and K are the deterministic moments around z and x, which take into account the hydrodynamic effects from the hull movements and forces exerted on the ship by the rudder and by the propulsion system. Such forces and moments are usually described by regarding X, Y, N and K as polynomial expansion in terms of state variables, control actions and hydrodynamic coefficients Lewis[13].

The effects of external disturbances, i.e. wind and waves, consist of related forces X_w, Y_w and moments N_w, K_w acting as perturbation terms in the corresponding right hand parts of equation (1). Such terms, owing to their intrinsically random nature, are generally quite difficult to be characterised through explicit mathematical relations: for example, as to the waves, they should be calculated by integrating the wave pressure over the immersed surface of the hull, on the assumption that the pressure within the waves is unaffected by the presence of the ship. As it has been shown in Lewis[13] and Price & Bishop[14], a reasonable simplifying assumption consists in applying a linear superposition principle, which makes

it possible to separate the ship motion due to the environment from the motion induced by the rudder and by the propeller thrust. According to this modelling approach, waves and wind are regarded as finite order linear realisations of stochastic processes characterised by known spectral densities.

By limiting attention to sea waves, which are by far the dominant disturbance, it is possible to regard a long crested irregular sea height $\zeta(t)$, at time t, as described by a one-dimensional amplitude spectrum, the main parameters of which are the significant wave height, h and the average wave period T. This spectrum, accepted by the International Ship Structure Congress (ISSC) is given by:

$$G_{\varsigma}(\omega)=\frac{173h^2}{\omega^5T^4}\exp\left(\frac{-691}{T^4\omega^4}\right) \tag{3}$$

The relation between the response of each individual component of the wave induced ship state vector $x_w = [u_w\ v_w\ r_w\ p_w]^T$, can be obtained in terms of the spectrum:

$$G_{x_w^i}(\omega,\chi,U)=\left|R_{x_w^i}(\omega,\chi,U)\right|^2 G_{\varsigma}(\omega) \qquad \textbf{i=1,..4} \tag{4}$$

where χ is the angle of encounter between ship and waves, U is the ship velocity and $R_{x_w^{(i)}}$ is the receptance operator, which is assumed to be known from experimental tests, describing the response of the ship i^{th} motion to the waves, Blanke & Jessen[11]. In order to obtain the corresponding spectrum relative to the ship centre of mass, it is finally necessary to express the spectrum given by equation (4) as a function of the frequency of encounter between ship and waves $\omega_e=\omega\left(1-\frac{\omega U}{g}\cos(\chi)\right)$. Once the waves induced ship state vector x_w is computed the total ship state vector is represented by:

$$x_{tot}=x_W+x$$

According to this approach, it is possible to implement an accurate and numerically reliable simulation of sea wave induced ship motions.
In order to take into account the effect of shallow water in the ship's dynamics, based on the work of Sheng[15] and Clarke[16], the correction of the following six hydrodynamic parameters with respect the deep of water are as follow:

$$\frac{Y_{\dot v}'}{Y_{\dot v_\infty}'}=K_0+\frac{2}{3}K_1\frac{B}{T}+\frac{8}{15}K_2\left(\frac{B}{T}\right)^2 \qquad \frac{N_{\dot r}'}{N_{\dot r_\infty}'}=K_0+\frac{2}{5}K_1\frac{B}{T}+\frac{24}{105}K_2\left(\frac{B}{T}\right)^2$$

$$\frac{Y_{v}'}{Y_{v_\infty}'}=K_0+K_1\frac{B}{T}+K_2\left(\frac{B}{T}\right)^2 \qquad \frac{N_{v}'}{N_{v_\infty}'}=K_0+\frac{2}{3}K_1\frac{B}{T}+\frac{8}{15}K_2\left(\frac{B}{T}\right)^2 \tag{5}$$

$$\frac{Y_{r}'}{Y_{r_\infty}'}=K_0+\frac{2}{3}K_1\frac{B}{T}+\frac{8}{15}K_2\left(\frac{B}{T}\right)^2 \qquad \frac{N_{r}'}{N_{r_\infty}'}=K_0+\frac{1}{2}K_1\frac{B}{T}+\frac{1}{3}K_2\left(\frac{B}{T}\right)^2$$

where

$$K_0=1+\frac{0.0775}{F^2}-\frac{0.0110}{F^3};\quad K_1=-\frac{0.0643}{F}+\frac{0.0724}{F^2}-\frac{0.0113}{F^3};\quad K_2=\frac{0.0342}{F};$$

and

$$F = \left(\frac{H}{T} - 1 \right)$$

In the above formulae the subscript ∞ refers to the deep water value of the derivative. The parameters H, B and T are specified in figure 2. The correction suggested by Sheng and reported in equation (5) do not completely describe the effect of the shallow water, they are in fact limited to few hydrodynamic derivatives. However, since there is not a more complete model available in the literature, equation (5) is used in this simulation study.

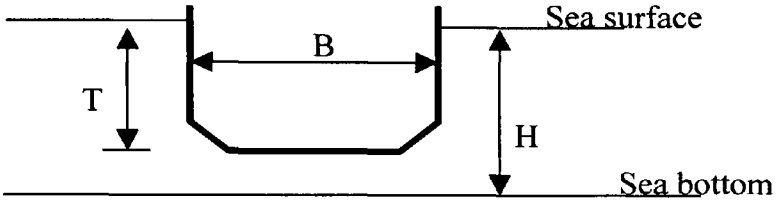

Figure 2: The ship in shallow water

3 Adaptive Controller

Adaptive control deals with the problem of controlling the output of a plant in the presence of parametric or structural uncertainty. In conventional adaptive control theory, to make the problem analytically tractable, the plant is assumed to be linear with unknown parameters. A suitable controller structure is chosen, and the parameters of the controller are adjusted using an adaptive law, so that the output of the plant follows the output of a reference model asymptotically. Assuring that a set of fixed parameters in the controller can achieve the desired response makes the problem well-posed and represent the algebraic part of the problem, while the generation of stable adaptive laws constitutes the analytic part. A general block diagram representing such adaptive system is sketched in figure 3. Here the controller can be thought of as consisting of two loops. The inner loop is an ordinary feedback loop composed of the process and the controller. The outer loop adjusts the controller parameters in such a way that the error, which is the difference between process output and model output is small.

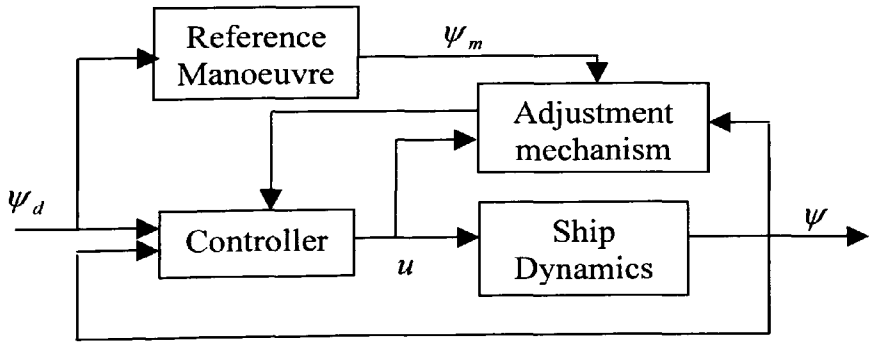

Figure 3: Model reference adaptive system

Two distinct approaches, named direct and indirect adaptive approach, have been proposed for the design of adaptive controllers. In the indirect approach, the parameters of the plant to be controlled are estimated and the parameters of the controller are adjusted based on these estimates. In the direct

approach, the control parameters are directly adjusted based on the observed output error. Narendra & Annaswamy[17]

3.1 Statement of the problem

As mentioned above, a stable reference model with input-output pair $\{\psi_d(k), \psi_m(k)\}$ can be chosen so that $\psi_m(k)$ represents the desired output behaviours for the unknown plant represented by the input-output pair $\{u(k), \psi(k)\}$. The object is to determine a bounded control input $u(.)$ so that the error $e(k) = \|\psi_m(k) - \psi(k)\|$, is bounded and tends to zero asymptotically. To makes the problem analytically tractable some assumptions on the non-linear plant dynamics must be done. In particular, it is assumed that, in the domain of interest the plant is identifiable with a finite input-output sequence and it is of known relative degree.

A possible representation of the ship's dynamics, is the non-linear Auto-Regressive-Moving-Average model:

$$\psi(k+1) = f[\psi(k),..,\psi(k-n+1)] + g[u(k),..,u(k-m+1)] \tag{6}$$

This representation is particularly interesting for control purposes, because if the function f and g are known, the control action can be computed as:

$$[u(k),..,u(k-m+1)] = g^{-1}\{\psi_m(k+1) - f[\psi(k),..,\psi(k-n+1)]\} \tag{7}$$

where ψ_m is the output of the reference model.

3.2 Reference model

As suggested by van Amerongen[18] a course-changing manoeuvre can be easily described by the step response of a second-order system. From this response, as shown figure 4, it is possible to identify three different phases: 1) a start of the turn, 2) a steady turning, and 3) an end of the turn. The turn should have a start, which clearly indicates to other ships the intention of the manoeuvre. The stationary part is determined both by limiting the rudder angle and by controlling the rate of turn. The end of the turn, for safety reason, should be completed without overshoot of the heading angle. In terms of Laplace transfer function such a model reference can be represented by equation (8):

$$\frac{\psi_m(s)}{\psi_d(s)} = \frac{K_{pm}/\tau_{pm}}{s^2 + s/\tau_m + K_{pm}/\tau_m} \tag{8}$$

where s is the Laplace operator. The time constant τ_m is chosen approximately 2 to 3 times smaller than the dominating time constant of the ship at cruise speed and must be such that the process is able to follow the model. If the rate-of-turn limiter is neglected, K_{pm} follows from the desired damping ratio (ξ) of the system:

$$K_{pm} = 1/(4\xi^2\tau_m) \tag{9}$$

Possible values of ξ are between ξ=1 which corresponds to a zero overshoot condition, to ξ=0.7 which corresponds to an overshoot of approximately 5% of the desired value. The selection of τ_m results from the following consideration: a reasonable course controller will have a rate-feedback gain

which makes the time constant of the ship 2 to 3 times smaller with respect to the case of the open-loop system (without controller). By choosing a similar time constant for the model reference this guarantees that the process can follow the model. However, with such a linear model reference, hard non-linearities such as saturation in the steering machine, can produce divergence from the perfect model following leading to instability of the closed-loop system. Instead of introducing non-linearity in the model reference, van Amerongen, suggests modifying the commanded input to the reference model such that the reference model remains linear. In van Amerongen[18], such a command generator has the same structure of the model reference equation (8), with the gain factor K_{pm} replaced by the term:

$$\frac{K_{pm} f}{s\tau_\delta + 1} \tag{10}$$

where f and τ_δ are computed on-line and are defined as

$$f = \frac{\delta_{\max}}{|\delta_r|} \qquad \text{and} \qquad \tau_\delta = \frac{|\delta_r - \delta|}{\dot{\delta}_{\max}}$$

where $\delta_{\max}$ is the maximum available rudder angle, $\dot{\delta}_{\max}$ is the maximum rudder speed and δ_r is the requested rudder angle from the controller.

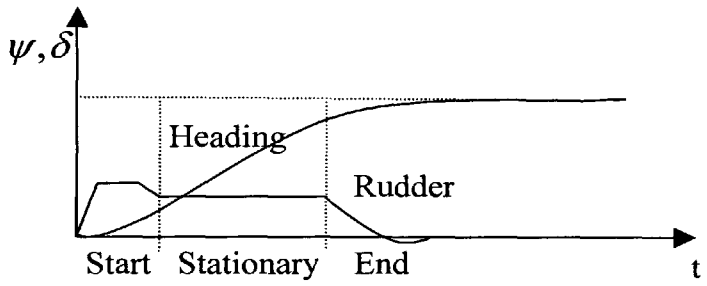

Figure 4: Course changing manoeuvre

The equation of the command generator will then be:

$$\dddot{\psi}_m + \left(\frac{1}{\tau_\delta} + \frac{1}{\tau_m}\right)\ddot{\psi}_m + \frac{1}{\tau_\delta \tau_m}\dot{\psi}_m + \frac{K_{pm} f}{\tau_\delta \tau_m}\psi_m = \frac{K_{pm} f}{\tau_\delta \tau_m}\psi_d \tag{11}$$

Although the structure of the model reference proposed by van Amerongen is retained, the design of the command generator, herein, is carried out through the use of a fuzzy system. The input of the fuzzy command generator are the requested final value of the ship's heading angle, the rudder speed and the maximum allowed rudder angle. The output is the interim set point for the second-order model reference. Figure 5 shows the block diagram of the overall system.

4 Neural-Control Design

If the functions f and g are known and g^{-1} exist, the output of the plant represented by equation (6), with the control law (7), follows the output of the reference model asymptotically. Moreover, because the reference model is linear means that the feedback system is also linear with the same transfer

function as the reference model. When the functions f, g and g^{-1} are unknown, two possible choices corresponding to the direct and indirect adaptive approach are possible.

In the direct adaptive approach, the desired control action $[u(k),..,u(k\text{-}m+1)]$, is realised as a non-linear function of $\psi_m(k+1)$ and $[\psi(k),...,\psi(k-n+1)]$ using a neural network in the feedback path. The most popular way to adjust the network's parameters is by the use of the back-propagation algorithm. This algorithm, adjust the parameters of the network in order to minimise the mean square error defined as:

$$F(x) = E[e^2] = E[(t-a)^2] \tag{12}$$

where x is the vector of network parameters, t is the desired output (or target) defined by the reference model and a is the actual output of the plant. However, since the error is measured at the output of the plant, to obtain the desired partial derivatives the equations describing the plant must be known. Different solutions to this problem have been proposed. In Saerens & Soquest[19] for instance, it is proposed to use of the sign of the partial derivative describing the ship's dynamics (the input-output relationship). However, as mentioned in Tiano[20]et al, especially for ships of large inertia and sailing subject to environmental excitation, the determination of the proper sign of the partial derivative is not always a trivial task. The wrong sign in the derivative could lead to ambiguity in training the neural network. Hence, unless further assumptions concerning the input-output characteristics of the plant are made, direct adaptive control under these circumstances is not possible.

The second way to determine the control action when the function f, g and g^{-1} are not known is based on the indirect adaptive approach. The unknown functions are estimated using neural networks and used in turn to determine the control action that will lead the plant to the desired behaviours.

In the following sections the indirect adaptive control design for the containership presented in the section 2 is outlined. Some simulation results are also presented showing the applicability of such an approach.

4.1 Indirect adaptive controller

Under the hypothesis on the ship's dynamics stated in equation (6), the object is to describe a systematic procedure for the identification of the functions f and g which in turn will be used for the indirect adaptive controller design. The architecture for the estimation of those functions is presented in figure 6. The networks NN_f and NN_g represent the estimation of the function f and g respectively. Since the input of the network $NN_f(\cdot)$ is fed with the ship's output $\psi(\cdot)$, instead of the estimated output $\hat{\psi}(\cdot)$, this estimation architecture is refereed as series-parallel identification.

When training a neural network to approximate a continuous functions over a compact set, both theoretical and practical considerations arises. There will be a trade-off between the size of the network chosen, which directly influences learning time, and the accuracy that can be achieved. From a practical point of view it is of considerable interest to know how large an error can be tolerated and how it will affect the control of the system. If the initial state can be chosen at the discretion of the designer, the task to identify the proper parameters, is simplified. By choosing initial values with uniform distribution in the state space domain, the function representing the dynamics of the ship can be approximated to any degree of accuracy off-line, Hornick[21]et al.

In many practical problems however, this is not the case and information about the function to be approximated, can be obtained only by the choice of suitable inputs $u(k)$ and the observation of the corresponding outputs. This implies that the state space is not completely explored, thus making the identification tasks much more difficult, if not impossible. Moreover, in this particular case, the

identification of the two functions f and g is also attempted through the same input-output pairs, where the output represent the sum of the output of the two functions. Therefore the above consideration on the choice of the input-output pairs is very important.

Using the mathematical model presented in section 2, a set of uniformly distributed initial states are chosen. Based on data collected from these simulations, the function NN_f and NN_g were identified off-line through the use of the back-propagation algorithm Rumelhart[22]et al. After different simulation tests, the best compromise between size and precision led to the following choices: i) the network representing the function g and f, are constituted by a three layers network with a non-linear hidden layer of forty neurons and a linear output layer, ii) the regression in the input and in the output is chosen to be n=m=1. The function g^{-1} is then computed from a random input-output collection of data, uniformly distributed in the interval [0 1] in such a way that $NN_g\left(NN_{g^{-1}}\right)=1$ (note that this is the inverse of the estimated NN_g, rather than the estimation of g^{-1}). Finally the function NN_f and $NN_{g^{-1}}$ are used to implement the controller as indicated in figure 7.

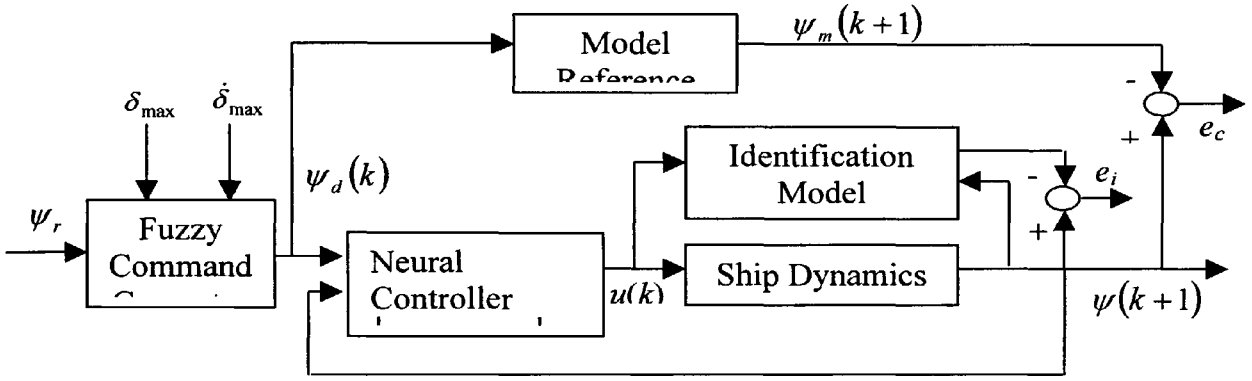

Figure 5: The Neuro-fuzzy model reference autopilot

The off-line identification of the networks NN_g and NN_g, has the purpose to find a suitable initialisation set of the network's parameters from which the on-line adaptation can be more easily accomplished. The on-line adaptation is demanded in order to comply with the parametric uncertainty due to a change in the sailing conditions (i.e. depth of water, load conditions etc.). However the use of more efficient identification algorithm could make this step unnecessary and an on-line identification can be directly realised.

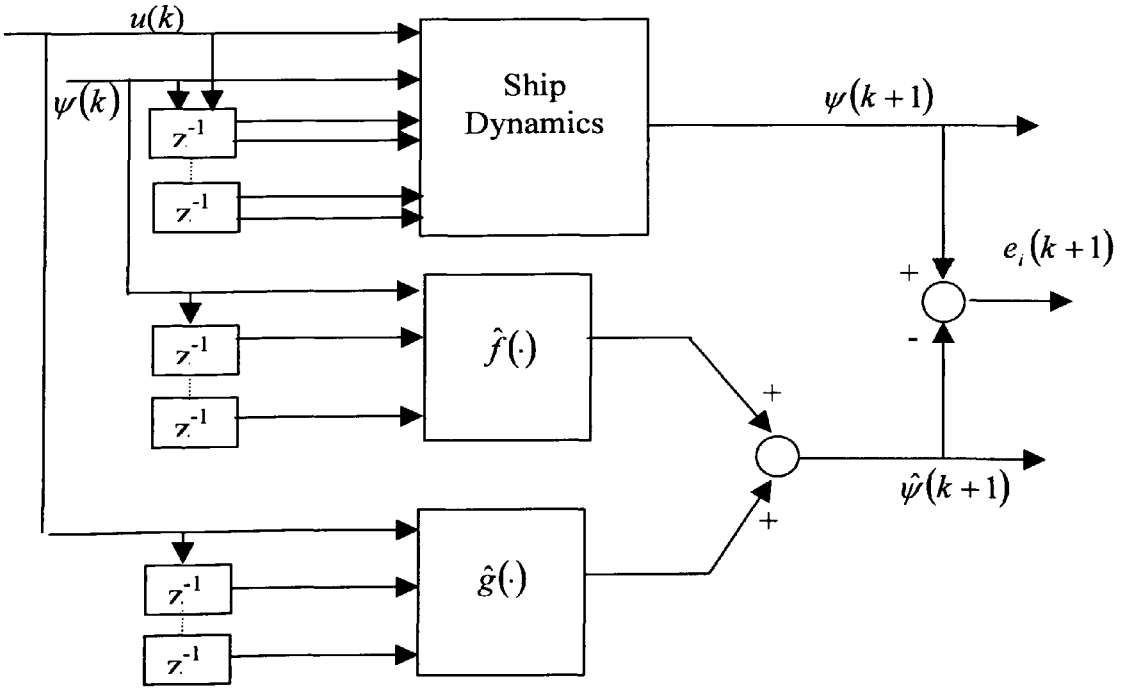

With this approach, the difficulty with using the back-propagation algorithm to compute the partial derivative with respect the unknown ship's dynamics is overcome.

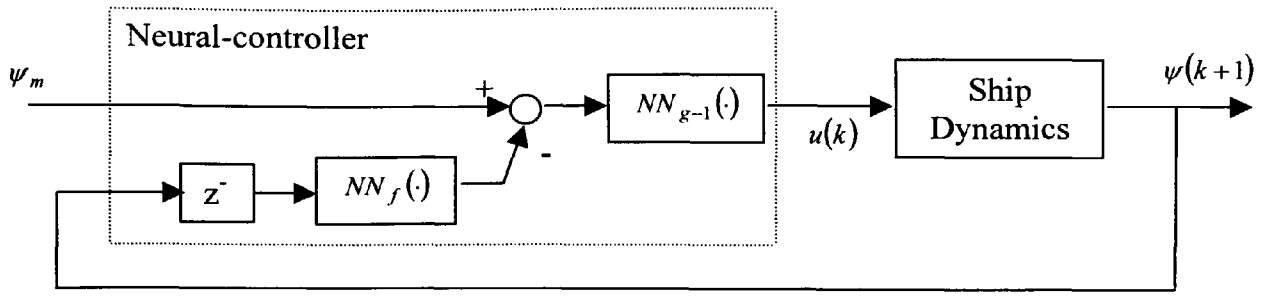

Figure 7: The neural controller structure

5 Simulation Results

The neuro-fuzzy model reference controller presented above was evaluated by a simulation study involving the containership model described in Tiano and Blanke[12]. The control algorithm can be summarised as:

Choice of the interim reference heading angle from the fuzzy command generator,
Apply the neural controller output to the ship mathematical model presented in equation (1),
If time is equal to KT_i then upgrade the neural ship model (function NN_f and NN_g) from the measured input-output,
If time is equal to KT_c then adapt the neural controller (function NN_f and $NN_{g^{-1}}$),
Back to step 1)

Steps three and four were settled at different sample time T_i and T_c respectively. In particular, for stable and efficient on-line control, the identification must be sufficiently accurate before control action can be initiated. Therefore the sample time T_i and T_c should be chosen with care. After different simulation experiments a reasonable choice seams to be T_i =5sec and T_c=10sec.

Figure 8, shows the changing in the hydrodynamic derivative presented in equation (5) (figures b, c and d), for a constant change in the deep of water (figure a). With respect to figure (2) the coefficients are:

B=32; % Breadth [m]
T=10.7; % mean draft [m]

The shallow water effect begin to take effect at water depth from 3 to 4 times T. Note that when $H=T$ the ship is running aground, F will be zero and the coefficients K_i will diverge to infinity. Therefore, in the simulations was set a minimum value for the water depth as, $H_{final} = T + \varepsilon$ with $\varepsilon > 0$.

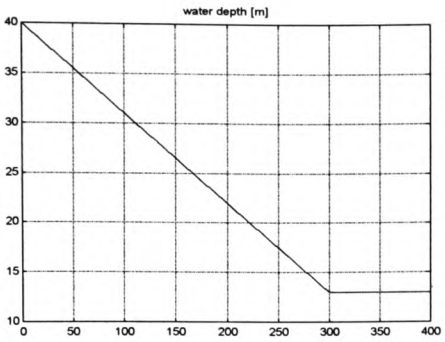

(a): water depth

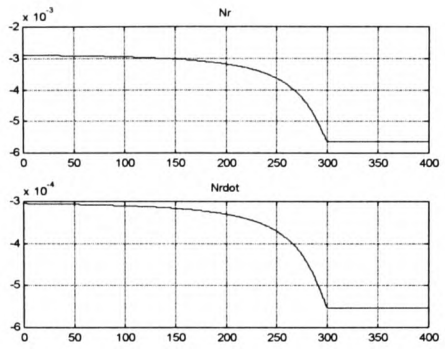

(b): $N_r, N_{\dot{r}}$

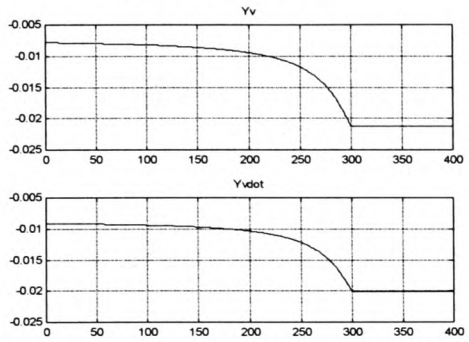

(c): $Y_v, Y_{\dot{v}}$

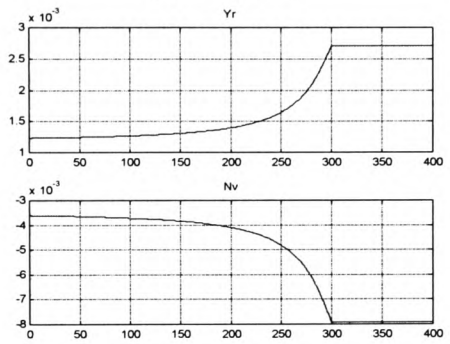

(d): Y_r, N_v

Figure 8: Shallow water effect on the hydrodynamic parameters

The equation describing the change in the deep of water *H*, as represented in figure 8.a) is:

```
if time<T_stranding
  H=C+m*time;
else
  H=T+epsilon;
end
```

where *T_stranding*=300 sec, $C=4*T$ and $m = [(T+\varepsilon)-C] / T_{stranding}$

Figure 9 shows a 10° course-changing manoeuvre with shallow water effect as defined in figure 8, and wave condition defined by a significant waves height h=3 m, an average period T=8 sec and a starting angle of attack of 30°.

Solid-yaw angle : dotted yaw

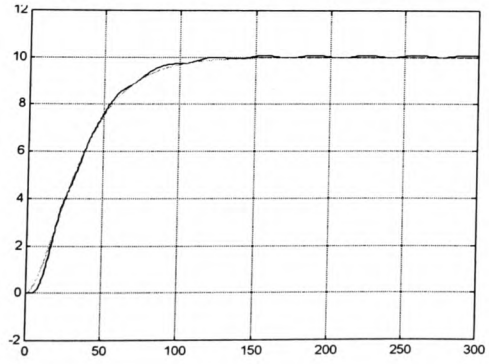

Solid-rudder angle : dotted-rudder

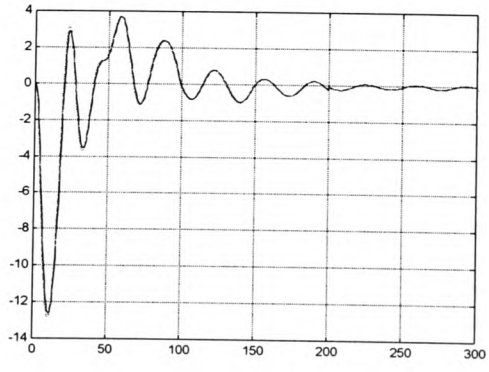

Figure 9: A 10° course-changing manoeuvre in shallow water and with waves

As can be appreciate from the rudder responses in figure 9, as a consequence of the command generator, the steering machine (solid line) can follow the demanded control signal (dotted line) without saturation. Finally, figure 10, shows a 30° course-changing manoeuvre with the same conditions for the shallow water effect and the waves disturbances, but with a starting angle of attack of 60°, leading to a final condition of a beam sea.

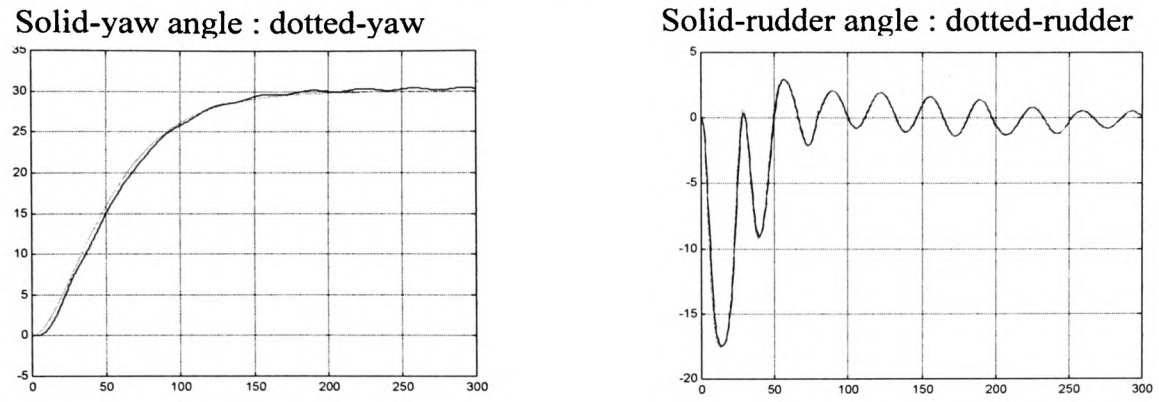

Figure 10: A 30° course-changing manoeuvre in shallow water and with waves

Also in this critical condition the neuro-fuzzy model reference autopilot is able to maintain properly the heading angle.

6 Concluding Remarks

Using the assumption that the ship's dynamics can be represented by an Auto-Regressive-Moving-Average model, the design of an indirect neural autopilot has been presented. The choice of the indirect approach for the design of the adaptive neural controller, especially when the back-propagation algorithm is used for the upgrading of the network's parameters, has also been demonstrated. In order to comply with the non-linearity introduced by the steering machine, a command generator has been introduced in the controller design. To test the performances of the controller, the mathematical equation representing the ship's dynamics have been extended in order to include the shallow water effects and the external disturbances due to the waves. With such an extension the parameters of the model become time varying. From the simulation results it is clear that the neuro-fuzzy controller is able to comply with such a parameter's change.

However, due to the off-line training, it can be argued that the proposed controller does not have the property of being truly adaptive. The off-line training, was proposed in order to overcome the problems related to the use of the back-propagation algorithm. The quality of such off-line training significantly influenced the controller performances, legitimating once more the above objection. It is in the authors' opinion that this problem is inherent to the back-propagation algorithm, therefore the investigation of new algorithms such those directly inspired from genetic behaviours could give a better solution to the problem.

References

2. Sperry E. 1922. Automatic steering. Trans. Society of Naval Architects and Marine Engineers, pp. 53-61.
3. Minorsky N. 1922. Directional Sability of Automatically Steered Bodies. *Journal of American Society of Naval Engineers,* **34**, pp. 280 309.
4. Norbin N.H. 1972. *On the added resistance due to steering on a straight course.* Proc. 13th International Towing Tank . Berlin.
5. Katebi M.R., Johnson M. A. Grimble M. J. 1993. *The design of Rudder Roll Stabilisation Control System using LQ control approach.* International Symposium on Marine Manouvering Craft. Southampton (U.K.).
6. Broome D.R., Keane A. J. and Marshall L. 1980. *The effect of varietions in ship operations on an adaptive autopilot.* Proc. Ship Steering and Automatic Control. Genova.
7. Honderd G. and Winkelman J.E. 1972. *An Adaptive Autopilot for Ships.* Proc. 3rd ship Control Systems Symposium.
8. Amerongen J. van and Udink Ten Cate A.J. 1975. Model reference adaptive autopilots for ships. *Automatica,* **Vol.11**, pp. 441-449.
9. Kallstrom C.G., Astrom K. J. Thorell N. E. Eriksson J. and Sten L. 1979. Adaptive autopiltos for tankers. *Automatica,* **Vol. 15**, pp. 254-284.
10. Brink A.W., Baas G. E. Tiano A. and Volta E. 1978. *Adaptive automatic course-keeping control of a supertanker and a container ship: a simulation study.* Proc. 5th Ship Control Systems Symposium. Annapolis.
11. Astrom K.J. 1980. Why Use Adaptive Techniques for Steering Large Tankers. *Int. J. Control,* **Vol.32, No4**, pp. 689-708.
12. Blanke M. and Jessen A.G. 1997. Dynamic properties of container vessel with low metacentric height. *Transactions of The Institute of Mesurement and Control,* **19** (2), pp. 78-93.
13. Tiano A., Blanke M. 1997. Multivariable identification of ship steering and roll mations. *Trans. Inst. Measurement and Control,* **19** (2), pp. 63-77.
14. Lewis E.W. 1988. Priciples of Naval Architecture. Society of Naval Architecture and Marine Engineers, New York,
15. Price W.G. and Bishop R. 1974. *Probabilistic Theory of Ship Dynamic.* London: Chapman and Hall.
16. Sheng Z.Y. 1981. *Shallow Water Effect on Hydrodynamic Derivatives of Ship Hull .* 2nd Symposium on Manoeuvrability. China.
17. Clarke D. 1983. The Application of Manoeuvring Criteria in Hull Design Using Linear Theory. *Transactions of Royal Institution of Naval Architects,* **125**, pp. 45-68.
18. Narendra K.S. and Annaswamy A.M. 1989. *Stable Adaptive Systems.* Englewood Cliffs, N.J. : Prentice-Hall.
19. Amerongen Van J. 1984. Adaptive steering of ships- A model reference approach. *Automatica,* **20** (1), pp. 3-14.
20. Saerens M. and Soquest A. 1991 Feb. *Neural controller based on back-propagation algorithm.* IEE Proc. Vol. 138 pp.55-62.
21. Tiano A., Mort N. Derradji D. A. Cuneo M. Ranzi A. and Zhou W. W. 1994. *Rudder Roll Stabilisation by Neural Network-Based Control Systems.* Proc. 3rd int. conference Manoeuvering and Control of Marine Craft. pp. 33-44,
22. Hornick K., Stinchcombe M. and White H. 1989. Multilayer Feedforward Networks are Universal Approximators. *Neural Network,* **2** pp.359-366
23. Rumelhart D., James L. Mcclelland and the PDP Research Group 1986. *Parallel Distributed Processing.* Eighth edition 1988 end. USA: The Massachusetts Institute of Technology.

An adaptive autopilot for ships based on neural network controller

Zirilli[1], G.N. Roberts[1], A. Tiano[2] and R Sutton[3]
[1]Mechatronics Research Centre, University of Wales College, Newport
Allt-yr-yn Campus, P.O. ox 180, Newport, NP20 5XR, U.K.

[2]Department of Information and Systems, University of Pavia, Pavia, Italy
Via Ferrata 1, I-27100 Pavia, Italy. Also: Institute of Ship Automation C.N.R
Via de Marini 6, I-16149 Genoa, Italy.

[3]*Department of Mechanical Engineering, University of Plymouth,*
Drake's Circus, Plymouth, PL4 8AA, UK.

SYNOPSIS

Neural Networks for control and system analysis have been intensively investigated during the last ten years, not only in terms of the research being carried out, but perhaps more importantly in terms of the potential range of applications. The main characteristics of neural networks for control applications can be summarised as: they can be used to approximate any continuos mapping, they perform this approximation through learning, parallel processing and fault tolerance are easily accomplished. This paper describes the development of a new Model-Reference-Adaptive autopilot for ships based on neural network controller. The system's behaviour is defined by a model reference through a setting of specific parameters, while the neural controller is properly trained in order to comply with the desired performances. For sailing in restricted water, where the manoeuvre precision is the most important target, the model reference must be tuned to give a zero desired-overshoot in the ship heading angle response, in order to avoid the risk of a dangerous path. A high value for the initial yaw rate can also be selected in order to clearly shown the intention of the manoeuvre to others ships, on the contrary during navigation in open water, a more relaxed performance could be selected, in order to minimise fuel consumption and drag force due to the rudder motion.

1 INTRODUCTION

Historically the first generation of ship control systems were introduced by Sperry and Minorsky in 1922. The aim of these autopilots was to maintain the course of the ship using a simple proportional action on the heading error angle. The implementation and use of such a simple autopilot demonstrated that thanks to a better course keeping there was also a reduction in propulsion losses and therefore a saving in fuel costs. A further improvement of the control law was the inclusion of a derivative term for the heading error and a further integrating term leading to the better known PID autopilot. Due to the relatively simplicity in the implementation of PID autopilot, this kind of controller dominated the scenario until the early 1970s.
Owing to the increasing cost of fuel, controlling the ship motion became a problem of major interest. The new challenge was to develop and put into operation new ship's control systems,

which could perform the desired task in a safe and economical way. For this purpose the coupling between the different motions could not be neglected. The most popular approach was the Linear Quadratic (LQ) Controller, in which the controller parameters are selected in order to satisfy certain optimal criteria expressed as a quadratic cost function. Different cost functions taking into account yaw and rudder deviation, fuel consumption, etc., were proposed Norrbin (3) and Katebi et al (4). Although the LQ technique fits very nicely in the formulation of the ship's course-keeping control problem and appeared to be robust for parameter changes, other researchers were investigating the applicability of adaptive control techniques such as model reference Honderd and Winkelman (5), Amerongen and Udink Ten Cate (6) or self-tuning adaptive controller Kallstrom et al (7), Brink et al (8).

The fast development of small and inexpensive microcomputers and advances in computing technology have fuelled the so-called 'Intelligent Control' theory, in which control algorithms are developed by emulating certain characteristics of intelligent biological systems. The foundation of such systems can be found at the intersection of disciplines like cybernetics, artificial intelligent and informatic Zi-Xing Cai (9). The ship's autopilot proposed in this paper is based on well-known model reference adaptive approach. The solution adopted in order to deal with certain class of non-linearity due to the ship steering machine, is based on the work of van Amerongen (10) then the design of a non-linear adaptive controller based on model reference theory and neural network concepts is presented.

2 MATHEMATICAL MODEL

The mathematical model of a container ship used in this study is described in detail in Tiano and Blanke (11)and Blanke and Jessen (12). It is herein considered a stochastic extension of such models capable to describe the ship response in irregular sea waves, which is expressed by the following non-linear equations:

$$\begin{aligned} m\left(\dot{u} - vr - x_g r^2 + z_g pr\right) &= X + X_w \\ m\left(\dot{v} + ur - z_g \dot{p} + x_g \dot{r}\right) &= Y + Y_w \\ I_{zz}\dot{r} + mx_g\left(\dot{ur} + \dot{v}\right) &= N + N_w \\ I_{xx}\dot{p} - mz_g\left(\dot{ur} + \dot{v}\right) &= K + K_w - \rho g D R_z(\varphi) \end{aligned} \tag{1}$$

The above equations with reference to the co-ordinate system shown in figure 1, describe the coupled surge, sway, yaw and roll motions, where D is the displacement, g the gravity constant, ρ the water mass density, $R_Z(\varphi)$ is the action of the rightening arm that depends on the roll angle φ, while $(x_G,0,z_G)$ are the co-ordinates of the mass centre. The mass is denoted by m whereas Ixx and Izz are the inertial moments about x and z, respectively. The linear velocity of surge and sway are u and v and the angular ones of yaw and roll are respectively r and p. The rightening arm function can be expressed as:

$$R_z(\varphi) = \sin\varphi\left(GM + \frac{BM}{2}\tan^2\varphi\right) \tag{2}$$

where GM is the ship metacentric height and BM is the distance from the centre of buoyancy to the metacentre.

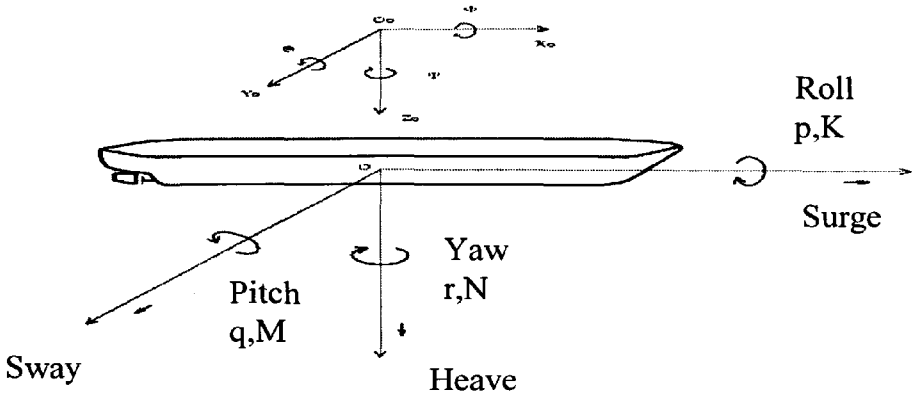

Figure 1: Ship's system frame

Terms X, Y denote the deterministic forces acting along x and y while N and K are the deterministic moments around z and x, which take into account the hydrodynamic effects from the hull movements and forces exerted on the ship by the rudder and by the propulsion system. Such forces and moments are usually described by regarding X, Y, N, K as polynomial expansion in terms of state variables, control actions and hydrodynamic coefficients Lewis (13). The effects of external disturbances, i.e. wind and waves, consist of related forces X_w, Y_w and moments N_w, K_w acting as perturbation terms in the corresponding right hand parts of equation (1). Such terms, owing to their intrinsically random nature, are generally quite difficult to be characterised through explicit mathematical relations: for example, as to the waves, they should be calculated by integrating the wave pressure over the immersed surface of the hull, on the assumption that the pressure within the waves is unaffected by the presence of the ship. As it has been shown in Lewis (13) and Price and Bishop (14), a reasonable simplifying assumption consists in applying a linear superposition principle, which makes it possible to separate the ship motion due to the environment from the motion induced by the rudder and by the propeller thrust. According to this modelling approach, waves and wind are regarded as finite order linear realisations of stochastic processes characterised by known spectral densities.

By limiting attention to sea waves, which are by far the dominant disturbance, it is possible to regard a long crested irregular sea height $\zeta(t)$, at time t, as described by a one-dimensional amplitude spectrum, the main parameters of which are the significant wave height, h and the average wave period T. This spectrum, accepted by the International Ship Structure Congress (ISSC) is given by:

$$G_{\varsigma}(\omega) = \frac{173h^2}{\omega^5 T^4} \exp\left(\frac{-691}{T^4\omega^4}\right) \tag{3}$$

The relation between the response of each individual component of the wave induced ship state vector $x_w = [u_w\ v_w\ r_w\ p_w]^T$, can be obtained in terms of the spectrum:

$$G_{x_w^i}(\omega,\chi,U) = \left|R_{x_w^i}(\omega,\chi,U)\right|^2 G_{\varsigma}(\omega) \qquad \text{i=1,4} \tag{4}$$

where χ is the angle of encounter between ship and waves, U is the ship velocity and R_{x_w} is the receptance operator, which is assumed to be known from experimental tests, describing the response of the ship i^{th} motion to the waves Blanke and Jessen (12). In order to obtain the corresponding spectrum relative to the ship centre of mass, it is finally necessary to express the spectrum given by equation (4) as a function of the frequency of encounter between ship and waves $\omega_e = \omega\left(1 - \frac{\omega U}{g}\cos(\chi)\right)$. Once the waves induced ship state vector x_w is computed the total ship state vector is represented by:

$$x_{tot}=x_w+x$$

According to this approach, it is possible to implement an accurate and numerically reliable simulation of sea wave induced ship motions.

3 ADAPTIVE CONTROLLER

Adaptive control deals with the problem of controlling the output of a plant in the presence of parametric or structural uncertainty. In conventional adaptive control theory, to make the problem analytically tractable, the plant is assumed to be linear with unknown parameters. A suitable controller structure is chosen, and the parameters of the controller are adjusted using an adaptive law, so that the output of the plant follows the output of a reference model asymptotically. Assuring that a set of fixed parameters in the controller can achieve the desired response makes the problem well posed and represent the algebraic part of the problem, while the generation of stable adaptive laws constitutes the analytic part. A general block diagram representing such adaptive system is sketched in figure 2. Here the controller can be thought of as consisting of two loops. The inner loop is an ordinary feedback loop composed of the process and the controller. The outer loop adjusts the controller parameters in such a way that the error, which is the difference between process output and model output is small.

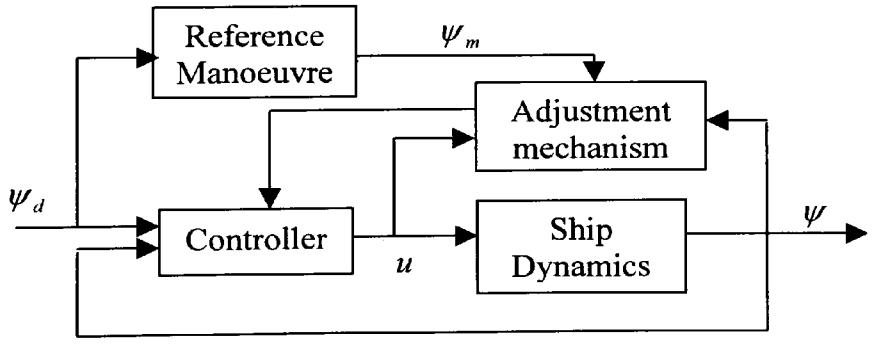

Figure 2: Model reference adaptive controller

Two distinct approaches, named *direct* and *indirect* adaptive approach, have been proposed for the design of adaptive controllers. In the indirect approach, the parameters of the plant to be controlled are estimated and the parameters of the controller are adjusted based on these estimates. In the direct approach, the control parameters are directly adjusted based on the observed output error. Narendra and Annaswamy (15)

3.1 Reference model

As suggested by van Amerongen (10) a course-changing manoeuvre can be easily described by the step response of a second-order system. From this response, as shown figure 3, it is possible to identify three different phases: 1) a start of the turn, 2) a steady turning, and 3) an end of the turn. The turn should have a start, which clearly indicates to other ships the intention of the manoeuvre. The stationary part is determined both by limiting the rudder angle and by controlling the rate of turn. The end of the turn, for safety reason, should be completed without overshoot of the heading angle. In terms of Laplace transfer function such a model reference can be represented by equation (5):

$$\frac{\psi_m(s)}{\psi_d(s)} = \frac{K_{pm}/\tau_{pm}}{s^2 + s/\tau_m + K_{pm}/\tau_m} \tag{5}$$

where s is the Laplace operator. The time constant τ_m is chosen approximately 2 to 3 times smaller than the dominating time constant of the ship at cruise speed and must be such that the process is able to follow the model. If the rate-of-turn limiter is neglected, K_{pm} follows from the desired damping ratio (ξ) of the system:

$$K_{pm} = 1/(4\xi^2\tau_m) \tag{6}$$

Possible values of ξ are between ξ=1 which corresponds to a zero overshoot condition, to ξ=0.7 which corresponds to an overshoot of approximately 5% of the desired value. The selection of τ_m results from the following consideration: a reasonable course controller will have a rate-feedback gain which makes the time constant of the ship 2 to 3 times smaller with respect to the case of the open-loop system (without controller). By choosing a similar time constant for the model reference this guarantees that the process can follow the model.

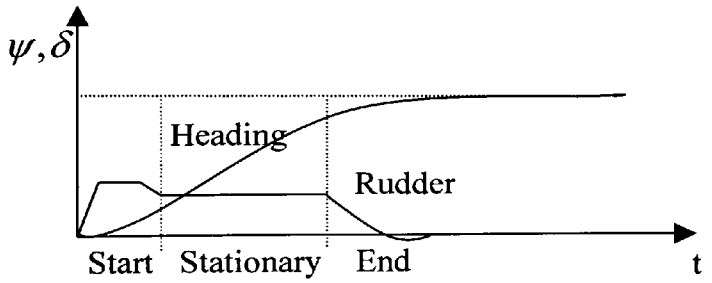

Figure 3: Course-changing manoeuvre.

However, with such a linear model reference, hard non-linearities such as saturation in the steering machine, can produce divergence from the perfect model following leading to instability of the closed-loop system. Instead of introducing non-linearity in the model reference, van Amerongen, suggests modifying the commanded input to the reference model such that the reference model remains linear. In (10), such a command generator has the same structure of the model reference equation (5), with the gain factor K_{pm} replaced by the term:

$$\frac{K_{pm} f}{s\tau_\delta + 1} \tag{7}$$

where f and τ_δ are computed on-line and are defined as

$$f = \frac{\delta_{\max}}{|\delta_r|} \qquad \text{and} \qquad \tau_\delta = \frac{|\delta_r - \delta|}{\dot{\delta}_{\max}}$$

where $\delta_{\max}$ is the maximum available rudder angle, $\dot{\delta}_{\max}$ is the maximum rudder speed and δ_r is the requested rudder angle from the controller. The equation of the command generator will then be expressed by equation (8):

$$\dddot{\psi}_m + \left(\frac{1}{\tau_\delta} + \frac{1}{\tau_m}\right)\ddot{\psi}_m + \frac{1}{\tau_\delta \tau_m}\dot{\psi}_m + \frac{K_{pm} f}{\tau_\delta \tau_m}\psi_m = \frac{K_{pm} f}{\tau_\delta \tau_m}\psi_d \tag{8}$$

4 NEURAL NETWORK FOR CONTROL

The ability of neural networks to approximate arbitrary well non-linear functions plays a fundamental role in the use of such networks as components or subsystems in identifiers and controller. Mainly inspired by biological systems, different types of neural networks have been proposed. Multilayer Perceptron Networks (MPN), Radial Basis Function Networks (RBFN), Cerebellar Model Articulation Controller (CMAC) are few examples that share the above mentioned ability to be universal approximator. However a fundamental difference between the different types of neural networks is represented by the way the output of the network is related to its parameters. For instance, when MPN are used as universal approximator at least one non-linear hidden layer is required, this in turns imply that the output of the network is related in a non-linear fashion to the network's parameters. On the contrary, in the RBFN with fixed parameters in the input layer, the parameters are related in a linear fashion to the output of the network. This fundamental difference will imply whether or not well-known stability results of adaptive control theory can be applied and which kind of learning algorithm for the adjustment of the network's parameters has to be used.

As stated previously, for the adaptive control problem two main architectures can be classified named *direct* and *indirect control*. In the first architecture, the plant to be controlled can be viewed as an additional and not modifiable layer of the network while in the *indirect* controller architecture the two steps of dynamic identification and plant control are involved. It is worth noting that when the *direct* control architecture is used, a neural model of the plant, that constitutes the not modifiable layer of the network, should be available. Therefore as well in the adaptive case, where the ship's dynamics are unknown as well in the case when the ship's dynamic is unstable, *direct* adaptive control is not possible.

With respect the neural network learning strategies, two main categories can be distinguished named *general* and *specialised learning*. In the former, the input space of the plant to be controlled is populated with training samples so that the network can interpolate for intermediate points. For such methods to be numerically efficient it is important that the input space is sampled with an appropriate interval. In the *specialised* learning, the controller learns

by directly evaluating the control accuracy, which can be defined as the difference between the actual and the desired output of the plant. The learning procedure in both cases is aimed to updating (adjusting) the network's parameters.

In the following sections an *indirect* adaptive neural controller is presented. In order to make the problem analytically tractable some assumptions on the non-linear ship's dynamics are formulated. Based on these assumptions follow the choice of the identifier and controller structures that are implemented by RBFN.

4.1 Statement of the problem

As mentioned above, a stable reference model with input-output pair $\{\psi_d(k), \psi_m(k)\}$ can be chosen so that $\psi_m(k)$ represents the desired output behaviours for the unknown plant represented by the input-output pair $\{u(k), \psi(k)\}$. The object is to determine a bounded control input $u(.)$ so that the error $e(k) = \|\psi_m(k) - \psi(k)\|$, is bounded and tends to zero asymptotically. To makes the problem analytically tractable some assumptions on the non-linear plant dynamics must be done. In particular, it is assumed that, in the domain of interest the plant is identifiable with a finite input/output sequence and can be described by the non-linear difference equation:

$$\psi(k+1) = \sum_{i=1}^{N} \alpha_i f_i[\psi(k), \psi(k-1), .., \psi(k-n+1)] + \sum_{j=0}^{m-1} \beta_j u(k-j+1) \tag{9}$$

This representation is particularly interesting for control purposes, because if the functions $f_i(\cdot)$ and the parameters α_i and β_j are known the control action can be computed as:

$$u(k) = \frac{1}{\beta_0}\left[\psi_m(k+1) - \sum_{1=1}^{N} \alpha_i f_i[\psi(k), .., \psi(k-n+1)] - \sum_{j=1}^{m-1} \beta_j u(k-j)\right] \tag{10}$$

where $\psi_m(k+1)$ is the output of the reference model and the parameter β_0 is supposed to be not equal to zero. When the functions $f_i(\cdot)$ and the parameters α_i and β_j are unknown as in the case of adaptive systems, based on the above considerations it is possible to attempt a first estimation of those parameters by means of neural networks and then based on the certainty equivalence principle apply the control law:

$$u(k) = \frac{1}{\hat{\beta}_0}\left[\psi_m(k+1) - \sum_{1=1}^{N} \hat{\alpha}_i \hat{f}_i[\psi(k), .., \psi(k-n+1)] - \sum_{j=1}^{m-1} \hat{\beta}_j u(k-j)\right] \tag{11}$$

where the hat denote the estimation of the parameters.

4.2 Indirect controller design

Under the hypothesis on the ship's dynamics stated in equation (9), the object is to describe a systematic procedure for the identification of the functions $f_i(\cdot)$ and the parameters α_i and β_j which in turn will be used for the indirect adaptive controller design (equation 11). The architecture for the estimation of those functions and parameters is presented in figure 4. The networks NN_f, that will approximate the first part of the equation (9), has selected as a RBFN while for the estimation of the parameters β_j a linear neural network is used. Since the input of the network $NN_f(\cdot)$ is fed with the ship's output $\psi(\cdot)$, instead of the estimated output $\hat{\psi}(\cdot)$, this estimation architecture is refereed as series-parallel identification.

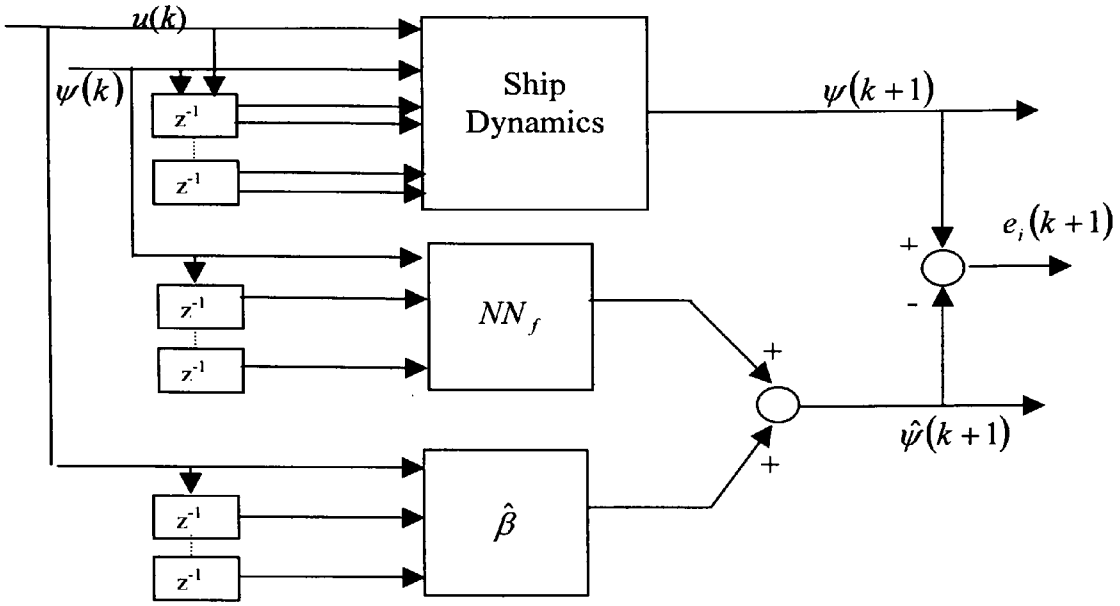

Figure 4: Architecture for the estimation of the controller's parameters

The radial basis functions used for the purpose to approximate the functions f_i are represented by the equation:

$$f_i = e^{-\frac{\|x_i - x\|}{\sigma_i}} \tag{12}$$

where $\|x_i - x\|$ represent the Euclidean distance between the input vector x and the centre x_i of the lattice input space while σ_i is the deviation of the basis function. The input of the RBFN is the two-dimensional vector $[\psi(k), \psi(k-1)]$. For this particular application it is assumed that the region of interest is represented by the interval [-50,50] degrees. The interval [-50,50] in each dimension has been sampled uniformly with sampling step of 5. Therefore the total number of lattice centres is $N = 21^2 = 441$. The deviation is assumed the same for each basis functions and equal to 5 so that a sufficient overlapping of the basis function is assured. As stated above a liner network can be used for the estimation of the parameters β_j with as input the two-dimensional vector $[u(k), u(k-1)]$. Choosing the bias of the linear neuron equal to zero the output of the network can be expressed as $\beta_1 u(k) + \beta_2 u(k-1)$. The weights of the network (β_1, β_2) are then the parameters of the model to be estimated leading to total number of parameters to be estimated of 443. Finally, once the parameters are estimated by the above procedure, they are used to implement the control law defined by equation (11).

5 SIMULATION RESULTS

The indirect neural controller presented above with the model reference presented in section 3.1 was evaluated by simulation involving the non-linear model of the containership presented in section 2. Different sailing condition by means at different wave conditions with varying angles of attack and a rouge of sea states were simulated. In all those conditions the neural controller performed acceptably well showing the viability of the proposed control scheme. Figure 5 shown a 30° course-changing manoeuvre with sea state characterised by an

average period of T=10 sec, a significant wave height of h=5 m and an initial angle of attack of 60°, leading to a final condition of beam sea. It can be appreciated from the figure, also in this critical condition the controller is able to maintain properly the heading angle.

On the left hand side of figure 5 it is shown in dotted line the desired heading angle (the output of the reference model) and in solid line the ship's heading angle. From this figure it is

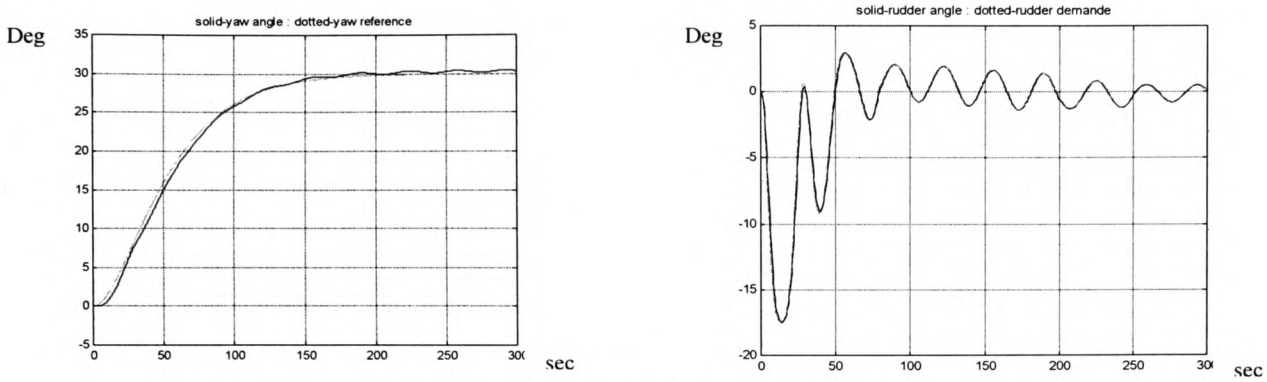

Figure 5: 30 degree course-changing manoeuvre

possible to appreciate the good tracking performance of the controller. The right hand side of figure 5 shown the demanded rudder angle in dotted line and the actual rudder angle in solid line. It is clear from this figure that as a consequence of the command generator the saturation of the steering machine are never reached.

It is important to note however that the two steps involved in the indirect adaptive control technique of identification and control, have to be properly set. In particular it is important that before a control action is attempted good identification of the parameters is achieved. This requirement can be fulfilled by either setting two different sample times for the identification and control or requiring that the identification error is lower then a minimum bound before attempting the controller design. The former approach, although more heuristic seems more viable for practical application.

6 CONCLUDING REMARKS

Under the assumption that the non-linear ship's dynamics can be described by the model presented in equation 9, the design of an indirect adaptive autopilot based on neural networks is presented. The motivation for selecting the indirect control approach has also given. However the design procedure outlined is affected by the *a-priori* knowledge required on the ship's dynamics. Namely the nature of the non-linear functions f, which has been approximated by a radial basis networks. This *a-priori* knowledge is used in order to choose the centre and the deviation for each basis functions that result in an acceptable approximation. It is clear therefore that the proper choice of these parameters are application dependent. In this particular case, a total number of 443 parameters has to be estimated. However for some application it is possible that the choice on the number of the centres lead to a numerically intractable number of parameters to be estimated. The use of different architecture like MPN can lead to few parameters to be estimated however as discussed earlier the stability analysis of the system became much more involved.

Reference List

1. Sperry E. 1922. Automatic steering. *Trans. Society of Naval Architects and Marine Engineers,* pp. 53-61.

2. Minorsky N. 1922. Directional Stability of Automatically Steered Bodies. *Journal of American Society of Naval Engineers,* 34, pp. 280 309.

3. Norrbin N.H. 1972. *On the added resistance due to steering on a straight course.* Proc. 13th International Towing Tank . Berlin.

4. Katebi M.R., Johnson M. A. Grimble M. J. 1993. *The design of Rudder Roll Stabilisation Control System using LQ control approach.* International Symposium on Marine Manoeuvring Craft. Southampton (U.K.).

5. Honderd G. and Winkelman J.E. 1972. *An Adaptive Autopilot for Ships.* Proc. 3rd ship Control Systems Symposium.

6. Amerongen J. van and Udink Ten Cate A.J. 1975. Model reference adaptive autopilots for ships. *Automatica,* Vol.11, pp. 441-449.

7. Kallstrom C.G., Astrom K. J. Thorell N. E. Eriksson J. and Sten L. 1979. Adaptive autopilots for tankers. *Automatica,* Vol. 15, pp. 254-284.

8. Brink A.W., Baas G. E. Tiano A. and Volta E. 1978. *Adaptive automatic course-keeping control of a supertanker and a container ship: a simulation study.* Proc. 5th Ship Control Systems Symposium. Annapolis.

9. Zi-Xing Cai 1997. *Intelligent Control: Principles, Techniques and Applications.* Singapore: World Scientific Publishing Co. Pte. Ltd. 981-02-2564-4.

10. Amerongen Van J. 1984. Adaptive steering of ships- A model reference approach. *Automatica,* 20 (1), pp. 3-14.

11. Tiano A., Blanke M. 1997. Multivariable identification of ship steering and roll motions. *Trans. Inst. Measurement and Control,* 19 (2), pp. 63-77.

12. Blanke M. and Jessen A.G. 1997. Dynamic properties of container vessel with low metacentric height. *Transactions of The Institute of Measurement and Control,* 19 (2), pp. 78-93.

13. Lewis E.W. 1988. Principles of Naval Architecture. *Society of Naval Architecture and Marine Engineers, New York,*

14. Price W.G. and Bishop R. 1974. *Probabilistic Theory of Ship Dynamic.* London: Chapman and Hall.

15. Narendra K.S. and Annaswamy A.M. 1989. *Stable Adaptive Systems.* Englewood Cliffs, N.J. : Prentice-Hall.

AN ADAPTIVE FUZZY AUTOPILOT FOR A CONTAINERSHIP

A. Zirilli[1], G.N. Roberts[1], A. Tiano[2] and R. Sutton[3]

[1]*Mechatronics Research Centre, University of Wales College, Newport Allt-yr-yn Campus, P.O. Box 180, Newport, NP20 5XR, UK*
[2]*Department of Information and Systems, University of Pavia, Pavia, Italy Via Ferrata 1, I-27100 Pavia, Italy. Also: Institute of Ship Automation C.N.R Via de Marini 6, I-16149 Genoa, Italy.*
[3]Department of Mechanical and Marine Engineering, University of Plymouth, Drake Circus, Plymouth, PL4 8AA, UK.

Abstract: During the last few years, fuzzy controllers have emerged as a viable alternative to others conventional control design techniques. The primary advantage of fuzzy systems, is the ability to manipulate uncertainties and expert knowledge. In this paper, the problem of designing an indirect adaptive fuzzy autopilot for a containership is addressed. The proposed adaptation mechanism is based on the interpretation of a performance function by a fuzzy system, which in turn will infer the change (adaptation) in the fuzzy controller parameters. The main advantages of using a fuzzy system to perform the adaptation with respect the use of a classical adaptation algorithms (i.e. back-propagation, least-square, MIT rule etc.), is related to the amount and form of a-priori information needed about the system to be controlled. The speed with which the adaptation is achieved makes this approach viable for on-line implementation. Simulations on a non-linear model of a containership are presented for both course-changing and course-keeping manoeuvres in the presence of environmental disturbances.

Keywords: Fuzzy system, adaptive controller, indirect adaptation.

1. INTRODUCTION

Historically the first generation of ship control systems were introduced by (Sperry 1922) and (Minorsky 1922) in 1922. The aim of these autopilots was to maintain the course of the ship using a simple proportional action on the heading error angle. The implementation and use of such a simple autopilot demonstrated that thanks to a better course keeping there was also a reduction in propulsion losses and therefore a saving in fuel costs. A further improvement of the control law was the inclusion of a derivative term for the heading error and a further integrating term leading to the better known PID autopilot. Due to the relatively simplicity in the implementation of PID autopilot, this kind of controller dominated the scenario until the early 1970s.

Owing to the increasing cost of fuel, controlling the ship motion became a problem of major interest. The new challenge was to develop and put into operation new ship's control systems, which could perform the desired task in a safe and economical way. For this purpose the coupling between the different motions could not be neglected. The most popular approach was the Linear Quadratic (LQ) Controller, in which the controller parameters are selected in order to satisfy certain optimal criteria expressed as a quadratic cost function. Different cost functions taking into account yaw and rudder deviation, fuel consumption, etc., were proposed (Broome 1980), and (Honderd and Winkelman 1972). Although the LQ technique fits very nicely in the formulation of the ship's course-keeping control problem and appeared to be robust for parameter changes, other researchers were investigating the applicability of adaptive control techniques such as model reference (Brink et al 1978), (Amerongen and Udink Ten Cate 1975) or self-tuning adaptive controller (Kallstrom 1979), which are much appropriate for the formulation of the ship's course-changing problem. Adaptive control is also needed to maintain optimal performances, even when the process characteristics change due to the changing in forward speed, load condition, water depth etc. (Astrom 1980).

The fast development of small and inexpensive microcomputers and advances in computing technology have fuelled the so-called "Intelligent Control" theory, in which control algorithms are developed by emulating certain characteristics of intelligent biological systems. The foundation of such systems can be found at the intersection of disciplines

like cybernetics, artificial intelligent and informatic (Zi-Xing 1997). The ship's autopilot proposed in this paper is based on well-known model reference adaptive approach and fuzzy systems theory. Two fuzzy systems, named *fuzzy controller* and *fuzzy adjustment mechanism*, perform respectively the controller and the adaptation law for the proposed adaptive controller.

2. THE NON-LINEAR MODEL OF A CONTAINERSHIP

The mathematical model of a container ship used in this study is described in detail in (Tiano and Blanke 1997) and (Blanke and Jessen 1997). It is herein considered a stochastic extension of such models capable to describe the ship response in irregular sea waves, which is expressed by the following non-linear equations:

$$\begin{aligned} m\left(\dot{u}-vr-x_g r^2+z_g pr\right) &= X+X_w \\ m\left(\dot{v}+ur-z_g\dot{p}+x_g\dot{r}\right) &= Y+Y_w \\ I_{zz}\dot{r}+mx_g\left(ur+\dot{v}\right) &= N+N_w \\ I_{xx}\dot{p}-mz_g\left(ur+\dot{v}\right) &= K+K_w-\rho gDR_z(\varphi) \end{aligned} \qquad (1)$$

The above equations with reference to the co-ordinate system shown in figure 1, describe the coupled surge, sway, yaw and roll motions, where D is the displacement, g the gravity constant, ρ the water mass density, $R_Z(\varphi)$ is the action of the rightening arm that depends on the roll angle φ, while $(x_G,0,z_G)$ are the co-ordinates of the mass centre. The mass is denoted by m whereas Ixx and Izz are the inertial moments about x and z, respectively. The linear velocity of surge and sway are u and v and the angular ones of yaw and roll are respectively r and p. The rightening arm function can be expressed as:

$$R_z(\varphi)=\sin\varphi\left(GM+\frac{BM}{2}\tan^2\varphi\right) \qquad (2)$$

where GM is the ship metacentric height and BM is the distance from the centre of buoyancy to the metacentre. Terms X, Y denote the deterministic forces acting along x e y while N and K are the deterministic moments around z and x, which takes into account the hydrodynamic effects from the hull movements and forces exerted on the ship by the rudder and by the propulsion system. Such forces and moments are usually described by regarding X,Y,N,K as polynomial expansion in terms of state variables, control actions and hydrodynamic coefficients (Lewis 1988).

The effects of external disturbances, i.e. wind and waves, consist of related forces X_w, Y_w and moments N_w, K_w acting as perturbation terms in the corresponding right hand parts of equation (1). Such terms, owing to their intrinsically random nature, are generally quite difficult to be characterised through explicit mathematical relations. For example, as to the waves, they should be calculated by integrating the wave pressure over the immersed surface of the hull, on the assumption that the pressure within the waves is unaffected by the presence of the ship. As it has been shown in (Price and Bishop 1974) and (Lewis 1988), a reasonable simplifying assumption consists in applying a linear superposition principle, which makes it possible to separate the ship motion due to the environment from the motion induced by the rudder and by the propeller thrust. According to this modelling approach, waves and wind are regarded as finite order linear realisations of stochastic processes characterised by known spectral densities.

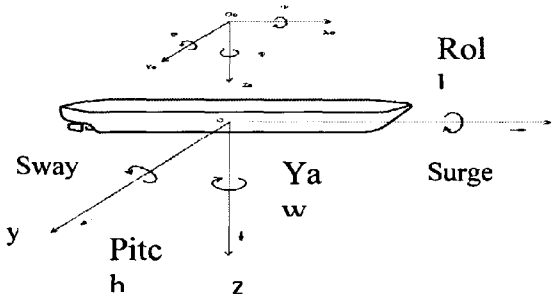

Figure:1 Ship's system frame

By limiting attention to sea waves, which are by far the dominant disturbance, it is possible to regard a long crested irregular sea height $\zeta(t)$, at time t, as described by a one-dimensional amplitude spectrum, the main parameters of which are the significant wave height, h and the average wave period T. This spectrum, accepted by the International Ship Structure Congress (ISSC) is given by:

$$G_\zeta(\omega)=\frac{173h^2}{\omega^5T^4}\exp\left(\frac{-691}{T^4\omega^4}\right) \qquad (3)$$

The relation between the response of each individual component of the wave induced ship state vector $\mathbf{x_w}=[u_w\ v_w\ r_w\ p_w]^T$, can be obtained in terms of the spectrum:

$$G_{x_w^i}(\omega,\chi,U)=\left|R_{x_w^i}(\omega,\chi,U)\right|^2 G_\zeta(\omega)\ \text{i=1,..,4} \qquad (4)$$

where χ is the angle of encounter between ship and waves, U is the ship velocity and $R_{x_w(i)}$ is the receptance operator, which is assumed to be known from experimental tests, describing the response of the ship i^{th} motion to the waves (Blanke and Jessen 1997). In order to obtain the corresponding spectrum relative to the ship centre of mass, it is finally necessary to

express the spectrum given by equation (4) as a function of the frequency of encounter between ship and waves $\omega_e = \omega\left(1 - \frac{\omega U}{g}\cos(\chi)\right)$. Once the waves induced ship state vector x_w is computed the total ship state vector is represented by:

$$x_{tot}=x_w+x$$

According to this approach, it is possible to implement an accurate and numerically reliable simulation of sea wave induced ship motions.

3. STEERING CRITERIA

In order to design an optimal controller, performances indexes have to be defined. In this respect, for a particular sailing condition different factors may be considered: 1) economy (fuel consumption), 2) safety (related to accuracy and manoeuvrability), 3) user predilections. In the design of steering control systems, it is common practice to distinguish between two main different modes of sailing. These modes are: *course-keeping* and *course-changing*.

Course-keeping: In the course-keeping mode of operating, the control system has to maintain a fixed direction of sailing, compensating for the different external environmental disturbances (i.e. wind, waves and current). The controller has to select the best trade-off between precision (which will minimise the elongation of the sailed distance) and control effort (rudder movement, which will produce additional drag force and consequent loss of speed). As a consequence of the problem definition it is clear that this optimisation problem fits very nicely in the formulation of the Linear Quadratic Gaussian control problem. Different papers have shown the applicability of this control technique for steering a large tanker in different sailing condition by a proper choice of the weighting matrices. However, the majority of such papers propose a solution for the LQG problem based on a linearisation of the ship's dynamics around an equilibrium point, achieved considering the first-order truncation of the power series expansion of the ship's equations of motion. The assumption that the rudder angle is "small" (does not exceed approximately 10 degrees) therefore has to be fulfilled.

Course-changing: During course-changing manoeuvres the ship heading angle is changed in such a way that the ship can sail in the new direction specified by a new (desired) heading angle. During this manoeuvre it is possible to distinguish between three main parts as: 1) the start of the manoeuvre, where for safety reasons, the intention of the manoeuvre must be clearly indicated to others ships, 2) a stationary turning, characterised by a constant turning rate, and 3) the end of the manoeuvre, where it is important to control the overshoot of the manoeuvre in order to avoid dangerous paths. The specification of this manoeuvre in the time domain, in each of its parts, can be done in terms of the step response of a second order reference model. Model reference adaptive technique can be used in order to design optimal controller for this particular mode of operation (Amerongen and Naute Lemke 1980). Generally speaking there are two main approaches to the synthesis of a Model Reference Adaptive Controller (MRAC), (Hang and Parks 1973). The first is based on the definition of a Lyapunov function which in turn is used to determine the adaptation law that guarantees the stability of the overall system, while the second is based on the minimisation of a predefined performance index. The most common choice for the performance index is represented by the tracking error defined with respect to figure 2 as, $e_t(kT) = \psi(kT) - \psi_m(kT)$.

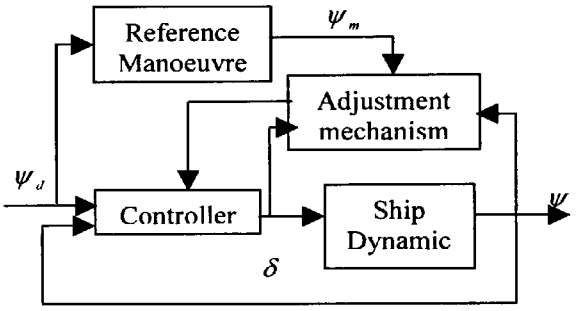

Fig.2: Model reference adaptive system

4. ADAPTIVE CONTROLLER

Adaptive control deals with the problem of controlling the output of a plant in the presence of parametric or structural uncertainty. In conventional adaptive control theory, to make the problem analytically tractable, the plant is assumed to be linear with unknown parameters. A suitable controller structure is chosen, and the parameters of the controller are adjusted using an adaptive law, so that the output of the plant follows the output of a reference model asymptotically. Assuring that a set of fixed parameters in the controller can achieve the desired response makes the problem well-posed and represents the algebraic part of the problem, while the generation of stable adaptive laws constitutes the analytic part. A general block diagram representing such adaptive system is shown in figure 2. Here the controller can be thought of as consisting of two loops. The inner loop is an ordinary feedback loop composed of the process and the controller. The outer loop adjusts the controller parameters in such a way that the error, which is the difference between process output and model output is small.

Two distinct approaches, named direct and indirect adaptive approach, have been proposed for the design of adaptive controllers. In the indirect approach, the parameters of the plant to be controlled are estimated and the parameters of the controller are adjusted based on these estimates. In the direct approach, the control parameters are directly adjusted based on the observed output error. (Narendra and Annaswamy 1989).

The two categories of adaptive controller defined above have their equivalent within the framework of adaptive fuzzy control (Wang 1993). In particular, if an adaptive fuzzy controller uses fuzzy logic systems as controller, it is called direct adaptive fuzzy controller. On the other hand if an adaptive fuzzy controller uses fuzzy logic systems as model of the plant, it is called indirect adaptive fuzzy controller.

In the remaining of this section the design of an indirect fuzzy controller based on optimisation criteria is presented. The performance index to be minimised is represented by the tracking error defined as $e_t(kT)=\psi(kT)-\psi_m(kT)$. The optimisation is performed through a fuzzy logic system (the fuzzy adaptation mechanism), which will infer about the change in the controller parameters. The design of the fuzzy adjustment mechanism is based on some heuristic knowledge about the ship's dynamics.

4.1 Indirect Fuzzy Controller

Different papers have been published, concerning the design of stable adaptive fuzzy controller (Tang et al 1999), (Spooner and Passino 1996), (Wang 1992). Although the authors in (Tang et al. 1999) claim that their control schema has better stability performance without relaying on the assumption that the tracking error is square integrable, (a necessary condition in Wang in order to prove stability), all the above mentioned design procedures rely on the assumption that a linear parameterisation of the control parameters is possible. Once this particular parameterisation is achieved the adaptive law is motivated by a Lyapunov based stability analysis.

Although a stability analysis of the proposed fuzzy adaptive controller is not addressed in this paper, the assumption that the unknown control parameters appear linearly is retained. In particular the fuzzy logic system used to implement the controller is the same proposed in (Wang 1993), with center-average defuzzification, product inference and singleton fuzzification. It is possible to prove that the above-defined fuzzy logic system is described by the following mathematical equation:

$$y(\bar{x})=\frac{\sum_{i=1}^{m} b_i\left(\prod_{j=1}^{n}\mu_{A_j}(x_j)\right)}{\sum_{i=1}^{m}\left(\prod_{j=1}^{n}\mu_{A_j}(x_j)\right)} \quad (5)$$

Where b_i is the maximum of the output membership function, μ_{A_j} is the fuzzy set associated with the antecedent part of each rule of the base knowledge, n is the number of input and m the number of rules. If the parameters of the input membership functions are known and fixed, equation (5) can be reparameterised as

$$y(\bar{x})=\theta^T\xi(\bar{x}) \quad (6)$$

Where $\xi(\bar{x})=\frac{\left(\prod_{j=1}^{n}\mu_{A_j}(x_j)\right)}{\sum_{i=1}^{m}\left(\prod_{j=1}^{n}\mu_{A_j}(x_j)\right)}$ is the regressor vector and $\theta^T=[b_1,...,b_m]$ is the parameter vector. The main reasons for considering the fuzzy system expressed by equation (6) as a building block for the design of adaptive systems, are i) it has been proved that equation (5) is a universal approximator, ii) the fuzzy logic system expressed by this equation is constructed from a set of IF-THEN rules, therefore linguistic information from human expert can be easily incorporated into the system, iii) the parameterisation (equation 6) allows for the application of well-known results of linear adaptive theory.

The fuzzy controller is designed with inputs as the reference error (*e*) and change in error (*ce*) and output as the rudder angle δ. The universe of discourse of the input variables is chosen, after some experiment to be equal to $[-\pi;\pi]$ [-0.5;0.5] for the error and change of error respectively while [-0.6;0.6] for the output universe of discourse. Seven linguistic variables are chosen to describe the input variables such as "Zero", "Positive-Small", "Positive", "Positive-Big", "Negative-Small", "Negative" and "Negative-Big".

The output fuzzy sets are chosen as singletons while the input fuzzy sets are described by Gaussian membership functions. To guarantee completeness of the base knowledge 49 rules are chosen of the form:

IF *e* is Z and *ce* is Z THEN $\delta=\theta_1$

The 49 parameters θ_m that define the consequent part of each rule, are the unknown controller parameters that have to be tuned by the fuzzy adjustment mechanism (the parameters b_i in equation 5). The tuning of these parameters is performed trough a fuzzy system, named fuzzy adjustment mechanism, described below.

4.2 Fuzzy adjustment mechanism

The fuzzy adjustment mechanism has to produce the change in the controller parameters (the adaptation law), in such a way that the performance measured by the tracking error is optimised. A possible strategy to enhance the performance of the fuzzy controller is based on the following considerations. Suppose that with input $\delta(kT)$ the tracking error at time T ($e_t(kT)=\psi(kT)-\psi_m(kT)$) is positive. If the input at time kT would have been $\delta(kT)+\varepsilon$, where ε represents an extra effort from the controller, it is expected that the error at that time would have been less. Therefore ε represent the correction that the controller has to produce in its output as a consequence of the adaptation. In others words, ε can be thought as a measure of the correction (adaptation) that has to be produced by the fuzzy adaptation mechanism. A rule that can represent this situation is

IF tracking error is Positive Then ε is Positive.

Because of the particular choice made on the fuzzy controller, it possible to understand that in order to increase the output of the fuzzy controller (by an amount ε) it is sufficient to increase the value of b_i in equation (5). By changing b_i with $b_i+\varepsilon$ the output of the fuzzy controller will increase. It is important to note, that at each time (kT) with inputs e(kT) and ce(kT) the output of the fuzzy controller is mainly determined by those rules whit the antecedent part described by membership functions with centre close to the inputs value. It is possible to consider this local behaviour of the system in order to speed up the adaptation process by changing only the parameters θ_i that belong to those rules for which the actual contribution to the output is greater then a certain threshold. Therefore using the fuzzy logic system described by equation (6), with inputs the tracking error and the change in the tracking error, and output the amount of change in the controller parameters and the same seven linguistic variable defined before the 49 rules describing the adaptation strategy are as follows:

IF e_t is Z and ce_t is Z THEN $\varepsilon = \varepsilon_1$

In this way, the optimisation of the performance function is achieved by a non-linear equation defined through a set of rules while in conventional adaptive control it is used to rely on gradient based optimisation algorithms or its modifications. It is worth nothing that it is also possible to expand the base knowledge of the fuzzy adjustment mechanism in such a way to include in the adaptation strategy rules that account for the saturation of the rudder angle and/or weather conditions.

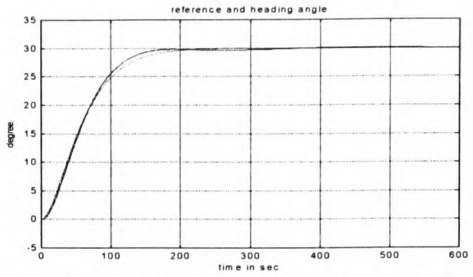

Fig.3: 30° course-changing control

5. SIMULATION RESULTS

The fuzzy adaptive controller presented above was evaluated by simulation study involving the non-linear model of the containership presented in section 2. For this purpose, different sailing conditions characterised by a different sea state and travelling directions were considered. Also different initial conditions for the controller' parameters were considered; i.e. all parameters being set to zero or all parameters randomly initialised. Figure 3 shown a 30° course changing manoeuvre performed with beam sea characterised by a significant wave height h=3 meters and a period T=8 sec. With dotted line is represented the reference manoeuvre while with solid line is the ship' heading angle. Figure 4 shows the rudder angle and the demanded change in the controller parameters from the fuzzy adjustment mechanism. As it can be appreciated from this figure the mean value of the parameter ε converges to zero while the instantaneous value is always different from zero. This is due to the presence of the external disturbance. For this instance, it is possible to consider a dead-zone in the adaptation algorithm. In particular, if the demanded change in the controller parameters (value of ε) is less then a certain

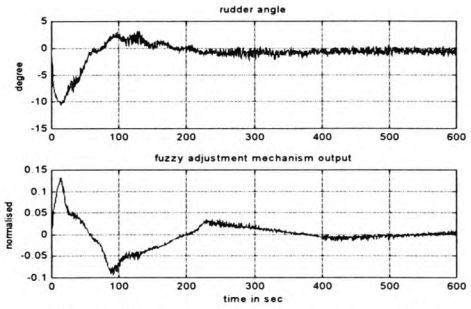

Fig.4: 30° course-changing control

threshold the controller parameters θ_i are not adjusted.

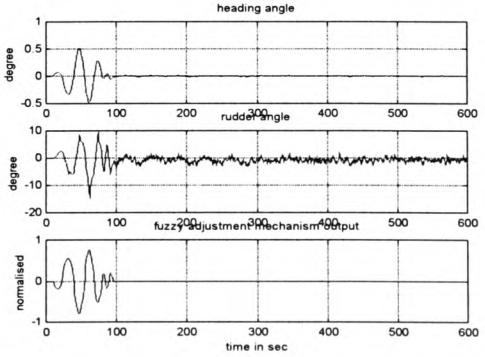

Fig.5: Course-Keeping control

This is seen better in figure 5 where is shown the ship's heading angle the parameter ε and the rudder angle for a course-keeping manoeuvre with the same sea conditions and angle of attack of 135°.
In order to test the ability of the adaptive controller to retain previously learned manoeuvres the same sequence of reference heading angle can be repeated. In figure 6 it is shown a typical sequence of such reference angles. Figure 7 shows the rudder angle and the parameter ε. From this figure it is possible to appreciate that the fuzzy adaptive autopilot need less adjustment of the controller parameters, when the requested manoeuvre has been already performed in the past.

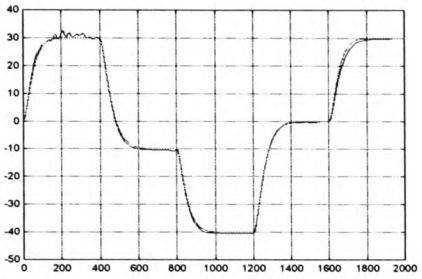

Fig. 6: Course-changing manoeuvre

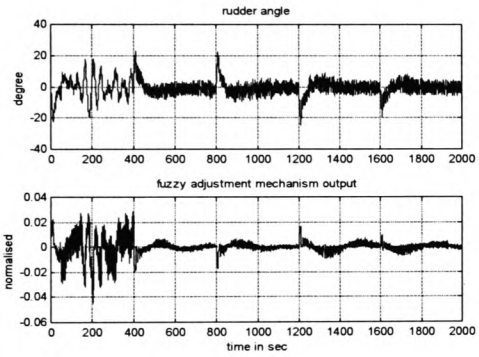

Fig.7: Course-changing manoeuvre

6. CONCLUDING REMARKS

In this paper an indirect fuzzy adaptive autopilot for a containership is presented. The structure of the fuzzy controller with its mathematical representation has been presented and justified. The controller parameters are adjusted trough a fuzzy system, the design of which is based on some heuristic knowledge of the ship's dynamics. Except for this weak requirement the design procedure is very general and does not rely on any mathematical model of the ship. Moreover, it is easy to expand the knowledge base of the fuzzy adjustment mechanism in such a way that the optimisation process will be constrained. It is believed that rules accounting for the saturation on the control signal or for the noise in the measured tracking error can increase the overall performances of the control system. The simulation results presented in section 5 are based on a four-degree of freedom non-linear mathematical model of a containership. In order to take into account the wave effects, a stochastic model of the ship waves induced motions has been considered. The proposed autopilot has been tested for both course-keeping and course-changing manoeuvres. All the simulations carried out at different sea conditions and different sailing direction confirms the viability of the proposed approach.

REFERENCES

Amerongen van J. and Udink Ten Cate A.J. Model reference adaptive autopilots for ships. Automatica. 1975; Vol.11:441-449.

Amerongen van J. and Naute Lemke van H.R. Criteria for optimum steering of ships. Symp. on Ship Steering Aut. Cont.; 1980; Genova. 1980.

Astrom K.J. Why Use Adaptive Techniques for Steering Large Tankers. Int. J. Control. 1980; Vol.32, No4:689-708.

Blanke M. and Jessen A.G. Dynamic properties of container vessel with low metacentric height. Trans. of The Inst. of Meas. and Cont. 1997; 19(2):78-93.

Brink A.W., Baas G. E. Tiano A. and Volta E. Adaptive automatic course-keeping control of a supertanker and a container ship: a simulation study. Proc. 5th Ship Control Syst. Symp. Annapolis. 1978: Vol 4.

Broome D.R., Keane A. J. and Marshall L. The effect of variations in ship operations on an adaptive autopilot. Proc. Ship Steering and Automatic Control; Genova. 1980: 77-95.

Hang C.C. and Parks P.C. Comparative studies of Model Reference Adaptive Control Systems. IEEE Transc. on Automatic Control. 1973 Oct; AC-18(5):419-28.

Honderd G. and Winkelman J.E. An Adaptive Autopilot for Ships. Proc. 3rd ship Control Systems Symposium Bath; 1972: Vol.2.

Kallstrom C.G., Astrom K. J. Thorell N. E. Eriksson J. and Sten L. Adaptive autopilots for tankers. Automatica. 1979; Vol. 15:254-284.

Lewis E.W. Principles of Naval Architecture. SNAME, New York. 1988.

Minorsky N. Directional Stability of Automatically Steered Bodies. Journal of American Society of Naval Engineers. 1922; 34:280 309.

Narendra K.S. and Annaswamy A.M. Stable Adaptive Systems.: Englewood Cliffs, N.J. : Prentice-Hall; 1989.

Price W.G. and Bishop R. Probabilistic Theory of Ship Dynamic. London: Chapman and Hall; 1974.

Sperry E. Automatic steering. Trans. Society of Naval Architects and Marine Eng.. 1922; 53-61.

Spooner J.T. and K.M. Passino. Stable adaptive control using fuzzy systems and neural

networks. IEEE Trans. on Fuzzy Systems. 1996 Aug; 4(3):339-359.

Tang Y., Zhang N. and Li Y. Stable fuzzy adaptive control of nonlinear systems. Fuzzy Sets and Systems. 1999; 104:279-288.

Tiano A. and Blanke M. Multivariable identification of ship steering and roll motions. Trans. Inst. Meas. and Cont. 1997; 19(2):63-77.

Wang L.X. Stable adaptive control of nonlinear systems. IEEE Proc. of 31th Conf. Decision and Control. 1992; 2511-2516.

Wang L.X.. Stable adaptive fuzzy control of nonlinear systems. IEEE Trans. Fuzzy Systems. 1993; 1(2):146-155.

Zi-Xing Cai. Intelligent Control: Principles, Techniques and Applications. Singapore: World Scientific Publishing Co. Pte. Ltd.; 1997. ISBN: 981-02-2564-4.

FEEDBACK-LINEARISATION CONTROLLER BASED ON NEURAL NETWORKS FOR THE COURSE-KEEPING PROBLEM OF A CONTAINERSHIP.

A. Zirilli[1], G.N. Roberts[1], A. Tiano[2] and R. Sutton[3]

[1] Mechatronics Research Centre, University of Wales, Newport U.K.
[2] University of Pavia Italy. Also Institute of Ship Automation C.N.R. Genova Italy
[3] University of Plymouth, Plymouth U.K.

Abstract. Neural Networks for control and system analysis have been intensively investigated during the last ten years, not only in terms of the research being carried out, but perhaps more importantly in terms of the potential range of applications. The main characteristics of neural networks for control applications can be summarised as: they can be used to approximate any continuos mapping, they perform this approximation through learning, parallel processing and fault tolerance are easily accomplished. In this paper the problem to stabilise a non-linear ship's dynamics around an equilibrium point is considered. This particular mode of operation is known as *course-keeping* manoeuvre. Steering criteria for this mode of operating is introduced and the classical results of optimal Linear Quadratic controller are extended by means of a feedback linearisation of the non-linear dynamics is achieved through the use of neural networks. Simulation results are included to show the viability of the proposed approach.

INTRODUCTION

The increasing cost of fuel during the 1970s produced a growth interest in the ship motion control problem. The main challenge was to develop and put into operation new ship's control systems, which could perform the desired task in a safe and economical way. For this purpose the coupling between the different motions could not be neglected. The most popular approach was the Linear Quadratic (LQ) Controller, in which the controller parameters are selected in order to satisfy certain optimal criteria expressed as a quadratic cost function. Different cost functions taking into account yaw and rudder deviation, fuel consumption, etc., were proposed Norrbin (1), Katebi et al (2), and Broome et al (3). Although the LQ technique appeared to be robust for parameter changes, other researchers were investigating the applicability of adaptive control techniques such as model reference Honderd and Winkelman (4), Amerongen and Udink Ten Cate (5) or self-tuning adaptive controller Kallstrom et al (6), Brink et al (7). Adaptive control is also needed to maintain optimal performances, even when the process characteristics change due to the changing in forward speed, load condition, water depth etc. Astrom (8).

The ship's autopilot proposed in this paper, is based on well-known results of non-linear control theory. The solution adopted herein is based on the assumption that the ship's dynamics can be linearized through feedback linearisation technique. Two neural networks are therefore trained in order to produce respectively the desired change in the systems co-ordinate and the new input signal, in such a way that the feedback linearisation of the ship's dynamics is achieved. With respect to the feedback linearized system, standard LQ theory is applied in order to deduce the optimal control law for the course-keeping problem.

NON-LINEAR MODEL OF A CONTAINERSHIP

The mathematical model of a container ship used in this study is described in detail in Tiano and Blanke (9) and Blanke and Jessen (10). It is herein considered a stochastic extension of such models capable to describe the ship response in irregular sea waves, which is expressed by the following non-linear equations:

$$\begin{aligned} m\left(\dot{u}-vr-x_g r^2+z_g pr\right) &= X+X_w \\ m\left(\dot{v}+ur-z_g\dot{p}+x_g\dot{r}\right) &= Y+Y_w \\ I_{zz}\dot{r}+mx_g\left(\dot{ur}+\dot{v}\right) &= N+N_w \\ I_{xx}\dot{p}-mz_g\left(\dot{ur}+\dot{v}\right) &= K+K_w-\rho gDR_z(\varphi) \end{aligned} \tag{1}$$

The above equations with reference to the co-ordinate system shown in figure 1, describe the coupled surge, sway, yaw and roll motions, where D is the displacement, g the gravity constant, ρ the water mass density, $R_Z(\varphi)$ is the action of the rightening arm that depends on the roll angle φ, while $(x_G,0,z_G)$ are the co-ordinates of the mass centre. The mass is denoted by m whereas Ixx and Izz are the inertial moments about x and z, respectively. The linear velocity of surge and sway are u and v and the angular ones of yaw and roll are respectively r and p. The rightening arm function can be expressed as:

$$R_z(\varphi)=\sin\varphi\left(GM+\frac{BM}{2}\tan^2\varphi\right) \tag{2}$$

where GM is the ship metacentric height and BM is the distance from the centre of buoyancy to the metacentre. Terms X, Y denote the deterministic forces acting along x e y while N and K are the deterministic moments around z and x, which take into account the hydrodynamic effects from the hull movements and forces exerted on the ship by the rudder and by the propulsion system. Such forces and moments are usually described by regarding X,Y,N,K as polynomial expansion in terms of state variables, control actions and hydrodynamic coefficients Lewis (11).

The effects of external disturbances, i.e. wind and waves, consist of related forces X_w, Y_w and moments N_w, K_w acting as perturbation terms in the

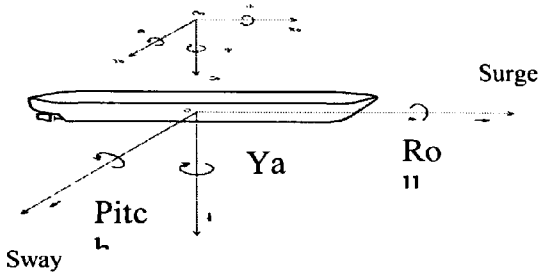

Fig. 1: Co-ordinate system

corresponding right hand parts of equation 1. Such terms, owing to their intrinsically random nature, are generally quite difficult to be characterised through explicit mathematical relations: for example, as to the waves, they should be calculated by integrating the wave pressure over the immersed surface of the hull, on the assumption that the pressure within the waves is unaffected by the presence of the ship. As it has been shown in Lewis (11) and Price and Bishop (12), a reasonable simplifying assumption consists in applying a linear superposition principle, which makes it possible to separate the ship motion due to the environment from the motion induced by the rudder and by the propeller thrust. According to this modelling approach, waves and wind are regarded as finite order linear realisations of stochastic processes characterised by known spectral densities. By limiting attention to sea waves, which are by far the dominant disturbance, it is possible to regard a long crested irregular sea height $\zeta(t)$, at time t, as described by a one-dimensional amplitude spectrum, the main parameters of which are the significant wave height, h and the average wave period T. This spectrum, accepted by the International Ship Structure Congress (ISSC) is given by:

$$G_\zeta(\omega) = \frac{173h^2}{\omega^5 T^4} \exp\left(\frac{-691}{T^4\omega^4}\right) \qquad (3)$$

The relation between the response of each individual component of the wave induced ship state vector $\mathbf{x}_w = [u_w\ v_w\ r_w\ p_w]^T$, can be obtained in terms of the spectrum:

$$G_{x_w^i}(\omega,\chi,U) = \left|R_{x_w^i}(\omega,\chi,U)\right|^2 G_\zeta(\omega) \quad i=1,4 \quad (4)$$

where χ is the angle of encounter between ship and waves, U is the ship velocity and R_{x_w} is the receptance operator, which is assumed to be known from experimental tests, describing the response of the ship i[th] motion to the waves Blanke and Jessen (10). In order to obtain the corresponding spectrum relative to the ship centre of mass, it is finally necessary to express the spectrum given by equation 4 as a function of the frequency of encounter between ship and waves $\omega_e = \omega\left(1 - \frac{\omega U}{g}\cos(\chi)\right)$. According to this approach, it is possible to implement an accurate and numerically reliable simulation of sea wave induced ship motions.

MODELS USED FOR CONTROL

Owing to the complexity and to the strong couplings between the different motion of a ship, when designing motion control systems, it is a usual convention to divide the total motions into two different sets:

1) *Vertical plane motion*, in which only surge, pitch and heave motion are considered,
2) *Lateral plane motion*, which includes yaw, sway and roll motions.

For most of the traditional ships such as RO-ROs, containerships, super-tankers and so on, pitch and heave motions could be neglected in comparison with the others and only the coupling between the remaining should be taken into account. However, for motions of small amplitudes it is possible to neglect the coupling between those remaining and consider the design of control systems regarding only the motion of interest Abkowitz (13), Lloyd (14). It is possible then to consider autopilots designed only for course keeping or course changing, or stabilisation systems designed only for roll damping motion. The most popular models used for the purpose to design yaw motion control systems are the ones by Nomoto et al (15) and Norrbin (16). For the former the models are deduced combining the linear equation representing the yaw and the sway motions and removing the dependence on roll. Such models basically represent the relationship between the rudder position and the yaw angle.

The Nomoto Model is a second-order differential equation where the coefficients are functions of the hydrodynamic derivatives:

$$\tau_1\tau_2\ddot{r} + (\tau_1+\tau_2)\dot{r} + r = k\left(\delta + \tau_3\dot{\delta}\right) \qquad (5)$$

Using the transfer function representation, equation (5) can be expressed:

$$\frac{r(s)}{\delta(s)} = \frac{k(1+\tau_3 s)}{(1+\tau_1 s)(1+\tau_2 s)} \qquad (6)$$

where,

$$\tau_1+\tau_2 = \frac{-Y_v\left(I_{zz}-N_{\dot{v}}\right) - N_r\left(m-Y_{\dot{v}}\right) + (mu-Y_r)N_{\dot{v}} - Y_{\dot{r}}N_r}{N_v(mu-Y_r)+N_rY_v}$$

$$k\tau_3 = \frac{Y_vN_\delta - N_vY_\delta}{N_v(mu-Y_r)+N_rY_v}$$

$$\tau_1\tau_2 = \frac{\left(m-Y_{\dot{v}}\right)\left(I_{zz}-N_{\dot{r}}\right)-N_{\dot{v}}Y_{\dot{r}}}{N_v\left(mu-Y_r\right)+N_rY_v}$$

$$k\tau_3 = \frac{-N_\delta\left(m-Y_{\dot{v}}\right)-N_{\dot{v}}Y_\delta}{N_v\left(mu-Y_r\right)+N_rY_v}$$

Nomoto further reduced this model to,

$$\tau r + r = k\delta \tag{7}$$

or in Laplace form in to

$$\frac{r(s)}{\delta(s)} = \frac{k}{(1+\tau s)} \tag{8}$$

where

$$\tau = \tau_1 + \tau_2 - \tau_3 \tag{9}$$

The Nomoto model is accurate in predicting ship yaw for a large class of vessels, however it is inaccurate either when large rudder angles and manoeuvres are concerned or when the ship is directionally unstable.

The Norrbin model tries to take into account the non-linearity of the ship introducing a non-linear term in the equation,

$$\tau r + H(r) = k\delta \tag{10}$$

Under steady-state condition it must be $H(r) = k\delta$. A non-linear approximation of H(r) may be given as a third order polynomial:

$$H(r) = \alpha_3 r^3 + \alpha_2 r^2 + \alpha_1 r + \alpha_0 \tag{11}$$

Norrbin suggested that the parameter α_0 assume a zero value caused by asymmetric hull or flow conditions. The parameter $\alpha_1 = +1$ for course stable ships and the parameter $\alpha_2 = -1$ for course unstable ships. Finally α_3 could describe by itself the non-linearity of the ship.

Steering criteria

In order to design an optimal controller, performances indexes have to be defined. In this respect, for a particular sailing condition different factors may be considered: 1) economy (fuel consumption), 2) safety (related to accuracy and manoeuvrability), 3) user predilections. It is common practice to distinguish between two main different modes of sailing for the specification of the ship steering control system performances. These modes are : *course changing* and *course keeping*.

Course changing: During a course changing manoeuvre the ship heading angle is changed in such a way that the ship can sail in the new direction specified by a new (desired) heading angle. During this manoeuvre it is possible to distinguish between three main parts as : 1) the start of the manoeuvre, where for safety reasons, the intention of the manoeuvre must be clearly indicated to others ships, 2) a stationary turning, characterised by a constant turning rate, and 3) the end of the manoeuvre, where it is important to control the overshoot of the manoeuvre in order to avoid dangerous paths. The specification of this manoeuvre in the time domain can be done in terms of the step response of a reference model. Model reference adaptive technique can be used in order to design optimal controllers for this particular mode of operation Amerongen and Naute Lemke (17).

Course-keeping: In the course-keeping mode of operating, the control system has to maintain a fixed direction of sailing, compensating for the different external environmental disturbances (i.e. wind, waves and current). The controller has to select the best trade-off between precision (which will minimise the elongation of the sailed distance) and control effort (rudder movement, which will produce additional drag force and consequent loss of speed). A first approximation of the relative increase in drag force due to steering can be represented by the equation:

$$\frac{\Delta R}{R} = \frac{\alpha}{T}\int_0^T \left(vr + \rho\delta^2\right)dt$$

The first term in the parenthesis represents the Coriolis force due to the coupling between sway and yaw while the second term represents the drag induced by the rudder movement. As a consequence of the problem definition it is clear that this optimisation problem fits very nicely in the formulation of the Linear Quadratic Gaussian control problem. Different papers have shown the applicability of this control technique for steering a large tanker in different sailing conditions by a proper choice of the weighting matrices. However, the majority of such papers propose a solution for the LQG problem based on a linearisation of the ship's dynamics around an equilibrium point, achieved considering the first-order truncation of the power series expansion of the ship's equations of motion. The assumption that the rudder angle is "small" (does not exceed approximately 8/10 degrees) therefore has to be fulfilled.

In the following sections the feedback-linearisation technique is introduced. Further, it is shown how the same design procedure (namely the LQ) applied to a linearisation of the plant achieved by feedback linearisation technique can, under a certain extent guarantee a large stability region around the equilibrium point, with respect to that achieved by considering the linearisation of the plant equation by simply considering the first-order terms of the non-linear equations.

FEEDBACK LINEARISATION

The problem to examine to what extent the behaviour of a non-linear system could be made linear under the effect of an appropriate feedback control law have been studied extensively during the 1980s and today represents a well-established subject in the non-linear system analysis Isidori (18) Slotine and L (19) Freeman Randy and Kokotovic (20). The problem of feedback linearisation of a non-linear system can be stated as follow:

1) find a suitable change of co-ordinates in the state space $z = \phi(x)$

2) and a feedback law $u(k) = \alpha[x(k), v(k)]$

such that the feedback system with new input $v(k)$ and state $z(k)$ is equivalent to a liner one. Suppose that the single-input, single-output (SISO) non-linear system with accessible states is represented by the equation:

$$x(k+1) = f[x(k), u(k)] \qquad (12)$$

where $x \in \Re^n$ is the state and $u \in \Re^1$ is the control input. If the system (12) is feedback linearizable it follows that:

$$z(k+1) = \phi[x(k+1)] = \phi[f(x(k), \alpha(x(k), v(k)))] = \\ = Az(k) + Bv(k) \qquad (13)$$

where A and B represent the behaviour of the linear system. However, when the non-linear function f is known, it is possible to check the conditions under which the system is feedback linearizable. In the adaptive problem, however where the function f is supposed to be unknown it is only possible to suppose the feedback linearisability of the plant and search for two mapping $NN_\phi : \Re^n \to \Re^n$ and $NN_\alpha : \Re \to \Re$ of $\phi(\cdot)$ and $\alpha(\cdot)$ respectively, using neural network such that equation (13) is verified.

In the following section an automatic procedure to find the mapping NN_ϕ and NN_α in order to achieve the feedback linearisation through neural networks is presented. Once linearized through feedback linearisation technique, the system is controlled by the optimal feedback gains calculated from the standard LQ theory. Comparison of the proposed approach and a standard LQ controller by simulation results are presented in the final section.

Course-keeping controller by feedback linearisation

In the adaptive problem the ship's dynamics are unknown, therefore an estimated model is used in order to carry out the controller design. A model of the ship's dynamics can be estimated from a collection of input/output data via neural network as shown in figure 2. The network $NN_f(\cdot)$ represent the estimation of the ship's dynamic and since it is fed with the ship output $\psi(\cdot)$ instead of the estimated output $\hat{\psi}(\cdot)$, this

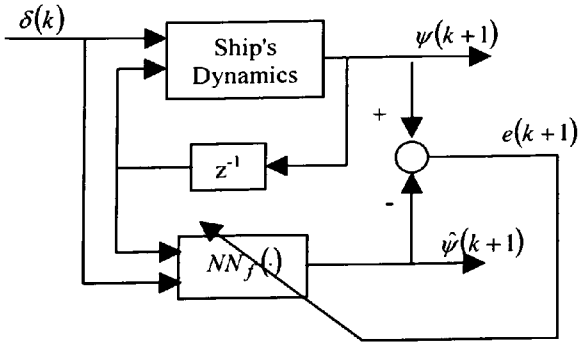

Fig. 2: Ship's dynamics estimation

architecture is referred to as series-parallel identification.

The question that arises is whether feedback linearisation of the real system (equation 12), implies feedback linearisation of the estimated system $(NN_f(\cdot))$ with the architecture shown in figure 2. Because neural networks are universal approximator Hornick et al (21), it follows that it is possible to approximate with bounded error any non-linear function over a compact region D, i.e.

$$\|NN_f(x,u) - f(x,u)\| < \|e(x,u)\| < \varepsilon \qquad \forall x, u \in D$$

Applying the mapping ϕ and α to NN_f (the estimation of the ship's dynamics) from equation 12 follows:

$$\phi[NN_f(x(k), \psi(x(k), v(k)))] = \\ = \phi[f(x(k), \psi(x(k), v(k))) + e(x(k), \psi(x(k), v(k)))] \qquad (14)$$

Since $\phi(\cdot)$ is a smooth function and $\|e(x,u)\|$ is assumed to be small, equation 14 can be rewritten;

$$\phi[f(x(k), \alpha(x(k), v(k))) + e(x(k), \alpha(x(k), v(k)))] = \\ = \phi[f(x(k), \alpha(x(k), v(k)))] + e_1(x(k), \alpha(x(k), v(k))) = \\ = Az + Bv + e_1 \qquad (15)$$

If the neural model of the ship is sufficiently good (e_1 is sufficiently small), equation 15 is an approximation of a linear system.

The objective now is to simultaneously train two neural networks $NN_\phi(\cdot)$ and $NN_\alpha(\cdot)$ that can approximate the unknown mapping $\phi(\cdot)$ and $\alpha(\cdot)$ respectively, in such a way that when the input to the neural model is given by $u(k) = NN_\alpha(x, v)$ the transformed state $\hat{z}(k+1) = NN\phi(x)$ will follow the output of a linear model $z(k+1)$ as shown in figure 3.

SIMULATION RESULTS

The linear system shown in figure 3, from which the unknown mapping $\phi(\cdot)$ and $\alpha(\cdot)$ are trained, is obtained by a straightforward linearisation of the non-linear ship equation 1, at a ship speed 12.5 m/s and GM=83 cm. The resulting state space representation is as follows:

$$x(k+1) = Ax(k) + Bu(k) \qquad (16)$$

where $x(\cdot) \in \Re^5$ is the state vector defined as $x = [v, r, p, \varphi, \psi]^T$, $u(\cdot) \in \Re$ is the rudder angle. The matrices of the linear system are defined as:

$$A = \begin{bmatrix} -0.0122 & -4.4802 & -0.0300 & -0.0256 & 0 \\ -0.0012 & -0.2211 & -0.0062 & -0.0009 & 0 \\ 0.0025 & -0.6504 & -0.0252 & -0.0282 & 0 \\ 0 & 0 & 1 & 0 & 0 \\ 0 & 1 & 0 & 0 & 0 \end{bmatrix}$$

$$B = \begin{bmatrix} 0.1315 \\ -0.0050 \\ -0.0043 \\ 0 \\ 0 \end{bmatrix}$$

A pseudo binary random manoeuvre with rudder $\delta \in [\pm 10^o]$, has been performed in order to collect the input/output pair $\{v(\cdot), z(\cdot)\}$ used for the training of the unknown mapping $NN_\phi(\cdot)$ and $NN_\alpha(\cdot)$. Once the unknown mapping $NN_\phi(\cdot)$ and $NN_\alpha(\cdot)$ have been trained the overall non-linear system shown in figure 4 has been simulated in different sailing conditions.

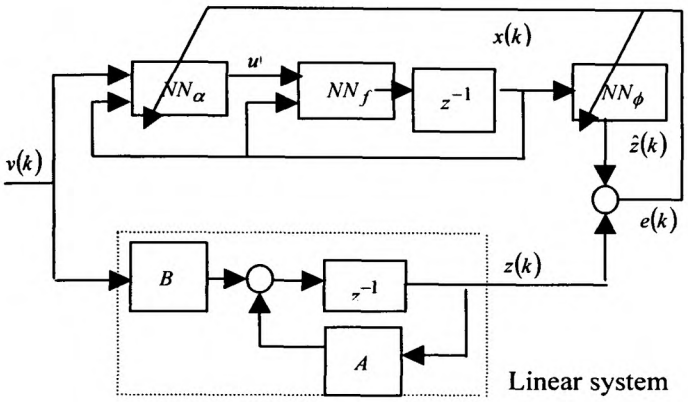

Fig. 3: Architecture for feedback linearisation

For the linearized system (equation 16) an optimal LQ controller has been designed and figure 5 and 6 shows a course-keeping manoeuvre with waves disturbances characterised by an angle of attack of 90 degrees, an average period of 10 second and a significant wave height of 7 meters. As can be appreciated from the figure, in this particular situation, both controllers the LQ linear controller (figure 5) and the non-linear LQ controller obtained by feedback-linearisation (figure 6) are able to maintain properly the heading angle.

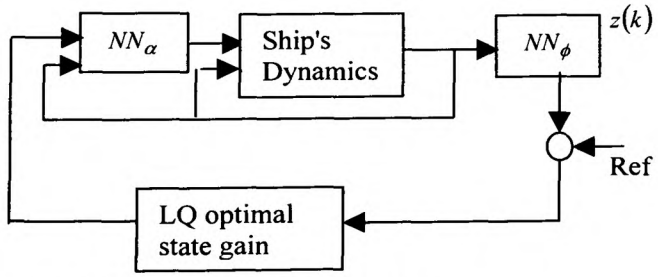

Fig. 4: Control system architecture

However, as shown in figure 7 and 8, for an initial state vector defined by x_1=[0,0,0.2,0,0], the linear approximation is not anymore valid and the linear LQ controller perform poorly while the non-linear LQ still maintain good performances. It is possible to show that the system controlled with the linear controller became unstable for an initial state vector of x=[0,0.3,0.2,0,0], while the non-linear LQ remain stable.

CONCLUDING REMARKS

In this paper a feedback-linearisation of a non-linear unknown ship's dynamic achieved by neural networks as been proposed. Once feedback-linearized the non-linear ship's dynamic has been controlled by a standard LQ optimal controller. Furthermore, has been shown by simulations, that the non-linear controller achieved with this approach can guarantee a bigger stability region around the equilibrium point with respect the linear controller. However, it is clear that for practical implementation of the proposed approach, the feedback linearizability of the non-linear plant is necessary and especially in the adaptive case, where the plant's dynamics are supposed unknown this condition can not be verified a-priori. The hypothesis used in this paper that the state of the system is accessible makes the controller design simpler, however as in the case of not accessible state the use of observer or identifier can represent a further concern.

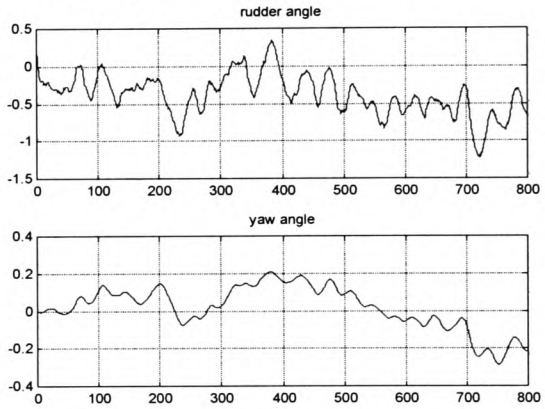

Fig. 5: Course-keeping for the linear LQ controller

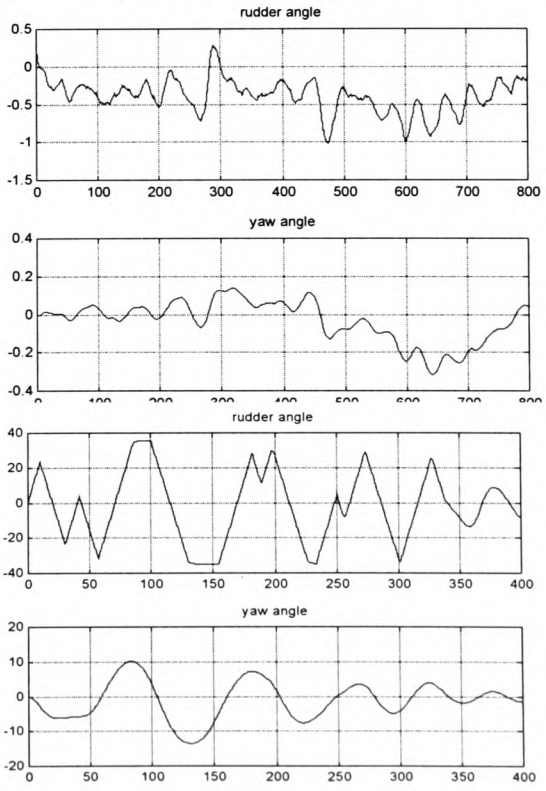

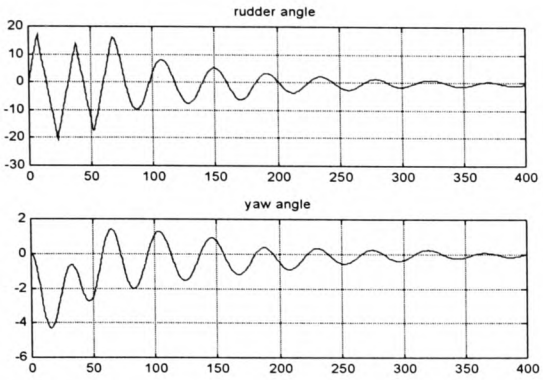

Fig. 8: Non-linear controller for initial condition x_1

Reference List

1. Norrbin N.H. 1972. On the added resistance due to steering on a straight course. Proc. 13th International Towing Tank .

2. Katebi M.R., Johnson M. A. Grimble M. J. 1993. The design of Rudder Roll Stabilisation Control System using LQ control approach. International Symposium on Marine Manoeuvring Craft.

3. Broome D.R., Keane A. J. and Marshall L. 1980. The effect of variations in ship operations on an adaptive autopilot. Proc. Ship Steering and Automatic Control.

4. Honderd G. and Winkelman J.E. 1972. An Adaptive Autopilot for Ships. Proc. 3rd ship Control Systems SymposiumBath.

5. Amerongen J. van and Udink Ten Cate A.J. 1975. Model reference adaptive autopilots for ships. Automatica Vol.11: 441-9.

6. Kallstrom C.G., Astrom K. J. Thorell N. E. Eriksson J. and Sten L. 1979. Adaptive autopilots for tankers. Automatica Vol. 15: 254-84.

7. Brink A.W., Baas G. E. Tiano A. and Volta E. 1978. Adaptive automatic course-keeping control of a supertanker and a container ship: a simulation study. Proc. 5th Ship Control Systems Symposium.

8. Astrom K.J. 1980. Why Use Adaptive Techniques for Steering Large Tankers. Int. J. Control Vol.32, No4: 689-708.

9. Tiano A., Blanke M. 1997. Multivariable identification of ship steering and roll motions. Trans. Inst. Measurement and Control 19, no. 2: 63-77.

10. Blanke M. and Jessen A.G. 1997. Dynamic properties of container vessel with low metacentric height. Transactions of The Institute of Measurement and Control 19, no. 2: 78-93.

11. Lewis E.W. 1988. Principles of Naval Architecture. Society of Naval Architecture and Marine Engineers, New York.

12. Price W.G. and Bishop R. 1974. Probabilistic Theory of Ship Dynamic. London: Chapman and Hall.

13. Abkowitz M.A. 1972. Stability and Motion Control of Ocean Vehicles. MIT Press.

14. Lloyd A.R.J.M. 1989. Seakieeping: Ship Behaviour in Rough Weather. Ellis Horwood.

15. Nomoto K.G., Tagachi K. Honda T. and Hirano S. 1957. On the steering quality of Ships, Vol. Vol. 4: International Shipbuilding Progress.

16. Norrbin N.H. 1963. On the design and analysis of the Zig-Zag Test on base of Quasi-Linear Frequency Response. 10th International Towing Tank Conference.

17. Amerongen van J. and Naute Lemke van H.R. 1980. Criteria for optimum steering of ships. Symposium on Ship Steering Automatic Control.

18. Isidori A. 1985. Nonlinear Control Systems: An Introduction. Berlin: Springer-Verlag.

19. Slotine JJ.E. and Li W. 1992. Applied Nonlinear Control. Prentice Hall.

20. Freeman Randy A. and Petar V. Kokotovic. 1996. Robust Nonlinear Control Design. State-Space and Lyapunov Techinques. Boston: Birkhauser.

21. Hornick K., Stinchcombe M. and White H. 1989. Multilayer Feedforward Networks are Universal Approximators. Neural Network 2: 359